Chemoresistance of Head and Neck Cancer Stem Cells

by

Alexandra Eileen Herzog

A dissertation submitted in partial fulfillment
of the requirements for the degree of
Doctor of Philosophy
(Oral Health Sciences)
in the University of Michigan
2024

Doctoral Committee:

Dean Jacques E. Nör, Chair
Associate Professor Rogerio M. Castilho
Associate Professor Alexander T. Pearson, The University of Chicago
Professor Peter J. Polverini

“It just takes some time
Little girl, you’re in the middle of the ride
Everything, everything’ll be just fine
Everything, everything’ll be alright, alright”

– *Jimmy Eat World*

Alexandra E. Herzog

aoklejas@umich.edu

ORCID iD: 0000-0002-8386-8045

DEDICATION

To Curtis, our family, and our dreams. To my friends and family, who have helped me along this path. To the graduate student, who doubts themselves.

And lastly, to the patients afflicted with this horrible disease. It is my most primal hope that this body of work can contribute to the advancement in improvements of systemic therapy to improve the quality and quantity of life of patients with head and neck cancer.

ACKNOWLEDGEMENTS

From the bottom of my heart, I would like to thank every individual who has supported me in this journey. There were times that I didn't think I could have made it through without you. They say it takes a village, and I am eternally grateful for mine.

First and foremost, I would like to thank Dr. Jacques Nör, my dissertation advisor and thesis committee chair, for his deep investment in me and my training. Jacques, I could not have dreamed of a better mentor for my journey in this program and beyond. Through all the twists and turns on this journey, you always knew what I needed, and I always knew I could count on you. You exemplify the epitome of what a leader should be, with a kind-hearted and patient nature in harmony with discipline and a standard for excellence. You will always be one of my biggest role models and I truly cannot thank you enough for the impact you have made in my life.

I would like to thank my thesis committee members, Dr. Rogerio Castilho, Dr. Peter Polverini, and Dr. Alexander Pearson for their invaluable feedback and guidance even long before my committee was formed. Rogerio, thank you for all your support in collaborating on experiments, interpreting results, and always being a source of positivity and encouragement. Pete, I am grateful for the many candid discussions, to have been able to work on exciting side projects with you, and to always be "kiddo." And Alex P. (or "big Alex"), thank you for taking a chance on me as an undergraduate to work with you during my gap semester and for investing so much into my development as a blossoming

graduate student. You inspired not only my dissertation project, but me as a young clinician-scientist. I am extremely grateful to have such brilliant and admirable individuals to learn from and call my mentors. I simply could not have imagined a more special thesis committee for me.

Thank you to the past and present members of the Nör lab: Drs. Kristy Warner, Zhaocheng Zhang, Tatiana Botero, Andrea Pobocik, Min Oh, Takafumi Nakano, Sosuke Sahara, Jaqueline Vanini, Ririko Tsuboi, and Christie Rodriguez who I have been fortunate to work with. I would like to especially thank Kristy, who has been there for me in immeasurable ways both in the lab and personally, for which words do not suffice. Zhang, who in my eyes is a science wizard and demonstration to it being an art – thank you for teaching me so much and challenging my ideas and findings. Jaque, thank you for being an amazing friend and lab partner – you made those 12-hour, nonstop flow cytometry days a near breeze. Min, thank you for having selected me as your undergraduate student and introducing me to the world of dental research. One of the most fulfilling parts of graduate school has been mentoring undergraduate students. Especially to Meera Bhagat, Reagan Malcolm, Ritu Somayaji, Shirley Zheng, and Madelynn Johnson: It was my honor to guide your first steps in the research lab, to practicing your first poster presentations, and witnessing you become independent young scientists. I hope you enjoyed our time together as much as I did and can't wait to continue hearing about your endeavors. My time as a graduate student may be coming to an end, but the Nör lab will always be a home to me.

Thank you to the Oral Health Sciences Ph.D. program and Office of Research staff (past and present), including Dr. Jan Hu, Dr. Vesa Kaartinen, Dr. Yuji Mishina, Kimberly

Smith, Amy Watson, Rebecca Chelberg, Patrick Lagua, and Chad Perkins for your unwavering support and guidance throughout my training. I would like to thank my fellow OHS PhD students: You guys have inspired and impressed me beyond measure. Erika, for giving the warmest hugs, always providing a safe space and shoulder to cry on, and for having a steady supply of chocolates in the pick-me-up jar. Tina, for having fulfilled your self-proclaimed role as social glue and talking me off the ledge prior to a handful of journal club presentations. Marsha-Kay, for exemplifying the definition of grace, composure, and true sisterhood. Shawn, for the scientific or dental-related discussions at 5 A.M. and consistent encouragement. To my two cohort-mates, Ben and Erica, I am grateful to have shared this journey with you. Erica, I cherish the many memories we've made and times we've laughed (and cried) together. Ben, I appreciate your accountability and meaningful discussions surrounding navigating the current and post-program plans. It takes a unique type of person to pursue this dual-degree program, and I cannot wait to see where each of our paths take us.

I would like to thank the School of Dentistry faculty and staff, for their support in navigating this dual-degree program that at times had me feeling like I was living a double life. I would like to particularly thank Dr. Don Heys, for *always* supporting the dual-degree students, leading and teaching with common sense and practicality, while maintaining the highest standard for professionalism and patient care. Dr. Elliott Hill, thank you for supporting my ambitious "Alex-appointments" in fixed prosthodontics, for your <u>many</u> words of wisdom that helped me monumentally, and your genuine care for your students. Drs. Marcia Campos and Bruno Cavalcanti, for having supported my learning and professional development beyond measure, as well as for introducing me to *churrasco*.

Clarissa Lusk and Teresa Patterson for your support, friendship, and example of character. Thank you, for being outstanding mentors and teachers. I look up to each and every one of you, and feel the deepest gratitude for you.

I am proud to be a pure-bred Michigan Wolverine and grateful to my extended community at the university for their continued support, some for over a decade. Dr. Mark Meyerhoff, for having believed in me since I was an undergraduate in your analytical chemistry class, your steadfast continued support over the many years, and for the regular lunches at *Mama Satto*. Dr. Kathleen Nolta, for being one of the greatest professors of all time, which I aspire to live up to a fraction of. Thank you both for having supported my application to this program in the first place. To Dr. Pamela Harnick – how do I synopsize the profound role you played in my journey? I could not image where or who I'd be, if I hadn't spent dozens of hours sitting in the comfortable chair across from you facing myself and what I feared most. On that note, I feel extremely privileged to be a student at this world-renowned institution and happily look forward to spending another three years here for my residency.

To my friends and family, I owe my deepest gratitude to you for having been there for me throughout this arduous journey, even when I missed opportunities to spend time together or didn't always have the capacity to be the friend or family member I would like to have been. Especially to my parents (through both blood and marriage), thank you for your unwavering support in countless ways, whether through basic necessities, care packages, visits, or phone calls; none of this would have been possible without you. To my family no longer on this earth (Oma, Opa, and Dad), you have remained a constant source of strength and reminder of where I come from. Dad, for better or worse, I think I

owe both my best and worst qualities to you and am learning to be grateful for exactly that. I also want to express my appreciation for my brothers Alex and Matt (and their families), my sister Katja, my aunt Maryann and uncle Mat, Hannah Tuller, and Omi. You never failed to make me feel loved and cared for, and I can't put into words what that has meant over the years. Thank you to Andrea Pesch, for having been an inspiration to me since our first class together in undergrad through watching you defend your Ph.D. and one of the best friends I could ask for. We miss game nights with you and Nick so much. Thank you to my classmates, the gym bros (Denzel Harris, Maxwell Shin, Mohab Louis, and Danjel Popaj) – y'all are real ones. I look forward to many more years of friendship and Tough Mudders. Especially Denzel, thank you for having felt like a familiar spirit from the moment we were partners for stab lab. Together with 'your Alex,' we've made some of my favorite memories, including the myriad of hours playing games, home-cooked family dinners, and adventures. Alexandra Gomez, thank you for having been such a good friend to Curtis and a light in my life – your energy is infectious. Thank you, Maxwell Beattie, for having been a great friend, who I am very grateful for both personally and professionally (even when you snowball about endodontics and the meaning of life). Thank you to Gerry Eaton, for caring for two of the beings who mean the most to me, for calling me out when I deserve it, and for having taught me much about horses and people.

Lastly, I would like to thank my other half and husband, Curtis, and the family we have grown over the years: Kylo, Ruby, Loki, Lady, and Moonshine. Sharing our lives with our animal family members has been one of the greatest gits from God. Kylo, thank you for being my emotional sponge, the cat that never fails to snuggle into my arms like a stuffed animal when I can't sleep. Loki, few beings have inspired me as much as you –

with three broken legs following a horrific, life-threatening accident as a kitten, your unyielding spirit and playful character were my guiding force when I concurrently suffered from my M.S. attack. Ruby, thanks for being my reminder that every girl deserves to be a princess and to never be afraid to speak up. Lady, you are my childhood dream come true and my soul's mirror. There isn't a day I don't thank God for bringing us together and that you haven't been able to make better. Moonshine, the epitome of a workhorse, commitment, and relentless drive – it was love at first ride in Wyoming and bringing you home was meant to be. Thank you for asking more of me and showing me what it means to show up no matter what. You all are magical creatures who I am deeply grateful for being their human. And Curtis, you deserve the world for putting up with me and everything we have been through. Like me at the start of this journey, you had no idea what you were getting into when you asked me out nine years ago. Through this program, we lost a parent, started grad school, got cats, got engaged, got you into residency, survived a pandemic, were married, started another round of dental school, got another cat, dealt with crippling disease, despaired, healed, bought a horse, grew both individually and together, made lifelong friends, bought another horse – I'll stop. That does not even hold a light to the life we've built throughout. Thank you for loving me so well and never giving up when I make it hard to. Thank you for having been my rock, my partner, and my whole world. I love you.

Finally, and above all: Thanks be to God, for his grace, his blessings, and his steadfast guidance for me on this path.

FINANCIAL ACKNOWLEDGEMENTS

I would like to acknowledge the funding resources that supported me throughout my graduate training. Thank you to the School of Dentistry Dean's Scholarship for having supported me when I first entered this program and to the support from research grants F30-DE029097 (A. E. Herzog), K08-DE026500 (A. T. Pearson), P50-CA097248 (G. T. Wolf), R01-DE021139 (J. E. Nör), and R01-DE023220 (J. E. Nör) from the National Institute of Dental and Craniofacial Research (NIDCR), National Institutes of Health (NIH). I am grateful to the Rackham Graduate School for the graduate student research grants and their annual research conference travel grants. Throughout my graduate training, the American Association for Dental, Oral, and Craniofacial Research (AADOCR) played an especially meaningful role through the opportunities I had to participate in various award programs (e.g. SCADA Program, Edward H. Hatton Competition, 411 Rapid Research Competition, and Student Research Fellowships) and my involvement within the National Student Research Group, for which I had the honor of serving as President (-elect) in 2020-2022. I am tremendously grateful for these opportunities, as they have undoubtedly supported and propelled my development as a young scientist.

PREFACE

Earning a Ph.D. is not only about obtaining the degree, but about the journey that it brings you on. Seven years ago, I was prepared for this to be an experience devised to push me to my limits, requiring personal growth, with demands only few people would understand. That 21-year-old girl who accepted her position in this D.D.S./Ph.D. program – filled with excitement and a vision – was not ready to embark on this journey two months after her dad died unexpectedly. She could not imagine the deep-rooted grief and trauma she would work relentlessly to unpack and heal from over the next years. She did not expect to receive the diagnosis of "Multiple Sclerosis" in her first year of dental school, or that she would support her husband through a grueling surgical residency. No, that girl truly had no idea what she was in for.

My journey through this program has taught me far more than the subject matter at hand, formed who I am today, and consistently demanded me to evaluate my definition of success: Seeing the bright side through the dark times when there isn't one. Being brave enough to live as your authentic self. Listening to what your mind, body, and soul need – and taking care of them. Being intentional. Resilience. Faith. The list goes on – maybe I'll write about it one day. The following dissertation is more than just a culmination of scientific experiments and synthesized conclusions. It's a body of work that encompasses more than anyone but myself can truly understand, and I am so honored and grateful to share it with you.

TABLE OF CONTENTS

DEDICATION ..... **ii**

ACKNOWLEDGEMENTS ..... **iii**

FINANCIAL ACKNOWLEDGEMENTS ix

PREFACE ..... **x**

LIST OF FIGURES ..... **xvi**

LIST OF ABBREVIATIONS ..... **xviii**

ABSTRACT ..... **xx**

CHAPTER 1: Overcoming Head and Neck Cancer Stem Cells **1**

1.1 Abstract 1

1.2 Introduction 2

1.3 The Cancer Stem Cell Hypothesis 3

1.4 Identifying Head and Neck Cancer Stem Cells 5

1.5 CSC Functional Assays 8

1.6 The Cancer Stem Cell Niche 9

1.7 Cell-Cell Crosstalk 10

1.7.1 Endothelial Cells 11

1.7.2 Cancer-Associated Fibroblasts 11

1.7.3 Immune Cells 12

1.7.4 Neural Cells 13

1.8 CSC Signaling Pathways 14

1.9 Epithelial-Mesenchymal Transition and Cell Plasticity 17

1.10 Therapeutic Resistance..... 18

1.11 Targeting Cancer Stem Cells 22

1.12 Conclusion..... 27

1.13 Acknowledgements 28

1.14 Figures 29

1.15 References 32

CHAPTER 2: The IL-6R and Bmi-1 Axis Controls Self-Renewal and Chemoresistance of Head and Neck Cancer Stem Cells 53

2.1 Abstract 53

2.2 Introduction..... 54

2.3 Results..... 56

2.3.1 IL-6/Bmi-1 signaling axis regulates cancer cell self-renewal and correlates with recurrence-free survival of HNSCC patients. 56

2.3.2 Therapeutic inhibition of IL-6R abrogates Cisplatin-induced cancer stemness in vivo..... 58

2.3.3 Tocilizumab suppresses Cisplatin-induction of CSC-associated signaling pathways. 59

2.3.4 Tocilizumab inhibits STAT3 signaling and self-renewal of HNSCC cells. .. 61

2.3.5 Therapeutic inhibition of IL-6R decreases self-renewal and CSC fraction in Cisplatin-resistant HNSCC cells. 63

2.3.6 Tocilizumab suppresses growth and Bmi-1 expression of Cisplatin-resistant xenografts. 64

2.4 Discussion 65

2.5 Materials and Methods 69

2.5.1 Cisplatin-resistant cell lines and cell culture 69

2.5.2 HNSCC Patient-Derived Xenograft (PDX) Mouse Model 70

2.5.3 HNSCC subcutaneous scaffold xenograft mouse model..... 70

2.5.4 Flow cytometry 71
2.5.5 Orosphere assay 71
2.5.6 Pluripotent stem cell array 72
2.5.7 IL-6R gene silencing 72
2.5.8 Western blot 73
2.5.9 Histological staining and analyses 73
2.5.10 Statistical Analysis 74
2.6 Acknowledgements 75
2.7 Figures 76
2.8 Supplemental Figures 85
2.9 References 92
CHAPTER 3: Bmi-1: A Master Regulator of Head and Neck Cancer Stemness 98
3.1 Abstract 98
3.2 Introduction 99
3.3 Cancer Stem Cells in Head and Neck Cancer 100
3.4 Biomarkers of Cancer Stem Cells 101
3.5 Bmi-1 and Cancer Stem Cells 104
3.5.1 Physiological Bmi-1 Function and Regulation 104
3.5.2 Bmi-1 Regulation in Cancer 107
3.5.3 Bmi-1 in Tumorigenesis and Metastasis 110
3.6 Bmi-1 in Cancer Therapeutics 112
3.6.1 Bmi-1 in Chemoresistance 112
3.6.2 Bmi-1 in Radioresistance 114
3.6.3 Bmi-1 as a Prognostic Factor 116
3.6.4 Therapeutic Targeting of Bmi-1 118

3.7 Conclusion 119

3.8 Acknowledgements 120

3.9 Figures 121

3.10 References 124

CHAPTER 4: Bmi-1 Mediates Resistance of Head and Neck Cancer Stem Cells to Cytotoxic Chemotherapy 143

4.1 Abstract 143

4.2 Introduction 144

4.3 Results 146

4.3.1 Bmi-1 knockdown decreases expression of the IL-6/STAT3 signaling axis and regulates cancer cell self-renewal. 146

4.3.2 Bmi-1 knockdown suppresses increase in CSC fraction by treatment with cytotoxic chemotherapy and mediates the DNA damage response. 147

4.3.3 Bmi-1 inhibition with PTC596 prevents the Cisplatin-induced self-renewal and fraction of CSCs. 149

4.3.4 PTC596 suppresses Cisplatin-induced CSC fraction in subcutaneous xenograft model of HNSCC in vivo. 151

4.3.5 Bmi-1 defines the self-renewal capacity of HNSCC cells. 153

4.4 Discussion 154

4.5 Materials and Methods 159

4.5.1 Cell culture 159

4.5.2 Bmi-1 gene silencing 160

4.5.3 Conventional orosphere assay 160

4.5.4 Automated orosphere assay 161

4.5.5 Western blot 161

4.5.6 Flow cytometry 162

4.5.7 HNSCC subcutaneous scaffold xenograft model 162

4.5.8 Statistical analyses 163
4.6 Acknowledgements 164
4.7 Figures 165
4.8 Supplemental Figures 172
4.9 References 177
CHAPTER 5: Conclusion 182
5.1 Summary 182
5.2 Future Directions 185
5.2.1 Biological processes underlying Bmi-1-mediated CSC fraction changes 185
5.2.2 Untangling the Bmi-1-mediated DNA damage response 187
5.2.3 Bmi-1 as a putative prognostic marker 188
5.3 Concluding Remarks 192
5.4 References 192

LIST OF FIGURES

Figure 1-1: The cancer stem cell niche. 29

Figure 1-2: Selective pressure of conventional anticancer therapies 30

Figure 1-3: Clinical trials targeting cancer stem cells in head and neck cancer. 31

Figure 2-1: IL-6/Bmi-1 signaling axis regulates cancer cell self-renewal and correlates with recurrence-free survival of HNSCC patients. 76

Figure 2-2: Tocilizumab suppresses Cisplatin-induced CSC phenotype in PDX models of HNSCC *in vivo.* 78

Figure 2-3: Combination therapy suppresses STAT3 signaling, Bmi-1 induction, and expression of stem cell markers *in vitro.* 80

Figure 2-4: Tocilizumab prevents the Cisplatin-induced self-renewal of orospheres. .. 81

Figure 2-5: Tocilizumab decreases CSC fraction and self-renewal of Cisplatin-resistant HNSCC cells. 82

Figure 2-6: Tocilizumab decreases tumor growth and Bmi-1 expression in a Cisplatin-resistant xenograft model. 83

Figure 2-7: Flow cytometry gating and orosphere size measurements for CSC analysis of IL-6R knockdown cells. 85

Figure 2-8: Therapeutic effect of Tocilizumab and/or Cisplatin in in vivo HNSCC models. 86

Figure 2-9: Tocilizumab suppresses Cisplatin-induction of cancer cell stemness. 87

Figure 2-10: Tocilizumab decreases orosphere growth and Bmi-1 expression. 88

Figure 2-11: Flow cytometry gating for CSC analysis of Cisplatin resistant HNSCC cell line variants. 89

Figure 2-12: Tocilizumab decreases size of orospheres in Cisplatin-resistant HNSCC cell line variants. 90

Figure 2-13: Effect of Tocilizumab and/or Cisplatin in a Cisplatin-resistant xenograft model. 91

Figure 3-1: Markers of head and neck cancer stem cells. 121

Figure 3-2: Potential involvement of Bmi-1 in key signaling pathways. 122

Figure 3-3: Chemotherapeutic induction of Bmi-1 increases the cancer stem cell population. 123

Figure 4-1: Bmi-1 knockdown decreases activation of the IL-6/STAT3 signaling axis and regulates cancer cell self-renewal. 165

Figure 4-2: Bmi-1 knockdown suppresses increase in CSC fraction by treatment with cytotoxic chemotherapy and mediates the DNA damage response. 167

Figure 4-3: Bmi-1 inhibition with PTC596 prevents the Cisplatin-induced self-renewal and fraction of CSCs. 169

Figure 4-4: PTC596 suppresses Cisplatin-induced CSC fraction in subcutaneous xenograft model of HNSCC *in vivo.* 170

Figure 4-5: Bmi-1 defines the self-renewal capacity of HNSCC cells. 171

Figure 4-6: Orosphere size measurements for analysis of Bmi-1 knockdown cells. .. 172

Figure 4-7: Orosphere size measurements and flow cytometry gating strategy for analysis of Bmi-1 knockdown cells treated with Cisplatin or Carboplatin. 173

Figure 4-8: Orosphere size measurements and flow cytometry gating strategy for analysis of HNSCC cells treated with Cisplatin and/or PTC596. 174

Figure 4-9: Therapeutic effect of PTC596 and/or Cisplatin in *in vivo* HNSCC subcutaneous xenograft model. 175

Figure 4-10: Optimization of cell seeding number for orosphere assay using an automated liquid handler. 176

Figure 5-1: The IL-6R and Bmi-1 axis controls self-renewal and chemoresistance of head and neck cancer stem cells. 183

Figure 5-2: Bmi-1 mediates resistance of head and neck cancer stem cells to cytotoxic chemotherapy. 184

Figure 5-3: Reciprocal exchange of cytokine mediators between cancer stem cells (CSC), endothelial cells (EC), and macrophages (M1 and M2). 191

LIST OF ABBREVIATIONS

ACC	Adenoid cystic carcinoma
ALDH	Aldehyde-dehydrogenase
CAF	Cancer-associated fibroblast
CSC	Cancer stem cell
EV	Extracellular vesicle
FACS	Fluorescence-activated cell sorting
HNSCC	Head and neck squamous cell carcinoma
IGF	Insulin-like growth factor
IGFBP7	Insulin-like growth factor binding protein 7
IL-6	Interleukin-6
LDA	Limiting dilution assay
MAST1	Microtubule-associated serine/threonine kinase 1
MFG-E8	Milk-fat globule-epidermal growth factor-VIII
NCCN	National comprehensive cancer network
PD-L1	Programmed death-ligand 1
PDX	Patient-derived xenograft
PNI	Perineural invasion
PRC1	Polycomb repressive complex 1
PTK7	Protein tyrosine kinase 7

SDF-1 Stromal cell-derived factor-1

STAT3 Signal transducer and activator of transcription 3

TEC Tumor endothelial cell

ABSTRACT

Head and neck squamous cell carcinoma (HNSCC) is a frequent and deadly malignancy. Despite significant advances in understanding the pathobiology of this disease, patient morbidity associated with invasive treatment modalities along with a high frequency of tumor recurrence and metastasis typically result in unacceptably low patient survival and poor quality of life. The cancer stem cell (CSC) hypothesis provides an explanation for the observed disease relapse following current treatment paradigms, with pivotal malignant features of a cancer cell deriving from a shift towards stem-like features. CSCs, identified as $ALDH^{high}CD44^{high}$ cells, constitute only around 5% of total tumor cells but function as drivers of tumor initiation, mediate therapeutic evasion, and promote recurrence and metastases of HNSCC.

We previously demonstrated that interleukin-6 (IL-6) secreted by endothelial cells within the perivascular niche in the tumor microenvironment enhances CSC survival, self-renewal, and tumorigenic potential. Cisplatin, the most common chemotherapy for HNSCC, activates the IL-6 pathway, which potentiates Cisplatin-induction of the CSC fraction and Bmi-1 expression. Bmi-1 is a master regulator of stem cell self-renewal and highly expressed in CSCs. Notably, cytotoxic chemotherapy enhances Bmi-1 expression and increases the CSC fraction in HNSCC. By virtue of their high tumorigenic potential and resistance to a multitude of therapies, CSCs present an imperative target for developmental therapeutics in HNSCC.

This project sought to understand signaling mechanisms underlying chemoresistance of CSCs. Our central hypothesis is that therapeutic blockade of the IL-6 and Bmi-1 signaling axis suppresses chemotherapy-induced CSC self-renewal and inhibits CSC resistance. In this work, we aimed to: 1) determine the effect of IL-6/STAT3 inhibition on Cisplatin-induced phenotypic changes in the cancer cell population and downstream signaling effectors, 2) determine the therapeutic effect of IL-6/STAT3 inhibition on resistance to conventional Cisplatin therapy in HNSCC, and 3) elucidate the role of Bmi-1 in increasing the fraction of CSCs in response to cytotoxic chemotherapy.

We demonstrate that blockade of IL-6R via lentiviral knockdown or pharmacologic inhibition with a humanized monoclonal antibody (Tocilizumab) is sufficient to inhibit Bmi-1 expression, sphere formation, and to decrease the CSC fraction even in a Cisplatin-resistant HNSCC model. IL-6R inhibition with Tocilizumab abrogates Cisplatin-mediated increase in the CSC fraction and induction of Bmi-1 in patient-derived xenograft (PDX) models of HNSCC. Notably, Tocilizumab inhibits Bmi-1 and suppresses growth of xenograft tumors generated with Cisplatin-resistant cells. Our results from human tumor specimens of 216 HNSCC patients show that high Bmi-1 expression correlates with decreased recurrence-free survival time. Moreover, both genetic knockdown of Bmi-1 as well as pharmacologic inhibition using the small molecule inhibitor PTC596 abrogates the increase of CSC fraction, sphere formation, and DNA damage response by cytotoxic chemotherapy. Treatment with PTC596 also suppressed Cisplatin-mediated increase of the CSC fraction in a scaffold xenograft model *in vivo*.

Altogether, these studies demonstrate that therapeutic blockade of IL-6R suppresses Bmi-1 function, thus inhibiting cancer stemness. We showed that Bmi-1

contributes to chemoresistance of CSCs, which may occur through induction of DNA damage repair mechanisms as Bmi-1 plays an important role in the DNA repair response. Further investigation into the role of Bmi-1 in DNA damage elicited by platinum-based chemotherapy is still necessary. This work unveils important molecular mechanisms underlying CSC maintenance and therapeutic resistance, which have the potential to inform novel mechanism-based therapies targeting CSCs to improve survival and quality of life of patients with head and neck cancer.

CHAPTER 1:
Overcoming Head and Neck Cancer Stem Cells[1]

1.1 Abstract

Head and neck cancer is a frequent and deadly malignancy. Despite significant advances in the understanding of the pathobiology of head and neck cancer, patient morbidity associated with invasive treatment and the high frequency of tumor recurrence/metastasis typically result in an unacceptably short patient survival and poor quality of life. The cancer stem cell hypothesis attempts to explain the observed heterogeneity of cancer cells within a tumor, with many malignant features of a cancer cell deriving from a shift towards stem-like features. Cancer stem cells function as drivers of tumor initiation, mediate therapeutic evasion, and promote recurrence and metastases of head and neck cancer. Notably, cancer stem cells are highly resistant to conventional chemotherapy and radiotherapy. Therefore, cancer stem cells represent an attractive target for developmental therapeutics. In this chapter, we discuss cancer stem cell-mediated resistance to treatment and approaches that might sensitize patients to therapy by targeting these cells.

[1] This chapter was originally published in *Improving the Therapeutic Ratio in Head and Neck Cancer*. Oklejas AE, Nör JE. Overcoming Head and Neck Cancer Stem Cells. In: R. Kimple (Ed.), *Improving the Therapeutic Ratio in Head and Neck Cancer* (1st Edition, pp. 135-150). Academic Press; 2019.

1.2 Introduction

Key malignant features of a cancer cell have been shown to derive from the acquisition of stem-like features [1]. Indeed, we will discuss here the scientific evidence that suggests that cancer stem cells (CSC) define the pathobiology and the response to treatment of head and neck squamous cell carcinomas (HNSCC) [2-4]. Cancer stem cells represent a self-renewing, multipotent, and highly tumorigenic subpopulation of cancer cells generally ranging from 1 to 10% of the overall tumor cell population in HNSCC. These cells have been shown to engage in cellular crosstalk within the dynamic tumor microenvironment, which plays a major role in governing their maintenance and cell fate. The preferred chemotherapeutic treatment for HNSCC remains platinum-based agents, Cisplatin being the most commonly used. Though their survival benefit is well recognized, Cisplatin-based treatment regimens are associated with substantial patient morbidity [5] and disease relapse, with locoregional recurrence accounting for 20-40% of HNSCC mortality of patients at 5 years [6]. Cancer stem cells have been shown to be highly resistant to conventional chemotherapy [7] and radiation [8], which may account for the fact that many head and neck cancer patients experience tumor recurrence. Advancements in the knowledge of cancer stem cell biology have provided scientific rationale for targeted elimination of the cancer stem cell pool to benefit the survival and quality of life of patients with head and neck malignancies. Here, we will review the evidence on the biology of head and neck cancer stem cells and will discuss their therapeutic targeting as a means to overcome treatment resistance and disease progression.

1.3 The Cancer Stem Cell Hypothesis

Over the past decade, the idea of stem-like cells within tumors has received significant attention. It has now been accepted that not all tumor cells are equal, and that a tumor is vastly heterogenous. The CSC hypothesis postulates that among the bulk of neoplastic cells, cancer stem cells make up a small fraction of cells endowed with characteristics of self-renewal, multipotency, and uniquely high tumorigenic potential [1]. These characteristics are demonstrated by (1) the unique ability of CSCs to initiate and propagate tumors *in vivo*, (2) the observation that the resulting tumors consist of a heterogeneous population that recapitulates the CSC's original tumor, and (3) the capability of these tumors to be serially transplanted [9]. On the other hand, the bulk of the tumor is composed of rapidly proliferating transit amplifying cells and post-mitotic differentiated cells, both of which are not capable of initiating tumors. These cells lack longevity and have only limited proliferative potential, as opposed to the cancer stem cell population [1].

A principal feature of stem cells is their ability to recapitulate a heterogeneous organ from a single cell. Rather than proposing a tumor arises from normal stem cells, the CSC hypothesis attempts to explain the observation that a tumor may be hierarchically organized in much the same manner as physiological tissues [10]. Similar to their physiological counterparts, cancer stem cells share the attributes of self-renewal and the capacity to differentiate into committed progenitor cells. However, a distinguishing feature of cancer stem cells is their uniquely high tumorigenic potential, making these cells a crucial part of tumor initiation and disease progression to metastasis and/or recurrence [1]. In parallel to the functional role of stem cells in physiological tissues, the

relatively small number of cancer stem cells fuels tumor growth and gives rise to the bulk tumor cells. The bulk tumor cells are not able to self-renew and do not contribute to the long-term viability of the tumor, therefore becoming less relevant in the grand scheme of disease progression and treatment [11]. Unfortunately, the line between what is a cancer stem cell and what is a bulk tumor cell is blurred. Cancer stem cells maintain plasticity to transition between epithelial- and mesenchymal cell stages, with molecular and environmental cues shifting the equilibrium of stem-like *versus* non-stem-like characteristics [12].

The CSC hypothesis is especially appealing due to the explanation it provides for several poorly understood clinical phenomena. A patient may present a robust response to chemo- and radiation therapy in the form of tumor shrinkage and disease remission. However, a small fraction of cancer stem cells survives these treatment attempts. Thus, the inevitable outcome of seemingly effective treatments is oftentimes local recurrence or metastatic spread. Cancer stem cells are resilient cells that can maintain their population through self-renewal, and their quiescent nature allows them to evade the majority of chemotherapeutic approaches. Cancer stem cells are highly migratory to distant sites within the body, where they can initiate a new tumor and lead to metastasis, even long after the patient was initially treated. In clinical assessments, the CSC content within tumors has been shown to be a predictive factor [13] and to define the tumor's heterogenous phenotypical and molecular traits [14]. Therefore, cancer stem cells present an enticing avenue for research into more effective therapeutic developments, as the goal is to target the "warhead" of the tumor instead of simply eradicating the, by comparison, harmless tumor bulk.

1.4 Identifying Head and Neck Cancer Stem Cells

The identification of cancer stem cells is an area of ongoing research in many different cancer types. Cancer stem cell identification relies predominantly on the expression of cell surface molecules or intracellular enzymes, which can vary depending on the cancer. Flow cytometry/fluorescence-activated cell sorting (FACS) remains the most commonly used technique to identify and isolate cancer stem cells based on cell-specific markers.

In HNSCC, cancer stem cells were first identified as $CD44^+$ expressing cells by Prince and colleagues [2]. CD44 is a cell surface adhesion receptor involved in cell-to-cell interaction, adhesion, and migration, which can bind to hyaluronic acid (among other extracellular matrix ligands). The small fraction of $CD44^+$ cells flow-sorted from primary HNSCC tumor samples was shown to be highly tumorigenic when implanted into immunodeficient mice, as compared to the $CD44^-$ cancer cells [2]. Interestingly, the $CD44^+$ cancer cells co-stained with epithelial basal cell marker Cytokeratin 5/14, which is highly expressed in mitotically active basal stem cells and down-regulated as these cells differentiate [15]. The tumors generated from $CD44^+$ cells reproduced a heterogenous tumor expressing both $CD44^+$ and $CD44^-$ cells, which demonstrated multipotency of these cells. Gene expression analysis also revealed differential expression of the self-renewal marker Bmi-1 in $CD44^+$ versus $CD44^-$ cells. This work was among the first to unveil a subpopulation of cancer cells in HNSCC that follow the principles put forth by the CSC hypothesis. It has since then been shown that CD44 is highly expressed in several stem cells and many cancers, in which it helps promote the migration and invasion processes involved in metastasis [16]. However, though CD44 expression has been shown to select

for a subset of cells with stem-like characteristics, it is not sufficient to distinguish between normal, benign, or malignant epithelia of the head and neck [17].

Another widely used marker for cancer stem cell identification is aldehyde dehydrogenase (ALDH), which has emerged as a rather universal CSC marker. The aldehyde dehydrogenase family of enzymes is crucial for maintenance, differentiation, and normal development of stem cells, and functions in cellular detoxification, retinoic acid metabolism and signaling, and protection from reactive oxygen species [18]. Increased ALDH activity was first shown to isolate cancer stem cells in leukemia, where $ALDH^{high}$ cells demonstrated superior tumorigenic potential as compared to $ALDH^{low}$ cells, and were co-expressed with the leukemia stem cell marker CD34 [19]. Concurrently in the breast cancer field, the Wicha laboratory identified high ALDH activity as a marker for a subpopulation of tumor cells characterized by multipotency, self-renewal, and enhanced tumorigenicity [20]. It was a few years later that the role of ALDH was first determined in the context of head and neck cancer stem cells, where Chen and colleagues demonstrated $ALDH^{high}$ HNSCC cells displayed evidence of epithelial-mesenchymal transition (EMT) shifting, radioresistance, and high tumorigenicity as compared to $ALDH^{low}$ cells in a xenotransplanted tumorigenicity study [21]. Further, it was shown that the $ALDH^{high}$ and $CD44^{+}$ cells purified an even more tumorigenic population, with 1,000 $ALDH^{high}CD44^{+}$ cells capable of initiating more tumors *in vivo* (*i.e.* in 13 mice out of 15), as compared to 10,000 $ALDH^{low}$ $CD44^{-}$ cells (*i.e.* in 2 mice out of 15) [22]. In another study, tumors generated from $ALDH^{high}$ cells were able to be serially passaged *in vivo* while reproducing the original tumor heterogeneity, thus confirming ALDH as a highly selective marker for cancer stem cells in HNSCC [23]. Currently, ALDH activity is being

successfully used as a cancer stem cell marker in many cancers including melanoma [24], colon [25], lung [26], prostate [27], liver [28], pancreatic [29], and salivary gland cancers [30] among many others.

The increasing evidence for the use of both CD44 and ALDH as cancer stem cell markers in HNSCC led to studies in which the combined expression of both markers further enhanced the ability to isolate cancer stem cells. $ALDH^{high}CD44^{+}$ cells were confirmed to be highly tumorigenic, capable of self-renewing as orospheres, and were able to be serially passaged *in vitro* and *in vivo* while reproducing original tumor histology and heterogeneity. These studies also demonstrated that the $ALDH^{high}CD44^{+}$ subpopulation of cells localized in close proximity to blood vessels, suggesting the existence of a perivascular cancer stem cell niche in HNSCC [22]. In head and neck cancer patients, CD44 and ALDH expression/activity in tumors have been correlated with worse prognosis, disease grade, and overall survival [31-33]. The prognostic significance of ALDH and CD44 suggests that they could be perhaps considered as potential diagnostic tools for patients [34].

In addition to CD44 and ALDH, a large cohort of other potential cancer stem cell markers have been identified in HNSCC. One of these includes the transmembrane glycoprotein CD133, which has been implicated as a potential marker for cancer stem cells in HNSCC. $CD133^{+}$ cells showed a marked capacity for self-renewal and multilineage differentiation *in vitro* [35], as well as correlated with worse patient survival when co-expressed with Oct-4 and Nanog [36]. In Cisplatin-resistant HNSCC cells, increased $CD10^{+}$ expression was shown to enhance sphere formation *in vitro* and tumorigenicity *in vivo*, and may be associated with therapeutic resistance and CSC-like

properties of these tumors [37]. In yet another study, $CD166^+$ stem-like HNSCC cells were shown to be significantly related to poorer clinical outcome, as compared to the correlation of CD44 [38]. There have been a plethora of other efforts to identify CSC-specific biomarkers in HNSCC, including more functional approaches such as dye-dependent isolation [39] or measuring intracellular reactive oxygen species [40] to enrich for cancer stem cells.

1.5 CSC Functional Assays

The perfect CSC-specific marker, *i.e.* only expressed in cancer stem cells, has not been identified. This complicates the attempt to isolate absolutely pure populations of cancer stem cells and to perform CSC-targeted developmental therapeutics studies, as the majority of cancer stem cell markers are also expressed in physiological stem cells [41]. Efforts to develop CSC-specific biomarkers could also provide insight into whether these markers are only useful for identifying this subpopulation or whether they also have a functional role in modulating the cancer stem cell phenotype. Other methods that allow enrichment and investigation of cancer stem cells that are independent of CSC biomarkers include functional cancer stem cell assays, which utilize the abilities of cancer stem cells to self-renew, differentiate into other cell types, and generate new tumors.

For example, to study the stem-like phenotype *in vitro*, the orosphere assay is a method which exploits the fact that stem cells are capable of surviving and proliferating in low/no serum and anchorage-independent conditions, unlike differentiated cells [42]. Culturing cancer cells in serum-free ultra-low attachment conditions allows only cancer stem cells to survive in the form of spheres, and their passaging is an indication of self-renewal [43]. Head and neck cancer cells cultured as orospheres exhibited high

expression/activity of ALDH and CD44 [42], were more radio- and chemo-resistant, and demonstrated enhanced tumorigenic potential *in vivo* [44]. The stem-like phenotype can also be investigated *in vivo*, where FACS-sorted CSCs and non-CSCs can be transplanted into immunodeficient mice by a limiting dilution assay (LDA) and serially passaged [45]. This *in vivo* LDA is a common approach for cancer stem cell research and is used to study differences in tumorigenic potential, self-renewal, and differentiation capacity of cancer stem cells *in vivo*, with orosphere assay complementing this method *in vitro*. Most recently, cancer stem cells have been studied in 3D tumor organoids, which can recapitulate the *in vivo* architecture and functionality of the original tumor microenvironment and have been shown to enable stable culture of the cancer stem cell population [46]. This method can provide a more biologically representative *in vitro* assay to study metabolic effects of a variety of anti-cancer therapies [47].

1.6 The Cancer Stem Cell Niche

Although there are significant efforts in place to discover CSC-specific biomarkers, the ones identified so far cannot be therapeutically targeted. However, this prompts other therapeutic approaches to be attractive, such as targeting signaling pathways that are active in cancer stem cells specifically. Because physiological stem cells and cancer stem cells share many attributes, it seems reasonable that many pathways that regulate normal stem cell development and function may be hijacked by cancer cells. Similarly, this suggests that cancer stem cells depend on their immediate microenvironment for cues that regulate their self-renewal and differentiation just as normal stem cells do [48].

Stem cells are typically found in perivascular niches in close proximity to blood vessels, which enable ease of access to signaling cues and provide a dynamic and

protective microenvironment [22,49]. In this niche, stem cells can engage in crosstalk with stromal cells to maintain their self-renewal and regulate their differentiation. As with many similarities between normal stem cells and CSCs, their choice in residence bares no exception (**Fig. 1-1**). The exploration of a CSC niche was ignited in brain cancers, as existing knowledge suggested that endothelial-cell secreted factors maintain neural stem cells [50]. In fact, some of the pioneering research about the CSC niche was performed in brain tumors, where cancer stem cells in glioblastoma multiforme were shown to reside in close proximity to endothelial cells [51].

Head and neck cancer stem cells reside in the invasive fronts within the tumor in perivascular niches, where they engage in crosstalk with stromal cells, endothelial cells, cancer-associated fibroblasts, immune cells, and others [22, 52]. Other important constituents of the CSC niche are comprised by signaling molecules secreted from a variety of cells and the extracellular matrix [53]. Cancer stem cell survival depends on the tumor microenvironment and their location within perivascular niches, which also provides a protective environment [3, 22].

1.7 Cell-Cell Crosstalk

Tumors are often referred to as “wounds that do not heal”. It is reasonable to believe then, that similar cell types involved in the response to injury and wound healing may contribute to the pathobiology of a tumor. There is increasing evidence that growth and survival of cancer stem cells are highly influenced by the tumor microenvironment and molecular signaling crosstalk. An important component of solid tumors are nonepithelial stromal cells, which include vascular endothelial cells, fibroblasts, and inflammatory cells that together play a key role in tumor growth and pathobiology through

either cell-cell contact or secreted signaling effectors [54]. The stromal cell component in HNSCC tumors has also been shown to contribute to invasion and metastasis [55].

1.7.1 Endothelial Cells

The close proximity between cancer stem cells and endothelial cells of blood vessels in the perivascular niche enables their active crosstalk. It has been demonstrated that the crosstalk between CSCs and endothelial cells through endothelial cell-secreted factors enhances cancer stem cell self-renewal and survival [22, 56, 57]. One of the most potent CSC-inducing endothelial cell-secreted factors is interleukin-6 (IL-6), an important inflammatory cytokine. IL-6 specifically enhances the tumorigenic potential and self-renewal of cancer stem cells via JAK/STAT3 signaling [58, 59]. It has also been shown that the $ALDH^{+}CD44^{+}$ head and neck cancer cells express higher levels of both IL-6 co-receptors (IL-6R and gp130) than non-CSCs [59]. Other endothelial cell-secreted candidate targets have been shown to play a role in cancer stem cell maintenance [60]. Endothelial-cell secreted EGF was shown to induce epithelial to mesenchymal transition (EMT) and promote the stem-like phenotype in HNSCC cancer cells [58]. Orosphere formation and cell motility was enhanced by EGF *in vitro*, and silencing of EGF expression in co-transplanted endothelial cells decreased the fraction of cancer stem cells in tumor xenografts engineered *in vivo*. Furthermore, conditioned media from primary human endothelial cells protected head and neck cancer stem cells from anoikis [57]. Collectively, these findings suggest that endothelial-cell secreted factors within the perivascular niche maintain the cancer stem cell population and induce a more stem-like phenotype in HNSCC cells.

1.7.2 Cancer-Associated Fibroblasts

Along with other cell types of the CSC niche, cancer-associated fibroblasts (CAFs) activate pathways that play major roles in cancer cell stemness and secrete growth factors, chemokines, and extracellular matrix components involved in angiogenic recruitment of other stromal cells [61]. Given the physiological roles of fibroblasts, CAFs function as builders of the tumor microenvironment and regulators of cell differentiation, inflammation, and tumor progression. Stromal myofibroblasts were shown to activate canonical Wnt signaling in colorectal cancer stem cells. The cancer stem cells with high Wnt activity were located in close proximity to these fibroblasts. Myofibroblast-secreted factors were also capable of restoring the stem-like phenotype in more differentiated cancer cells [62]. In lung cancer stem cells, IGF1R signaling activation by CAF-secreted IGF-II was shown to be necessary to sustain cancer cell stemness [63]. In HNSCC, fibroblasts recruit cancer stem cells to supportive niches through secretion of stromal cell-derived factor-1 (SDF-1) and stimulate podia formation in cancer cells [64]. The SDF-1/CXCR4 signaling axis has been shown to play an important role in tumor metastasis in various cancers [65, 66]. Periostin secreted by CAFs has also been linked to metastasis, and in HNSCC was shown to promote the stem-like phenotype via protein tyrosine kinase 7 (PTK7)-Wnt/β-catenin signaling, as well as induce tumor initiation and invasion *in vivo* [67]. These findings signify the role of CAFs within the tumor microenvironment in supporting the CSC niche.

1.7.3 Immune Cells

One of the hallmarks of cancer is the ability of tumor cells to evade destruction by the immune system [68]. The immune system interacts with cancer cells before and after clinical detection of a tumor and engages in a process called tumor immunoediting, which

consists of three phases: elimination, equilibrium, and escape [69]. During elimination, most of the cancer cells are recognized and destroyed by the immune system. However, some cancer cells manage to escape this immunosurveillance, leading to a phase of equilibrium between tumor growth and immunological elimination. Cancer stem cells have been shown to have advantages in evading immune detection and elimination, thereby augmenting their tumorigenic ability, ultimately leading to the escape phase of tumor immunoediting [70]. In HNSCC, the T-cell inhibitory molecule PD-L1 has been shown to be preferentially expressed on CD44+ tumor-initiating cells, which suppressed T-cell mediated immunity and supported an EMT phenotype of the cancer stem cells [71, 72]. Likewise, head and neck cancer stem cells downregulate various immunogenic components and can inhibit proliferation of T-cells, regulatory T-cells, and myeloid-derived suppressor cells [73]. Immune cells can also help sustain the stem-like phenotype, as MFG-E8 and IL-6 secreted by tumor-associated macrophages has been shown to enhance cancer stem cell tumorigenicity and drug resistance [74]. Although the immune system does not primarily play a CSC-supporting role in the tumor microenvironment, it plays a crucial role in allowing cancer stem cells to overcome immunosurveillance of tumor growth. This presents another fascinating crosstalk to be investigated for sensitization towards eliminating cancer stem cells through targeted activation of host immune defenses.

1.7.4 Neural Cells

Lastly, the nervous system has been shown to have direct effects on proliferation patterns of epithelial stem cells and plays a role in various contexts of tissue development and regeneration [75]. The stimulatory role of nerves is not restricted to physiological

tissues, as denervation of primary tumors has been shown to suppress tumor growth and metastasis, suggesting a function for nerves in cancer progression [76, 77]. This denervation was linked with suppression of stem cell expansion and tumorigenesis, as well as inhibition of Wnt signaling [76]. In HNSCC, a high incidence of perineural invasion (PNI) is associated with tumor recurrence and poor survival [78], as nerves present a significant route of tumor metastasis [79]. As the nerve-tumor distance decreases in human biopsy specimens, the estimated relative death rate increases [80]. Nerves in HNSCC tumors have been shown to secrete a variety of neurotrophic factors, adhesion molecules, and chemokines that function in crosstalk with cancer cells, which also attract nerve fibers [81]. A recent study has shown that human cancer stem cells from gastric and colorectal carcinoma can differentiate into functional neurons that are involved in tumor neurogenesis and progression in tumor xenograft models [82].

We can gather from these findings investigating the CSC niche that the tumor microenvironment is highly complex, which may contribute to the functional diversity of cancer cells (**Fig. 1-1**). Although there are many players in these interactions between cancer stem cells and stromal cells, an underlying common ground can be found in the signaling pathways that are employed by the various cell types.

1.8 CSC Signaling Pathways

In addition to studying the cellular crosstalk between cancer stem cells and other cells in the tumor microenvironment, a pathway-oriented perspective can be taken to understand cancer stem cell biology. Elucidating basic molecular mechanisms can provide insight into what governs phenotypic changes within the cancer cell population that lead to the acquisition of this stem-like phenotype.

In epidemiological studies, high levels of pre-treatment serum IL-6 and tumor IL-6 receptor (IL-6R) expression correlate with poor survival of HNSCC patients and a higher rate of tumor recurrence, which propounds the use of IL-6 as a marker to predict survival and risk of recurrence in HNSCC [41, 83]. IL-6 was found to regulate head and neck cancer stem cell function and induces their self-renewal, as shown by an increase in expression of the self-renewal marker Bmi-1 [7]. There is a direct correlation between levels of IL-6 secreted by tumor-associated endothelial cells and the tumorigenicity of cancer stem cells *in vivo* [59]. Endothelial cell-secreted IL-6 enhances orosphere formation, STAT3 activation, and self-renewal of cancer stem cells *in vitro*. Activation of STAT3 plays an important role in the self-renewal and stemness of a variety of normal stem cells and cancer stem cells [84, 85]. STAT3 is constitutively phosphorylated in head and neck cancer stem cells ($ALDH^{high}CD44^{+}$), as compared to the $ALDH^{low}CD44^{-}$ population [59]. This STAT3 expression is enhanced by endothelial cell-secreted IL-6 and EGF, and its inhibition reduces the sphere-forming ability of cancer stem cells [57, 59]. In a study investigating cancer stem cell interactions with T-cell-mediated immunity, constitutive phosphorylation of STAT3 was observed in $CD44^{+}$ cells that selectively expressed PD-L1 [86]. Activation of STAT3 in head and neck cancer overall has been implicated in treatment resistance and immune escape [87].

The protein Bmi-1 is an important transcriptional repressor and component of the polycomb repressive complex 1 (PRC1). It is highly expressed in self-renewing normal stem cells [88, 89], in which it inhibits cell cycle regulators $p16^{Ink4a}$ and $p19^{Arf}$ to regulate various important stem cell functions [90, 91]. In HNSCC, Bmi-1 has been shown to be highly expressed specifically in cancer stem cells, and that this effect is enhanced by

endothelial cell-secreted factors [22]. The importance of Bmi-1 in the maintenance of cancer stem cells has also been implicated [2], as Bmi-1$^+$ head and neck cancer cells express the known cancer stem cell markers ALDH and CD44 [92]. Currently no mechanistic studies have determined the regulation of Bmi-1 in head and neck cancer stem cells, but a body of literature has demonstrated IL-6/STAT3 signaling to orchestrate epithelial-mesenchymal transition (EMT) in breast cancer through activation of Bmi-1 by transcription factor Twist [93, 94], thus conferring tumors with migratory and self-renewal abilities.

A variety of other signaling pathways have been implicated in cancer stem cell biology in head and neck cancers specifically. For example, Wnt signaling serves a vital role in normal stem cell regulation, especially during embryonic development, but also in adult tissue self-renewal and cancer [95]. In HNSCC, Wnt/β-catenin signaling was shown to be crucial in the maintenance of cancer stem cell self-renewal and tumorigenicity [96]. In these studies, β-catenin was co-expressed with ALDH and CD44 staining, suggesting that this signaling axis is primarily restricted to cancer stem cells. They demonstrated that β-catenin positively regulated sphere formation and expression of the stem cells markers Oct4 and Sox2, as well as chemoresistance to Cisplatin. Other signaling pathways that have been shown to play significant roles in head and neck cancer stem cells include the Notch and Hedgehog pathways [97, 98].

Many of these pathways regulate common downstream embryonic stem cell transcription factors that are relevant in cancer stem cell function. Octamer-binding transcription factor 4 (Oct4) regulates many genes in embryonic stem cell development and cancer, and has been linked to a less differentiated phenotype, increased tumor

aggressiveness, and resistance to radiation therapy in HNSCC [99]. Ectopic expression of Oct4 promotes the stem-like phenotype, sphere formation, invasion capacity, and xenograft tumorigenicity in head and neck cancer [100]. Nanog is another transcription factor required for the maintenance of embryonic stem cells [101], and has been recently implicated as a prognostic cancer stem cell marker in HNSCC [102]. Another major downstream signaling effector is the protein p53. One of the most frequent genomic mutations in HNSCC is within the *TP53* gene, which has been correlated with poor patient survival [103, 104]. Normally, p53 functions to repair DNA damage by either transiently arresting the cell cycle or irreversibly triggering apoptosis. In both normal and cancer stem cells, p53 is involved in mechanisms of self-renewal and differentiation [105, 106], specifically affecting stem cell expansion [107]. MDM2 functions as a major negative regulator of p53 by targeting it for proteasomal degradation and has also been shown to independently drive stemness characteristics [108, 109].

1.9 Epithelial-Mesenchymal Transition and Cell Plasticity

When discussing the acquisition of stem-like features, the physiological phenomenon of epithelial-mesenchymal transition has been strongly associated with cancer progression, endowing cancer cells with enhanced migratory characteristics and invasive ability [110]. Induction of EMT in normal epithelial cells has been shown to transform these cells into cancer stem cells capable of forming spheres *in vitro* and tumors in preclinical models of breast cancer *in vivo* [111]. In HNSCC, EGF and Snail were shown to induce EMT and maintain the cancer stem cell phenotype [57, 112]. Endothelial cell-derived IL-6 has also been shown to induce EMT, motility, and invasive capacity of head and neck cancer stem cells by creating a chemotactic gradient towards blood vessels

[41]. EMT induced by IL-6 converted non-metastatic tumors into metastatic ones *in vivo*, also through STAT3/Snail pathway activation [113].

These studies incite the idea of cancer cell plasticity and the conversion of bulk cancer cells to cancer stem cells, or vice versa. This leads to consideration of how these signaling pathways in cancer stem cell biology might influence fate decisions during cell division. Drawing another parallel to physiological tissues, the regulation of cell fate in cancer stem cells is a homeostatic balance of self-renewal and cell differentiation. This becomes apparent through one of many examples in which a pure population of sorted cancer stem cells will revert to the same percentage of CSCs versus non-CSCs prior to the sort [23]. The decision that cancer stem cells face between self-renewal and differentiation into bulk tumor cells comes down to a single cycle of mitosis. Cancer stem cell divisions can be symmetrical, creating two self-same daughter cells, or asymmetrical, creating one cancer stem cell and one differentiated cell [114]. Cues from the tumor microenvironment can affect these decision processes [85, 115]. The signaling pathways implicated in connecting cancer cell plasticity to EMT transitions have been reviewed elsewhere [12, 116]. Collectively, these findings support the roles of various signaling pathways in head and neck cancer stem cells. Many pathways share common downstream effectors, which may provide opportunities for investigating potential therapeutic targets.

1.10 Therapeutic Resistance

Head and neck squamous cell carcinoma (HNSCC) is the sixth most-common solid tumor [117]. Although multiple treatment modalities exist, including surgical resection, radiation therapy, and/or chemotherapy, they frequently are associated with unacceptably

poor patient survival and low quality of life [118]. Unfortunately, the improved control of tumor-growth achieved with platinum-based drugs correlates with an increased incidence of evasive resistance and recurrence of HNSCC [119]. Although platinum-based drugs have improved control of local disease [120], increases in incidence of resistance and metastasis have essentially nullified their benefits [121].

Evasive resistance is a process by which cancer cells acquire an invasive phenotype to escape the unfriendly tumor microenvironment generated by chemotherapy [119]. Clinical observations suggest that some tumor cells are resistant to chemotherapy and have the capability to migrate and initiate a new tumor (**Fig. 1-2**). Indeed, traditional platinum-based chemotherapy induces phenotypic changes in cancer cells, suggesting that conventional therapy causes a shift in the tumor cell population towards self-renewal [122-124]. This primes residual HNSCC cells for a more aggressive phenotype and leads to therapeutic resistance and disease progression [125]. Cancer stem cells have been shown to drive tumor initiation, therapeutic evasion and resistance, metastasis, and recurrence in HNSCC [1, 2, 57, 126]. Due to their defining characteristics of self-renewal, multipotency, and tumorigenic potential, it is not surprising that cancer stem cells are capable of reforming an entire heterogenous tumor post-treatment. Not surprisingly, many of the same pathways that sustain the cancer stem cell niche also play a role in CSC-mediated therapeutic resistance.

Cisplatin is considered the standard of care in the treatment of HNSCC patients (NCCN Practice Guidelines in Oncology-Head Neck Cancer). Similar to other cytotoxic chemotherapies and platinum-based agents, Cisplatin forms DNA crosslinks to trigger apoptosis in dividing cells. Both Cisplatin and radiotherapy target actively dividing, rapidly-

proliferating cells. Cancer stem cells have been shown to be slow-cycling cells, which may explain their resistance to conventional chemotherapeutics and radiation therapy, as both target actively dividing cells [127, 128]. Cisplatin causes a shift in the head and neck cancer cell population towards more stem-like features [7, 122, 129], but there is no well-defined mechanistic evidence demonstrating how this cancer stem cell increase occurs. Cisplatin has been shown to increase the cancer stem cell fraction and induce stem cell self-renewal in a dose-dependent manner, as determined by Bmi-1 expression [7]. When comparing Cisplatin-resistant with Cisplatin-sensitive head and neck cancer cells, the resistant cells show a marked increase in expression of stemness markers, particularly in Oct4, Nanog, and Bmi-1 [7, 122].

These findings suggest that the cancer stem cell increase post-chemotherapy is due to preferential killing of non-CSCs while simultaneously supporting symmetric division of surviving cancer stem cells (**Fig. 1-2**). Both a (1) numerator and (2) denominator effect can be responsible for this shift in balance towards cancer stem cell expansion. In (1), conventional chemotherapy may kill the bulk tumor cells, but simultaneously induce self-renewal mechanisms that support cell plasticity or symmetric division of cancer stem cells. In (2), conventional chemotherapy may kill the bulk tumor cells and decrease the total tumor volume, whereas the cancer stem cells survive and then compose a greater fraction of total cells. The evidence provided in the literature supports both of these hypotheses, with the biologically observed effect likely being due to a combination of these factors.

The crosstalk between endothelial cells and cancer stem cells has been shown to play a crucial role in HNSCC resistance to conventional chemotherapy [130-132]. The IL-

6 pathway is activated upon Cisplatin exposure [130] and potentiates the Cisplatin-induced increase in the fraction of $ALDH^{high}CD44^{+}$ and Bmi-1 expression [7]. In Cisplatin-resistant versions of HNSCC parental cell lines, IL-6 was shown to enhance their resistance to Cisplatin *in vitro*. The resistant cell lines express higher levels of Bmi-1 and pSTAT3, and have higher sphere-forming ability compared to parental cells [7]. IL-6 and MFG-E8 secreted in context of tumor-associated inflammation has also been shown to amplify anticancer drug resistance through activating both STAT3 and Hedgehog signaling [133]. A large body of literature has demonstrated that endothelial cells regulate cancer cell aggressiveness. Recently, Cao and colleagues described a mechanism by which tumor-associated endothelial cells (TECs) confer stem-like activity to indolent cancer cells [134]. They show that naïve tumor cells are converted to chemoresistant cancer stem cells through a complex feedback loop between TECs and cancer cells. Normally, insulin growth factor (IGF) binding protein-7 (IGFBP7) expressed by TECs blocks IGF1 signaling to cancer cells, thereby inhibiting their stem-like traits. However, conventional chemotherapy deregulates this balance, inhibiting IGFBP7 and elevating IGF1 in TECs, which activates a positive angiocrine cascade that promotes CSC-mediated invasiveness and progression.

In a recent publication, Jin and colleagues defined MAST1 as the main driver of Cisplatin-resistance across various human cancers [135]. They demonstrated that Cisplatin, but no other DNA-damaging agent, inhibits the MAPK pathway by dissociating cRaf from MEK1. MAST1 replaces cRaf and was shown to contribute to platinum resistance and worse clinical outcome both before and after Cisplatin induction. Additionally, the authors showed that inhibiting MAST1 with the targeted agent

Lestaurtinib restores Cisplatin sensitivity. These findings suggest that Cisplatin-resistance may be explained by the fact that platinum-based therapies directly affect major signaling pathways that are also important in cancer stem cell biology, as inactivation of MAPK has been shown to contribute to stem-like properties [136]. Other novel findings have described the wide-ranging effects of cytotoxic chemotherapy in eliciting release of tumor-derived extracellular vesicles (EVs), which have been shown to promote seeding and growth of metastatic cancer cells in distant organ sites *in vivo* [137]. These chemotherapy-induced EVs were shown to promote NF-kB-dependent activation of endothelial cells, one of the key players in the maintenance of the cancer stem cell niche.

Although therapeutic reduction in tumor size is successful at first, long-term clinical improvement is often not attained. This can be accounted for by chemoresistance of the cancer stem cell subpopulation. Growing knowledge about CSC-associated resistance mechanisms in HNSCC has demonstrated a need for treatment strategies that take into account CSC-driven tumor biology and target these cells specifically. Thus, cancer stem cells constitute an attractive target for developmental therapeutics studies in head and neck cancer.

1.11 Targeting Cancer Stem Cells

Targeting cancer stem cells is difficult, as they share many characteristics and markers with normal stem cells and exhibit high drug efflux through ATP-binding cassette transporters [138]. Currently, no HNSCC treatment strategies for patients exist that directly target cancer stem cells despite their important pathological properties and identifiable population. Notably, the goal of CSC-targeted therapy is not necessarily to

“shrink tumors.” Rather, the aim is to eliminate the fraction of tumor cells (~5%), which are therapy-resistant cancer stem cells that drive tumor recurrence and HNSCC progression. Therefore, CSC-driven tumor biology requires a combination therapy approach to expose the effects of CSC-targeted treatment on the HNSCC cell population. The increased knowledge about cancer stem cells has sparked an avid interest in developing novel therapeutic strategies that incorporate targeted ablation of cancer stem cells in anticancer treatments. Here, we highlight a select number of preclinical and clinical trials for targeting cancer stem cells in head and neck cancer (**Fig. 1-3**). As mentioned by Saygin and colleagues in a cross-cancer review of CSC-targeted clinical trials [139], the interpretation of these trials is limited by the fact that most of these studies lack a concrete stem cell readout to prove the efficacy of these therapies in eradicating cancer stem cells specifically. However, we will focus here on clinical trials with mechanistic approaches that have been validated in head and neck cancer stem cell biology.

The importance of cellular crosstalk within the perivascular niche, particularly on endothelial cell-secreted IL-6, has been discussed above. Therefore, the IL-6 pathway presents an appealing target within CSC-specific therapies. It has been shown that IL-6 defines the tumorigenic potential of head and neck cancer stem cells [59], and that inhibition of IL-6R signaling with Tocilizumab (Genentech) decreases the cancer stem cell fraction in preclinical models of different head and neck cancers *in vitro* and *in vivo* [58, 140]. The clinically relevant agent Tocilizumab (Genentech) is a humanized, monoclonal anti-IL-6R antibody and was FDA-approved for rheumatoid arthritis in 2010. An already approved agent such as Tocilizumab presents an attractive adjunct therapy, as

developing a new FDA-approved drug proves highly difficult and costly. In one study, combination therapy with Tocilizumab enhanced the antitumor effects of Cisplatin and Paclitaxel chemotherapy, and decreased VEGF expression and tumor microvessel density [140]. Inhibition of IL-6 signaling did not affect cancer cell viability, but robustly inhibited STAT3 signaling. Within the endothelial-cancer cell crosstalk, the clinical results of anti-angiogenic therapies have been attractive. However, issues arise in the fact that a decrease in tumor microvasculature leads to hypoxia, which creates a hypoxic environment that cancer stem cells thrive in [141]. This suggests that the observed decrease in the cancer stem cell fraction and enhanced antitumor effect may either be due to preferential killing of only the small cancer stem cell population, or due to blocking essential mechanisms that support cancer stem cell self-renewal, forcing these cells to lose their stem-like traits instead.

Many other signaling pathways that are implicated in head and neck cancer stem cell self-renewal have been targeted in preclinical studies. In nasopharyngeal carcinoma, both a Wnt inhibitor (Wnt-C59) and an mTor inhibitor (Rapamycin) were shown to downregulate cancer stem cell properties [142, 143]. The findings from inhibiting mTor signaling corroborated the successfully completed phase II clinical trial studying the efficacy of an mTor inhibitor (Temsirolimus) in head and neck cancer (**Fig. 1-3**). Inhibiting Bmi-1 (PCT-209) was also shown to robustly abrogate cancer stem cell function in HNSCC and colorectal cancer, and sensitized cancer stem cells to Cisplatin therapy [92, 144]. Approaches such as these are riveting, as they suggest a method for sensitizing otherwise resistant cancer stem cells to conventional chemotherapy by targeting the cancer stem cell population in addition to having a direct effect on the more differentiated

cells. Epigenetic regulations have also been shown to influence tumor behavior. The effects of a histone deacetylase inhibitor (Vorinostat) was studied in a phase II clinical trial, but was terminated due to the targeted agent showing no clinical activity (**Fig. 1-3**). This may be explained by the observation that although HDAC inhibition decreased the fraction of $ALDH^{high}CD44^{+}$ cells, it paradoxically induced epithelial to mesenchymal transition and expression of Bmi-1 [145]. This suggests that histone acetylation status may bivalently regulate different mechanisms involved in cancer stem cell biology.

Cancer stem cells play an important role in tumor progression, particularly in locoregional tumor recurrence [146]. A possible explanation for tumor recurrence might be that conventional platinum-based therapies and radiotherapy target fast-proliferating cells, but spare the quiescent cancer stem cells that can re-establish the tumor. Based on the cancer stem cell hypothesis, eliminating cancer stem cells should prevent tumor recurrence [147]. In head and neck cancer, MDM2 inhibition has been shown to activate endogenous p53 in tumors *in vivo* [148] and sensitize HNSCC tumors to chemotherapy [149]. Preclinical recurrence studies mimicking a clinical trial using adenoid cystic carcinoma (ACC) patient-derived xenograft (PDX) models have been conducted *in vivo*, where therapeutic inhibition of the MDM2-p53 interaction decreased the cancer stem cell fraction and sensitized adenoid cystic carcinoma PDX tumors to Cisplatin therapy [150]. Neoadjuvant administration of the targeted therapy followed by surgical resection of the primary tumors completely eliminated tumor recurrence with a post-surgical follow-up of over 300 days, as compared to 62.5% tumor recurrence in the control group. Ablation of cancer stem cells through MDM2-p53 inhibition was also demonstrated in mucoepidermoid carcinoma [151]. MDM2 inhibitors have been in clinical trials for the

treatment of several cancers [76, 152], and now are on the cusp of beginning a Phase I/II clinical trial in salivary gland cancers (**Fig. 1-3**).

In context of immunotherapy in head and neck cancer, most targeted therapies have focused on modulating T-cell interactions with bulk tumor cells. Although these strategies produce promising results, the same long-term problems may arise through CSC-mediated cancer progression and may require targeting cancer stem cells specifically through immunologic approaches. ALDH1A1, the most specific cancer stem cell marker in HNSCC, has been investigated as a potential CD8+ T-cell-defined tumor antigen in head and neck cancer [153, 154]. The development of an anticancer vaccine has been a promising, ongoing area of research. Antitumor immunity was achieved by vaccinating immunocompetent mice with sera from cancer stem cells of syngeneic murine tumors [155]. In a recent phase 1 clinical trial (**Fig. 1-3**), the safety and efficacy of a nasopharyngeal cancer stem cell vaccine was preliminarily proven, where the CSC-specific patient response was significantly enhanced with few side effects [156].

Novel treatment strategies involving targeting cancer stem cells are highly complex. However, it is very apparent that in comparison to other cancers, HNSCC is one of the last to follow with new paradigms. This is directly reflected in the number of past and current clinical trials of CSC-targeted therapies in head and neck tumors (**Fig. 1-3**), which are few and far between CSC-targeting clinical trials in other cancers [139]. Collectively, these studies present at least two strategies for incorporating CSC-targeted therapies into novel treatment paradigms for head and neck cancer: (A) an approach targeting crucial crosstalk between cancer stem cells and the tumor microenvironment (*i.e.*, cutting off the supportive supply), or (B) an approach targeting vital signaling

pathways in cancer stem cell maintenance (*i.e.,* using intrinsic cancer stem cell mechanisms to either eliminate or differentiate these cells). Preclinical evidence supports efficacy of both strategies in suppressing CSC-mediated tumor progression, but more clinical trials are direly necessary to determine their impact, especially in head and neck cancer.

1.12 Conclusion

The existence of heterogeneity within the cancer cell population of a tumor has become indisputable with recent advancements in tumor biology. Head and neck tumors have been demonstrated to be composed of cancer cells that exhibit significant plasticity in phenotypic characteristics, directed by cues within the tumor microenvironment. In this chapter, we have explored the biology and clinical relevance of the cancer stem cell subpopulation, which can be therapeutically targeted.

Evidence suggests that while conventional chemotherapy is effective in debulking the tumor, it does not eradicate the uniquely resistant cancer stem cells. Conversely, while using a CSC-targeted approach alone would eliminate the small fraction of cancer stem cells within the tumor, it would leave behind the bulk tumor cells that still have growth potential and are capable of repopulating the cancer stem cell niche through cell plasticity. In attempt to achieve optimal therapeutic outcomes, both cancer stem cells and tumor bulk cells need to be targeted with a combination therapy approach, which could effectively inhibit the cancer stem cell population in HNSCC and prevent disease progression. Therefore, elucidating critical processes that define the fate of head and neck cancer stem cells will inform mechanism-based therapies to prevent CSC-driven tumor growth and recurrence. Targeting pathways that play a significant role in the

maintenance of cancer stem cells could sensitize these cells to conventional therapies and result in better treatment outcomes. Strategic and innovative approaches to understand CSC-driven tumor biology will fundamentally advance and provide rationale for novel treatment paradigms, which aim to improve the survival and quality of life of patients with head and neck cancer.

1.13 Acknowledgements

We are thankful to the support received by grants R01-DE021139 and R01-DE023220 from the National Institutes of Health/National Institutes of Dental and Craniofacial Research (NIH/NIDCR).

1.14 Figures

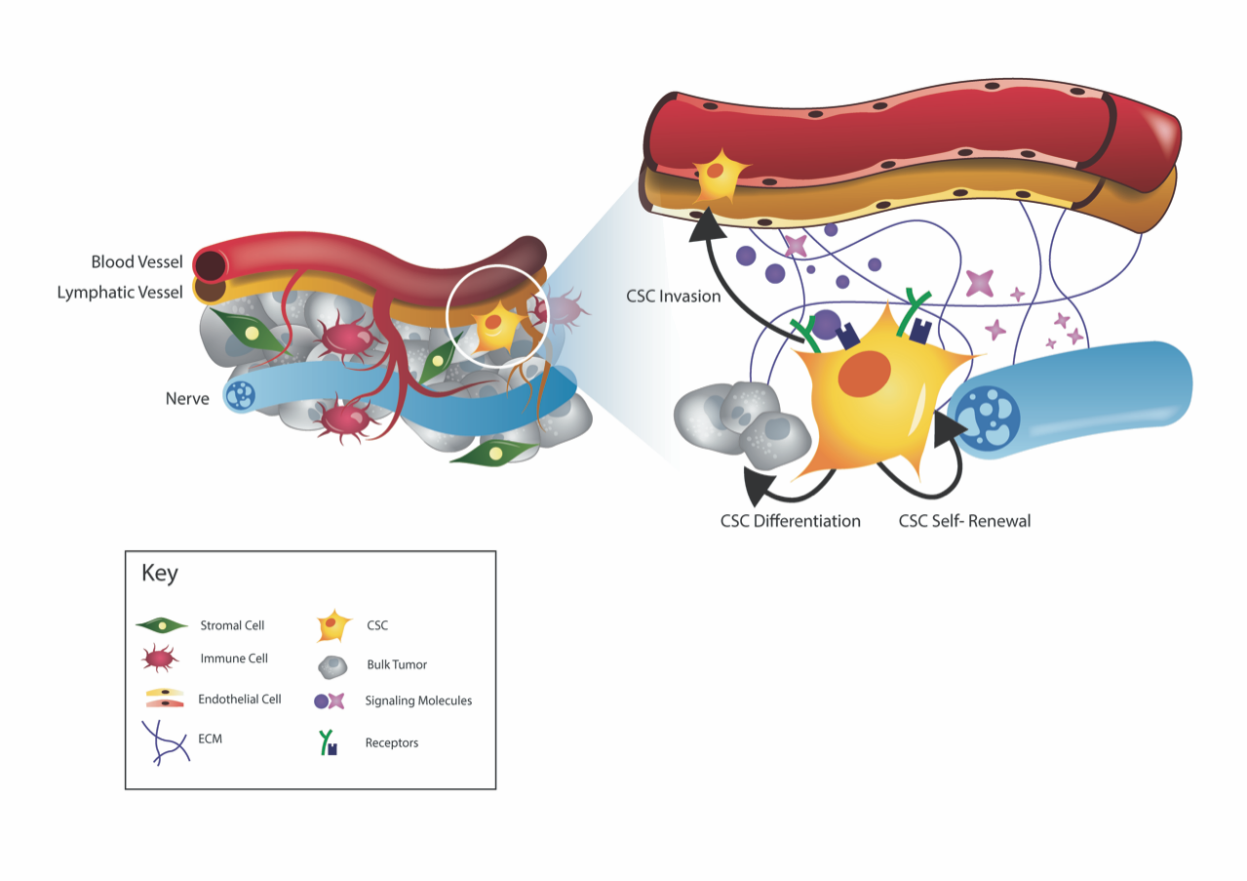

Figure 1-1: The cancer stem cell niche.

Cancer stem cells reside in a perivascular niche that serves as a protective environment and consists of multiple cell types, including endothelial cells, fibroblasts, immune cells, and nerve cells. Cellular crosstalk between cancer stem cells and stromal cells regulate cancer stem cell self-renewal, differentiation, and invasion. These processes are supported by the cancer stem cell niche and enable dissemination of cancer stem cells, ultimately leading to metastasis. Interfering with environmental cues that sustain the cancer stem cell niche may allow targeted elimination of cancer stem cells.

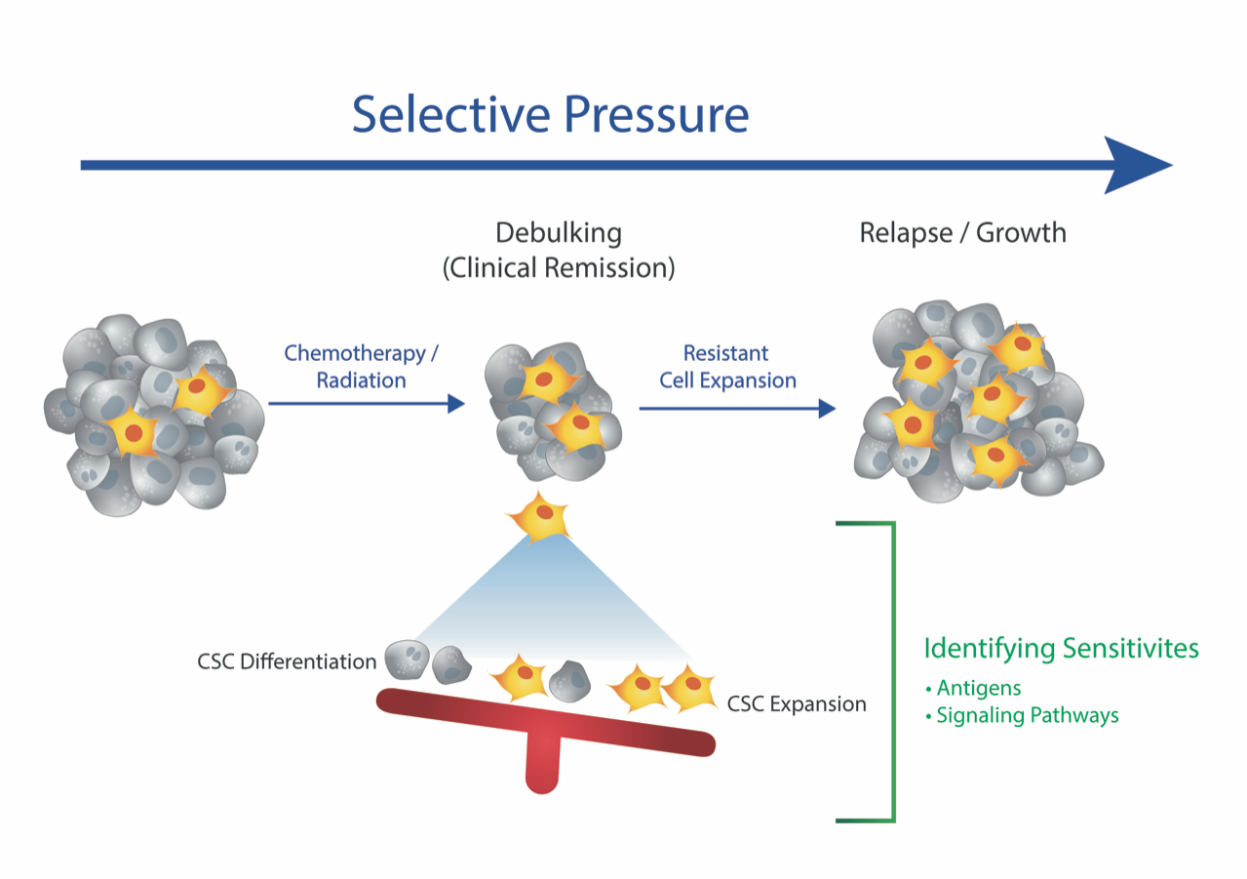

Figure 1-2: Selective pressure of conventional anticancer therapies

Conventional anticancer therapies successfully debulk tumors, leading to clinical remission. However, cancer stem cells are resistant, leading to their expansion within the tumor and acquisition of a more aggressive disease phenotype and therapeutic evasion. Cancer stem cell proliferation can occur symmetrically or asymmetrically, leading to their expansion, maintenance, or differentiation. These cell division events are regulated by signaling pathways that can be targeted therapeutically to shift the scale towards cancer stem cell differentiation, which supports their sensitization to conventional anticancer therapies.

TABLE 1

Drug class/ mechanism	Agent name	Title	Suggested patient population	Phase	Enrollment	Status	Identifier
EGFR inhibitor/ Hedgehog inhibitor	Cetuximab/IPI-926	Pilot Study of Cetuximab and the Hedgehog Inhibitor IPI-926 in Recurrent Head and Neck Cancer	Recurrent head and neck cancer	I	9	Completed	NCT01255800
Tyrosine kinase inhibitor	Sunitinib/ cetuximab	Sunitinib, Cetuximab, and Radiation Therapy in Treating Patients With Locally Advanced or Recurrent Squamous Cell Carcinoma of the Head and Neck	Head and neck squamous cell carcinoma	I	36	Terminated	NCT00906360
MDM2 Inhibitor	APG-115 +/− Carboplatin	A Phase I/II Trial of APG-115 in Patients With Salivary Gland Carcinoma	Malignant salivary gland cancer	I/II	62	Not yet recruiting	NCT03781986
Cancer stem cell vaccine	N/A	The Immunotherapy of Nasopharyngeal Cancer Using Cancer Stem Cells Vaccine	Nasopharyngeal cancer	I/II	40	Completed	NCT02115958
Histone deacetylase inhibitor/Cytotoxic chemotherapy	Vorinostat/ Capecitabine	Capecitabine and Vorinostat in Treating Patients With Recurrent and/or Metastatic Head and Neck Cancer	Recurrent and/or metastatic head and neck cancer	II	25	Terminated	NCT01267240
mTor inhibitor	Temsirolimus	Efficacy Study of Temsirolimus to Treat Head and Neck Cancer	Head and neck squamous cell carcinoma	II	42	Completed	NCT01172769
Tyrosine kinase inhibitor	Dasatinib	Dasatinib in Treating Patients With Recurrent or Metastatic Malignant Salivary Gland Tumors	Salivary gland tumors	II	55	Completed	NCT00859937
FGFR inhibitor	BGJ398	BGJ398 in Treating Patients With FGFR Positive Recurrent Head and Neck Cancer	Recurrent head and neck cancer	II	20	Recruiting	NCT02706691

Figure 1-3: Clinical trials targeting cancer stem cells in head and neck cancer.

1.15 References

[1] Reya T, Morrison SJ, Clarke MF, Weissman IL. Stem cells, cancer, and cancer stem cells. Nature. 2001 Nov 1;414(6859):105-11.

[2] Prince ME, Sivanandan R, Kaczorowski A, Wolf GT, Kaplan MJ, Dalerba P, Weissman IL, Clarke MF, Ailles LE. Identification of a subpopulation of cells with cancer stem cell properties in head and neck squamous cell carcinoma. Proc Natl Acad Sci U S A. 2007 Jan 16;104(3):973-8.

[3] Krishnamurthy S, Nör JE. Head and neck cancer stem cells. J Dent Res. 2012 Apr;91(4):334-40.

[4] Steinbichler TB, Dudás J, Skvortsov S, Ganswindt U, Riechelmann H, Skvortsova II. Therapy resistance mediated by cancer stem cells. Semin Cancer Biol. 2018 Dec;53:156-167.

[5] Vermorken JB, Mesia R, Rivera F, Remenar E, Kawecki A, Rottey S, Erfan J, Zabolotnyy D, Kienzer HR, Cupissol D, Peyrade F, Benasso M, Vynnychenko I, De Raucourt D, Bokemeyer C, Schueler A, Amellal N, Hitt R. Platinum-based chemotherapy plus cetuximab in head and neck cancer. N Engl J Med. 2008 Sep 11;359(11):1116-27.

[6] Carvalho AL, Nishimoto IN, Califano JA, Kowalski LP. Trends in incidence and prognosis for head and neck cancer in the United States: a site-specific analysis of the SEER database. Int J Cancer. 2005 May 1;114(5):806-16.

[7] Nör C, Zhang Z, Warner KA, Bernardi L, Visioli F, Helman JI, Roesler R, Nör JE. Cisplatin induces Bmi-1 and enhances the stem cell fraction in head and neck cancer. Neoplasia. 2014 Feb;16(2):137-46.

[8] Reid PA, Wilson P, Li Y, Marcu LG, Bezak E. Current understanding of cancer stem cells: Review of their radiobiology and role in head and neck cancers. Head Neck. 2017 Sep;39(9):1920-1932.

[9] Prince ME, Ailles LE. Cancer stem cells in head and neck squamous cell cancer. Journal of Clinical Oncology. 2008 Jun 10;26(17):2871-5.

[10] Shackleton M, Quintana E, Fearon ER, Morrison SJ. Heterogeneity in cancer: cancer stem cells versus clonal evolution. Cell. 2009 Sep 4;138(5):822-9.

[11] Clevers H. The cancer stem cell: premises, promises and challenges. Nat Med. 2011 Mar;17(3):313-9.

[12] Zhu Y, Luo M, Brooks M, Clouthier SG, Wicha MS. Biological and clinical significance of cancer stem cell plasticity. Clinical Transl Med 2014;3(1):32.

[13] Tao Y, Li H, Huang R, Mo D, Zeng T, Fang M, Li M. Clinicopathological and Prognostic Significance of Cancer Stem Cell Markers in Ovarian Cancer Patients: Evidence from 52 Studies. Cell Physiol Biochem. 2018;46(4):1716-26.

[14] Pece S, Tosoni D, Confalonieri S, Mazzarol G, Vecchi M, Ronzoni S, Bernard L, Viale G, Pelicci PG, Di Fiore PP. Biological and molecular heterogeneity of breast cancers correlates with their cancer stem cell content. Cell. 2010 Jan 8;140(1):62-73.

[15] Alam H, Sehgal L, Kundu ST, Dalal SN, Vaidya MM. Novel function of keratins 5 and 14 in proliferation and differentiation of stratified epithelial cells. Mol Biol Cell. 2011 Nov;22(21):4068-78.

[16] Senbanjo LT, Chellaiah MA. CD44: A Multifunctional Cell Surface Adhesion Receptor Is a Regulator of Progression and Metastasis of Cancer Cells. Front Cell Dev Biol.

2017;5:18.

[17] Mack B, Gires O. CD44s and CD44v6 expression in head and neck epithelia. PLoS One. 2008;3(10):e3360.

[18] Clark DW, Palle K. Aldehyde dehydrogenases in cancer stem cells: potential as therapeutic targets. Ann Transl Med. 2016;4(24):518.

[19] Cheung AM, Wan TS, Leung JC, Chan LY, Huang H, Kwong YL, Liang R, Leung AY. Aldehyde dehydrogenase activity in leukemic blasts defines a subgroup of acute myeloid leukemia with adverse prognosis and superior NOD/SCID engrafting potential. Leukemia. 2007 Jul;21(7):1423-30.

[20] Ginestier C, Hur MH, Charafe-Jauffret E, et al. ALDH1 is a marker of normal and malignant human mammary stem cells and a predictor of poor clinical outcome. Cell Stem Cell. 2007;1(5):555-67.

[21] Chen YC, Chen YW, Hsu HS, Tseng LM, Huang PI, Lu KH, Chen DT, Tai LK, Yung MC, Chang SC, Ku HH, Chiou SH, Lo WL. Aldehyde dehydrogenase 1 is a putative marker for cancer stem cells in head and neck squamous cancer. Biochem Biophys Res Commun. 2009 Jul 31;385(3):307-13.

[22] Krishnamurthy S, Dong Z, Vodopyanov D, Imai A, Helman JI, Prince ME, Wicha MS, Nör JE. Endothelial cell-initiated signaling promotes the survival and self-renewal of cancer stem cells. Cancer Res. 2010 Dec 1;70(23):9969-78.

[23] Clay MR, Tabor M, Owen JH, Carey TE, Bradford CR, Wolf GT, Wicha MS, Prince ME. Single-marker identification of head and neck squamous cell carcinoma cancer stem cells with aldehyde dehydrogenase. Head Neck. 2010;32(9):1195–201.

[24] Boonyaratanakornkit JB, Yue L, Strachan LR, et al. Selection of tumorigenic melanoma cells using ALDH. J Invest Dermatol. 2010;130(12):2799-808.

[25] Carpentino JE, Hynes MJ, Appelman HD, et al. Aldehyde dehydrogenase-expressing colon stem cells contribute to tumorigenesis in the transition from colitis to cancer. Cancer Res. 2009;69(20):8208-15.

[26] Jiang F, Qiu Q, Khanna A, et al. Aldehyde dehydrogenase 1 is a tumor stem cell-associated marker in lung cancer. Mol Cancer Res. 2009;7(3):330-8.

[27] Li T, Su Y, Mei Y, et al. ALDH1A1 is a marker for malignant prostate stem cells and predictor of prostate cancer patients' outcome. Lab Invest. 2009;90(2):234-44.

[28] Ma S, Chan KW, Lee TK, Tang KH, Wo JY, Zheng BJ, Guan XY. Aldehyde dehydrogenase discriminates the CD133 liver cancer stem cell populations. Mol Cancer Res. 2008 Jul;6(7):1146-53.

[29] Rasheed ZA, Yang J, Wang Q, et al. Prognostic significance of tumorigenic cells with mesenchymal features in pancreatic adenocarcinoma. J Natl Cancer Inst. 2010;102(5):340-51.

[30] Adams A, Warner K, Pearson AT, et al. ALDH/CD44 identifies uniquely tumorigenic cancer stem cells in salivary gland mucoepidermoid carcinomas. Oncotarget. 2015;6(29):26633-50.

[31] Chen J, Zhou J, Lu J, Xiong H, Shi X, Gong L. Significance of CD44 expression in head and neck cancer: A systemic review and meta-analysis. BMC Cancer. 2014 Jan 13;14:15.

[32] Kokko LL, Hurme S, Maula SM, Alanen K, Grenman R, Kinnunen I, Ventela S. Significance of site-specific prognosis of cancer stem cell marker CD44 in head

and neck squamous-cell carcinoma. Oral Oncol. 2011 Jun;47(6):510–6.

[33] Dong Y, Ochsenreither S, Cai C, Kaufmann AM, Albers AE, Qian X. Aldehyde dehydrogenase 1 isoenzyme expression as a marker of cancer stem cells correlates to histopathological features in head and neck cancer: A meta-analysis. PLoS One. 2017;12(11):e0187615.

[34] Qian X, Wagner S, Ma C, Coordes A, Gekeler J, Klussman JP, Hummel M, Kaufmann AM, Albers AE. Prognostic significanc of ALDH1A1-positive cancer stem cells in patients with locally advanced, metastasized head and neck squamous cell carcinoma. J Cancer Res Clin Oncol. 2014 Jul;140(7):1151–8.

[35] Zhou L, Wei X, Cheng L, Tian J, Jiang JJ. CD133, one of the markers of cancer stem cells in Hep-2 cell line. Laryngoscope. 2007 Mar;117(3):455-60.

[36] Chiou SH, Yu CC, Huang CY, Lin SC, Liu CJ, Tsai TH, Chou SH, Chien CS, Ku HH, Lo JF. Positive correlations of Oct-4 and Nanog in oral cancer stem-like cells and high-grade oral squamous cell carcinoma. Clin Cancer Res. 2008 Jul 1;14(13):4085-95.

[37] Fukusumi T, Ishii H, Konno M, et al. CD10 as a novel marker of therapeutic resistance and cancer stem cells in head and neck squamous cell carcinoma. Br J Cancer. 2014;111(3):506-14.

[38] Yan M, Yang X, Wang L, et al. Plasma membrane proteomics of tumor spheres identify CD166 as a novel marker for cancer stem-like cells in head and neck squamous cell carcinoma. Mol Cell Proteomics. 2013;12(11):3271-84.

[39] Song J, Chang I, Chen Z, Kang M, Wang CY. Characterization of side populations in HNSCC: highly invasive, chemoresistant and abnormal Wnt signaling. PLoS One.

2010;5(7), e11456.

[40] Chang CW, Chen YS, Chou SH, Han CL, Chen YJ, Yang CC, Huang CY, Lo JF. Distinct subpopulations of head and neck cancer cells with different levels of intracellular reactive oxygen species exhibit diverse stemness, proliferation, and chemosensitivity. Cancer Res. 2014;74(21):6291–305.

[41] Kim WT, Ryu CJ. Cancer stem cell surface markers on normal stem cells. BMB Rep. 2017;50(6):285-298.

[42] Krishnamurthy S, Nör JE. Orosphere assay: a method for propagation of head and neck cancer stem cells. Head Neck. 2013 Jul;35(7):1015-21.

[43] Dontu G, Abdallah WM, Foley JM, Jackson KW, Clarke MF, Kawamura MJ, Wicha MS. In vitro propagation and transcriptional profiling of human mammary stem/progenitor cells. Genes Dev 2003;17:1253-70.

[44] Chen SF, Chang YC, Nieh S, Liu CL, Yang CY, Lin YS. Nonadhesive culture system as a model of rapid sphere formation with cancer stem cell properties. PLoS One. 2012;7(2): e31864.

[45] O'Brien CA, Kreso A, Jamieson CH. Cancer stem cells and self-renewal. Clin Cancer Res. 2010 Jun 15;16(12):3113-20.

[46] Dutta D, Heo I, Clevers H. Disease Modeling in Stem Cell-Derived 3D Organoid Systems. Trends Mol Med. 2017 May;23(5):393-410.

[47] Shah AT, Heaster TM, Skala MC. Metabolic Imaging of Head and Neck Cancer Organoids. PLoS One. 2017 Jan 18;12(1):e0170415.

[48] Fuchs E, Tumbar T, Guasch G. Socializing with the neighbors: stem cells and their niche. Cell. 2004 Mar 19;116(6):769-78.

[49] Oh M, Nör JE. The Perivascular Niche and Self-Renewal of Stem Cells. Front Physiol. 2015 Dec 2;6:367.

[50] Jin K, Mao XO, Sun Y, Xie L, Greenberg DA. Stem cell factor stimulates neurogenesis in vitro and in vivo. J Clin Invest. 2002;110(3):311–9.

[51] Calabrese C, Poppleton H, Kocak M, Hogg TL, Fuller C, Hamner B, Oh EY, Gaber MW, Finklestein D, Allen M, Frank A, Bayazitov IT, Zakharenko SS, Gajjar A, Davidoff A, Gilbertson RJ. A perivascular niche for brain tumor stem cells. Cancer Cell. 2007;11(1):69–82.

[52] Hildebrand LC, Carvalho AL, Lauxen IS, Nör JE, Cerski CT, Sant'Ana M. Spatial distribution of cancer stem cells in head and neck squamous cell carcinomas. J Oral Pathol Med 43(7):499-506, 2014.

[53] Korkaya H, Liu S, Wicha MS. Breast cancer stem cells, cytokine networks, and the tumor microenvironment. J Clin Invest. 2011;121(10):3804–9.

[54] Kenny PA, Lee GY, Bissell MJ. Targeting the tumor microenvironment. Front Biosci. 2007 May 1;12:3468-74.

[55] Markwell SM, Weed SA. Tumor and stromal-based contributions to head and neck squamous cell carcinoma invasion. Cancers (Basel). 2015;7(1):382–406.

[56] Campos M, Neiva K, Meyers K, Krishnamurthy S, Nör JE. Endothelial derived factors inhibit anoikis of head and neck cancer stem cells. Oral Oncol 2012 Jan;48(1):26-32.

[57] Zhang Z, Dong Z, Lauxen I, Sant'Anna M, Nör JE. Endothelial cell-secreted EGF induces epithelial to mesenchymal transition and endows head and neck cancer cells with stem-like phenotype. Cancer Res 2014a;74(10):2869-2881.

[58] Kim HS, Chen YC, Nör F, Warner KA, Andrews A, Wagner VP, Zhang Z, Zhang Z, Martins MD, Pearson AT, Yoon E, Nör JE. Endothelial-derived interleukin-6 induces cancer stem cell motility by generating a chemotactic gradient towards blood vessels. Oncotarget. 2017 Nov 1;8(59):100339-100352.

[59] Krishnamurthy S, Warner KA, Dong Z, Imai A, Nör C, Ward BB, Helman JI, Taichman RS, Bellile EL, McCauley LK, Polverini PJ, Prince ME, Wicha MS, Nör JE. Endothelial interleukin-6 defines the tumorigenic potential of primary human cancer stem cells. Stem Cells. 2014 Nov;32(11):2845-57.

[60] Neiva KG, Zhang Z, Miyazawa M, Warner KA, Karl E, Nör JE. Crosstalk initiated by endothelial cells enhances migration and inhibits anoikis of squamous cell carcinoma cells through STAT3/Akt/ERK signaling. Neoplasia. 2009;11:583–93.

[61] Kalluri R, Zeisberg M. Fibroblasts in cancer. Nat Rev Cancer. 2006 May;6(5):392-401.

[62] Vermeulen L, De Sousa E Melo F, van der Heijden M, Cameron K, de Jong JH, Borovski T, Tuynman JB, Todaro M, Merz C, Rodermond H, Sprick MR, Kemper K, Richel DJ, Stassi G, Medema JP. Wnt activity defines colon cancer stem cells and is regulated by the microenvironment. Nat Cell Biol. 2010;12(5):468–76.

[63] Chen WJ, Ho CC, Chang YL, Chen HY, Lin CA, Ling TY, Yu SL, Yuan SS, Chen YJ, Lin CY, Pan SH, Chou HY, Chen YJ, Chang GC, Chu WC, Lee YM, Lee JY, Lee PJ, Li KC, Chen HW, Yang PC. Cancer-associated fibroblasts regulate the plasticity of lung cancer stemness via paracrine signaling. Nat Commun. 2014;5:3472.

[64] Faber A, Aderhold C, Goessler UR, Hoermann K, Schultz JD, Umbreit C, Walliczek

U, Stern-Straeter J. Interaction of a CD44+ head and neck squamous cell carcinoma cell line with a stromal cell-derived factor-1-expressing supportive niche: An in vitro model. Oncol Lett. 2014;7(1):82–6.

[65] Taichman RS, Cooper C, Keller ET, Pienta KJ, Taichman NS, McCauley LK. Use of the stromal cell-derived factor-1/CXCR4 pathway in prostate cancer metastasis to bone. Cancer Res. 2002 Mar 15;62(6):1832-7.

[66] Geminder H, Sagi-Assif O, Goldberg L, Meshel T, Rechavi G, Witz IP, Ben-Baruch A. A possible role for CXCR4 and its ligand, the CXC chemokine stromal cell-derived factor-1, in the development of bone marrow metastases in neuroblastoma. J Immunol. 2001;167(8):4747–57.

[67] Yu B, Wu K, Wang X, Zhang J, Wang L, Jiang Y, Zhu X, Chen W, Yan M. Periostin secreted by cancer-

associated fibroblasts promotes cancer stemness in head and neck cancer by ac tivating protein tyrosine kinase 7. Cell Death Dis. 2018 Oct 22;9(11):1082.

[68] Hanahan D, Weinberg RA. Hallmarks of cancer: the next generation. Cell. 2011 Mar 4;144(5):646-74.

[69] Dunn GP, Old LJ, Schreiber RD. The three Es of cancer immunoediting. Annu Rev Immunol. 2004;22:329-60.

[70] Sultan M, Coyle KM, Vidovic D, Thomas ML, Gujar S, Marcato P. Hide-and-seek: the interplay between cancer stem cells and the immune system. Carcinogenesis. 2017 Feb 1;38(2):107-118.

[71] Lee Y, Sunwoo J. PD-L1 is preferentially expressed on CD44+ tumor-initiating cells in head and neck squamous cell carcinoma. J Immunother Cancer. 2014; 2(Suppl

3): P270.

[72] Lee Y, Shin JH, Longmire M, Wang H, Kohrt HE, Chang HY, Sunwoo JB. CD44+ Cells in head and neck squamous cell carcinoma suppress T-cell-mediated immunity by selective constitutive and inducible expression of PD-L1. Clin Cancer Res. 2016 Jul 15;22(14):3571–81.

[73] Chikamatsu K, Takahashi G, Sakakura K, Ferrone S, Masuyama K. Immunoregulatory properties of CD44+ cancer stem-like cells in squamous cell carcinoma of the head and neck. Head Neck. 2011 Feb;33(2):208-15.

[74] Jinushi M, Chiba S, Yoshiyama H, Masutomi K, Kinoshita I, Dosaka-Akita H, Yagita H, Takaoka A, Tahara H. Tumor-associated macrophages regulate tumorigenicity and anticancer drug responses of cancer stem/initiating cells. Proc Natl Acad Sci U S A. 2011 Jul 26;108(30):12425-30.

[75] Davis EA, Zhou W, Dailey MJ. Evidence for a direct effect of the autonomic nervous system on intestinal epithelial stem cell proliferation. Physiol Rep. 2018 Jun;6(12):e13745.

[76] Zhao Y, Aguilar A, Bernard D, Wang S. Small-molecule inhibitors of the MDM2-p53 protein–protein interaction (MDM2 inhibitors) in clinical trials for cancer treatment. J Med Chem. 2015 Feb 12;58(3):1038–52.

[77] Magnon C, Hall SJ, Lin J, Xue X, Gerber L, Freedland SJ, Frenette PS. Autonomic nerve development contributes to prostate cancer progression. Science. 2013 Jul 12;341(6142):1236361.

[78] Kurtz KA, Hoffman HT, Zimmerman MB, Robinson RA. Perineural and vascular invasion in oral cavity squamous carcinoma: increased incidence on re-review of

slides and by using immunohistochemical enhancement. Arch Pathol Lab Med. 2005;129:354–359.

[79] Johnston M, Yu E, Kim J. Perineural invasion and spread in head and neck cancer. Expert Rev Anticancer Ther. 2012;12:359–371.

[80] Schmitd LB, Beesley LJ, Russo N, Bellile EL, Inglehart RC, Liu M, Romanowicz G, Wolf GT, Taylor JMG, D'Silva NJ. Redefining Perineural Invasion: Integration of Biology With Clinical Outcome. Neoplasia. 2018 Jul;20(7):657-667.

[81] Boilly B, Faulkner S, Jobling P, Hondermarck H. Nerve Dependence: From Regeneration to Cancer. Cancer Cell. 2017 Mar 13;31(3):342-354.

[82] Lu R, Fan C, Shangguan W, Liu Y, Li Y, Shang Y, Yin D1, Zhang S, Huang Q, Li X, Meng W, Xu H, Zhou Z, Hu J, Li W, Liu L, Mo X. Neurons generated from carcinoma stem cells support cancer progression. Signal Transduct Target Ther. 2017 Jan 6;2:16036.

[83] Interleukin-6 predicts recurrence and survival among head and neck cancer patients. Cancer. 2008;113:750-7.

[84] Marotta LL, Almendro V, Marusyk A, et al. The JAK2/STAT3 signaling pathway is required for growth of CD44+CD24- stem cell-like breast cancer cells in human tumors. J CLIN INVEST. 2011;121:2723–2735.

[85] Matthews JR, Sansom OJ, Clarke AR. Absolute requirement for STAT3 function in small-intestine crypt stem cell survival. CELL DEATH DIFFER. 2011;18:1934–1943.

[86] Lee G, Hall RR, 3rd, Ahmed AU. Cancer stem cells: Cellular plasticity, niche, and its clinical relevance. J Stem Cell Res Ther. 2016 Oct;6(10):363.

[87] Geiger JL, Grandis JR, Bauman JE. The STAT3 pathway as a therapeutic target in head and neck cancer: Barriers and innovations. Oral Oncol. 2016 May;56:84-92.

[88] Molofsky AV, Pardal R, Iwashita T, Park IK, Clarke MF, Morrison SJ. Bmi-1 dependence distinguishes neural stem cell self-renewal from progenitor proliferation. Nature. 2003 Oct 30;425(6961):962-7.

[89] Park IK, Qian D, Kiel M, Becker MW, Pihalja M, Weissman IL, Morrison SJ, Clarke MF. Bmi-1 is required for maintenance of adult self-renewing haematopoietic stem cells. Nature. 2003 May 15;423(6937):302-5.

[90] Jacobs JJ, Kieboom K, Marino S, DePinho RA, van Lohuizen M. The oncogene and Polycomb-group gene bmi-1 regulates cell proliferation and senescence through the ink4a locus. Nature. 1999 Jan 14;397(6715):164-8.

[91] Bmi-1 promotes neural stem cell self-renewal and neural development but not mouse growth and survival by repressing the p16Ink4a and p19Arf senescence pathways. Genes Dev. 2005 Jun 15;19(12):1432-7.

[92] Chen D, Wu M, Li Y, Chang I, Yuan Q, Ekimyan-Salvo M, Deng P, Yu B, Yu Y, Dong J, Szymanski JM, Ramadoss S, Li J, Wang CY. Targeting BMI1+ Cancer Stem Cells Overcomes Chemoresistance and Inhibits Metastases in Squamous Cell Carcinoma. Cell Stem Cell. 2017 May 4;20(5):621-634.e6.

[93] Sullivan NJ, Sasser AK, Axel AE, Vesuna F, Raman V, Ramirez N, Oberyszyn TM, Hall BM. Interleukin-6 induces an epithelial-mesenchymal transition phenotype in human breast cancer cells. Oncogene. 2009 Aug 20;28(33):2940-7.

[94] Cheng GZ, Zhang WZ, Sun M, Wang Q, Coppola D, Mansour M, Xu LM, Costanzo C, Cheng JQ, Wang LH. Twist is transcriptionally induced by activation of STAT3

and mediates STAT3 oncogenic function. J Biol Chem. 2008 May 23;283(21):14665-73.

[95] Clevers H. Wnt/β-catenin signaling in development and disease. Cell. 2006;127:469–80.

[96] Lee SH, Koo BS, Kim JM, Huang S, Rho YS, Bae WJ, Kang HJ, Kim YS, Moon JH, Lim YC. Wnt/β- catenin signaling maintains self-renewal and tumourigenicity of head and neck squamous cell carcinoma stem-like cells by activating Oct4. J Pathol. 2014;234(1):99–107.

[97] Mao L, Zhao ZL, Yu GT, Wu L, Deng WW, Li YC, Liu JF, Bu LL, Liu B, Kulkarni AB, Zhang WF, Zhang L, Sun ZJ. γ-Secretase inhibitor reduces immunosuppressive cells and enhances tumour immunity in head and neck squamous cell carcinoma. Int J Cancer. 2018 Mar 1;142(5):999-1009. doi: 10.1002/ijc.31115. Epub 2017 Nov 2.

[98] Gan GN, Eagles J, Keysar SB, Wang G, Glogowska MJ, Altunbas C, Anderson RT, Le PN, Morton JJ, Frederick B, Raben D, Wang XJ, Jimeno A. Hedgehog signaling drives radioresistance and stroma-driven tumor repopulation in head and neck squamous cancers. Cancer Res. 2014 Dec 1;74(23):7024-36.

[99] Ventelä S, Sittig E, Mannermaa L, Mäkelä JA, Kulmala J, Löyttyniemi E, Strauss L, Cárpen O, Toppari J, Grénman R, Westermarck J. CIP2A is an Oct4 target gene involved in head and neck squamous cell cancer oncogenicity and radioresistance. Oncotarget. 2015 Jan 1;6(1):144-58.

[100] Koo BS, Lee SH, Kim JM, Huang S, Kim SH, Rho YS, Bae WJ, Kang HJ, Kim YS, Moon JH, Lim YC. Oct4 is a critical regulator of stemness in head and neck

squamous carcinoma cells. Oncogene. 2015;34(18):2317–24.

[101] Mitsui K, Tokuzawa Y, Itoh H, Segawa K, Murakami M, Takahashi K, Maruyama M, Maeda M, Yamanaka S. The homeoprotein Nanog is required for maintenance of pluripotency in mouse epiblast and ES cells. Cell. 2003 May 30;113(5):631–42.

[102] Fan Z, Li M, Chen X, Wang J, Liang X, Wang H, Wang Z, Cheng B, Xia J. Prognostic Value of Cancer Stem Cell Markers in Head and Neck Squamous Cell Carcinoma: a Meta-analysis. Sci Rep. 2017 Feb 21;7:43008.

[103] Cancer Genome Atlas Network. Comprehensive genomic characterization of head and neck squamous cell carcinomas. Nature. 2015 Jan 29;517(7536):576–82.

[104] Poeta ML, Manola J, Goldwasser MA, Forastiere A, Benoit N, Califano JA, Ridge JA, Goodwin J, Kenady D, Saunders J, Westra W, Sidransky D, Koch WM. TP53 Mutations and survival in squamous-cell carcinoma of the head and neck. N Engl J Med. 2007 Dec 20;357(25):2552–61.

[105] Stiewe T. The p53 family in differentiation and tumorigenesis. Nat Rev Cancer. 2007 Mar;7(3):165–8.

[106] Verga Falzacappa MV, Ronchini C, Reavie LB, Pelicci PG. Regulation of self-renewal in normal and cancer stem cells. FEBS J. 2012 Oct;279(19):3559–72.

[107] Cicalese A, Bonizzi G, Pasi CE, Faretta M, Ronzoni S, Giulini B, Brisken C, Minucci S, Di Fiore PP, Pelicci PG. The tumor suppressor p53 regulates polarity of self-renewing divisions in mammary stem cells. Cell. 2009 Sep 18;138(6):1083–95.

[108] Kubbutat MH, Jones SN, Vousden KH. Regulation of p53 stability by MDM2. Nature. 1997 May 15;387(6630):299–303.

[109] Wienken M, Dickmanns A, Nemajerova A, Kramer D, Najafova Z, Weiss M, Karpiuk O, Kassem M, Zhang Y, Lozano G, Johnsen SA, Moll UM, Zhang X, Dobbelstein M. MDM2 Associates with Polycomb Repressor Complex 2 and Enhances Stemness Promoting Chromatin Modifications Independent of p53. Mol Cell. 2016 Jan 7;61(1):68-83.

[110] De Craene B, Berx G. Regulatory networks defining EMT during cancer initiation and progression. Nat Rev Cancer. 2013;13(2):97–110.

[111] Mani SA, Guo W, Liao MJ, Eaton EN, Ayyanan A, Zhou AY, Brooks M, Reinhard F, Zhang CC, Shipitsin M, Campbell LL, Polyak K, Brisken C, Yang J, Weinberg RA. The epithelial-mesenchymal transition generates cells with properties of stem cells. Cell. 2008;133(4):704–15.

[112] Ota I, Masui T, Kurihara M, Yook JI, Mikami S, Kimura T, Shimada K, Konishi N, Yane K, Yamanaka T, Kitahara T. Snail-induced EMT promotes cancer stem cell-like properties in head and neck cancer cells. Oncol Rep. 2016 Jan;35(1):261-6.

[113] Yadav A, Kumar B, Datta J, Teknos TN, Kumar P. IL-6 promotes head and neck tumor metastasis by inducing epithelial-mesenchymal transition via the JAK-STAT3-SNAIL signaling pathway. Mol Cancer Res. 2011;9(12):1658–67.

[114] Pearson AT, Ingram P, Bai S, O'Hayer P, Chung J, Yoon E, Jackson T, Buckanovich RJ. Sampling from single-cell observations to predict tumor cell growth *in-vitro* and *in-vivo.* Oncotarget. 2017 Dec 19; 8(67): 111176–111189.

[115] Heddleston JM, Li Z, McLendon RE, Hjelmeland AB, Rich JN. The hypoxic microenvironment maintains glioblastoma stem cells and promotes

reprogramming towards a cancer stem cell phenotype. Cell Cycle 2009 Oct 15;8(20):3274–84.

[116] Morrison SJ, Kimble J. Asymmetric and symmetric stem-cell divisions in development and cancer. Nature. 2006 Jun 29;441(7097):1068-74.

[117] Siegel R, Ma J, Zou Z, Jemal A. Cancer statistics, 2014. CA Cancer J Clin. 2014 Jan-Feb;64(1):9-29.

[118] Jemal A, Bray F, Center MM, Ferlay J, Ward E, Forman D. Global cancer statistics. CA Cancer J Clin. 2011;61:69–90.

[119] Bergers G, Hanahan D. Modes of resistance to anti-angiogenic therapy. Nat Rev Cancer. 2008 Aug;8(8):592-603.

[120] Forastiere AA. Chemotherapy in the treatment of locally advanced head and neck cancer. J Surg Oncol. 2008;97:701-7.

[121] Seiwert TY, Salama JK, Vokes EE. The chemoradiation paradigm in head and neck cancer. Nat Clin Pract Oncol. 2007 Mar;4(3):156-71.

[122] Tsai LL, Yu CC, Chang YC, Yu CH, Chou MY. Markedly increased Oct4 and Nanog expression correlates with cisplatin resistance in oral squamous cell carcinoma. J Oral Pathol Med. 2011 Sep;40(8):621-8.

[123] Goldman A, Majumder B, Dhawan A, Ravi S, Goldman D, Kohandel M, Majumder PK, Sengupta S. Temporally sequenced anticancer drugs overcome adaptive resistance by targeting a vulnerable chemotherapy-induced phenotypic transition. Nat Commun. 2015 Feb 11;6:6139.

[124] Sharma SV, Lee DY, Li B, Quinlan MP, Takahashi F, Maheswaran S, McDermott U, Azizian N, Zou L, Fischbach MA, Wong KK, Brandstetter K, Wittner

B, Ramaswamy S, Classon M, Settleman J. A chromatin-mediated reversible drug-tolerant state in cancer cell subpopulations. Cell. 2010 Apr 2;141(1):69-80.

[125] Davis SJ, Divi V, Owen JH, Bradford CR, Carey TE, Papagerakis S, Prince ME. Metastatic potential of cancer stem cells in head and neck squamous cell carcinoma. Arch Otolaryngol Head Neck Surg. 2010 Dec;136(12):1260-6.

[126] Chinn SB, Darr OA, Owen JH, Bellile E, McHugh JB, Spector ME, Papagerakis SM, Chepeha DB, Bradford CR, Carey TE, Prince ME. Cancer stem cells: mediators of tumorigenesis and metastasis in head and neck squamous cell carcinoma. Head Neck. 2015 Mar;37(3):317-26.

[127] Chang JC. Cancer stem cells: Role in tumor growth, recurrence, metastasis, and treatment resistance. Medicine (Baltimore). 2016 Sep;95(1 Suppl 1):S20-5.

[128] Chaffer CL, Weinberg RA. A perspective on cancer cell metastasis. Science 2011;331(6024):1559-64.

[129] McDermott SC, Rodriguez-Ramirez C, McDermott SP, Wicha MS, Nör JE. FGFR signaling regulates resistance of head and neck cancer stem cells to cisplatin. Oncotarget. 2018 May 18;9(38):25148-25165.

[130] Eyler CE, Rich JN. Survival of the fittest: cancer stem cells in therapeutic resistance and angiogenesis. J Clin Oncol. 2008;26:2839-45.

[131] Li Z, Bao S, Wu Q, Wang H, Eyler C, Sathornsumetee S, Shi Q, Cao Y, Lathia J, McLendon RE, Hjelmeland AB, Rich JN. Hypoxia-inducible factors regulate tumorigenic capacity of glioma stem cells. Cancer Cell. 2009;15:501-13.

[132] Gilbert LA, Hemann MT. DNA damage-mediated induction of a chemoresistant

niche. Cell. 2010; 29;143(3):355-66.

[133] Jinushi M, Chiba S, Yoshiyama H, Masutomi K, Kinoshita I, Dosaka-Akita H, Yagita H, Takaoka A, Tahara H. Tumor-associated macrophages regulate tumorigenicity and anticancer drug responses of cancer stem/initiating cells. Proc Natl Acad Sci U S A. 2011 Jul 26;108(30):12425-30.

[134] Cao Z, Scandura JM, Inghirami GG, Shido K, Ding BS, Rafii S. Molecular Checkpoint Decisions Made by Subverted Vascular Niche Transform Indolent Tumor Cells into Chemoresistant Cancer Stem Cells. Cancer Cell. 2017 Jan 9;31(1):110-126.

[135] Jin L, Chun J, Pan C, Li D, Lin R, Alesi GN, Wang X, Kang HB, Song L, Wang D, Zhang G, Fan J, Boggon TJ, Zhou L, Kowalski J, Qu CK, Steuer CE, Chen GZ, Saba NF, Boise LH, Owonikoko TK, Khuri FR, Magliocca KR, Shin DM, Lonial S, Kang S. MAST1 Drives Cisplatin Resistance in Human Cancers by Rewiring cRaf-Independent MEK Activation. Cancer Cell. 2018 Aug 13;34(2):315-330.e7.

[136] Fang Y, Wang J, Wang G, Zhou C, Wang P, Zhao S, Zhao S, Huang S, Su W, Jiang P, Chang A, Xiang R, Sun P. Inactivation of p38 MAPK contributes to stem cell-like properties of non-small cell lung cancer. Oncotarget. 2017 Apr 18; 8(16): 26702–26717.

[137] Keklikoglou I, Cianciaruso C, Güç E, Squadrito ML, Spring LM, Tazzyman S, Lambein L, Poissonnier A, Ferraro GB, Baer C, Cassará A, Guichard A, Iruela-Arispe ML, Lewis CE, Coussens LM, Bardia A, Jain RK, Pollard JW, De Palma M. Chemotherapy elicits pro-metastatic extracellular vesicles in breast cancer models. Nat Cell Biol. 2018 Dec 31. [Epub ahead of print]

[138] Zhou S, Schuetz JD, Bunting KD, Colapietro AM, Sampath J, Morris JJ, Lagutina I, Grosveld GC, Osawa M, Nakauchi H, Sorrentino BP. The ABC transporter Bcrp1/ABCG2 is expressed in a wide variety of stem cells and is a molecular determinant of the side-population phenotype. Nat Med. 2001;7:1028–1034.

[139] Saygin C, Matei D, Majeti R, Reizes O, Lathia JD. Targeting Cancer Stemness in the Clinic: From Hype to Hope. Cell Stem Cell. 2019 Jan 3;24(1):25-40.

[140] Mochizuki D, Adams A, Warner KA, Zhang Z, Pearson AT, Misawa K, McLean SA, Wolf GT, Nör JE. Anti-tumor effect of inhibition of IL-6 signaling in mucoepidermoid carcinoma. Oncotarget. 2015 Sep 8;6(26):22822-35.

[141] Schöning JP, Monteiro M, Gu W. Drug resistance and cancer stem cells: the shared but distinct roles of hypoxia-inducible factors HIF1α and HIF2α. Clin Exp Pharmacol Physiol. 2017 Feb;44(2):153-161.

[142] Cheng Y, Phoon YP, Jin X, Chong SY, Ip JC, Wong BW, Lung ML. Wnt-C59 arrests stemness and suppresses growth of nasopharyngeal carcinoma in mice by inhibiting the Wnt pathway in the tumor microenvironment. Oncotarget. 2015 Jun 10;6(16):14428-39.

[143] Yang C, Zhang Y, Zhang Y, Zhang Z, Peng J, Li Z, Han L, You Q, Chen X, Rao X, Zhu Y, Liao Z. Downregulation of cancer stem cell properties via mTOR signaling pathway inhibition by rapamycin in nasopharyngeal carcinoma. Int J Oncol. 2015 Sep;47(3):909-17.

[144] Kreso A, van Galen P, Pedley NM, Lima-Fernandes E, Frelin C, Davis T, Cao L, Baiazitov R, Du W, Sydorenko N, Moon YC, Gibson L, Wang Y, Leung C, Iscove NN, Arrowsmith CH, Szentgyorgyi E, Gallinger S, Dick JE, O'Brien CA.

Self-renewal as a therapeutic target in human colorectal cancer. Nat Med. 2014 Jan;20(1):29-36.

[145] Giudice FS, Pinto Jr DS, Nör JE, Squarize CH, Castilho RM. Inhibition of histone deacetylase impacts cancer stem cells and induces epithelialmesenchyme transition of head and neck cancer. PLoS One. 2013;8(3):e58672.

[146] Islam F, Gopalan V, Smith RA, Lam AK. Translational potential of cancer stem cells: A review of the detection of cancer stem cells and their roles in cancer recurrence and cancer treatment. Exp Cell Res. 2015 Jul 1;335(1):135-47.

[147] Schatton T, Frank NY, Frank MH. Identification and targeting of cancer stem cells. Bioessays. 2009;31(10):1038-49.

[148] Warner KA, Nör F, Acasigua GA, Martins MD, Zhang Z, McLean SA, Spector ME, Chepeha DB, Helman J, Wick MJ, Moskaluk CA, Castilho RM, Pearson AT, Wang S, Nör JE. Targeting MDM2 for Treatment of Adenoid Cystic Carcinoma. Clin Cancer Res. 2016;22(14):3550-9.

[149] Roh JL, Kang SK, Minn I, Califano JA, Sidransky D, Koch WM. p53-Reactivating small molecules induce apoptosis and enhance chemotherapeutic cytotoxicity in head and neck squamous cell carcinoma. Oral Oncol. 2011 Jan;47(1):8–15.

[150] Nör F, Warner KA, Zhang Z, Acasigua GA, Pearson AT, Kerk SA, Helman JI, Sant'Ana Filho M, Wang S, Nör JE. Therapeutic Inhibition of the MDM2-p53 Interaction Prevents Recurrence of Adenoid Cystic Carcinomas. Clin Cancer Res. 2017 Feb 15;23(4):1036-1048.

[151] Andrews A, Warner K, Rodriguez-Ramirez C, Pearson AT, Nör F, Zhang Z, Kerk S, Kulkarni A, Helman JI, Brenner JC, Wicha MS, Wang S, Nör JE. Ablation of Cancer

Stem Cells by Therapeutic Inhibition of the MDM2-p53 Interaction in Mucoepidermoid Carcinoma. Clin Cancer Res. 2018 Nov 29. [Epub ahead of print].

[152] de Jonge M, de Weger VA, Dickson MA, Langenberg M, Le Cesne A, Wagner AJ, Hsu K, Zheng W, Mace S, Tuffal G, Thomas K, Schellens JH. A phase I study of SAR405838, a novel human double minute 2 (HDM2) antagonist, in patients with solid tumours. Eur J Cancer. 2017 May;76:144–51.

[153] Visus C, Ito D, Amoscato A, Maciejewska-Franczak M, Abdelsalem A, Dhir R, Shin DM, Donnenberg VS, Whiteside TL, DeLeo AB. Identification of human aldehyde dehydrogenase 1 family member A1 as a novel CD8+ T-cell-defined tumor antigen in squamous cell carcinoma of the head and neck. Cancer Res. 2007 Nov 1;67(21):10538-45.

[154] Visus C, Wang Y, Lozano-Leon A, Ferris RL, Silver S, Szczepanski MJ, Brand RE, Ferrone CR, Whiteside TL, Ferrone S, DeLeo AB, Wang X. Targeting ALDHbright human carcinoma-initiating cells with ALDH1A1-specific CD8+ T cells. Clin Cancer Res. 2011 Oct 1;17(19):6174–84.

[155] Ning N, Pan Q, Zheng F, Teitz-Tennenbaum S, Egenti M, Yet J, Li M, Ginestier C, Wicha MS, Moyer JS, Prince ME, Xu Y, Zhang XL, Huang S, Chang AE, Li Q. Cancer stem cell vaccination confers significant antitumor immunity. Cancer Res. 2012;72(7):1853–64.

[156] Lin M, Yuan Y, Xu J, Cai X, Liu S, Niu L, Chen J, Li Q, Xu K. Safety and efficacy study of nasopharyngeal cancer stem cell vaccine. Immunol Lett. 2015;165(1):26–31.

CHAPTER 2:
The IL-6R and Bmi-1 Axis Controls Self-Renewal and Chemoresistance of Head and Neck Cancer Stem Cells[2]

2.1 Abstract

Despite major progress in elucidating the pathobiology of head and neck squamous cell carcinoma (HNSCC), the high frequency of disease relapse correlates with unacceptably deficient patient survival. We previously showed that cancer stem-like cells (CSC) drive tumorigenesis and progression of HNSCC. While CSCs constitute only 2-5% of total tumor cells, CSCs contribute to tumor progression by virtue of their high tumorigenic potential and their resistance to chemo-, radio- and immunotherapy. Not only are CSCs resistant to therapy, but cytotoxic agents actually enhance cancer stemness by activating transcription of pluripotency factors and by inducing expression of Bmi-1, a master regulator of stem cell self-renewal. We hypothesized therapeutic inhibition of Interleukin-6 receptor (IL-6R) suppresses Bmi-1 to overcome intrinsic chemoresistance of CSCs. We observed that high Bmi-1 expression correlates with decreased (p=0.04) recurrence-free survival time in HNSCC patients (n=216). Blockade of IL-6R by lentiviral knockdown or pharmacologic inhibition with a humanized monoclonal antibody (Tocilizumab) is sufficient to inhibit Bmi-1 expression, secondary sphere formation, and

[2] This chapter was originally published in *Cell Death & Disease*. Herzog AE, Warner KA, Zhang Z, Bellile E, Bhagat M, Castilho R, Wolf GT, Polverini PJ, Pearson AT, Nör JE. The IL-6R and Bmi-1 axis controls self-renewal and chemoresistance of head and neck cancer stem cells. *Cell Death Dis*. 2021 Oct 23;12(11):988.

to decrease the CSC fraction even in Cisplatin-resistant HNSCC cells. IL-6R inhibition with Tocilizumab abrogates Cisplatin-mediated increase in CSC fraction and induction of Bmi-1 in patient-derived xenograft (PDX) models of HNSCC. Notably, Tocilizumab inhibits Bmi-1 and suppresses growth of xenograft tumors generated with Cisplatin-resistant HNSCC cells. Altogether, these studies demonstrate that therapeutic blockade of IL-6R suppresses Bmi-1 function and inhibits cancer stemness. These results suggest therapeutic inhibition of IL-6R might be a viable strategy to overcome the CSC-mediated chemoresistance typically observed in HNSCC patients.

Significance: This work unveiled the impact of IL-6R/Bmi-1 signaling to CSC-mediated chemoresistance of HNSCC, and informed a new mechanism-based therapy that might improve survival and health standard of head and neck cancer patients.

2.2 Introduction

Head and Neck Squamous Cell Carcinoma (HNSCC) is the sixth most common solid tumor experiencing around 55,000 newly diagnosed cases every year in the U.S. (1). Treatment modalities for advanced HNSCC include surgical resection, radiation and chemotherapy, or chemotherapy alone, which commonly correlate with increased patient morbidity and disease relapse (2). Platinum-based agents persist as standard of care in chemotherapeutic treatment of HNSCC, of which Cisplatin is the most commonly used. Despite their well-recognized survival benefit through refined control of tumor growth, treatment with platinum-based chemotherapeutics is frequently associated with development of evasive resistance leading to tumor progression (3). In HNSCC, locoregional recurrence accounts for 20-40% of the 5-year patient mortality rate (4),

making it imperative that a treatment strategy that is more consistently effective be investigated. This is particularly true in HPV-negative HNSCC patients, as HPV-negative disease exhibits worse prognosis and higher recurrence rates when compared to HPV-positive disease (5). Improved comprehension of the pathobiology of HNSCC will enable establishing novel mechanism-based strategies to ameliorate the survival and health standard of HNSCC patients.

The cancer stem cell hypothesis proposes key malignant features of neoplastic cells originate from acquisition of stem-like features (6). Cancer stem-like cells (CSC) encompass a unique cellular subpopulation characterized by multipotency, uniquely high tumorigenic potential, and self-renewal. CSC in HNSCC are identified by high activity of aldehyde dehydrogenase (ALDH) and high expression of the surface glycoprotein CD44 (7-10). These cells drive tumor initiation, tumor progression and, ultimately, therapeutic evasion in HNSCC (7,11,12). Thus, targeted therapeutic ablation of cancer stem-like cells might benefit head and neck cancer patients.

Traditional cytotoxic chemotherapy is known to instigate phenotypic changes in cancer cells (13) by causing a shift towards self-renewal in the tumorigenic CSC population, priming a more aggressive phenotype in residual tumor cells that leads to tumor recurrence or metastatic spread (14,15). Cisplatin increases the head and neck CSC fraction and induces expression of Bmi-1, a master regulator of stem cell self-renewal (16). Clinical observations suggest that chemoresistant tumor cells possess the capacity to initiate a new tumor, resulting in either locoregional recurrence or metastasis (17). It has been recently demonstrated that Bmi-1^{+} cancer stem cells mediate chemoresistance and metastasis in HNSCC (18). In HNSCC, Cisplatin-resistant cancer

cells display a distinct increase in expression of Bmi-1 among other stemness markers, as opposed to Cisplatin-sensitive cancer cells (13,16). Recent work evaluating immunotherapy resistance in HNSCC have also found CSC to be a relevant immune-oncology target (19-21).

The molecular crosstalk within the tumor microenvironment has been shown to assume a crucial part in maintaining the CSC pool and mediating HNSCC resistance to conventional chemotherapy (22,23). It has been previously shown that interleukin-6 (IL-6) secreted from endothelial cells within the perivascular niche enhances CSC survival, self-renewal, and tumorigenic potential (24,25). Cisplatin exposure activates the interleukin-6 (IL-6) pathway (26), which potentiates the Cisplatin-induction of the CSC fraction and Bmi-1 expression (16). We have shown that $ALDH^{high}CD44^{high}$ head and neck CSCs display elevated levels of the IL-6 receptors (IL-6R) than non-CSC (24). Notably, high levels of tumor IL-6 receptor (IL-6R) and serum IL-6 expression are strongly correlated with poor survival of patients with HNSCC (25,27).

Here, we used Tocilizumab (Genentech), a humanized monoclonal anti-IL-6R antibody approved by the FDA since 2010 for rheumatoid arthritis as a prototypic inhibitor of the IL-6R signaling pathway. We demonstrated that therapeutic blockade of IL-6R inhibits Bmi-1 function, suppresses Cisplatin-induced CSC self-renewal and tumor growth. In summary, these data suggest that therapeutic inhibition of IL-6R might be a viable strategy to overcome CSC-mediated chemoresistance in head and neck cancer.

2.3 Results

2.3.1 IL-6/Bmi-1 signaling axis regulates cancer cell self-renewal and correlates with recurrence-free survival of HNSCC patients.

To perceive the clinical significance of Bmi-1 function in HNSCC patients, a tissue microarray of human HNSCC tumors (n=216) was independently evaluated for Bmi-1 staining by two trained oral pathologists blind for patient outcome. Immunostaining for Bmi-1 was almost exclusively nuclear, varying from mild to intense and primarily associated with nuclear chromatin, resulting in a granular-like pattern (**Fig. 2-1A**). Bmi-1 expression formed a gradient towards high intensity in the basal epithelial layer, where stem cells reside in normal oral epithelium. Bmi-1 expression clearly correlated with shorter recurrence-free survival (p=0.04) (**Fig. 2-1B**). No association was found between Bmi-1 expression and gender (p=0.30), age (p=0.82), tobacco use (p=0.96), or clinical stage (p=0.92), propounding that Bmi-1 may be cogitated an impartial identifier of tumor recurrence. High levels of pre-treatment tumor IL-6 receptor (IL-6R) and serum IL-6 expression have been shown to correlate with a higher rate of tumor recurrence and reduced survival of HNSCC patients, which emphasizes the relevance of inhibiting this signaling pathway to mitigate the risk of recurrence in HNSCC (25,27). To assess the role of the IL-6R signaling pathway in maintaining the CSC population and self-renewal, we used lentiviral short hairpin RNA (shRNA) constructs to knockdown IL-6R protein levels in the UM-SCC-1, UM-SCC-22A, and UM-SCC-22B cells. Western blots revealed that IL-6R knockdown was sufficient to inhibit STAT3 phosphorylation and Bmi-1 expression (**Fig. 2-1C**). We have shown that CSCs exhibit constitutive phosphorylation of STAT3 and expression of Bmi-1 (24). To determine whether IL-6R knockdown affects expression of these signaling factors in CSC, we used the orosphere assay to functionally enrich cell cultures for CSCs (28). We observed that IL-6R knockdown also inhibited STAT3 phosphorylation and Bmi-1 expression in CSC-enriched orospheres (**Fig. 2-1D**).

Moreover, IL-6R knockdown decreased the orosphere-forming ability of all HNSCC cell lines evaluated by reducing both number and size of spheres, as compared to cells transduced with shRNA-control constructs (**Fig. 2-1E and F**, Supplementary Fig. 2-7A). Lastly, to determine the effect of IL-6R knockdown on the CSC fraction directly, flow cytometry analysis showed a decrease in $ALDH^{high}CD44^{high}$ cells (**Fig. 2-1G**, Supplementary Fig. 2-7B). These data underline the importance of IL-6R signaling in maintaining the phenotype and self-renewal of head and neck CSCs.

2.3.2 Therapeutic inhibition of IL-6R abrogates Cisplatin-induced cancer stemness in vivo.

Conforming to the cancer stem cell hypothesis, therapeutic eradication of CSCs prevents tumor progression and therapeutic resistance (6). As shown above and in previous publications (24,25), the IL-6 pathway is a particularly attractive target for CSC-specific therapy. To determine the outcome of combination therapy with Cisplatin and IL-6R inhibitor Tocilizumab on the CSC fraction, we utilized HNSCC patient-derived xenograft (PDX) mouse models characterized by our laboratory (31). When tumors grew to an average of approximately 450 mm^3 (Supplementary Fig. 2-8A and B), we began weekly treatment with Cisplatin and/or Tocilizumab for two weeks (**Fig. 2-2A**).

To evaluate the consequence of this treatment on the CSC fraction of PDX tumors *in vivo*, we conducted flow cytometry for ALDH activity and CD44 expression (**Fig. 2-2B and C**). Consistent with previously published findings (16), we observed here that Cisplatin is sufficient to increase the CSC fraction in HNSCC (**Fig. 2-2B**). Importantly, Tocilizumab decreased the CSC fraction and abrogated Cisplatin-induction of CSC fraction in both PDX models. These results corroborate similar findings *in vitro,* where

Tocilizumab suppressed Cisplatin-induction of the CSC fraction in UM-SCC-1, -22A, and -22B cell lines (**Fig. 2-2D**). Although the principal objective of this short-term experiment was to determine the treatment effect on tumor CSC fraction, we also observed significant suppression of tumor growth by Cisplatin and combination therapy, as compared to the untreated group (**Fig. 2-2E and F**). Tocilizumab alone suppressed tumor growth only in the UM-PDX-HNSCC-15 model. Notably, these data illustrate that although Cisplatin alone is effective in decreasing tumor growth, a combination therapy approach with Tocilizumab is required to decrease tumor CSC fraction (**Fig. 2-2A**). Likewise, a CSC-targeted therapy only targets a relatively small fraction of cancer cells and, therefore, may not inhibit tumor growth alone. Separately, we assessed the effect of this treatment strategy on long-term tumor regrowth using a scaffold xenograft model with UM-SCC-22B cells, because the PDX models exhibit much more rapid tumor growth that precludes their use for such an experiment. Here, Cisplatin chemotherapy was stopped after completion of the two-week primary treatment, while maintenance injections of Tocilizumab were continuously administered weekly (Supplementary Fig. 2-8). We observed a delay in tumor regrowth in the groups that received Tocilizumab (Supplementary Fig. 2-8D and E). Western blots of representative PDX tumor lysates showed that Tocilizumab inhibited Bmi-1 expression *in vivo*, even in presence of Cisplatin (**Fig. 2-2G**). These findings support the flow cytometry data and demonstrate that Tocilizumab inhibits Cisplatin-induced cancer stemness.

2.3.3 Tocilizumab suppresses Cisplatin-induction of CSC-associated signaling pathways.

To begin elucidating the mechanisms underlying the anti-CSC effect of therapeutic blockade of IL-6R, we examined the impact of the IL-6 pathway on downstream signaling effectors in three different HNSCC cell lines. Cells were exposed to recombinant human IL-6, Tocilizumab and/or Cisplatin (**Fig. 2-3A**). In a separate, analogous set of experiments, we exposed cells to rhIL-6 after treatment with Cisplatin and/or Tocilizumab to determine whether this inhibition is robust to excess activation of the IL-6 signaling pathway (**Fig. 2-3B**). We observed that rhIL-6 induced STAT3 phosphorylation as well as Bmi-1 expression (**Fig. 2-3A and B**). Similarly, Cisplatin activated STAT3 and Bmi-1 expression, which was enhanced by rhIL-6, but did not significantly affect expression of IL-6 co-receptors. Tocilizumab suppressed expression of IL-6 co-receptors, STAT3 activation, and Bmi-1, even in presence of excess rhIL-6 stimulus. To determine the effect of Tocilizumab in CSC versus bulk tumor cells, we sorted cells for subsequent Western blot analyses. Bmi-1 and IL-6R are both preferentially expressed in CSC, and Tocilizumab was shown to abrogate Cisplatin-induction of these proteins in both CSC as well as bulk tumor cells (**Fig. 2-3C**).

To determine whether the anti-stemness effect of Tocilizumab was specific to Bmi-1 or also affected other stemness pathways, we used a stem cell protein array. Combination therapy with Tocilizumab/Cisplatin decreased expression of several pluripotent stem cell markers as compared to controls (**Fig. 2-3D,** Supplementary Fig. 2-9B), suggesting that this therapeutic strategy may broadly suppress stemness phenotypes in HNSCC. To verify these results, we analyzed protein expression of Oct4 and Nanog via western blot, as these traditional stem cell markers have been implied in the maintenance of head and neck CSC (32,33). Interestingly, while IL-6 and Cisplatin

both induced expression of Oct4 and Nanog, Tocilizumab suppressed more effectively expression of these two regulators of stemness when used in combination with Cisplatin than when Tocilizumab was used alone (**Fig. 2-3E**).

To determine whether the change in cancer stem cell fraction occurs due to a numerator or a denominator effect, we used immunocytochemistry to evaluate ALDH1 and Bmi-1 expression on a single cell basis (**Fig. 2-3F**, Supplementary Fig. 2-9A). Interestingly, Cisplatin induced an overall shift in ALDH1 fluorescence, with a small subpopulation of cells expressing very high levels of ALDH1 (**Fig. 2-3G**). Cisplatin did not appear to induce an overall shift in Bmi-1 fluorescence, but also sharply increased its expression in a small proportion of cells (**Fig. 2-3H**). Tocilizumab and the combination therapy resulted in an overall suppression of ALDH1 and Bmi-1. Overall, these data suggest that IL-6R signaling regulates HNSCC stemness and that combination therapy with Cisplatin and Tocilizumab prevents acquisition of the stem-like phenotype within HNSCC cells observed upon single-agent Cisplatin exposure.

2.3.4 Tocilizumab inhibits STAT3 signaling and self-renewal of HNSCC cells.

To evaluate the consequence of Tocilizumab on inhibiting CSC stemness and self-renewal, we engaged the orosphere assay. Utilizing the orosphere assay enables functional measurement of stemness and self-renewal of CSCs in ultra-low attachment conditions (28). While primary orospheres serve as a read-out of cancer cell stemness, serial passaging of these cultures into secondary orospheres allows assessment of their self-renewal ability. We also sought to understand Bmi-1 and ALDH expression patterns within orospheres. It is known that CSC initiate orosphere formation, and orospheres express overall higher levels of ALDH, IL6-R, and Bmi-1 than cells under normal

attachment conditions (28,29,30). We found that within both small and large spheres, only a subset of cells expresses high levels of ALDH and Bmi-1. Interestingly, not all ALDH-expressing cells also express Bmi-1 and vice versa, which may suggest a self-renewing subpopulation of CSC (**Fig. 2-4A**). These findings mimic the heterogeneity of ALDH and Bmi-1 expression within a tumor.

Cisplatin treatment increased the number (**Fig. 2-4B**) and size (**Fig. 2-4C**) of primary orospheres, as well as enhanced their growth over time (Supplementary Fig. 2-10A and B), which is consistent with Cisplatin-induced increase in the CSC fraction (**Fig. 2-2A and B)**. In contrast, treatment with Tocilizumab suppressed orosphere formation, significantly decreasing both size and number of orospheres (**Fig. 2-4B and C)**. The combination therapy had a similar effect to Tocilizumab alone but was more effective in decreasing sphere number formed by UM-SCC-1 cells. Tocilizumab alone or in combination with Cisplatin also suppressed the Cisplatin-induction of the number and size of secondary orospheres (**Fig. 2-4D and E**). While Cisplatin alone did not further increase the size of secondary orospheres (Supplementary Fig. 2-10C), combination therapy nearly eliminated secondary orosphere formation (**Fig. 2-4D**). Notably, Tocilizumab suppresses the dose-dependent induction of Bmi-1 by Cisplatin (Supplementary Fig. 2-10D to 2-10F).

To validate our findings of protein expression changes presented in Figure 2-3A **and B**, we next sought to determine whether Tocilizumab inhibits STAT3 activation and Bmi-1 expression in the orospheres. Orosphere protein lysates showed via western blot analysis that Cisplatin induces STAT3 activation within the spheres and that Tocilizumab suppresses this activation even in presence of Cisplatin (**Fig. 2-4F**). As in Figure 2-3A

and B, Tocilizumab decreased expression of both IL-6 co-receptors. Interestingly, Cisplatin further induced Bmi-1 expression within orospheres from UM-SCC-1 cells but did not further increase Bmi-1 within UM-SCC-22A and UM-SCC-22B spheres. Tocilizumab fully suppressed Bmi-1 expression in orospheres, even in presence of Cisplatin (**Fig. 2-4F**). These findings further support IL-6 signaling as pivotal regulator of cancer stem cell self-renewal and overcoming Cisplatin-induction of CSC function.

2.3.5 Therapeutic inhibition of IL-6R decreases self-renewal and CSC fraction in Cisplatin-resistant HNSCC cells.

Clinical and laboratory observations suggest a subset of tumor cells are chemoresistant and acquire a migratory behavior, ultimately giving rise to the process of evasive resistance (34). CSC cells are known to be critical mediators of therapeutic evasion and resistance (6,7,12), suggesting that targeted elimination of this cellular subpopulation is necessary to prevent disease recurrence. To determine the efficacy of IL-6R inhibition as an avenue to conquer Cisplatin resistance, we used Cisplatin-resistant variants of the UM-SCC-1, -22A, and -22B cell lines that were generated in our lab (16). These variants were named Cis1, Cis4, Cis6, Cis12, each being resistant to the corresponding concentration of Cisplatin (μM). The naïve parent cells are here referred to as Cis0. First, we examined the CSC fraction in the Cisplatin-resistant variants as compared to the naïve parent cells (**Fig. 2-5A**; Supplementary Fig. 2-11A). The Cisplatin-resistant HNSCC cells showed a dose-dependent increase in the $ALDH^{high}CD44^{high}$ CSC fraction (**Fig. 2-5A**) as compared to the parent cell lines, likewise activation of STAT3 signaling and expression of Bmi-1 (**Fig. 2-5B**). This observation supports previously published findings of increases in CSC fraction and stemness markers in Cisplatin-resistant cells (13,16). Next, we

evaluated whether IL-6R inhibition with Tocilizumab could decrease Bmi-1 expression of Cisplatin-resistant cells. Cells were treated as in previous experiments with either rhIL-6, Cisplatin, with and without Tocilizumab. We observed that in all three Cisplatin-resistant HNSCC cell line sets, as well as each corresponding resistant variant, Tocilizumab suppressed Bmi-1 expression, even in the presence of Cisplatin treatment (**Fig. 2-5C**). Interestingly, treatment with Cisplatin further induced expression of Bmi-1 as compared to untreated cell line variants with lower Cisplatin resistance. However, Cisplatin did not further enhance Bmi-1 expression in the Cis12 cell lines, potentially indicating a saturated level of resistance (**Fig. 2-5C**). To address the efficacy of Tocilizumab in the inhibition of CSC self-renewal, the orosphere assay was employed (**Fig. 2-5D,** Supplementary Fig. 2-12A). Cisplatin increased orosphere formation in naïve HNSCC cells. In the Cisplatin-resistant variants, Cisplatin treatment either increased or did not further induce sphere-forming ability. However, Tocilizumab reduced the number and size of orospheres in all cell lines, both alone and in combination with Cisplatin (**Fig. 2-5E**, Supplementary Fig. 2-12B). Of note, the combination therapy was found to have a synergistic effect on decreasing sphere formation in all cell lines (Supplementary Fig. 2-12C).

2.3.6 Tocilizumab suppresses growth and Bmi-1 expression of Cisplatin-resistant xenografts.

To examine whether *in vitro* findings translate into *in vivo* results, we seeded UM-SCC-22B naïve and UM-SCC-22BCis6 resistant cells in biodegradable scaffolds embedded in SCID mice. We chose the UM-SCC-22BCis6 variant, because these cells had the highest level of Cisplatin resistance while not exhibiting inhibition of cell proliferation (data not shown). When tumors reached an average of 250 mm^3 (Supplementary Fig. 2-13G), we

began weekly treatment with Cisplatin and/or Tocilizumab for up to 8 weeks (**Fig. 2-6A**). Histological analyses suggested that UM-SCC-22BCis6-resistant tumors were histologically less differentiated and more vascularized, when compared to UM-SCC-22B-naïve tumors (**Fig. 2-6B**).

Treatment with Tocilizumab with or without Cisplatin slowed down tumor growth in both UM-SCC-22B and UM-SCC-22BCis6 xenograft tumors (**Fig. 2-6C and D**) and extended time to tumor volume doubling (**Fig. 2-6E**). In the resistant tumor model, Cisplatin was less effective in inhibiting tumor growth (**Fig. 2-6C and D**). In UM-SCC-22B-naïve tumors, Cisplatin suppressed tumor growth more potently during earlier doses and was later observed to lose efficacy in inhibiting tumor growth. The combination therapy approach was most effective in both xenograft models. Western blot analyses of tumor tissue lysates showed that Cisplatin induced Bmi-1 expression in UM-SCC-22B-naïve tumors (**Fig. 2-6F**). After treatment with Tocilizumab, both STAT3 and Bmi-1 expression were inhibited in UM-SCC-22B tumors (**Fig. 2-6G,** Supplementary Fig. 2-13A to 2-13F). These data support our findings from our experiments using PDX models shown above (**Fig. 2-2F**). Notably, Tocilizumab also inhibited Bmi-1 expression in the Cis6 resistant variants, with or without concurrent Cisplatin treatment (**Fig. 2-6H**). However, Tocilizumab did not affect total STAT3 expression in these tumors. These data showed that therapeutic IL-6R inhibition with Tocilizumab might be an effective strategy to inhibit self-renewal and overcome Cisplatin resistance in HNSCC.

2.4 Discussion

Platinum-based chemotherapy constitute core components within the treatment standard for advanced HNSCC. However, the high recurrence rate and poor overall survival

demand the development of a more effective therapeutic strategy. Evidence indicates that while tumors are effectively debulked by conventional therapies, the distinctively resistant cancer stem cells are not eradicated. In fact, platinum-based agents and cytotoxic chemotherapies have been demonstrated to increase the CSC fraction in tumors (13,14,35). However, using only a CSC-targeted approach as a novel treatment strategy would result in remnant bulk tumor cells with residual growth potential. In an attempt to achieve optimal therapeutic outcomes, the CSC hypothesis explains that a combination therapy approach is required to target both CSC and bulk tumor cells, which could effectively prevent disease progression. Our data illustrates this effect in that Tocilizumab alone successfully decreases self-renewal within tumors, but is not as potent in reducing tumor growth as in combination with Cisplatin.

Targeting signaling conduits that compose critical roles in the maintenance of CSC might sensitize them to standard platinum-based chemotherapy and provide better treatment outcomes. Our lab has extensively described the role of endothelial cell-secreted IL-6 inside the perivascular niche in supporting the maintenance of the CSC pool and their invasive properties (24,25). Our results further our previous observations that IL-6 augments Cisplatin-induced cancer cell stemness, implicating Cisplatin and IL-6R signaling as mediators of phenotypic changes in HNSCC tumors that result in enhanced stemness (16). Here, we showcase a pioneering potential therapeutic strategy to suppress these adverse effects of Cisplatin treatment that result in an increase in CSC. We have shown here that IL-6R inhibition using Tocilizumab can resolutely overcome CSC induction by Cisplatin and suppress the growth of Cisplatin-resistant tumors.

Further, we showed that both genetic and pharmacologic inhibition of IL-6R signaling could suppress Cisplatin-mediated induction of the CSC fraction, Bmi-1 expression, and self-renewal of HNSCC cells. Interestingly, we observe that IL-6R inhibition decreases expression of IL-6R and downstream STAT3 signaling, which has recently also been shown in another study (36). This might be explained by either internalization of the receptor via endocytosis and subsequent degradation, or by its shedding to increase levels of soluble IL-6R (37). Collectively, our data advocate that IL-6R signaling plays an essential role in resistance to Cisplatin that is frequently observed in patients with HNSCC. This observation, together with the fact that developing and obtaining FDA approval for a new drug proves highly difficult and costly, unveils the re-purposing of Tocilizumab as a highly attractive adjunct therapy with Cisplatin in a novel treatment strategy for HNSCC.

Although combination therapy is effective in decreasing cancer stemness, it is unclear which underlying processes drive this biologically observed effect. Comparable to other platinum-based agents, Cisplatin targets actively dividing, rapidly proliferating cells and triggers apoptosis. CSC resistance to conventional chemotherapeutics may be explicated by the fact that these cells are known to be slow cycling. Previous findings show that Cisplatin promotes CSC self-renewal, as deduced by Bmi-1 expression, and that Cisplatin-resistant cells express elevated levels of stemness markers (13,16), suggesting that the post-chemotherapy increase in CSC results from preferential eradication of non-CSC, while simultaneously promoting self-renewal of surviving CSC. Likewise, the synergy of the combination therapy observed in many of the data presented here could be explained similarly. As Tocilizumab has been shown to preferentially target

CSC (25), while Cisplatin targets bulk tumor cells, requiring a combination therapy approach to most effectively target the entire cancer cell population. Our data demonstrate that IL-6R inhibition can potently suppress Cisplatin induction of Bmi-1, even in Cisplatin-resistant cell line variants. Interestingly, others have shown that Bmi-1^{+} CSC represent only a subset of ALDH^{high}CD44^{high} CSC that might be responsible for therapeutic resistance and tumor recurrence (18). These observations underline the importance of elucidating the signaling mechanisms governing CSC self-renewal and stemness and provide a potential mechanism by which CSC can be re-programmed and re-sensitized to conventional chemotherapies. Further investigation of mechanisms mediating this shift in the CSC fraction may explore the role of IL-6R signaling in CSC plasticity, as well as CSC symmetric *versus* asymmetric cell division fates.

Bmi-1 is a principal controller of stem cell self-renewal (38-41). IL-6/STAT3 signaling has been revealed to choreograph epithelial-mesenchymal transition through activation of Bmi-1, a process known to confer tumors with self-renewal and migratory abilities (42,43). Bmi-1 is uniquely expressed in head and neck CSC (as opposed to bulk tumor cells), and we showed that this effect is enhanced by IL-6 signaling (24). It has been recently shown that direct inhibition of Bmi-1 abrogates CSC function and sensitizes cells to Cisplatin therapy in HNSCC (18). Here, we present data in support of the function of the IL-6R pathway in the modulation of Bmi-1 expression in HNSCC. Through both genetic and pharmacologic approaches, we demonstrated a compelling link between IL-6R signaling and Bmi-1 expression. The clinical importance of Bmi-1 in HNSCC was demonstrated through retrospective analysis of 216 patient samples that displayed a correlation among Bmi-1 levels and clinical outcomes. Interestingly, we found that Bmi-1

expression significantly correlated with recurrence-free patient survival time, which can be clarified by the CSC hypothesis. While the small CSC fraction within a tumor may not noticeably contribute to overall tumor growth, it is resistant to radiation and conventional chemotherapy and promotes tumor recurrence. Using Bmi-1 as a putative prognostic marker may enable risk assessment for recurrence in patients with HNSCC.

Collectively, these data provide preclinical evidence for an innovative mechanism-based treatment strategy that is based on targeted ablation of CSC with Tocilizumab in combination with Cisplatin to debulk the tumor. This new combination therapy has the potential to improve the survival and standard of health for head and neck squamous cell carcinoma patients.

2.5 Materials and Methods

2.5.1 Cisplatin-resistant cell lines and cell culture

Human HNSCC cell lines UM-SCC-1, UM-SCC-22A, and UM-SCC-22B (from T. Carey, University of Michigan) cultured in Dulbecco's modified Eagle medium (DMEM, Invitrogen) with 10% FBS (Atlanta Biologicals), 1% L-Glutamine (Gibco), and 1% Antibiotic-Antimycotic (Gibco). The cell lines' origin, confirmation of identity, and authentication by STR profiling are described elsewhere (44) and tested negative for mycoplasma (Mycoplasma Detection Kit, Invitrogen). Cisplatin-resistant cell line variants were produced from UM-SCC-1, UM-SCC-22A, and UM-SCC-22B cells, as described previously (16,45). Four Cisplatin-resistant variants were generated for each parent cell line, for example: UM-SCC-1Cis1 (UM-SCC-1 resistant to 1 μM Cisplatin), UM-SCC-1Cis4 (UM-SCC-1 resistant to 4 μM Cisplatin), UM-SCC-1Cis6 (UM-SCC-1 resistant to 6 μM Cisplatin), UM-SCC-1Cis12 (UM-SCC-1 resistant to 12 μM Cisplatin). Cisplatin

treatment was removed the passage before experiments being performed, waiting at least two days until cells were utilized for experiments.

2.5.2 HNSCC Patient-Derived Xenograft (PDX) Mouse Model

HNSCC tumor fragments were implanted into the dorsal subcutaneous space of immunodeficient mice (CB17 SCID, Charles River), as previously described and characterized (31). Once tumors grew to an average volume of 450 mm^3, mice were randomly assigned to treatment groups (*n*= 5-8, due to reduced tumor-take reliability in PDX models): 5 mg/kg Cisplatin; 10 mg/kg Tocilizumab; 10 mg/kg Tocilizumab + 5 mg/kg Cisplatin; or no treatment. Treatment was administered weekly intraperitoneally for two weeks. Mice were euthanized, and tumors retrieved two days after the end of treatment. Tumor measurements were taken 2-3 times per week, and volumes were calculated via the equation $V=length*width^2/2$. Notably, PDX tumors of *in vivo* passage five or below were used in this manuscript. All procedures and treatments were conducted under protocols reviewed and approved by UCUCA.

2.5.3 HNSCC subcutaneous scaffold xenograft mouse model

HNSCC subcutaneous xenograft tumors were generated as previously described (46) without the inclusion of HDMEC cells. Briefly, 1 x 10^5 tumor cells (UM-SCC-22B, UM-SCC-22BCis6) were seeded with a cell growth media and Matrigel (Corning) mixture in poly-(L)-lactic acid biodegradable scaffoldings and subsequently implanted into the dorsal subcutaneous space of SCID mice (CB17, Charles River). For long-term treatments, mice were randomly assigned to treatment groups and dosages as described above once tumors reached an average volume of 250 mm^3 (n=6).

2.5.4 Flow cytometry

Tumors were resected from mice, dissociated by collagenase and hyaluronidase (Stem Cell Technologies), incubated in ACK red blood cell lysis buffer (Invitrogen), and filtered through a sterile 40-μm cell strainer. ALDH enzymatic activity was stained using Aldefluor Kit (Stem Cell Technologies) or AldeRed ALDH Detection Assay (EMD Millipore). Briefly, $1x10^6$ cells were incubated with activated ALDH substrate or the equivalent volume of ALDH inhibitor diethyl aminobenzaldehyde (DEAB). DEAB controls were included for all treatment conditions. Cells were rinsed with PBS and stained for CD44 with either CD44-PE or CD44-APC (R&D Systems) for 15 minutes at 4°C. Human cells were identified by anti-HLA-ABC (P.E., BD Pharmingen). Viable cells were stained with DAPI (Molecular Probes). For cell sorting, $ALDH^{high}CD44^{high}$ CSC population was sorted against the combined bulk tumor cells ($ALDH^{high}CD44^{low}$, $ALDH^{low}CD44^{high}$, $ALDH^{low}CD44^{low}$). All flow cytometry analysis was conducted in a BD LSRFortessa flow cytometer (B.D. Biosciences). Results were analyzed with FlowJo software (LLC) in triplicate per condition.

2.5.5 Orosphere assay

HNSCC cells were grown in ultra-low attachment (ULA) culture ware (Corning) as previously described (28). 12,000 cells/well were passed through a single-cell strainer and seeded in 6-well ULA plates. 24 hours later, cells were treated with 1 μM Cisplatin and/or 0.1 μM Tocilizumab. Primary orospheres were fed by adding media held constant at the final treatment concentration and dissociated on day 10 with Accutase (StemCell Technologies), passed through a sterile single-cell strainer, and re-plated at the same cell density to generate secondary orospheres. Secondary orospheres were not further

treated and again cultured for 10 days. Orospheres were stated as non-adherent spheres containing ≥ 25 cells, as observed at high power magnification. Results are representative of at minimum two independent experiments, all performed in triplicate experimental conditions. Coefficient of drug interaction (CDI) was calculated as follows to analyze the effect of the combination therapy: CDI=AB/(AxB). AB represents the ratio of the combination therapy to control, whereas A or B represent the ratio of the individual treatments to control. CDI<1 specifies synergism (for CDI <0.7 significantly synergistic effect), CDI=1 specifies an additive effect, and CDI>1 specifies antagonism.

2.5.6 Pluripotent stem cell array

The proteome profiler human pluripotent stem cell array kit (R&D Systems) was used to evaluate expression of stem cell markers. Briefly, UM-SCC-1, UM-SCC-22A, and UM-SCC-22B cells were plated, serum-starved overnight, and treated with 0-1 μM Cisplatin and/or 0-0.1 μM Tocilizumab for 24 hours. Lysates were extracted and incubated with the antibody-spotted array following manufacturer's instructions. Biotinylated detection antibodies and streptavidin-HRP reagents enabled subsequent signal detection by chemiluminescence. The stem cell array was exposed on film and relative integrated densities of each dot were quantified using ImageJ software.

2.5.7 IL-6R gene silencing

HEK293T cells were used to produce lentiviral particles by co-transfecting packaging vectors pMD2.G and psPAX2 with either shRNA-control or shRNA-IL6R constructs on a pGIPZ backbone (University of Michigan Vector Core) using the calcium phosphate method. The supernatant was collected, and UM-SCC cells were infected

overnight with the supernatant in the presence of 4 μg/ml polybrene (Sigma-Aldrich). Successfully infected cells were selected with 1 μg/ml puromycin (Invivogen).

2.5.8 Western blot

Cells were plated, serum-starved overnight, and treated with 0-1 μM Cisplatin and/or 0.1 μM Tocilizumab. Alternatively, cells were pre-incubated with 0.1 μM Tocilizumab for 1 hour and then treated with 1 μM Cisplatin and/or 0-20 ng/ml rhIL-6 for 30 min or 24 hours. HNSCC cells and tumor tissues were lysed in NP-40 lysis buffer and loaded onto 9% SDS-PAGE gels. Membranes were blocked with 5% nonfat milk in TBST, then incubated with the following primary antibodies overnight at 4°C: p-STAT3, STAT3, Bmi-1, gp130, OCT4, Nanog (Cell Signaling), GAPDH (Chemicon), IL6Rα (Santa Cruz). Secondary anti-mouse or anti-rabbit antibodies conjugated with HRP (Jackson Laboratories) were used, and proteins were visualized by SuperSignal West Pico chemiluminescent substrate (Thermo Scientific).

2.5.9 Histological staining and analyses

Formalin-fixed, paraffin-embedded tissue sections were deparaffinized with xylene and rehydrated with graded ethanol. Orospheres were cryosectioned, and OCT compound was removed using PBS. HNSCC cells were plated in 4-well chamber slides, incubated overnight, and treated as described above. Chamber slide cultures were fixed in 10% buffered formalin. For immunohistochemical and immunofluorescence analyses, antigen retrieval was performed in citrate buffer (Thermo Fisher Scientific) using a decloaking chamber following the manufacturer's instructions (Biocare Medical). Sections were incubated with 0.1% Triton X-100 (Fisher Scientific), followed by 3% hydrogen

peroxide (Fisher Scientific), and Background Sniper (Biocare Medical). Orosphere sections were not incubated in hydrogen peroxide. Sections were exposed to primary antibodies at 4˚C overnight: anti-human ALDH1 (1:200; Abcam, Rabbit), anti-human CD44 (1:800; Cell Signaling, Mouse), anti-human Bmi-1 (1:200; Cell Signaling, Rabbit). For immunoperoxidase staining, sections were incubated with MACH3 probe and MACH3 HRP polymer (Biocare Medical), and then DAB until the desired staining was reached. Sections were counterstained with hematoxylin (Vector Laboratories). For immunofluorescence, specimens were incubated in secondary antibodies labeled with either mouse or rabbit Alexafluor 488 or 594 (Invitrogen). Specimens were mounted in Vectashield mounting medium for fluorescence with DAPI (Vector Laboratories). Fluorescence intensity was measured in randomly selected fields (at least 4 in triplicate experimental conditions) using ImageJ and analyzed in GraphPad Prism. Images were captured with a Nikon Eclipse E800 fluorescence microscope or a Nikon confocal microscope.

2.5.10 Statistical Analysis

Statistical analysis was achieved using GraphPad Prism. One-way ANOVA followed by appropriate post hoc tests (Tukey test) was used to analyze comparisons between two or more groups. Two-tailed student's t-test followed by appropriate post-hoc tests (Mann-Whitney U) was used to compare two groups. Kaplan-Meier graphs were evaluated using the Gehan Breslow-Wilcoxon test. Statistical significance was defined at $p<0.05$ throughout the manuscript. Intensity scores for individual TMA cores were averaged within patients across multiple cores and pathologists. Comparisons between levels of a clinical factor were tested for significance by nonparametric Kruskal-Wallis test.

Univariate and multivariable Cox regression models (adjusted for age, clinical stage, disease site, comorbidities, HPV status, and smoking) tested association with overall patient survival (O.S.) and recurrence-free time (RFT). For an illustration of adjusted analysis, adjusted survivor functions for intensity tertiles were plotted from the multivariable model. Statistical analysis of TMA data was performed in SAS v9.4.

2.6 Acknowledgements

We thank Dr. Thomas Carey for generously providing us with the UM-SCC-1, UM-SCC-22A, and UM-SCC-22B cell lines. We express our gratitude to the patients who donated tumor specimens to create the patient-derived xenograft (PDX) models and cell lines required for this research. We thank the surgeons and support staff from the University of Michigan Head and Neck SPORE, who enabled the tumor specimen collection used for the construction of the TMA used here. We thank the University of Michigan Flow Cytometry and Histology cores for their aid with experimental design, protocol troubleshooting, and data handling. All schematic diagrams were created with BioRender.com.

2.7 Figures

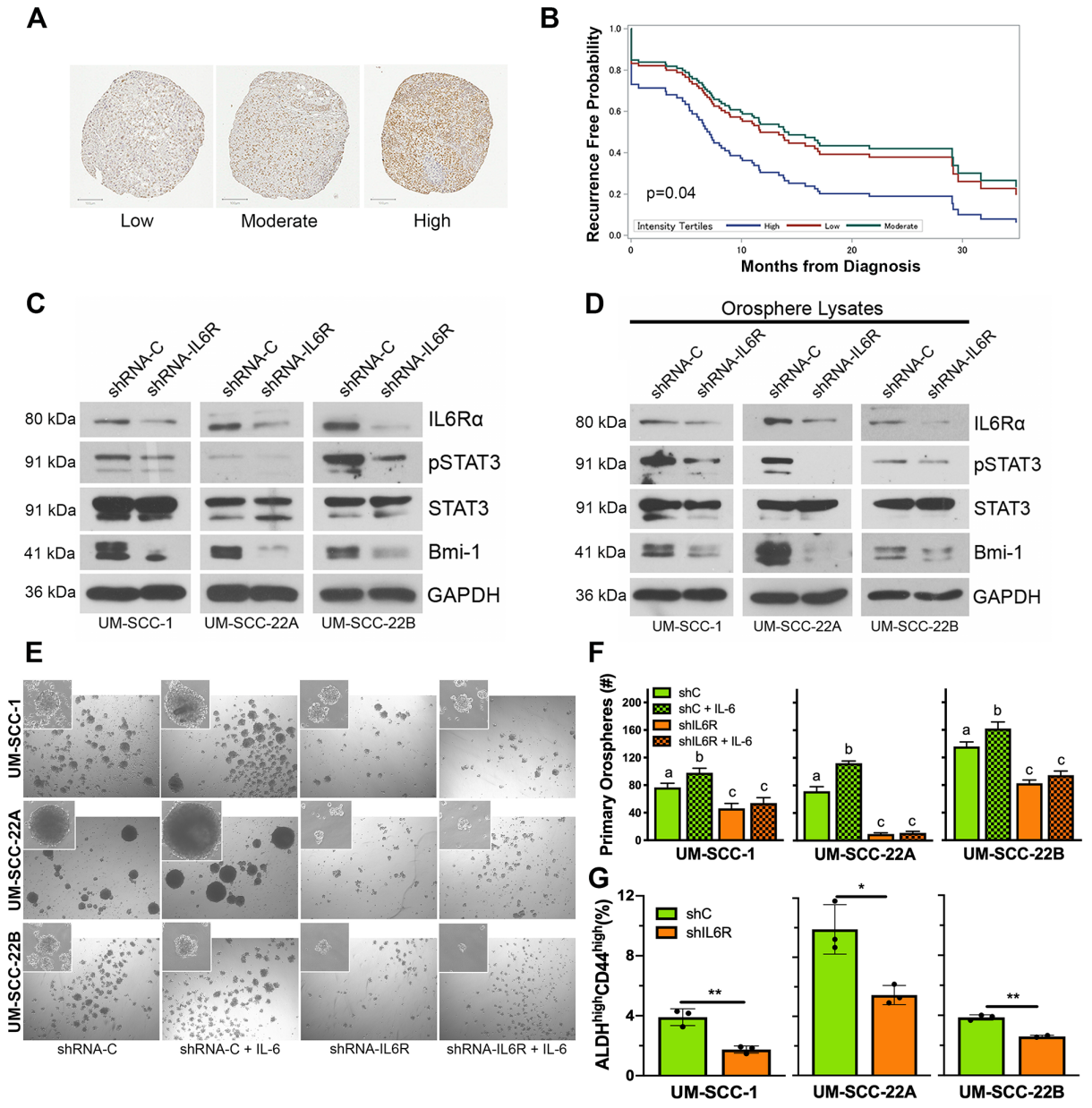

Figure 2-1: IL-6/Bmi-1 signaling axis regulates cancer cell self-renewal and correlates with recurrence-free survival of HNSCC patients.

(A) Immunohistochemistry staining Bmi-1 in human HNSCC tumor cores of the tissue microarray. Images representative of staining patterns in Bmi-1-low (left), Bmi-1-moderate (middle) and Bmi-1-high (right) specimens. **(B)** Graph depicting adjusted recurrence free survival functions over time in tumors with Bmi-1 expression separated into intensity tertiles. **(C)** Western blots showing baseline protein levels in IL-6R knockdown and control cells. **(D)** Western blots showing baseline protein levels in lysates isolated from primary orospheres formed by IL-6R knockdown and control cells. **(E)** Representative images (40x) of primary orospheres on day 8 formed by IL-6R

knockdown and control cells. Cells were treated with 20 ng/ml rhIL-6 the day after plating in ULA sphere conditions. Inserts at 100x magnification. Pictures acquired of 5 fields per well in three wells per treatment group. **(F)** Quantification depicting number of primary orospheres per well. Three wells were counted per treatment group. Bar graphs display mean ± S.D. (n=3) and significance denoted by letters at $p \leq 0.05$. **(G)** Flow cytometry graphs depicting the CSC fraction ($ALDH^{high}CD44^{high}$ cells) in IL-6R knockdown and control cells. Bar graphs display mean ± S.D. (n=3). Asterisks depict $p<0.05$ (*) or $p<0.01$ (**) as determined by t-test.

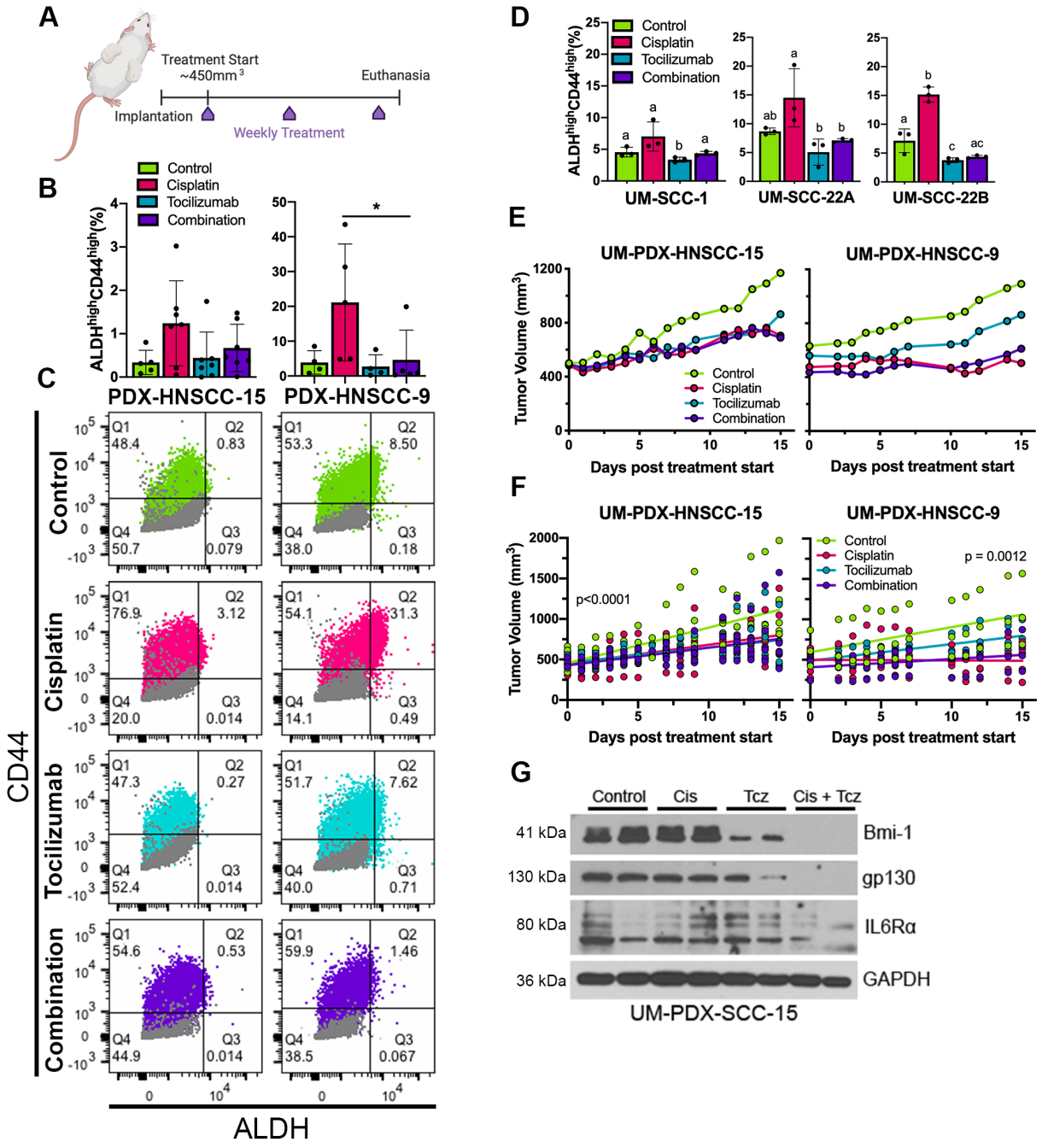

Figure 2-2: Tocilizumab suppresses Cisplatin-induced CSC phenotype in PDX models of HNSCC *in vivo.*

(A) Treatment schematic. Mice harboring PDX tumors began weekly treatment for 2 weeks (3 doses total), receiving either no treatment, Cisplatin (5 mg/kg, I.P.) and/or Tocilizumab (10 mg/kg, I.P.). Mice were euthanized on 2nd day after last dose. **(B)** Flow cytometry graphs depicting CSC fraction percentage ($ALDH^{high}CD44^{high}$ cells) in PDX tumors. **(C)** Flow cytometry graphs depicting DEAB/IgG controls (gray) for Aldefluor and CD44, respectively. One experimental replicate per group is shown to demonstrated gate setting strategy. $ALDH^{high}CD44^{high}$ cells were identified based on these gates. **(D)** Flow cytometry graphs depicting CSC fraction percentage

(ALDH^{high}CD44^{high} cells) in HNSCC cell lines. Bar graphs display mean ± S.D. (n=3) and significance denoted by letters at p≤0.05. **(E)** Line graph depicting mean tumor volume over time in the PDX models after treatment with Cisplatin and/or Tocilizumab. Tumor measurements were taken ~3 per week until study endpoints. **(F)** Simple linear regression model of mean tumor volumes over the duration of the experiment. **(G)** Western blot of representative PDX tumor tissue lysates from each treatment group.

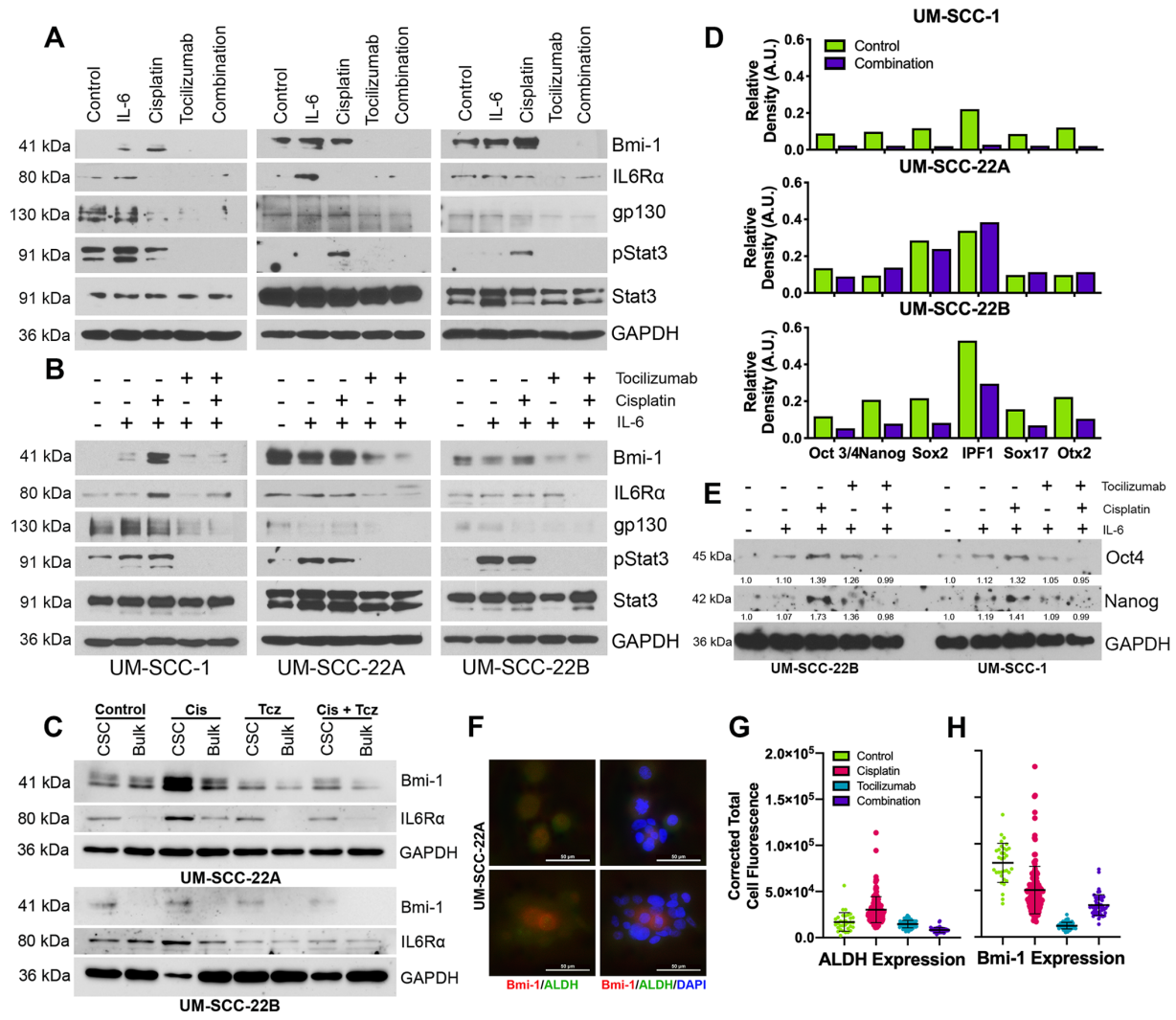

Figure 2-3: Combination therapy suppresses STAT3 signaling, Bmi-1 induction, and expression of stem cell markers *in vitro.*

(A) Western blot analysis of UM-SCC-1, UM-SCC-22A, and UM-SCC-22B cells treated with rhIL-6 (0-20 ng/ml), Cisplatin (0-1 μM) and/or Tocilizumab (0-0.1 μM). **(B)** Western blot analysis of UM-SCC-1, UM-SCC-22A, and UM-SCC-22B cells treated with rhIL-6 (0-20 ng/ml), Cisplatin (0-1 μM) and/or Tocilizumab (0-0.1 μM) for 24 hours, followed by additional rhIL-6 (0-20 ng/ml) for 24 hours. **(C)** Western blot analysis of UM-SCC-22A and UM-SCC-22B cells treated with 1μM Cisplatin and/or 0.1 μM Tocilizumab and sorted for $ALDH^{high}CD44^{high}$ CSC or bulk tumor cells. **(D)** Stem cell marker protein array analysis of UM-SCC-1, UM-SCC-22A, and UM-SCC-22B cells treated with Cisplatin (0-1 μM) and Tocilizumab (0-0.1 μM). **(E)** Western blot analysis of UM-SCC-1, UM-SCC-22A, and UM-SCC-22B cells treated with rhIL-6 (0-20 ng/ml), Cisplatin (0-1 μM) and/or Tocilizumab (0-0.1 μM). **(F)** Representative images of immunofluorescence staining of cells plate in chamber slides and treated with Cisplatin (0-1 μM) and/or Tocilizumab (0-0.1 μM). **(G)** Graph quantifying mean cellular fluorescence of ALDH normalized to DAPI stain in UM-SCC-22A cells treated with Cisplatin (0-1 μm) and/or Tocilizumab (0-0.1 μM). **(H)** Graph quantifying mean cellular fluorescence of Bmi-1 normalized to DAPI stain in UM-SCC-22A cells treated with Cisplatin (0-1 μM) and/or Tocilizumab (0-0.1 μM).

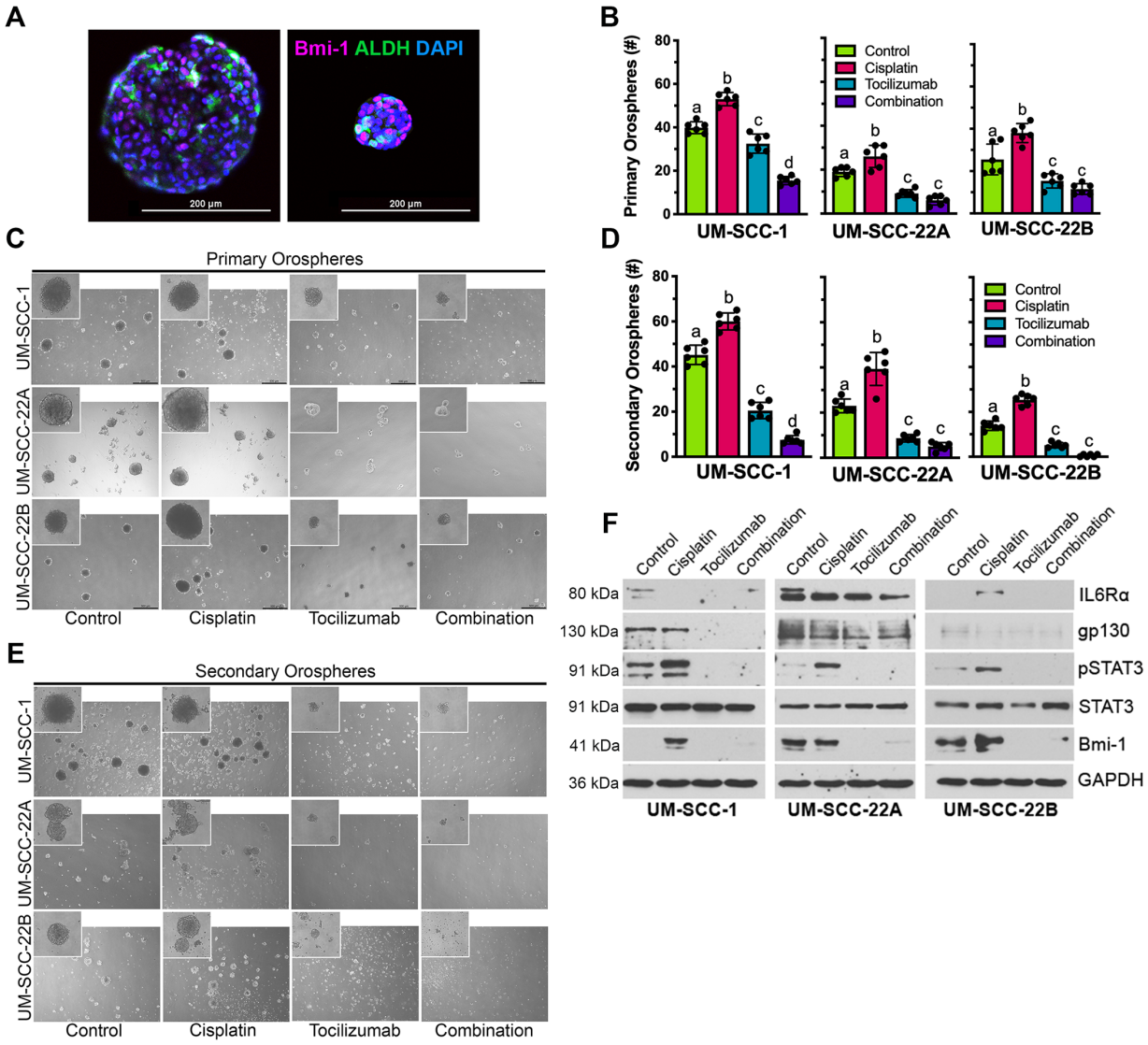

Figure 2-4: Tocilizumab prevents the Cisplatin-induced self-renewal of orospheres.

(A) Representative images of immunofluorescence staining of untreated, cryosectioned spheres on Day 8. Example images of both a large (left) and small (right) sphere are shown. **(B)** Quantification depicting number of primary orospheres per well. Six wells were counted per treatment group. Bar graphs display mean ± S.D. (n=6) and significance denoted by letters at p≤0.05. **(C)** Representative images (40x) of primary orospheres on day 8 after treatment with Cisplatin (0-1 µm) and/or Tocilizumab (0-0.1 µm). Cells were treated the day after plating in ULA sphere conditions. Inserts at 100x magnification. Pictures were taken of 5 fields per well in three wells per treatment group. **(D)** Quantification depicting number of secondary orospheres per well. Six wells were counted per treatment group. Bar graphs display mean ± S.D. (n=6) and significance denoted by letters at p≤0.05. **(E)** Representative images (40x) of secondary orospheres on day 8 after treatment with Cisplatin (0-1 µM) and/or Tocilizumab (0-0.1 µM). Cells were treated the day after plating in ULA sphere conditions. Inserts at 100x magnification. Pictures acquired of 5 fields per well in three wells per treatment group. **(F)** Western blots showing protein levels in lysates isolated from primary orospheres on day 8 after treatment with Cisplatin (0-1 µM) and/or Tocilizumab (0-0.1 µM).

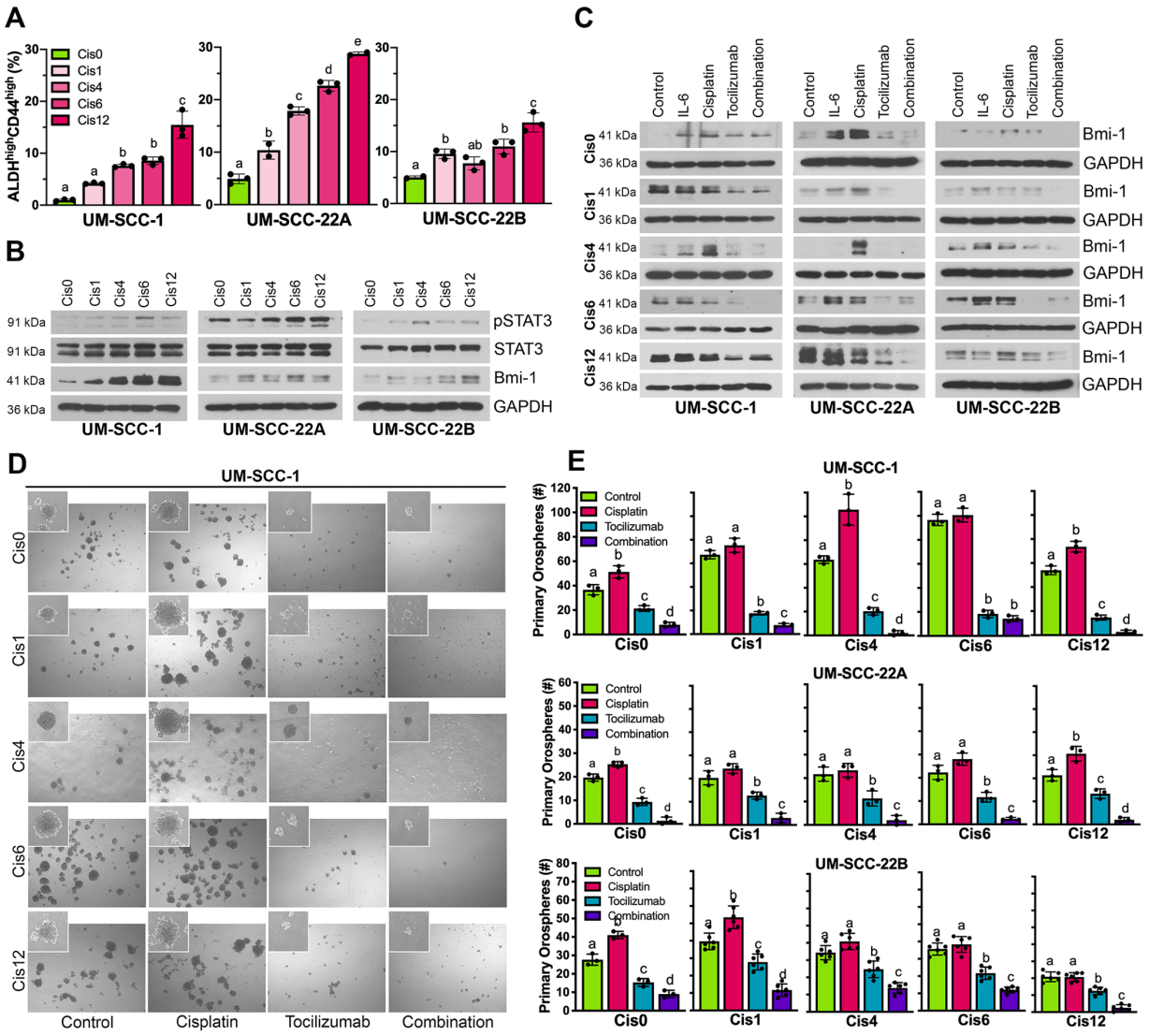

Figure 2-5: Tocilizumab decreases CSC fraction and self-renewal of Cisplatin-resistant HNSCC cells.

(A) Flow cytometry graphs depicting the CSC fraction ($ALDH^{high}CD44^{high}$ cells) in naïve and Cisplatin resistant variants of UM-SCC-1, UM-SCC-22A, and UM-SCC-22B cells. Bar graphs display mean ± S.D. (n=3) and significance denoted by letters at p≤0.05. **(B)** Western blots showing baseline activation of STAT3 and Bmi-1 expression in naïve and Cisplatin resistant HNSCC cell line variants. **(C)** Western blot analysis of Bmi-1 expression after treatment with rhIL-6 (0-20 ng/ml), Cisplatin (0-1 μm) and/or Tocilizumab (0-0.1 μM). **(D)** Representative images (40x) of naïve and Cisplatin-resistant UM-SCC-1 primary orospheres on day 8 after treatment with Cisplatin (0-1 μM) and/or Tocilizumab (0-0.1 μM). Cells were treated the day after plating in ULA sphere conditions. Inserts at 100x magnification. Pictures acquired of 5 fields per well in three wells per treatment group. **(E)** Quantification depicting number of primary orospheres per well. Three wells were counted per treatment group. Bar graphs display mean ± S.D. (n=3) and significance denoted by letters at p≤0.05.

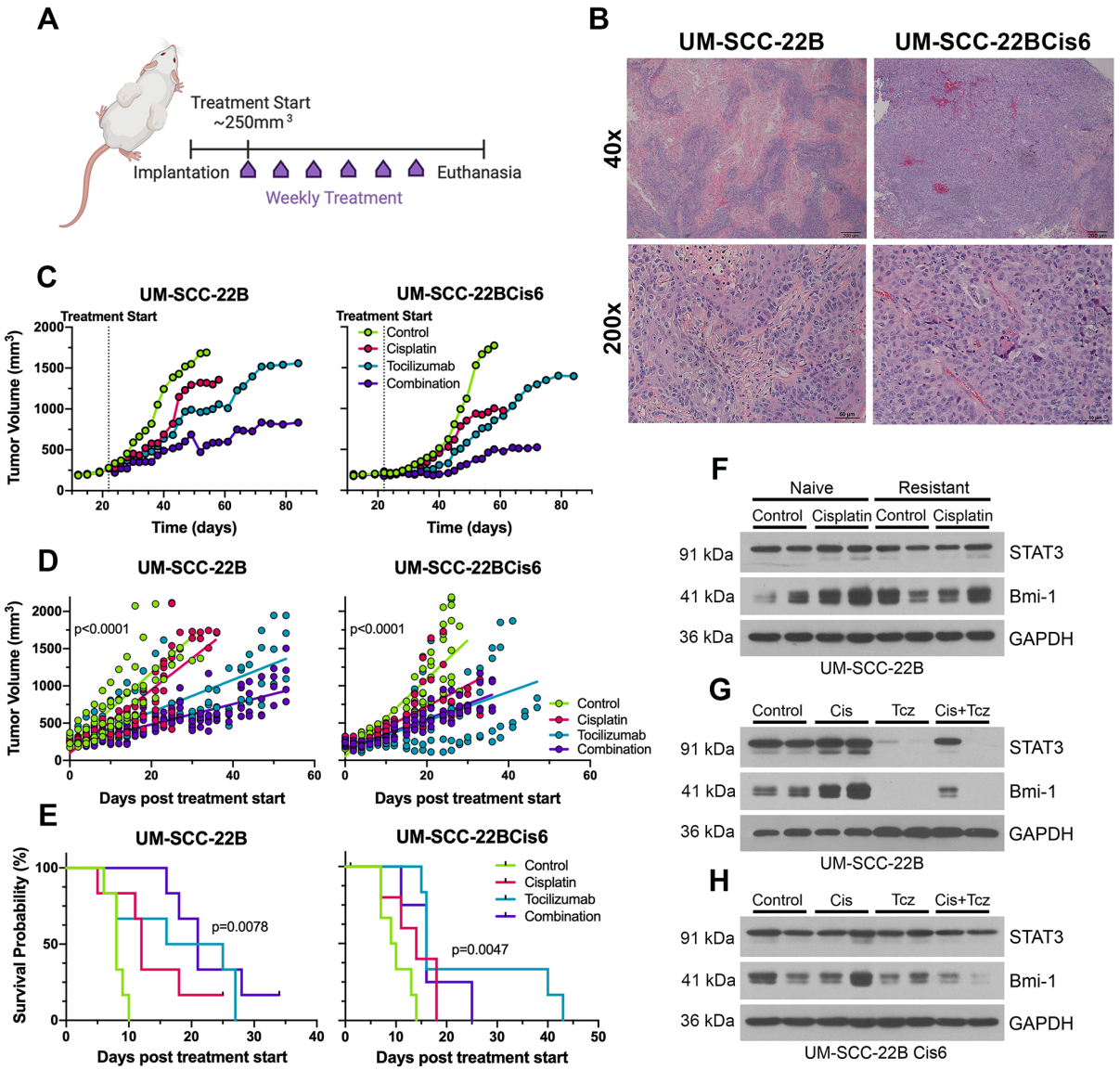

Figure 2-6: Tocilizumab decreases tumor growth and Bmi-1 expression in a Cisplatin-resistant xenograft model.

(A) Treatment schematic. Xenograft tumors generated from UM-SCC-22B or UM-SCC-22BCis6 cells and began weekly treatment for up to 8 weeks, receiving either no treatment, Cisplatin (5 mg/kg, I.P.) and/or Tocilizumab (10 mg/kg, I.P.). Mice were euthanized either at experiment endpoint (8 weeks post treatment start) or when reaching maximum tumor volume (2,000 mm^3). **(B)** Representative images of histological sections stained for H&E of UM-SCC-22B and UM-SCC-22BCis6 tumors. Scale bars represent 200 μm at 40x magnification and 50 μm at 200x magnification. **(C)** Line graph depicting mean tumor volume over time after treatment with Cisplatin and/or Tocilizumab. Tumor measurements were taken ~3 per week until study endpoints. **(D)** Simple linear regression model of mean tumor volumes over the duration of the experiment. **(E)** Kaplan-Meier graph for survival, as defined by time to doubling of tumor volume, as compared to pre-treatment tumor volume (n=6). **(F)** Western blot of representative tumor tissue lysates comparing control tumors with Cisplatin treated tumors in UM-SCC-22B and UM-SCC-

22BCis6 xenograft models. **(G)** Western blot of representative UM-SCC-22B tumor lysates of each treatment group. **(H)** Western blot of representative UM-SCC-22BCis6 tumor lysates of each treatment group.

2.8 Supplemental Figures

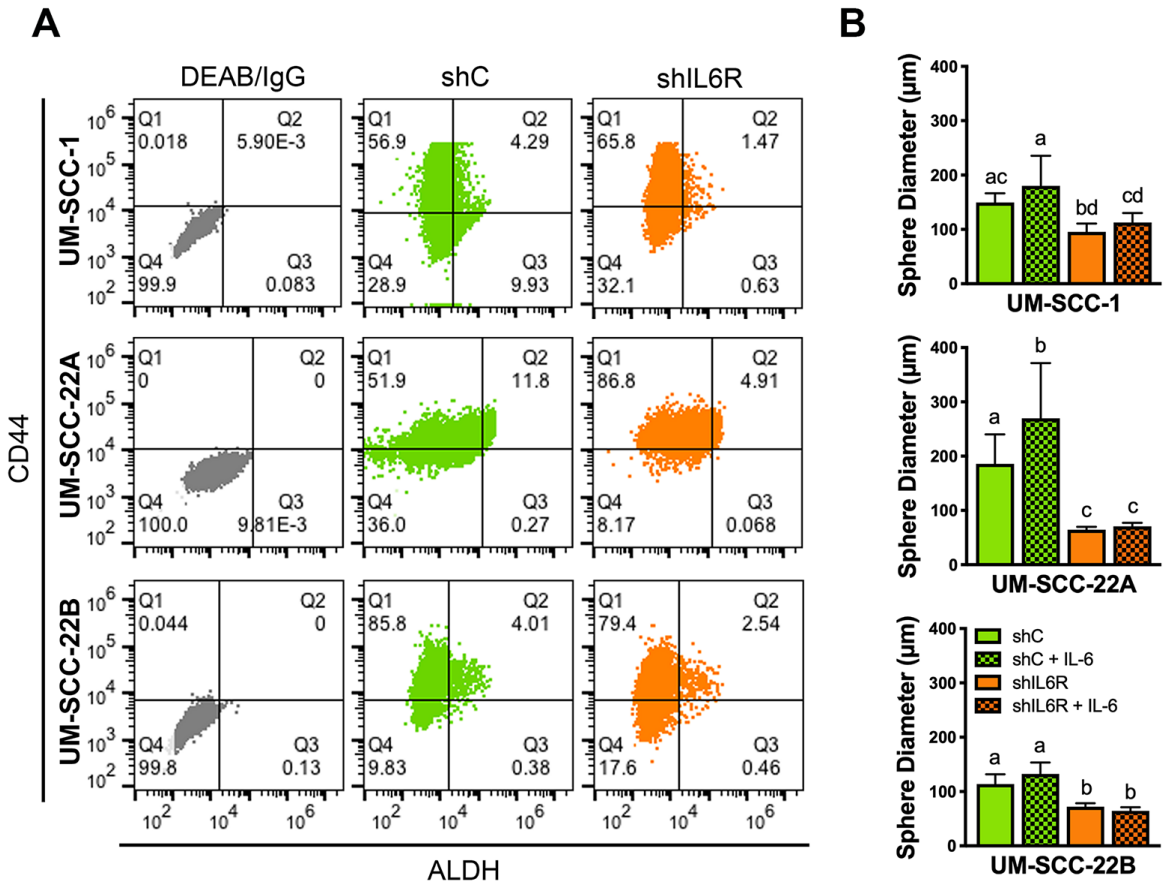

Figure 2-7: Flow cytometry gating and orosphere size measurements for CSC analysis of IL-6R knockdown cells.

(A) Bar graphs depicting the size of orospheres generated from IL-6R knockdown cells treated with rhIL-6 (0-20 ng/ml). Different low case letter depict statistical significance at $p<0.05$. **(B)** Flow cytometry graphs depicting DEAB/IgG controls for Aldefluor and CD44, respectively. One experimental replicate per group is shown to demonstrated gate setting strategy. $ALDH^{high}CD44^{high}$ cells were identified based on these gates.

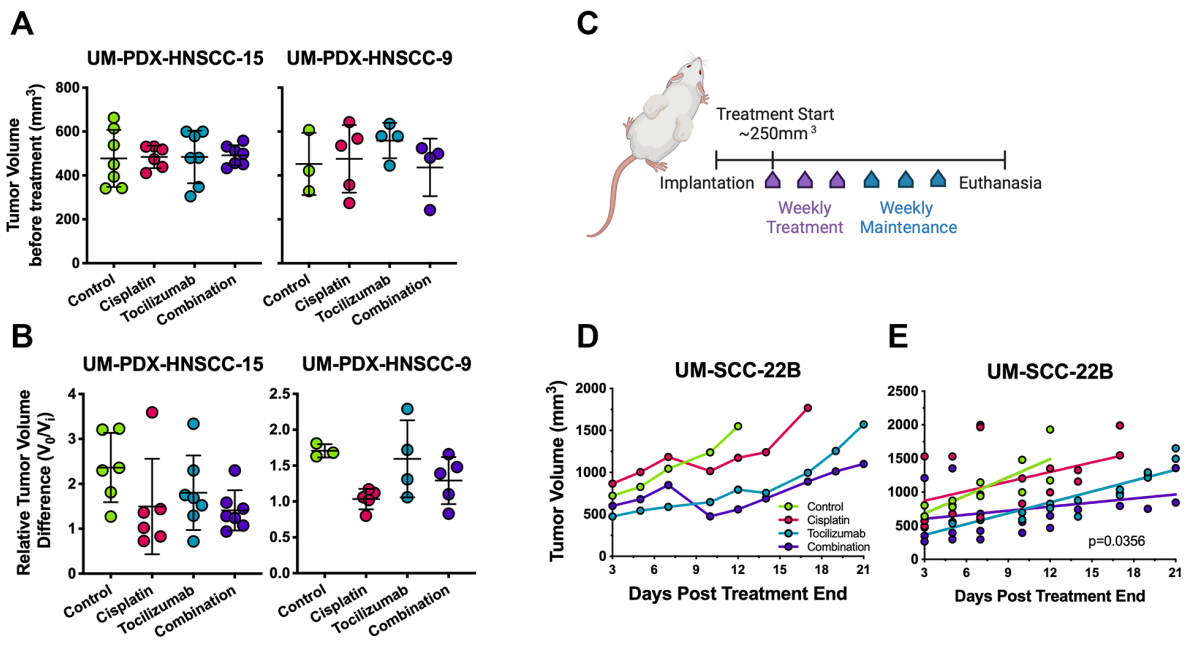

Figure 2-8: Therapeutic effect of Tocilizumab and/or Cisplatin in in vivo HNSCC models.

(A) Graphs depicting tumor volumes at treatment start. **(B)** Graphs depicting tumor volume at the end of experiment (V_0) normalized against tumor volume at treatment start (V_i). **(C)** Treatment schematic. Xenograft tumors generated from UM-SCC-22B cells and began main treatment for two weeks (three doses total), receiving either no treatment, Cisplatin (5 mg/kg, I.P.) and/or Tocilizumab (10 mg/kg, I.P.). Following the main treatment, those mice that had incorporated Tocilizumab in their treatment plan continued receiving weekly maintenance injections of Tocilizumab (10 mg/kg). Mice were euthanized three weeks post main treatment end, or when they reached maximum tumor volume (2,000 mm^3). **(D)** Line graph depicting mean tumor volume over time after main treatment end, when only Tocilizumab maintenance treatment was administered to the corresponding groups. Tumor measurements were taken 3 times per week until study endpoints. **(E)** Simple linear regression model of mean tumor volumes over the duration of the experiment. p=0.0356 for comparison of the combination to control group.

A

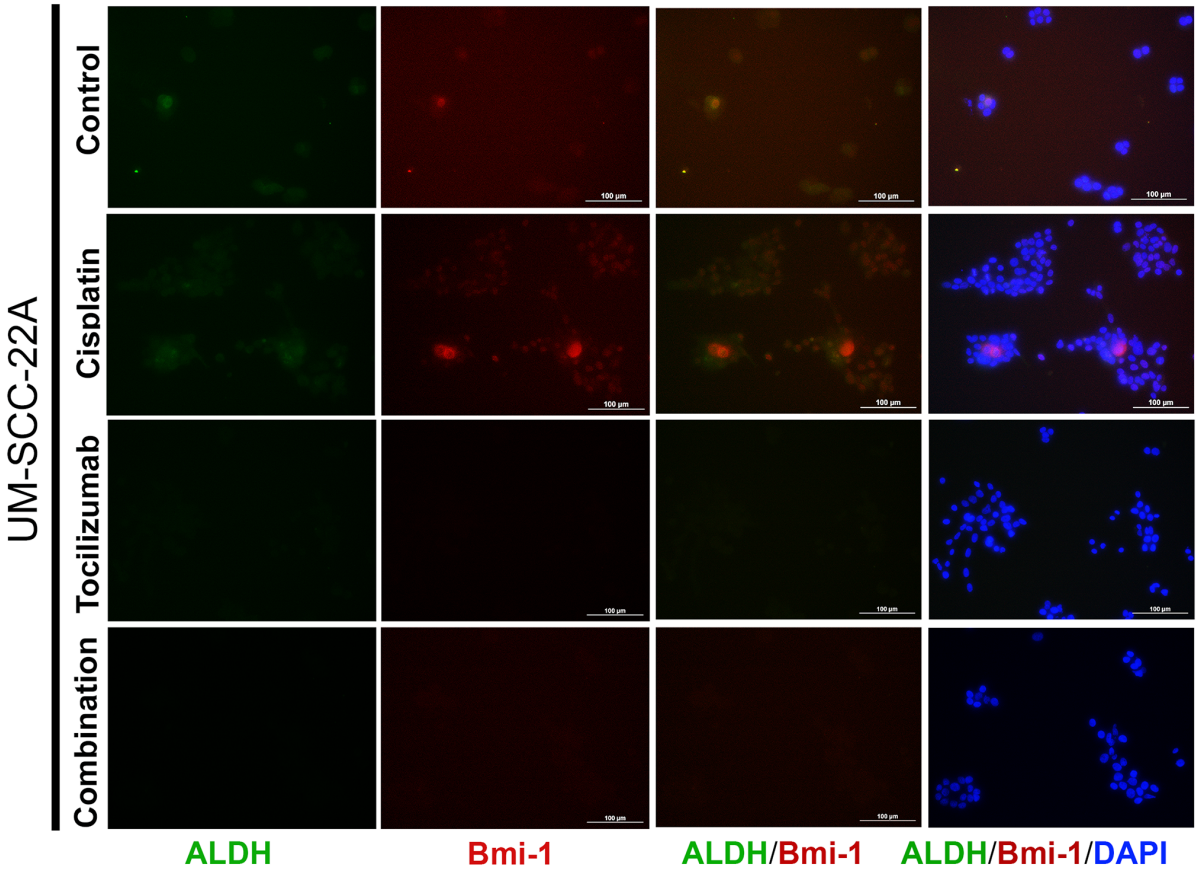

B

	UM-SCC-1				UM-SCC-2A				UM-SCC-22B			
	Control	Cis	Tcz	Cis + Tcz	Control	Cis	Tcz	Cis + Tcz	Control	Cis	Tcz	Cis + Tcz
Oct3/4	0.088	0.078	0.071	0.023	0.134	0.135	0.121	0.089	0.118	0.082	0.053	0.053
Nanog	0.097	0.057	0.056	0.021	0.094	0.229	0.142	0.138	0.208	0.164	0.150	0.078
Sox2	0.117	0.075	0.082	0.019	0.285	0.349	0.369	0.239	0.216	0.147	0.162	0.082
IPF1	0.221	0.144	0.104	0.027	0.338	0.435	0.444	0.384	0.529	0.446	0.360	0.295
Sox17	0.086	0.070	0.047	0.021	0.098	0.179	0.159	0.113	0.156	0.120	0.065	0.069
Otx2	0.121	0.076	0.066	0.021	0.098	0.179	0.159	0.113	0.223	0.205	0.171	0.105

Figure 2-9: Tocilizumab suppresses Cisplatin-induction of cancer cell stemness.

(A) Representative immunofluorescence images of UM-SCC-22A cells grown in chamber slides and stained for ALDH (green), Bmi-1 (red), and DAPI (blue) were captured at 200x for quantification. **(B)** Stem cell marker protein array analysis of UM-SCC-1, UM-SCC-22A, and UM-SCC-22B cells treated with Cisplatin (0-1 μM) and Tocilizumab (0-0.1 μM).

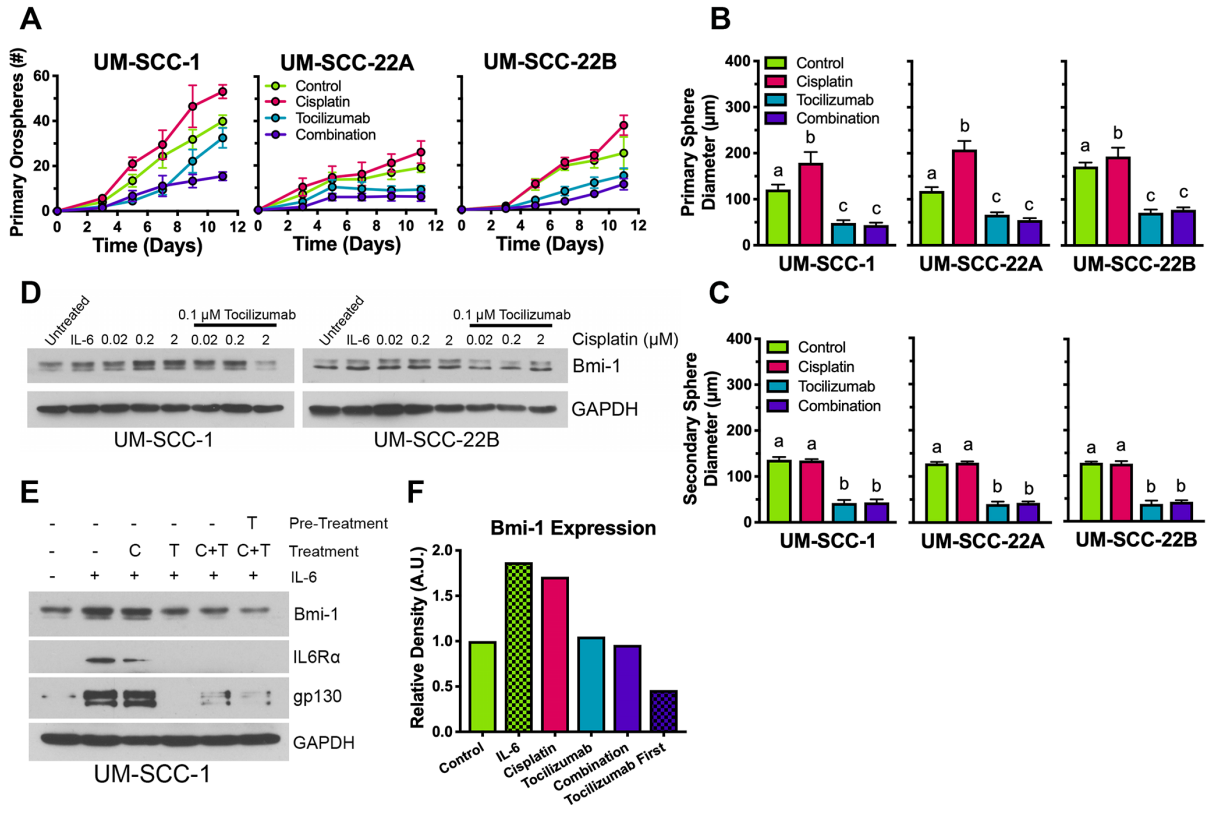

Figure 2-10: Tocilizumab decreases orosphere growth and Bmi-1 expression.

(A) Graph depicting orosphere growth over time after treatment with Cisplatin (0-1 μM) and/or Tocilizumab (0-0.1 μM). Cells were treated the day after plating in ULA sphere conditions. **(B)** Bar graphs depicting the size of primary orospheres after treatment with Cisplatin (0-1 μM) and/or Tocilizumab (0-0.1 μM). Different low case letter depict statistical significance at $p<0.05$. **(C)** Bar graphs depicting the size of secondary orospheres after treatment with Cisplatin (0-1 μM) and/or Tocilizumab (0-0.1 μM). Different low case letter depict statistical significance at $p<0.05$. **(D)** Western blot analysis of UM-SCC-1 and UM-SCC-22B cells treated with rhIL-6 (0-20 ng/ml), Cisplatin (0-2 μM) and/or Tocilizumab (0-0.1 μM) for 24 hours. **(E)** Western blot analysis of UM-SCC-1 cells treated with rhIL-6 (0-20 ng/ml), Cisplatin (0-1 μM) and/or Tocilizumab (0-0.1 μM) for 24 hours. Pre-treatment with Tocilizumab was applied 1 hour prior to subsequent combination therapy. **(F)** Bar graph depicting the quantification of Bmi-1 protein expression normalized to GAPDH.

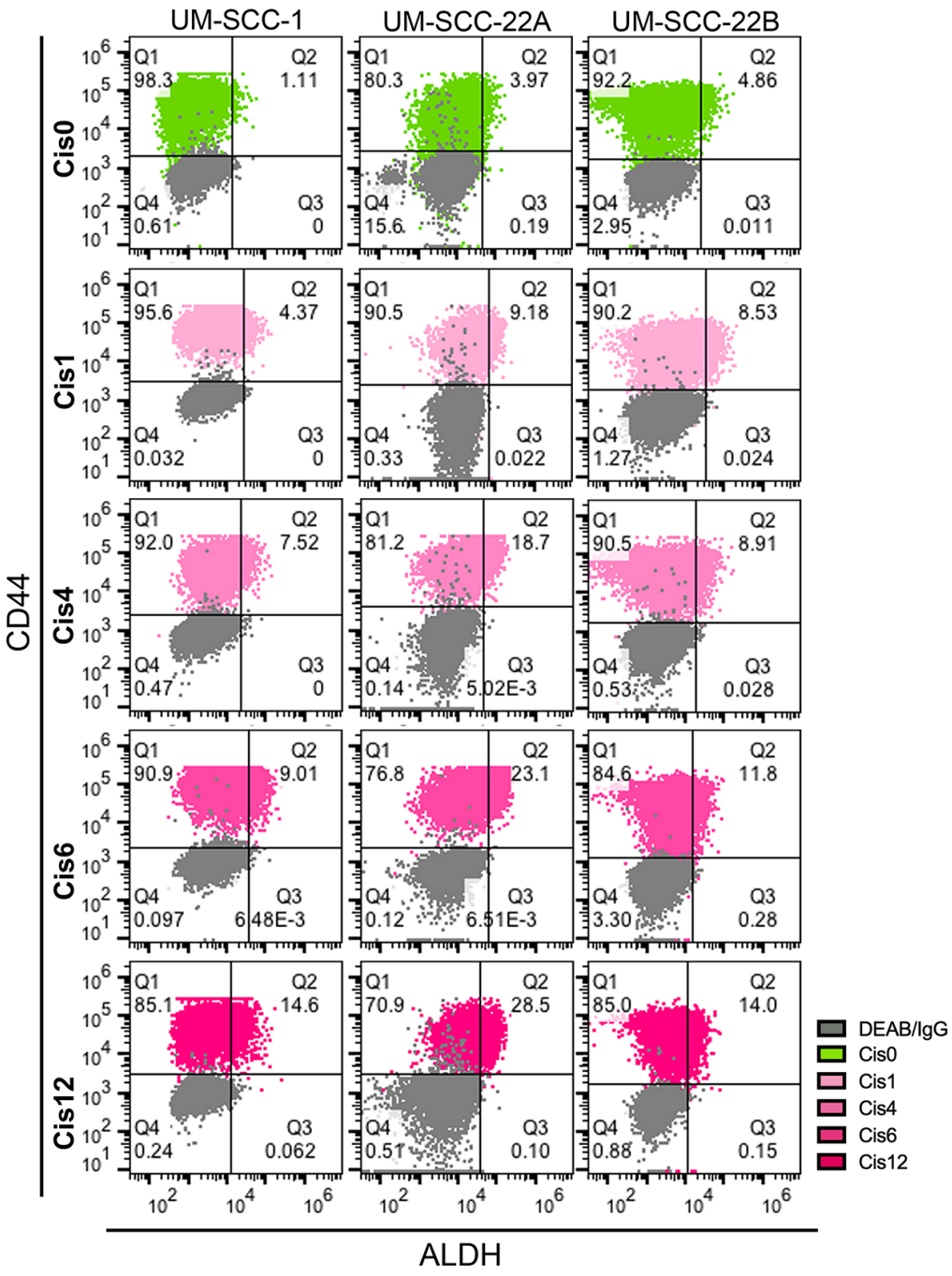

Figure 2-11: Flow cytometry gating for CSC analysis of Cisplatin resistant HNSCC cell line variants.

Flow cytometry gating strategies depicting DEAB/IgG controls for Aldefluor and CD44, respectively. One experimental replicate per group is shown to demonstrated gate setting strategy. $ALDH^{high}CD44^{high}$ cells were identified based on these gates.

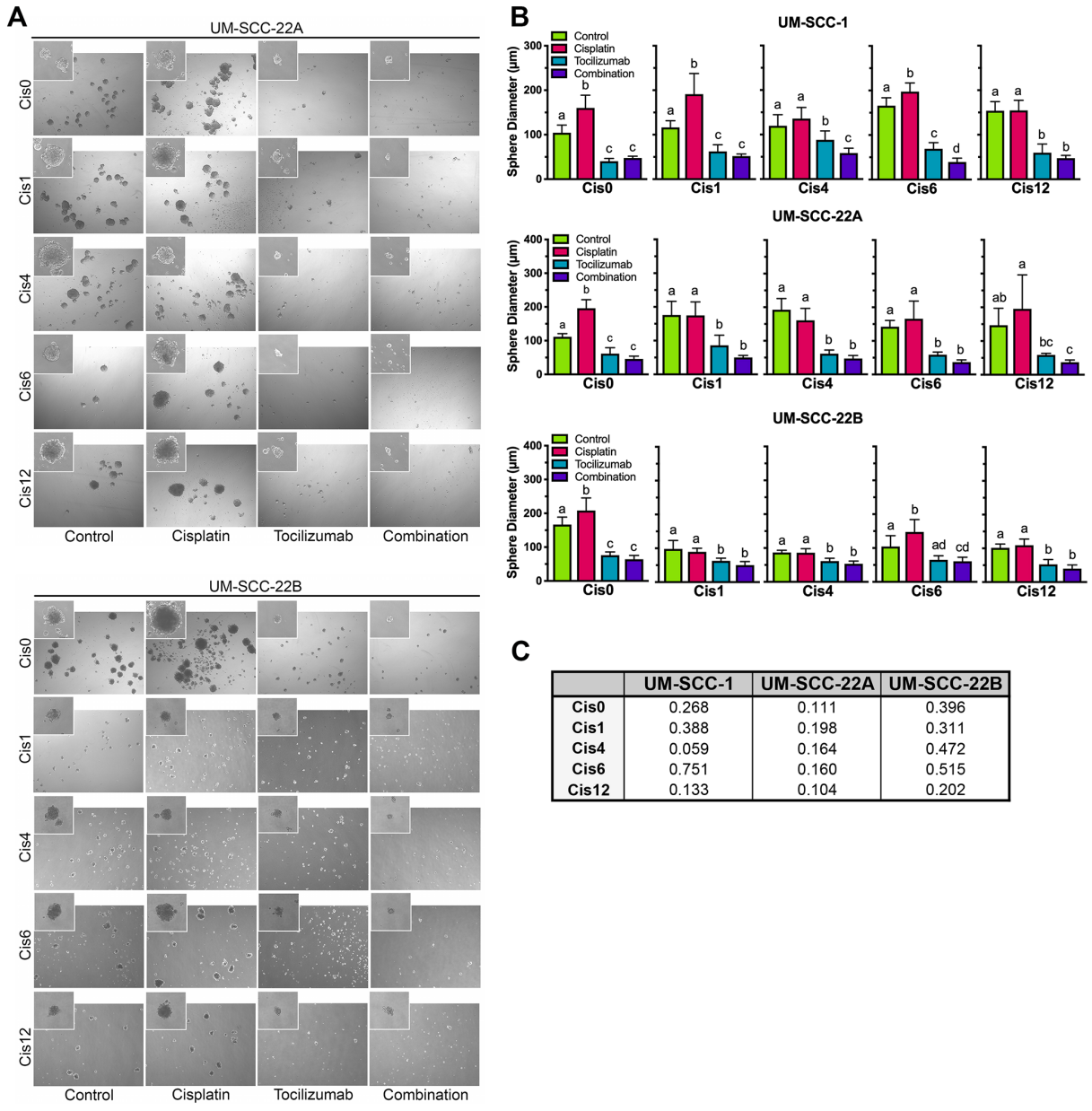

C

	UM-SCC-1	UM-SCC-22A	UM-SCC-22B
Cis0	0.268	0.111	0.396
Cis1	0.388	0.198	0.311
Cis4	0.059	0.164	0.472
Cis6	0.751	0.160	0.515
Cis12	0.133	0.104	0.202

Figure 2-12: Tocilizumab decreases size of orospheres in Cisplatin-resistant HNSCC cell line variants.

(A) Representative images (40x) of naïve and Cisplatin-resistant UM-SCC-22A and UM-SCC-22B primary orospheres on day 8 after treatment with Cisplatin (0-1 µM) and/or Tocilizumab (0-0.1 µM). Cells were treated the day after plating in ULA sphere conditions. Inserts are at 100x magnification. Pictures were taken of 5 fields per well in three wells per treatment group. **(B)** Bar graphs depicting the size of orospheres generated from Cisplatin resistant cell line variants treated with Cisplatin (0-1 µM) and/or Tocilizumab (0-0.1 µM). Different low case letter depict statistical significance at $p<0.05$. **(C)** Coefficient of drug interaction (CDI) for the combination effect of Cisplatin and Tocilizumab in primary orosphere formation, where CDI<1, =1, and >1 indicate synergism, additive effect, and antagonism (respectively).

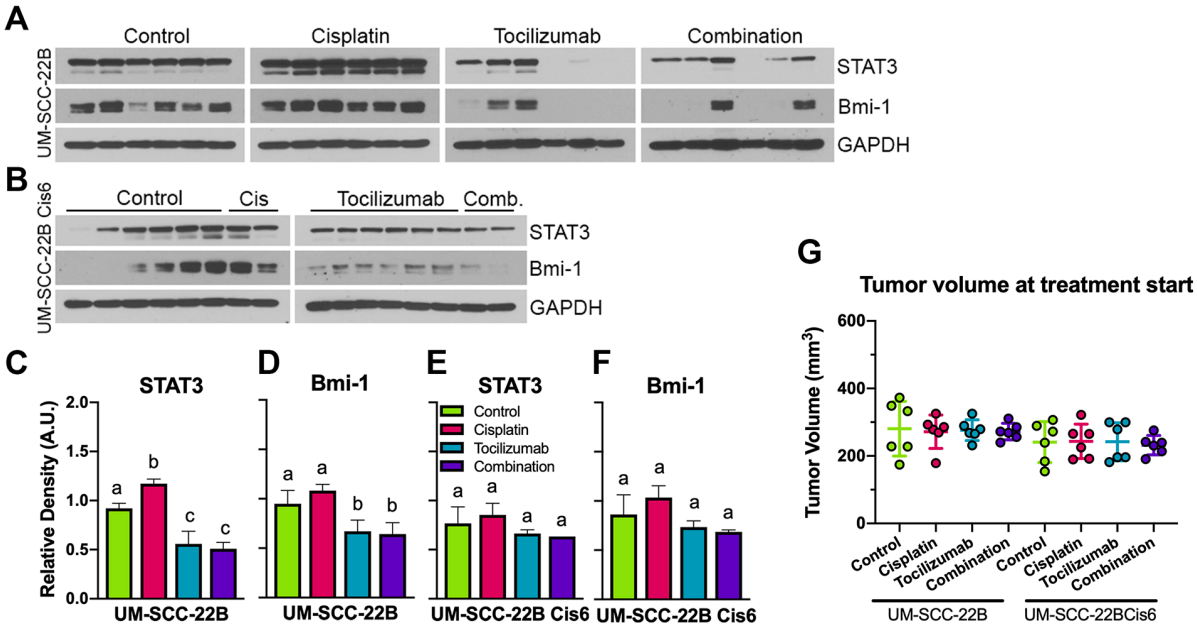

Figure 2-13: Effect of Tocilizumab and/or Cisplatin in a Cisplatin-resistant xenograft model.

(**A,B**) Western blots depicting the impact of Cisplatin and/or Tocilizumab on the expression of STAT3 and Bmi-1 in xenograft tumors generated with UM-SCC-22B (A) or UM-SCC-22BCis6 (B) cells. Lysates were prepared from whole tumors upon dissociation (n=6). (**C-F**) Graphs depicting the quantification of STAT3 (C,E) and Bmi-1 (D,F) protein expression normalized to GAPDH in UM-SCC-22B (C,D) or UM-SCC-22BCis6 (E,F) cells exposed to Cisplatin and/or Tocilizumab. Different low case letter depict statistical significance at $p<0.05$. **(G)** Graphs depicting tumor volumes at start of treatment.

2.9 References

[1] Siegel, R., Ma, J., Zou, Z. & Jemal, A. Cancer statistics. CA. Cancer J. Clin. 64(1), 9-29 (2014).

[2] Vermorken, J.B. et al. Platinum-based chemotherapy plus cetuximab in head and neck cancer. N. Engl. J. Med. 359(11),1116-1127 (2008).

[3] Seiwert, T.Y., Salama, J.K. & Vokes, E.E. The chemoradiation paradigm in head and neck cancer. Nat. Clin. Pract. Oncol. 4(3), 156-171 (2007).

[4] Carvalho, A.L., Nishimoto, I.N., Califano, J.A. & Kowalski, L.P. Trends in incidence and prognosis for head and neck cancer in the United States: a site-specific analysis of the SEER database. Int. J. Cancer 114(5), 806-816 (2005).

[5] Koneva, L.A. et al. HPV Integration in HNSCC Correlates with Survival Outcomes, Immune Response Signatures, and Candidate Drivers. Mol. Cancer Res. 16(1), 90-102 (2018).

[6] Reya, T., Morrison, S.J., Clarke, M.F. & Weissman, I.L. Stem cells, cancer, and cancer stem cells. Nature 414(6859),105-111 (2001).

[7] Prince, M.E. et al. Identification of a subpopulation of cells with cancer stem cell properties in head and neck squamous cell carcinoma. Proc. Natl. Acad. Sci. USA 104(3), 973-978 (2007).

[8] Chen, Y.C. et al. Aldehyde dehydrogenase 1 is a putative marker for cancer stem cells in head and neck squamous cancer. Biochem. Biophys. Res. Commun. 385(3), 307-313 (2009).

[9] Clay, M.R. et al. Single-marker identification of head and neck squamous cell carcinoma cancer stem cells with aldehyde dehydrogenase. Head Neck 32(9), 1195-1201 (2010).

[10] Krishnamurthy, S. et al. Endothelial cell-initiated signaling promotes the survival and self-renewal of cancer stem cells. Cancer Res. 70(23), 9969-9978 (2010).

[11] Krishnamurthy, S. & Nör, J.E. Head and neck cancer stem cells. J. Dent. Res. 91(4), 334-340 (2012).

[12] Chinn, S.B. et al. Cancer stem cells: mediators of tumorigenesis and metastasis in head and neck squamous cell carcinoma. Head Neck 37(3), 317-326 (2015).

[13] Tsai, L.L., Yu, C.C., Chang, Y.C., Yu, C.H. & Chou, M.Y. Markedly increased Oct4 and Nanog expression correlates with cisplatin resistance in oral squamous cell carcinoma. J. Oral Pathol. Med. 40(8), 621-628 (2011).

[14] Goldman, A. et al. Temporally sequenced anticancer drugs overcome adaptive resistance by targeting a vulnerable chemotherapy-induced phenotypic transition. Nat. Commun. 6, 6139 (2015).

[15] Davis, S.J. et al. Metastatic potential of cancer stem cells in head and neck squamous cell carcinoma. Arch. Otolaryngol. Head Neck Surg. 136(12), 1260-1266 (2010).

[16] Nör, C. et al. Cisplatin induces Bmi-1 and enhances the stem cell fraction in head and neck cancer. Neoplasia 16(2),137-146 (2014).

[17] Islam, F., Gopalan, V., Smith, R.A. & Lam, A.K. Translational potential of cancer stem cells: A review of the detection of cancer stem cells and their roles in cancer recurrence and cancer treatment. Exp. Cell Res. 335(1), 135-147 (2015).

[18] Chen, D. et al. Targeting BMI1+ cancer stem cells overcomes chemoresistance and inhibits metastases in squamous cell carcinoma. Cell Stem Cell 20(5), 621-634, e6 (2017).

[19] Ning, N. et al. Cancer stem cell vaccination confers significant antitumor immunity. Cancer Res. 72(7), 1853-1864 (2012).

[20] Lu, L. et al. Cancer stem cell vaccine inhibits metastases of primary tumors and induces humoral immune responses against cancer stem cells. Oncoimmunology 4(3), e990767, (2015).

[21] Kaur, K. et al. Novel Strategy to Expand Super-Charged NK Cells with Significant Potential to Lyse and Differentiate Cancer Stem Cells: Differences in NK Expansion and Function between Healthy and Cancer Patients. Front. Immun. 8, 297 (2017).

[22] Eyler, C.E. & Rich, J.N. Survival of the fittest: cancer stem cells in therapeutic resistance and angiogenesis. J. Clin. Oncol. 26, 2839-2845 (2008).

[23] Gilbert, L.A. & Hemann, M.T. DNA damage-mediated induction of a chemoresistant niche. Cell 143(3), 355-366 (2010).

[24] Krishnamurthy, S. et al. Endothelial interleukin-6 defines the tumorigenic potential of primary human cancer stem cells. Stem Cells 32(11), 2845-2857 (2014).

[25] Kim, H.S. et al. Endothelial-derived interleukin-6 induces cancer stem cell motility by generating a chemotactic gradient towards blood vessels. Oncotarget 8(59), 100339-100352 (2017).

[26] McDermott, S.C., Rodriguez-Ramirez, C., McDermott, S.P., Wicha, M.S. & Nör, J.E. FGFR signaling regulates resistance of head and neck cancer stem cells to Cisplatin. Oncotarget 9(38), 25148-25165 (2018).

[27] Duffy, S.A. et al. Interleukin-6 predicts recurrence and survival among head and neck cancer patients. Cancer 113(4), 750-757 (2008).

[28] Krishnamurthy, S. & Nör, J.E. Orosphere assay: a method for propagation of head and neck cancer stem cells. Head Neck 35(7), 1015-1021 (2013).

[29] Xu, R., Chen, L. & Yang, W.T. Aberrantly elevated Bmi1 promotes cervical cancer tumorigenicity and tumor sphere formation via enhanced transcriptional regulation of Sox2 genes. Oncology reports 42(2), 688-696 (2019).

[30] Chen, Y.C. et al. High-throughput single-cell derived sphere formation for cancer stem-like cell identification and analysis. Scientific reports 6(1), 1-2 (2016).

[31] Pearson, A.T. et al. Patient-derived xenograft (PDX) tumors increase growth rate with time. Oncotarget 7(7), 7993-8005 (2016).

[32] Koo, B.S. et al. Oct4 is a critical regulator of stemness in head and neck squamous carcinoma cells. Oncogene 34(18), 2317–2324 (2015).

[33] Mitsui, K. et al. The homeoprotein Nanog is required for maintenance of pluripotency in mouse epiblast and E.S. cells. Cell 113(5), 631–642 (2003).

[34] Bergers, G. & Hanahan, D. Modes of resistance to anti-angiogenic therapy. Nat. Rev. Cancer 8(8), 592-603 (2008).

[35] Sharma, S.V. et al. A chromatin-mediated reversible drug-tolerant state in cancer cell subpopulations. Cell 141(1), 69-80 (2010).

[36] Alraouji, N.N. et al. Tocilizumab potentiates cisplatin cytotoxicity and targets cancer stem cells in triple-negative breast cancer. Molecular Carcinogenesis 59(9), 1041-1051 (2020).

[37] Müllberg, J. et al. Differential shedding of the two subunits of the interleukin-6 receptor. FEBS letters 332(1-2), 174-178 (1993).

[38] Molofsky, A.V., Pardal, R., Iwashita, T., Park, I.K., Clarke, M.F. & Morrison, S.J. Bmi-1 dependence distinguishes neural stem cell self-renewal from progenitor proliferation. Nature 425(6961), 962-967 (2003).

[39] Park, I.K. et al. Bmi-1 is required for maintenance of adult self-renewing haematopoietic stem cells. Nature 423(6937), 302-305 (2003).

[40] Jacobs, J.J., Kieboom, K., Marino, S., DePinho, R.A. & van Lohuizen, M. The oncogene and Polycomb-group gene bmi-1 regulates cell proliferation and senescence through the ink4a locus. Nature 397(6715), 164-168 (1999).

[41] Molofsky, A.V., He, S., Bydon, M., Morrison, S.J. & Pardal, R. Bmi-1 promotes neural stem cell self-renewal and neural development but not mouse growth and survival by repressing the p16Ink4a and p19Arf senescence pathways. Genes Dev. 19(12), 1432-1437 (2005).

[42] Sullivan, N.J. et al. Interleukin-6 induces an epithelial-mesenchymal transition phenotype in human breast cancer cells. Oncogene 28(33), 2940-2947 (2009).

[43] Cheng, G.Z. et al. Twist is transcriptionally induced by activation of STAT3 and mediates STAT3 oncogenic function. J. Biol. Chem. 283(21), 14665-14673 (2008).

[44] Chad, B.J. et al. Genotyping of 73 UM-SCC head and neck squamous cell carcinoma cell lines. Head Neck 32(4), 417-426 (2010).

[45] Negoro, K. et al. Establishment and characterization of a cisplatin-resistant cell line, KB-R, derived from oral carcinoma cell line, K.B. Int. J. Oncol. 30, 1325–1332 (2007).

[46] Nör, J.E. et al. Engineering and characterization of functional human microvessels in immunodeficient mice. Lab Invest. 81, 453–463 (2007).

CHAPTER 3:

Bmi-1: A Master Regulator of Head and Neck Cancer Stemness[3]

3.1 Abstract

Head and neck cancers are composed of a diverse group of malignancies, many of which exhibit an unacceptably low patient survival, high morbidity and poor treatment outcomes. The cancer stem cell (CSC) hypothesis provides an explanation for the substantial patient morbidity associated with treatment resistance and the high frequency of tumor recurrence/metastasis. Stem cells are a unique population of cells capable of recapitulating a heterogenous organ from a single cell, due to their capacity to self-renew and differentiate into progenitor cells. CSCs share these attributes, in addition to playing a pivotal role in cancer initiation and progression by means of their high tumorigenic potential. CSCs constitute only a small fraction of tumor cells but play a major role in tumor initiation and therapeutic evasion. The shift towards stem-like phenotype fuels many malignant features of a cancer cell and mediates resistance to conventional chemotherapy. Bmi-1 is a master regulator of stem cell self-renewal as part of the polycomb repressive complex 1 (PRC1) and has emerged as a prominent player in cancer stem cell biology. Bmi-1 expression is upregulated in CSCs, which is augmented by tumor-promoting factors and various conventional chemotherapies. Bmi-1^{+} CSCs mediate chemoresistance and metastasis. On the other hand, inhibiting Bmi-1 rescinds

[3] This chapter was originally published in *Frontiers in Oral Health*. Herzog AE, Somayaji R, Nör JE. Bmi-1: a master regulator of head and neck cancer stemness. *Front Oral Health*. 2023 Jan 16;4:1080255.

CSC function and re-sensitizes cancer cells to chemotherapy. Therefore, elucidating the functional role of Bmi-1 in CSC-mediated cancer progression may unveil an attractive target for mechanism-based, developmental therapeutics. In this review, we discuss the parallels in the role of Bmi-1 in stem cell biology of health and disease and explore how this can be leveraged to advance clinical treatment strategies for head and neck cancer.

3.2 Introduction

Head and neck squamous cell carcinoma (HNSCC) is the sixth most common form of cancer worldwide with over 900,000 new cases and 400,000 deaths annually [1]. HNSCC incidence is strongly correlated with alcohol and tobacco use, as well as human papillomavirus (HPV) infection. While there has been a marked decrease in HNSCC associated with tobacco use, the incidence and mortality rate of HPV-induced HNSCC has increased significantly [2]. Current treatment modalities for HNSCC include surgery, radiation, chemotherapy, EGFR inhibitors (e.g. Cetuximab) and immunotherapy (e.g. Pembrolizumab) [3, 4]. However, the modest improvement in overall survival rates achieved with current therapies emphasizes the significant need for further research in this area.

Salivary gland cancers account for approximately 6% of all head and neck cancers, and present significant treatment challenges due to their rarity and biological diversity [5]. Mucoepidermoid carcinoma (MEC) is the most common subtype of salivary gland cancer, followed by adenoid cystic carcinoma (ACC) [6]. Conventional chemotherapies are ineffective in salivary gland cancers, and currently no systemic or targeted therapy is approved [7, 8]. Given the limited understanding of the underlying pathobiology of these diseases and lack of effective chemotherapeutic approaches, surgery remains the main

treatment option for these patients. Considering that both HNSCC and malignant salivary gland cancers follow the cancer stem cell hypothesis, the understanding of the pathobiology of these cells may unveil new therapeutic targets for these tumors.

3.3 Cancer Stem Cells in Head and Neck Cancer

The traditional, or stochastic, model of carcinogenesis postulates that tumor growth is initiated by a single cell harboring advantageous genetic mutations, which proliferates and dominates the tumor architecture [9]. In this model, all subsequently formed tumor cells possess equal potential for tumorigenesis. Nowadays, it is widely accepted that a tumor is highly heterogenous, constituted by cells of varying biological characteristics. The hierarchical model of carcinogenesis suggests that only a unique subset of tumor cells is capable of tumorigenesis, namely cancer stem cells (CSCs) [10]. The CSC hypothesis presents that these cells are endowed with the ability to self-renew and give rise to the various cell phenotypes of a heterogeneous tumor through asymmetric and symmetric cell division. CSCs and physiological stem cells share many attributes: the capacity for self-renewal and differentiation, the ability to survive for long periods of time, and strong resistance to harmful agents [11]. Hence, the most-accepted hypothesis for the genesis of CSCs remains that they arise from physiological stem cells [12]. Other hypotheses include that CSCs arise from physiological differentiated cells or progenitor cells.

Head and neck cancers have been shown to follow the CSC hypothesis and hierarchical model of carcinogenesis, as they are solid, heterogenous tumors consisting of both CSCs capable of tumorigenesis and bulk tumor cells. CSCs have been diligently studied and characterized in multiple types of head and neck cancers, including head and

neck squamous cell carcinoma (HNSCC), mucoepidermoid carcinoma (MEC) and adenoid cystic carcinoma (ACC) [13-17]. Head and neck CSCs are endowed with properties of invasiveness, quiescence, and epithelial-mesenchymal transition (EMT) – a crucial process in cancer metastasis [18]. These cells have been found to reside in perivascular niches, with the majority residing within a 100 μm radius of blood vessels, from which endothelial cell-secreted factors enhance their self-renewal and promote their tumorigenicity [19, 20]. This microenvironmental support, along with many other factors, contributes to the increased resistance to therapies observed in CSCs [21, 22].

The CSC hypothesis may explain the resistance to current cytotoxic treatments and propensity for recurrence and metastasis in head and neck squamous cell carcinoma, which are factors that have a negative impact on the long-term survival of these patients. CSCs are resistant to chemotherapies, because these agents generally target cells with high proliferation rates, whereas CSCs proliferate slowly and thus escape their cytotoxicity [23]. Therefore, the modest progress of therapies against HNSCC can at least partially be attributed to CSCs, rendering them to be a therapeutic target of interest.

3.4 Biomarkers of Cancer Stem Cells

In order to target CSCs, they must be identifiable by means of unique cellular markers and pathways, which is an area of active research in many cancers. Though differences in CSC biomarkers across cancer types exist, their identification relies heavily on intracellular enzymes, transcription factors, and cell surface molecules. Here, we briefly discuss some commonly used biomarkers of CSCs in head and neck cancer, which are illustrated in Figure 3-1.

CSCs were first identified in HNSCC as expressing high levels of CD44, a cell-surface glycoprotein for hyaluronic acid that is involved in cell proliferation, survival, adhesion, migration, and intercellular interactions [13]. CD44 is one of the most common CSC markers in several malignancies and has been shown to select for highly tumorigenic CSCs as compared to $CD44^-$ cells [24]. However, since most cells in epithelia of the head and neck express CD44, other biomarkers have been established to refine identification of head and neck CSCs [25]. Among these, aldehyde dehydrogenase (ALDH) activity has been accepted as a frequent marker of CSCs. In HNSCC patient-derived xenograft models and cell lines, $ALDH^{high}$ cells demonstrated increased tumorigenicity, therapy resistance, and EMT as compared to $ALDH^{low}$ cells [26-28]. As complementary markers, purified $CD44^+ALDH^{high}$ cells constitute an even more tumorigenic and invasive cancer cell population, as compared to the other combinations of both markers' expression status [15, 17, 19]. Additionally, these cells positively correlate with decreased overall survival, disease grade, and treatment prognosis in patients with HNSCC [29, 30].

CD133, a cell surface glycoprotein, is another prominent yet more debated head and neck CSC marker [31]. $CD133^+$ cells exhibit increased invasiveness, tumorigenicity, and chemoresistance, but may present only a subpopulation of CSCs in oral squamous cell carcinoma cell lines and tissues [32]. CD133 has also been shown to function as a regulatory switch of EMT and stemness properties [33]. Multiple other cell surface proteins have been implicated as head and neck CSC markers: CD10 expression correlates with poorer overall survival, local recurrences, and therapeutic resistance [34, 35]; $CD24^+$ cells promote angiogenesis and tumor progression [36]; $CD29^+$ cells are

highly invasive, migratory, and contribute to metastases [37]; $CD98^+$ cells are tumorigenic and demonstrate increased expression of DNA repair genes [38].

Various receptor tyrosine kinase (RTK) proteins have also been found to promote chemoresistance, metastasis, and CSC properties in head and neck cancer, with therapeutic targeting of these receptors providing clinical promise. CSCs responsible for Cisplatin-resistance and metastasis have been shown to express high levels of c-Met^+, and a Phase 1 trial of selective c-MET inhibitor ARQ197 has shown early clinical success [16, 39]. The epidermal-growth factor receptor (EGFR) is another example of RTK that is highly expressed in 90% of HNSCC patients and has been linked to treatment resistance, poor clinical outcomes, and higher fraction of CSCs, which, together with CD44, has been shown to promote tumor initiation and progression *in vivo* [40]. The EGFR receptor is the target of Cetuximab, an FDA-approved antibody-based therapy currently accepted for treatment of HNSCC [41]. The interleukin-6 receptor (IL-6R) is also strongly upregulated in head and neck CSCs and enhances tumorigenicity and self-renewal via STAT3 signaling [20]. Lastly, CD117 is highly implicated in salivary gland CSCs, where it is also commonly used to isolate progenitor cells of the submandibular gland [42].

Other markers of CSCs are intracellular proteins vital to maintaining stemness such as Oct4, Sox2, Nanog, and Bmi-1. Oct 4, Sox2, and Nanog are markers of pluripotency in embryonic stem cells and crucial for these cells' property of self-renewal [43]. CSCs from oral squamous cell carcinoma patient samples exhibited high expression of Oct4 and Nanog, along with CD133, which was correlated with greater tumor stage and worse overall survival prognosis [44]. Sox2 expression in head and neck CSCs was responsible for their self-renewal, chemoresistance, invasion, and tumorigenicity *in vitro*

and *in vivo* [45]. A meta-analysis revealed that Sox2 could be utilized as an unfavorable prognostic factor for higher tumor grade, stage, and metastases [46]. Bmi-1 is a polycomb group protein involved in the regulation of normal stem cells. Head and neck CSCs also exhibit high Bmi-1 expression, which has been shown to be required for sphere formation and self-renewal, indicating that Bmi-1 is an important cellular marker for CSC stemness [47]. Interestingly, knockdown of Bmi-1 in $ALDH^+$ CSCs was shown to also downregulate expression of Oct4, Nanog, Sox2, and c-Myc among other stemness markers in these cells [48]. In MEC, intense CD44 and Bmi-1 expression was observed in the tumor invasive front, while Oct4 and Nanog was highly associated with perineural invasion *in vivo* [49].

Many of these cellular proteins have been investigated as potential therapeutic targets for HNSCC, converging in a common denominator of regulating cancer cell stemness [50]. In this review, we specifically elaborate on the role and molecular regulatory network of Bmi-1 in mediating head and neck cancer stemness. Additionally, we discuss the current literature on Bmi-1 in promoting therapeutic evasion through chemo- and radioresistance, and the potential therapeutic implications of targeting this master regulator of stemness.

3.5 Bmi-1 and Cancer Stem Cells

3.5.1 Physiological Bmi-1 Function and Regulation

Bmi-1 (**B** cell-specific **M**oloney murine leukemia virus **I**ntegration site **1**) is a 37 kDA protein that consists of three domains: N-terminal RING domain, central domain, and C-terminal proline-serine domain. The RING domain at the N-terminal forms a complex with RING1B [51, 52]. Bmi-1 is a member of the Polycomb repressive complex 1 (PRC-

1) and is involved in H2A-K119 ubiquitination [53] facilitated in part through this interaction between Bmi-1 and RING1B. Polycomb group (PcG) proteins are a family of proteins involved in transcriptional regulation that form complexes such as PRC-1 to facilitate this regulation. The central domain of Bmi-1 contains a ubiquitin-like (UBL) fold that interacts with PHC2, a polyhomeotic protein that is a member of PRC-1; the UBL region also plays a role in the homo-oligomerization of Bmi-1 [54]. Lastly, the C-terminal is a proline-serine rich domain that serves as a regulatory domain for Bmi-1 through negative regulation [55].

Bmi-1 plays a direct role in cell cycle regulation and senescence as a negative regulator of the Ink4a locus that encodes $p16^{Ink4a}$ and $p19^{Arf}$, tumor suppressor proteins. Downregulation of Bmi-1 resulted in an increase in $p16^{Ink4a}$ and $p19^{Arf}$ expression leading to senescence, while upregulation of Bmi-1 resulted in a decrease in $p16^{Ink4a}$ and $p19^{Arf}$ expression leading to tumor formation *in vivo* [56]. $p19^{Arf}$ is an upstream regulator of p53, a key tumor suppressor protein that functions by blocking MDM2-induced p53 degradation [57]. $p16^{Ink4a}$ is an upstream regulator of another tumor suppressor protein: the retinoblastoma (Rb) protein. The phosphorylation of Rb proteins by cyclin D and cyclin E-dependent kinases activates E2F transcription factors, which promotes cellular senescence through entry into the S phase of the cell cycle [58]. Thus, Bmi-1 represses two tumor suppressor proteins, $p16^{Ink4a}$ and $p19^{Arf}$, which function by activating senescence and apoptosis respectively.

Bmi-1 has also been implicated in several developmental signaling pathways including Hox, Hedgehog, and Sox2 pathways. The role of Bmi-1 in H2A-K119 ubiquitination has been linked to Hox gene silencing in mouse embryonic fibroblasts when bound to various Hox gene promoters, while Bmi-1 knockdown resulted in de-repression

of these genes. This provided evidence that Hox genes are direct targets of Bmi-1-mediated transcriptional regulation and underlines the importance of Bmi-1 in regulation of key developmental processes in progenitor cells [53]. Experiments conducted in mammary stem cells illustrated that activating Hedgehog (Hh) signaling upregulated self-renewal and Bmi-1 expression. In these cells within an *in vivo* mouse model, upregulation of Gli1 and Gli2, two downstream transcription factors of the Hh pathway, led to upregulation of Bmi-1 which suggests that Hedgehog signaling mediates stem cell self-renewal through Bmi-1 [59]. Bmi-1 is also a downstream target of Sox2, a crucial transcription factor in maintaining stem cell pluripotency and stemness in concert with Wnt signaling. Sox2 inactivation leads to strong Bmi-1 downregulation in osteoblasts *in vivo*, whereas Sox2 overexpression causes Bmi-1 upregulation, and constitutive Bmi-1 expression rescues cell senescence promoted by Sox2 inactivation [60].

Bmi-1 is also regulated by the p38 mitogen-activated protein kinase (MAPK) and Akt pathways. Epidermal growth factor (EGF)-induced Akt activation directly phosphorylates and stabilizes Bmi-1, rendering it resistant to proteasomal degradation and allowing for its nuclear accumulation, whereas p38 inhibits Akt-induced phosphorylation, destabilizing Bmi-1 and promoting increased Bmi-1 degradation in neural stem cells *in vivo* [61]. MAPKAP kinase 3 (3pk), a downstream convergence point of p38 and ERK signaling, also regulates Bmi-1 through phosphorylation. 3pK phosphorylation and activation of Bmi-1 resulted in chromatin dissociation and de-repression of Bmi-1 targets, one of which is $p14^{ARF}$ – a tumor suppressor by means of MDM2 inhibition and subsequent p53 stabilization, arresting cells in G1 cell cycle phase [62, 63]. As Bmi-1 phosphorylation by 3pk illustrates, the phosphorylation status of Bmi-

1 is inversely related to its chromatin association, allowing for fine-tuned regulation of Bmi-1 binding to chromatin throughout the cell cycle [64].

In addition to cell cycle regulation and the maintenance of the stem cell phenotype, Bmi-1 plays a role in reactive oxygen species (ROS) damage and DNA repair. The transcription factor FoxM1c is expressed highly in proliferating cells and was shown to protect them from oxidative stress-induced senescence by directly activating Bmi-1 expression via c-Myc *in vitro* and *in vivo* [65]. Deletion of c-Myc lead to a decoupling in FoxM1c-induced Bmi-1 expression, emphasizing that c-Myc serves as a bona fide regulatory intermediate in Bmi-1 signaling. Similarly, Mel-18, another polycomb group ring finger protein, downregulates Bmi-1 expression through transcriptional repression of c-Myc in human fibroblasts [66]. The absence of Bmi-1 in mice leads to an accumulation of ROS that subsequently triggers the DNA damage response (DDR) pathway [67]. The $p16^{Ink4a}$ pathway, which is negatively regulated by Bmi-1, induces ROS accumulation to promote senescence [68]. Bmi-1 is necessary for the DDR pathway and is recruited to DNA double-strand breaks, where it contributes to the repair of the DNA lesion with H2A ubiquitination [69]. Thus, Bmi-1 contributes to DNA repair through the DDR pathway, but also by preventing elevated levels of ROS in the cell.

These reported findings suggest that Bmi-1-mediated repression is a finely regulated and dynamically controlled process, with all arrows pointing to Bmi-1 as a master regulator within the PcG-mediated transcriptional system (**Fig. 3-2**).

3.5.2 Bmi-1 Regulation in Cancer

In head and neck cancer, Bmi-1 is more highly expressed in tumorigenic cells as compared to normal cells. More specifically, elevated Bmi-1 expression is predominantly

observed in $ALDH^{high}CD44^{+}$ when compared to $ALDH^{low}CD44^{-}$ cells *in vitro* and *in vivo* [19, 70], and endothelial cell-secreted factors further induce Bmi-1 expression in the CSCs [19], revealing Bmi-1 as an important player in HNSCC CSC biology. Characterizing Bmi-1 as an oncogene is a novel, active area of research in head and neck cancer, with limited literature on the exact mechanism and signaling pathways in interplay with Bmi-1. Therefore, we will also review Bmi-1-associated signaling pathways in other types of cancer here.

As elaborated above, the Ink4a locus is a direct target of Bmi-1 in normal cells. In breast cancer and oral squamous cell carcinoma, changes in Bmi-1 expression did not affect $p16^{Ink4a}$ expression, suggesting that the oncogenic activity of Bmi-1 functions through a $p16^{Ink4a}$-independent signaling pathway [71, 72]. Conversely, in laryngeal cancer, colorectal cancer, gastrointestinal cancer, and non-small cell lung cancer a significant negative correlation between Bmi-1 and Ink4a locus gene expression was observed, suggesting that Bmi-1 promotes cellular renewal through the inhibition of senescence and apoptosis [73-76]. In yet another example, Bmi-1-mediated tumorigenesis in liver cancer was not at all related to Ink4a/Arf expression but required for RasV12-driven tumor induction [77]. These contrasting findings illuminate the complex dysregulation of Bmi-1 in cancer, highlighting the need for further research in this area.

Another paradoxical relationship has been observed between Bmi-1 and Hox signaling pathways in cancer. Typically, high expression of Bmi-1 results in lower expression of Hox signaling proteins. However, in both Ewing sarcoma and certain leukemias it was observed that despite the expected elevated levels of Bmi-1 expression, there were also elevated levels of Hox expression [78, 79]. The underlying mechanism of

these surprising findings is not clear, but one hypothesis suggests that this could be due to a mutation that unlinks Bmi-1 and Hox signaling [79] Unlike with Hox signaling, the direct relationship between Hh signaling and Bmi-1 observed in normal cells appears to be maintained in cancer cells. In breast cancer, Gli-1 and Gli-2 overexpression induced Bmi-1 expression, which was necessary to promote self-renewal of both normal and malignant mammary stem cells [59]. In ovarian cancer, overexpression of various protein signaling effectors of the Hh pathway also induced Bmi-1 expression [80].

A direct relationship between the Akt pathway regulation of Bmi-1 is also observed in various cancer cells. In MEC, CSCs exhibit constitutive activation of mTOR, Akt, S6K1, and Bmi-1, and it was shown that phosphorylation of S6K1 presents a crucial step in regulation of Bmi-1 *in vitro* and *in vivo* [81]. In pancreatic cancer, overexpression of Bmi-1 induced activation of the P13K/Akt pathway by negative regulation of PTEN in CSCs [82]. In endometrial cancer, a direct correlation was found between Bmi-1 expression and Akt expression; interestingly, lower levels of both Bmi-1 and the Akt pathway were associated with more aggressive cancer phenotypes, which stands in contrast to most other cancers [83]. In gastric cancer, the microRNAs miR-498 and miR-218 inhibited Bmi-1 function, as well as EMT and Akt signaling [84, 85]. A similar finding in breast cancer showed that the PcG protein Mel-18 inhibited Bmi-1 and Akt expression, and that constitutively active Akt rescued the tumor-suppressive function of Mel-18 and Bmi-1 inhibition [86]. As previously mentioned, Mel-18 suppresses Bmi-1 through inhibition of c-myc in normal cells. This relationship between c-myc and Bmi-1 was supported in a lymphoma mouse model: overexpression of both c-myc and Bmi-1 induced transformation primary embryo fibroblasts [87].

In salivary gland cancer, p53 has been shown to play a central role in regulating the CSC phenotype via Bmi-1 [70]. Here, it was suggested that p53 reduces CSC stemness not by inducing apoptosis, but rather by regulating Bmi-1 expression via downstream p21 signaling and promoting CSC differentiation, and that this mechanism was independent of MDM2. In ACC, therapeutic inhibition of MDM2-p53 was shown to decrease the CSC fraction via apoptosis as well as an increase in cells within the G_1 phase of the cell cycle *in vitro* and *in vivo* [88]. Altogether, while Bmi-1 regulation in cancer isn't necessarily conserved as compared to its physiological regulation, these findings highlight Bmi-1 as an important player in tipping the scales between health and disease.

3.5.3 Bmi-1 in Tumorigenesis and Metastasis

As previously mentioned, Bmi-1 is highly expressed in head and neck CSCs, which drive tumorigenesis, [13] and silencing Bmi-1 leads to a reduction in stemness and tumor formation in HNSCC [48, 47]. Bmi-1^+ CSCs were shown to mediate invasion and lymph node metastases in HNSCC, specifically through increased AP-1 activity and FOSL1 activation, as determined via lineage tracing and genetic ablation studies [47]. Bmi-1^+ tumor cells formed significantly more spheres and tumors than Bmi-1^- cells, providing strong evidence for the direct role of Bmi-1 in tumorigenesis both *in vitro* and *in vivo*. In MEC, downregulation of p53 promoted tumor growth through expansion of the CSC population and upregulation of Bmi-1, providing evidence for not only the role of Bmi-1 in regulating cancer cell stemness, but also for p53 being a master regulator of cell fate within this context [70]. Due to the high rate of metastasis and recurrence observed in head and neck cancer, these findings render the role of Bmi-1 particularly significant and may lead to new therapeutic strategies.

The tumor microenvironment plays a crucial role in supporting cancer cell growth, with microenvironment-associated cytokines and growth factors defining tumorigenic potential of CSCs. In HNSCC, endothelial cell-secreted IL-6 has been shown to promote tumorigenicity of CSCs through STAT3 signaling activation and Bmi-1 expression [89, 20]. In fact, endothelial cells were shown to produce a chemotactic gradient through secreted IL-6, which enhances survival and motility of tumorigenic head and neck CSCs [20].

The epithelial-mesenchymal transition (EMT), a process through which a cell shifts from an epithelial phenotype to a more migratory mesenchymal phenotype, is a key feature of invasive cancers and metastases. In nasopharyngeal carcinoma cells, silencing Bmi-1 resulted in a reversal of EMT, exhibited by a shift in epithelial and mesenchymal markers and a reduction in metastases, indicating that Bmi-1 induces EMT resulting in a more migratory and aggressive phenotype *in vitro* [90]. This occurs via the underlying mechanism of Bmi-1 repressing PTEN, a negative regulator of the PI3K/Akt pathway, which activates this pathway and down-regulates E-cadherin in a Snail-dependent manner. Likewise, upregulating Bmi-1 in $ALDH^-$ head and neck CSCs promotes stemness properties, tumorigenicity, and migration by upregulating Snail, an EMT regulatory protein [91]. A direct regulatory link has also been established between Bmi-1 and another EMT regulatory protein, Twist1. Twist1 directly binds to the regulatory region of Bmi-1, and both interdependently promote EMT especially under hypoxic conditions [92]. Endothelial cell-secreted EGF and IL-6 were also found to induce EMT to enhance the invasive capacity of head and neck CSCs [20, 93]. The human telomerase reverse transcriptase catalytic subunit (hTERT) is involved in maintaining the telomeres of cells, thereby

prolonging cell life, and also contributes to EMT. Bmi-1 expression mirrored that of hTERT and was required for hTERT-induced EMT marker expression of oral epithelial cells via suppression of $p16^{INK4a}$ [94]. Altogether, these findings demonstrate the direct role Bmi-1 plays in EMT and therefore, to the more aggressive stem-like and migratory phenotype of tumor cells.

3.6 Bmi-1 in Cancer Therapeutics

3.6.1 Bmi-1 in Chemoresistance

The lack of progress in HNSCC, MEC, and ACC treatment can largely be attributed to therapeutic resistance of each of these cancer types, which can lead to both metastasis and recurrence; notably, CSCs are particularly resistant to therapies compared to bulk tumor cells. In the context of head and neck CSCs, Bmi-1 has been strongly implicated in therapy resistance (**Fig. 3-3**).

Cisplatin is still the most common chemotherapy agent used in treatment of HNSCC, as well as many other cancers. However, it has been shown that treatment with Cisplatin actually increases the CSC fraction in HNSCC tumors, and Cisplatin-resistant cells intrinsically express elevated levels of Bmi-1; there is also a direct association between Cisplatin dosage or resistance and Bmi-1 expression *in vitro* and *in vivo* [22, 95]. Interestingly, it has been demonstrated that Cisplatin-induced apoptosis mainly occurred in Bmi-1^- tumor cells, and that in HNSCC recurrence specifically Bmi-1^+ CSC lineages were maintained in these tumors [47]. As has been previously mentioned, the IL-6/STAT3 pathway is highly upregulated in head and neck CSCs, and IL-6 augments the Cisplatin-induction of Bmi-1 expression and CSC fraction [22, 89]. Inhibition of IL-6 signaling decreased the CSC fraction *in vitro* and *in vivo*, as well as suppressed Cisplatin-induction

of Bmi-1 expression and the CSC fraction [20, 22, 95]. Similarly, a combination treatment of an AP-1 inhibitor and Cisplatin resulted in inhibition of Bmi-1$^+$ CSCs and a reduction in metastases, suggesting a possible mechanistic pathway for chemoresistance via Bmi-1 [47]. Altogether, these results suggest a clear link between Cisplatin resistance and Bmi-1 expression and support the therapeutic strategy to include the use of either a direct Bmi-1 inhibitor or an inhibitor of a Bmi-1-associated pathway, such as those mentioned above.

Interestingly, Salinomycin, a commonly used antibiotic, successfully targeted CSCs in HNSCC, resulting in reduced Bmi-1 expression and invasive phenotypes of CSCs. When used in combination with Cisplatin or Paclitaxel, Salinomycin greatly increased overall cell death. However, it was found to increase EMT markers, Akt, and mTor signaling, which may correlate with cancer cell stemness [96]. As mentioned previously, the PI3K/Akt pathway is highly upregulated in head and neck CSCs and therapeutic inhibition of the mechanistic target of rapamycin (mTOR) has shown clinical success in head and neck cancer [97]. mTOR inhibition ablates Cisplatin-induced stemness and blocks Bmi-1 expression in MEC [98]. As opposed to in HNSCC, p53 is not oftentimes mutated in salivary gland cancers, and a major therapeutic strategy that has since been translated into clinical trials involves targeting the MDM2-p53 interaction. A small-molecule inhibitor of MDM2-p53 complex (MI-773) has been shown to potently decrease the CSC fraction, Bmi-1 expression, and tumor recurrence in both MEC and ACC [70, 88, 99, 100]. Inhibition of MDM2-p53 triggered G_1 cell cycle arrest, and sensitized tumors to Cisplatin chemotherapy [99, 100]. Altogether, these findings

illuminate a variety of strategies to overcoming CSC-mediated chemotherapeutic resistance to Cisplatin.

Comparable to the effect of Cisplatin, treatment with Metformin (diabetes drug that has exhibited anticancer properties in various other cancers) lead to a reduction in bulk tumor cells but an increase in CSCs and Bmi-1 expression in HNSCC. Metformin increased expression of Bmi-1, Oct4, Nanog, and CD44, and was revealed to bind to mitochondrial complex III, suggesting a possible role of Metformin in mediating ROS [101]. Interestingly, in prostate cancer, Cisplatin functions by elevating intracellular ROS through NADPH oxidase activation [102]. Indeed, mechanistic studies revealed that Cisplatin induces a mitochondria-dependent ROS response in conjunction with, but independent from, its well-known cytotoxic effect through inducing DNA damage [103]. Therefore, it is hypothesized that many cytotoxic effects of chemotherapeutic agents function through ROS, eliciting protective effects on CSCs and Bmi-1 function. This relates to results described above regarding the role Bmi-1 plays in maintenance of low ROS levels and in the DDR pathway. By elevating ROS and DNA damage levels in the cell, Cisplatin is likely activating Bmi-1 for response to these stimuli, inadvertently activating cancer cell stemness properties.

Thus, further investigation into targeted therapies is necessary, but the treatment for head and neck cancers will likely entail a combination of systemic cytotoxic therapies and CSC-targeted therapies such as small molecule inhibitors of Bmi-1.

3.6.2 Bmi-1 in Radioresistance

In parallel to chemoresistance, radioresistance poses another obstacle in successful treatment of head and neck cancers. In HNSCC, silencing Bmi-1 activity in

$ALDH^+$ CSCs led to increased apoptotic activity as detected via Annexin V staining, resulting in decreased radioresistance and an overall higher survival rate in a mouse model [48]. In nasopharyngeal cancer, silencing Bmi-1 resulted in re-sensitization to radiation therapy through increased apoptotic activity of p53 and increased production of ROS [104]. These findings implicated Bmi-1 in contributing to HNSCC CSC radioresistance.

Further literature on the role of Bmi-1 in head and neck cancer radioresistance is limited. However, notable findings have been reported in other cancers. Elevated levels of Bmi-1 were also observed in adaptively radioresistant esophageal squamous cell carcinoma (ESCC) cells, where Bmi-1 silencing led to re-sensitization to radiation therapy [105]. Similar to the observations made in nasopharyngeal cancer, Bmi-1 conferred adaptive radioresistance to ESCC cells, and Bmi-1-depleted cells treated with radiotherapy expressed elevated levels of ROS and impaired DNA repair capacities, further supporting a common mechanism by which Bmi-1 mediates therapeutic resistance [105]. In breast cancer cells, Bmi-1 expression was also indicative of radioresistance. Upon Bmi-1 knockdown, increased DNA double strand breaks, reduced DNA repair, and increased apoptosis through elevated p53, p21 and Bax protein expression was observed [106]. In glioblastomas, radiation therapy primarily functions by halting senescence and it was shown that Bmi-1 confers radioresistance by inhibiting cell senescence through the p16 signaling pathway [107]. Reduction of Bmi-1 expression by overexpression of microRNA-128 in glioma cells also promoted radiosensitivity and prevalence of senescent cells [108].

Collectively, these studies suggest that Bmi-1 promotes radioresistance through decreased levels of ROS, increased DNA repair, and suppression of senescence through mechanisms resembling those that arbitrate chemoresistance. This also strongly implicates Bmi-1 as a powerful point of convergence in multiple therapeutic resistance mechanisms of different treatment modalities across many cancers.

3.6.3 Bmi-1 as a Prognostic Factor

We have reviewed the prominent impact Bmi-1 has on tumorigenesis, metastasis, and therapy resistance of head and neck cancers. Yet, there are many unanswered questions: How does this translate to overall patient survival? How can we leverage this knowledge to better make predictions about patient prognoses and treatment outcomes?

Few research studies to date have robustly investigated Bmi-1 expression patterns in head and neck cancer. Bmi-1 expression in tumor tissue of oropharyngeal squamous cell carcinoma was significantly higher as compared to normal mucosa, but no difference in expression was observed between the primary tumor and lymph node metastases [109]. This expression pattern was observed in both HPV-negative and HPV-positive samples (n=12). In another study, HPV-positive human oropharyngeal squamous cell carcinoma specimens showed lower Bmi-1 expression than HPV-negative tumors (n=202) [110]. In human tissue specimens, Bmi-1 expression was significantly higher in oral squamous cell carcinoma but showed no difference between normal mucosa and oral dysplasia (n=129) [111]. Thus, more elaborate studies are needed to determine the relevance of Bmi-1 expression in head and neck cancer, especially in relation to HPV status and disease progression.

In one study analyzing CSC markers as prognostic factors for HNSCC, it was observed that both Bmi-1 and CD44 are indicators for poorer prognosis of overall and disease-free survival in patients receiving primary radio-chemotherapy irrespective of HPV status (n=85) [112]. Conversely, in SCC of the tongue, a strong correlation was observed between low Bmi-1 expression and poor patient prognosis (n=73) [113], and in a separate meta-analysis (n=2143), Bmi-1 did not impact overall HNSCC survival significantly [114]. In another study, Bmi-1 expression in patient samples (n=216) was correlated with poor prognosis of recurrence-free survival, but not overall survival [95]. These observations may indeed be explained by the CSC hypothesis, since the small CSC fraction may not significantly contribute to overall tumor growth and survival, but to tumor recurrence or metastases. This ambiguity illustrates a definitive need for further research on Bmi-1 as a prognostic factor in HNSCC.

In other cancers, Bmi-1 has been a more promising negative prognosticator. Bmi-1 overexpression has been reported in a plethora of cancers, including gastric, ovarian, breast, head and neck, pancreatic, lung, hepatocellular, and endometrial carcinoma and correlated with a variety of indicators of poor prognoses as described elsewhere [82]. A meta-analysis of non-small cell lung cancer revealed a correlation between elevated Bmi-1 expression and increased tumor size, metastasis, and lower overall survival rates [115]. Bmi-1 was also found to be a negative prognostic factor in gastric cancer and endometrial adenocarcinoma, each demonstrating heightened Bmi-1 expression to be indicative of worse clinical stage, lymph node metastases, and overall survival [116, 117]. Based on these varied and contradictory findings, the utility of Bmi-1 as a prognostic factor remains unclear. One plausible explanation for this may be the lack of expression analyses

specific to a tumor subsite or clonal cell population. As mentioned previously, tumor cells as well as a plethora of stromal cells from the tumor microenvironment express Bmi-1, which highly clouds the prognostic value of this marker. While these studies do not yet provide convincing evidence for Bmi-1 serving as a possible way to prognosticate treatment response, Bmi-1 is undoubtedly an important master regulator of cancer cell stemness and therapeutic resistance, rendering it a putative therapeutic target, nonetheless.

3.6.4 Therapeutic Targeting of Bmi-1

Bmi-1 has emerged as an attractive therapeutic target in CSC-focused, mechanism-based cancer treatments. Therapeutic inhibition of Bmi-1 was first described in a primary colorectal cancer xenograft model, where it inhibited CSC self-renewal and thus abrogated their tumorigenic potential [118]. The anti-PD-1 immunotherapies Nivolumab and Pembrolizumab have been approved as first-line therapies for HNSCC and are commonly combined with Cisplatin treatment. In an *in vivo* mouse model of HNSCC, Bmi-1$^+$ CSCs were enriched in tumors following treatment with Cisplatin and anti-PD-1 therapy, but treatment with the Bmi-1 inhibitor PTC209 prevented induction of these cells and tumor progression [119]. In this study, Bmi-1 inhibition was also shown to promote CD8$^+$ T-cell infiltration by removing repressive H2A ubiquitination to induce transcription of chemokines necessary for their recruitment. Interestingly, Bmi-1 may play a significant role as immune modifier in several *in vivo* studies: Bmi-1 inhibition restored B-cell-mediated humoral immune responses via increased antibody function [120]. Immune escape of pancreatic cancer cells from NK cell-mediated elimination in a hyperglycemic tumor microenvironment was also shown to be mediated by upregulation

of Bmi-1 and subsequent MICA/B inhibition and GATA2 promotion [121]. In a murine myeloma model, Bmi-1 inhibition eliminated tumor-associated macrophages and mediated chemoresistance [122].

The therapeutic potential of Bmi-1 inhibitors has also been investigated in early human clinical trials. In a Phase 1 multi-center, open-label study in patients with advanced solid tumors, the second-generation Bmi-1 inhibitor PTC596 was determined to be tolerable with manageable side effects [123]. Notably, PTC596 was shown to be successful in the treatment of acute leukemia in an *in vitro* study irrespective of p53 mutational status, which could provide highly beneficial in the treatment of salivary gland cancers which typically demonstrate high mutational burden of p53 [124]. Another Bmi-1 inhibitor, PRT4165, prevents accumulation of all detectable H2A ubiquitination sites around DNA double-stranded breaks in an osteosarcoma model, which could be highly relevant in combination with antiproliferative chemotherapies that propagate the DNA damage response as mentioned in Figure 3-3 [125]. In an ovarian cancer model, the Bmi-1 inhibitor PTC028 was shown to selectively inhibit cancer cell growth while leaving normal cells unaffected, which could present a unique benefit as compared to conventional chemotherapeutic agents that do not selectively eliminate tumor cells [126]. While there are limited published studies on the efficacy of Bmi-1 inhibitors in head and neck cancers, the success of these small molecule drugs in treatment of other cancers in preclinical and clinical models strongly supports their therapeutic potential.

3.7 Conclusion

There has been modest progress in the outcome of head and neck cancer patients, in part due to therapy resistance which can be attributed to the function of CSCs in

tumorigenesis and tumor dissemination. This emphasizes the need for further research into the underlying mechanisms regulating the CSC phenotype. Bmi-1, a polycomb complex protein, has been established as a pivotal player in controlling cancer cell stemness. It has been implicated in many major signaling pathways such as the $p16^{Ink4a}$/$p19^{Arf}$, PI3K/Akt, MAPK, STAT3, and Hedgehog pathways. It also plays vital roles in cellular processes responding to ROS and DNA damage. In cancer, it has been widely linked to increased stemness, tumor formation and metastasis, as well as therapeutic resistance. This review attempted to synthesize the current evidence on Bmi-1 within the context of head and neck cancer stem cells, and to provide support for future research aimed at targeting this master regulator of cancer cell stemness using novel therapeutic approaches.

3.8 Acknowledgements

This work was funded by NIH/NIDCR F30-DE029097 (AEH), R01-DE21139 (JEN), and R01-DE23220 (JEN).

3.9 Figures

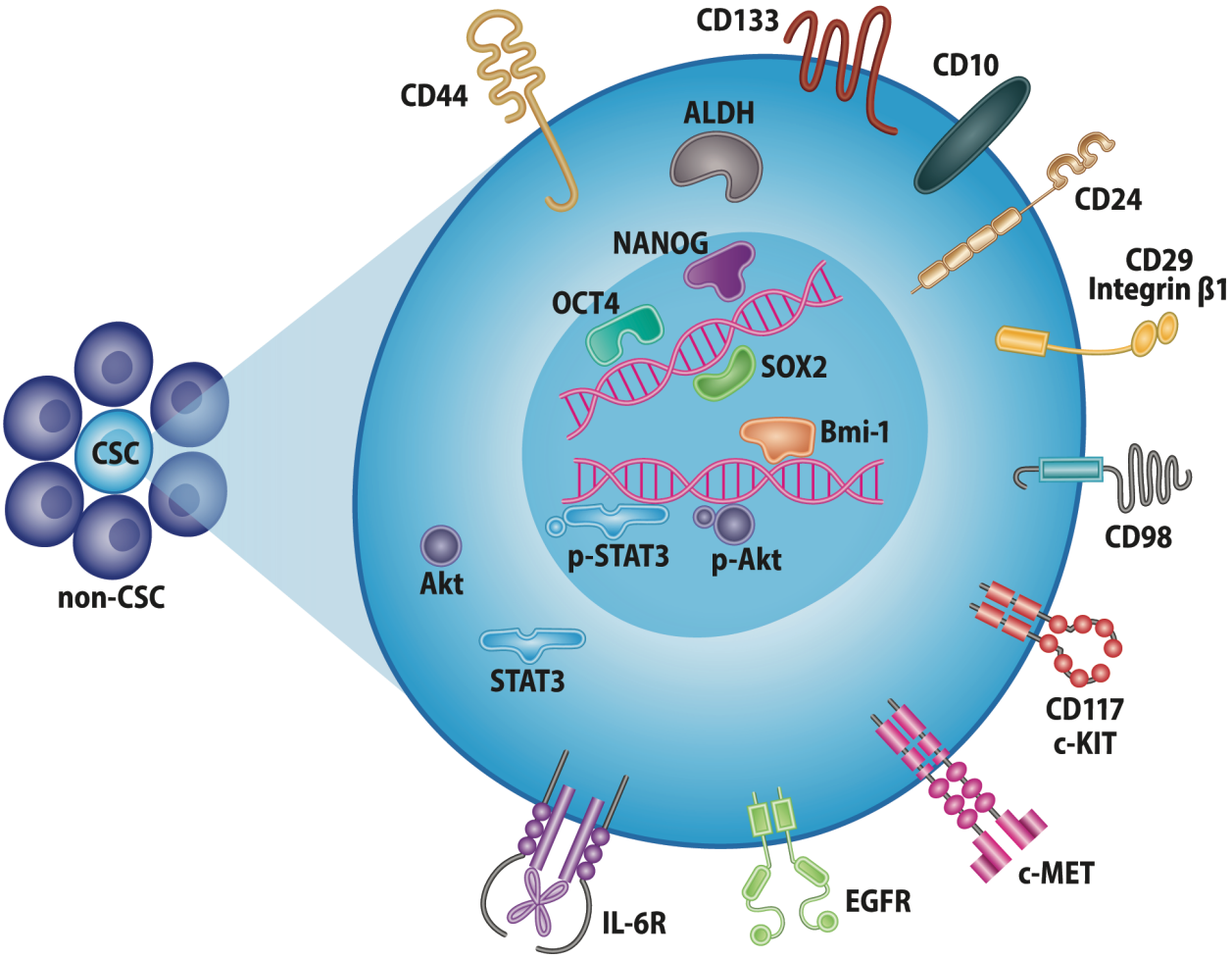

Figure 3-1: Markers of head and neck cancer stem cells.

Selected proteins currently used for identification of CSCs in head and neck cancer. These include, but are not limited to, various cell-surface glycoproteins, receptor tyrosine kinases, intracellular enzymes, and transcription factors.

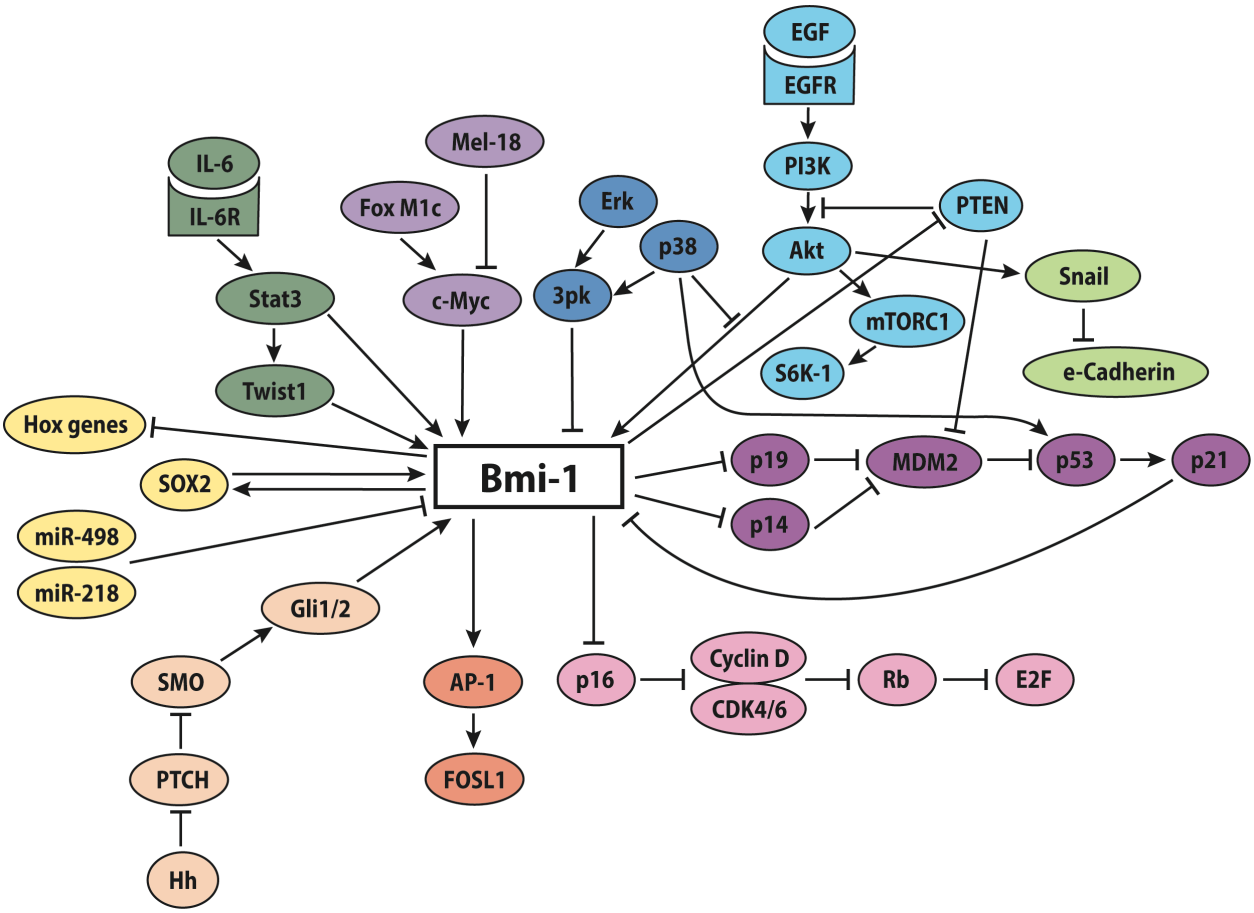

Figure 3-2: Potential involvement of Bmi-1 in key signaling pathways.

The proposed molecular signaling network of Bmi-1 promotes increased stemness, self-renewal, and proliferation, while decreasing apoptosis, differentiation, and senescence.

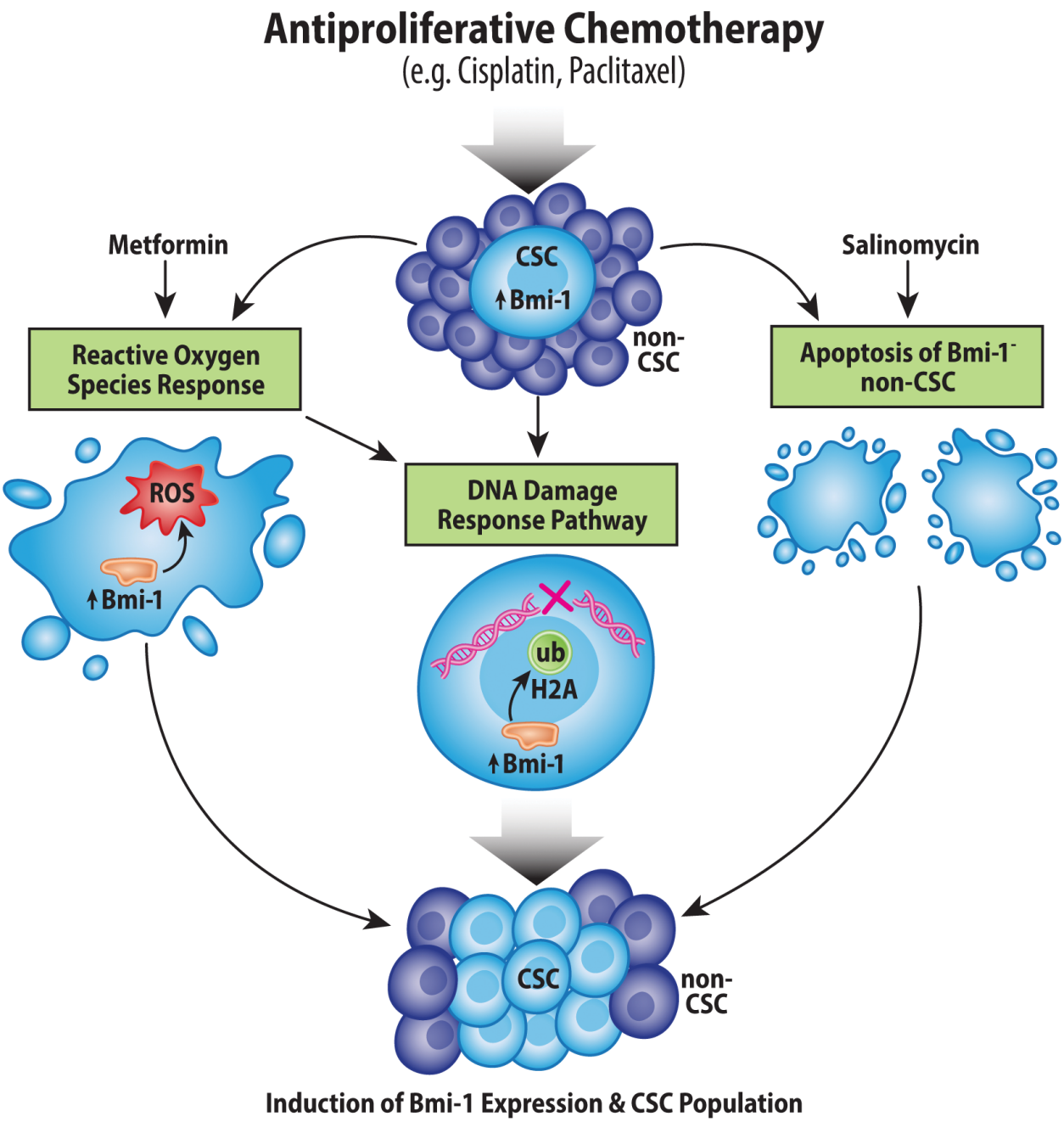

Figure 3-3: Chemotherapeutic induction of Bmi-1 increases the cancer stem cell population.

Antiproliferative chemotherapeutic agents currently used for treatment of head and neck cancers have been shown to increase the CSC fraction in tumors via multiple mechanisms, which include inducing the reactive oxygen species response, the DNA damage response pathway, and apoptosis of Bmi-1$^-$ CSCs.

3.10 References

[1] Siegel RL, Miller KD, Fuchs HE, Jemal A. Cancer statistics, 2021. Ca Cancer J Clin. 2021 Jan 12;71(1):7-33.

[2] Zaravinos A. An updated overview of HPV-associated head and neck carcinomas. Oncotarget. 2014 Jun;5(12):3956.

[3] Moskovitz J, Moy J, Ferris RL. Immunotherapy for head and neck squamous cell carcinoma. Current oncology reports. 2018 Feb;20(2):1-7.

[4] Cramer JD, Burtness B, Le QT, Ferris RL. The changing therapeutic landscape of head and neck cancer. Nature reviews Clinical oncology. 2019 Nov;16(11):669-83.

[5] Seethala RR, Stenman G. Update from the 4th edition of the World Health Organization classification of head and neck tumours: tumors of the salivary gland. Head and neck pathology. 2017 Mar;11(1):55-67.

[6] Speight PM, Barrett AW. Salivary gland tumours. Oral diseases. 2002 Sep;8(5):229-40.

[7] Chintakuntlawar AV, Okuno SH, Price KA. Systemic therapy for recurrent or metastatic salivary gland malignancies. Cancers of the Head & Neck. 2016 Dec;1(1):1-9.

[8] Sahara S, Herzog AE, Nör JE. Systemic therapies for salivary gland adenoid cystic carcinoma. American Journal of Cancer Research. 2021;11(9):4092.

[9] Nowell PC. The Clonal Evolution of Tumor Cell Populations: Acquired genetic lability permits stepwise selection of variant sublines and underlies tumor progression. Science. 1976 Oct 1;194(4260):23-8.

[10] Reya T, Morrison SJ, Clarke MF, Weissman IL. Stem cells, cancer, and cancer stem cells. nature. 2001 Nov;414(6859):105-11.

[11] Sell S. Stem cell origin of cancer and differentiation therapy. Critical reviews in oncology/hematology. 2004 Jul 1;51(1):1-28.

[12] Costea DE, Tsinkalovsky O, Vintermyr OK, Johannessen AC, Mackenzie IC. Cancer stem cells–new and potentially important targets for the therapy of oral squamous cell carcinoma. Oral diseases. 2006 Sep;12(5):443-54.

[13] Prince ME, Sivanandan R, Kaczorowski A, Wolf GT, Kaplan MJ, Dalerba P, Weissman IL, Clarke MF, Ailles L. Identification of a subpopulation of cells with cancer stem cell properties in head and neck squamous cell carcinoma. Proceedings of the National Academy of Sciences. 2007 Jan 16;104(3):973-8.

[14] Krishnamurthy S, Nör JE. Head and neck cancer stem cells. Journal of dental research. 2012 Apr;91(4):334-40.

[15] Adams A, Warner K, Pearson AT, Zhang Z, Kim HS, Mochizuki D, Basura G, Helman J, Mantesso A, Castilho RM, Wicha MS, Nor JE. ALDH/CD44 identifies uniquely tumorigenic cancer stem cells in salivary gland mucoepidermoid carcinomas. Oncotarget. 2015 Sep 9;6(29):26633.

[16] Sun S, Wang Z. Head neck squamous cell carcinoma c-Met+ cells display cancer stem cell properties and are responsible for cisplatin-resistance and metastasis. International Journal of Cancer. 2011 Nov 15;129(10):2337-48.

[17] Keysar SB, Eagles JR, Miller B, Jackson BC, Chowdhury FN, Reisinger J, Chimed TS, Le PN, Morton JJ, Somerset HL, Varella-Garcia M. Salivary Gland Cancer Patient-Derived Xenografts Enable Characterization of Cancer Stem Cells and

New Gene Events Associated with Tumor ProgressionSalivary Cancer Stem Cells Increase with Disease Progression. Clinical Cancer Research. 2018 Jun 15;24(12):2935-43.

[18] Chen C, Wei Y, Hummel M, Hoffmann TK, Gross M, Kaufmann AM, Albers AE. Evidence for epithelial-mesenchymal transition in cancer stem cells of head and neck squamous cell carcinoma. PloS one. 2011 Jan 27;6(1):e16466.

[19] Krishnamurthy S, Dong Z, Vodopyanov D, Imai A, Helman JI, Prince ME, Wicha MS, Nör JE. Endothelial Cell-Initiated Signaling Promotes the Survival and Self-Renewal of Cancer Stem Cells Head and Neck Cancer Stem Cell Niche. Cancer research. 2010 Dec 1;70(23):9969-78.

[20] Kim HS, Chen YC, Nör F, Warner KA, Andrews A, Wagner VP, Zhang Z, Zhang Z, Martins MD, Pearson AT, Yoon E. Endothelial-derived interleukin-6 induces cancer stem cell motility by generating a chemotactic gradient towards blood vessels. Oncotarget. 2017 Nov 11;8(59):100339.

[21] Reid PA, Wilson P, Li Y, Marcu LG, Bezak E. Current understanding of cancer stem cells: Review of their radiobiology and role in head and neck cancers. Head & neck. 2017 Sep;39(9):1920-32.

[22] Nör C, Zhang Z, Warner KA, Bernardi L, Visioli F, Helman JI, Roesler R, Nör JE. Cisplatin induces Bmi-1 and enhances the stem cell fraction in head and neck cancer. Neoplasia. 2014 Feb 1;16(2):137-W8.

[23] Sayed SI, Dwivedi RC, Katna R, Garg A, Pathak KA, Nutting CM, Rhys-Evans P, Harrington KJ, Kazi R. Implications of understanding cancer stem cell (CSC)

biology in head and neck squamous cell cancer. Oral oncology. 2011 Apr 1;47(4):237-43.

[24] Facompre N, Nakagawa H, Herlyn M, Basu D. Stem-like cells and therapy resistance in squamous cell carcinomas. Advances in pharmacology. 2012 Jan 1;65:235-65.

[25] Mack B, Gires O. CD44s and CD44v6 expression in head and neck epithelia. PloS one. 2008 Oct 9;3(10):e3360.

[26] Clay MR, Tabor M, Owen JH, Carey TE, Bradford CR, Wolf GT, Wicha MS, Prince ME. Single-marker identification of head and neck squamous cell carcinoma cancer stem cells with aldehyde dehydrogenase. Head & neck. 2010 Sep;32(9):1195-201.

[27] Bertrand G, Maalouf M, Boivin A, Battiston-Montagne P, Beuve M, Levy A, Jalade P, Fournier C, Ardail D, Magné N, Alphonse G. Targeting head and neck cancer stem cells to overcome resistance to photon and carbon ion radiation. Stem Cell Reviews and Reports. 2014 Feb;10(1):114-26.

[28] Chen YC, Chen YW, Hsu HS, Tseng LM, Huang PI, Lu KH, Chen DT, Tai LK, Yung MC, Chang SC, Ku HH. Aldehyde dehydrogenase 1 is a putative marker for cancer stem cells in head and neck squamous cancer. Biochemical and biophysical research communications. 2009 Jul 31;385(3):307-13.

[29] Kokko LL, Hurme S, Maula SM, Alanen K, Grénman R, Kinnunen I, Ventelä S. Significance of site-specific prognosis of cancer stem cell marker CD44 in head and neck squamous-cell carcinoma. Oral oncology. 2011 Jun 1;47(6):510-6.

[30] Dong Y, Ochsenreither S, Cai C, Kaufmann AM, Albers AE, Qian X. Aldehyde dehydrogenase 1 isoenzyme expression as a marker of cancer stem cells

correlates to histopathological features in head and neck cancer: A meta-analysis. PloS one. 2017 Nov 7;12(11):e0187615.

[31] Chen D, Wang CY. Targeting cancer stem cells in squamous cell carcinoma. Precision Clinical Medicine. 2019 Sep;2(3):152-65.

[32] Zhang Q, Shi S, Yen Y, Brown J, Ta JQ, Le AD. A subpopulation of CD133+ cancer stem-like cells characterized in human oral squamous cell carcinoma confer resistance to chemotherapy. Cancer letters. 2010 Mar 28;289(2):151-60.

[33] Chen YS, Wu MJ, Huang CY, Lin SC, Chuang TH, Yu CC, Lo JF. CD133/Src axis mediates tumor initiating property and epithelial-mesenchymal transition of head and neck cancer. PloS one. 2011 Nov 28;6(11):e28053.

[34] Fukusumi T, Ishii H, Konno M, Yasui T, Nakahara S, Takenaka Y, Yamamoto Y, Nishikawa S, Kano Y, Ogawa H, Hasegawa S. CD10 as a novel marker of therapeutic resistance and cancer stem cells in head and neck squamous cell carcinoma. British journal of cancer. 2014 Jul;111(3):506-14.

[35] Li Q, Wang Y, Xu L, Wang L, Guo Y, Guo C. High level of CD10 expression is associated with poor overall survival in patients with head and neck cancer. International Journal of Oral and Maxillofacial Surgery. 2021 Jul 1;50(7):857-64.

[36] Zimmerer RM, Ludwig N, Kampmann A, Bittermann G, Spalthoff S, Jungheim M, Gellrich NC, Tavassol F. CD24+ tumor-initiating cells from oral squamous cell carcinoma induce initial angiogenesis in vivo. Microvascular Research. 2017 Jul 1;112:101-8.

[37] Lin HC, Wu CL, Chen YL, Huang JS, Wong TY, Yuan K. High-level β1-integrin expression in a subpopulation of highly tumorigenic oral cancer cells. Clinical oral investigations. 2014 May;18(4):1277-84.

[38] Martens-de Kemp SR, Brink A, Stigter-van Walsum M, Damen JM, Rustenburg F, Wu T, van Wieringen WN, Schuurhuis GJ, Braakhuis BJ, Slijper M, Brakenhoff RH. CD98 marks a subpopulation of head and neck squamous cell carcinoma cells with stem cell properties. Stem cell research. 2013 May 1;10(3):477-88.

[39] Yap TA, Olmos D, Brunetto AT, Tunariu N, Barriuso J, Riisnaes R, Pope L, Clark J, Futreal A, Germuska M, Collins D. Phase I trial of a selective c-MET inhibitor ARQ 197 incorporating proof of mechanism pharmacodynamic studies. Journal of clinical oncology: official journal of the American Society of Clinical Oncology. 2011 Apr 1;29(10):1271-9.

[40] Perez A, Neskey DM, Wen J, Pereira L, Reategui EP, Goodwin WJ, Carraway KL, Franzmann EJ. CD44 interacts with EGFR and promotes head and neck squamous cell carcinoma initiation and progression. Oral oncology. 2013 Apr 1;49(4):306-13.

[41] Rehmani HS, Issaeva N. EGFR in head and neck squamous cell carcinoma: exploring possibilities of novel drug combinations. Annals of Translational Medicine. 2020 Jul;8(13).

[42] Adams A, Warner K, Nör JE. Salivary gland cancer stem cells. Oral oncology. 2013 Sep 1;49(9):845-53.

[43] Boiani M, Schöler HR. Regulatory networks in embryo-derived pluripotent stem cells. Nature reviews Molecular cell biology. 2005 Nov;6(11):872-81.

[44] Chiou SH, Yu CC, Huang CY, Lin SC, Liu CJ, Tsai TH, Chou SH, Chien CS, Ku HH, Lo JF. Positive correlations of Oct-4 and Nanog in oral cancer stem-like cells and high-grade oral squamous cell carcinoma. Clinical cancer research. 2008 Jul 1;14(13):4085-95.

[45] Lee SH, Oh SY, Do SI, Lee HJ, Kang HJ, Rho YS, Bae WJ, Lim YC. SOX2 regulates self-renewal and tumorigenicity of stem-like cells of head and neck squamous cell carcinoma. British journal of cancer. 2014 Nov;111(11):2122-30.

[46] Dong Z, Liu G, Huang B, Sun J, Wu D. Prognostic significance of SOX2 in head and neck cancer: a meta-analysis. International journal of clinical and experimental medicine. 2014;7(12):5010.

[47] Chen D, Wu M, Li Y, Chang I, Yuan Q, Ekimyan-Salvo M, Deng P, Yu B, Yu Y, Dong J, Szymanski JM. Targeting BMI1+ cancer stem cells overcomes chemoresistance and inhibits metastases in squamous cell carcinoma. Cell stem cell. 2017 May 4;20(5):621-34.

[48] Chen YC, Chang CJ, Hsu HS, Chen YW, Tai LK, Tseng LM, Chiou GY, Chang SC, Kao SY, Chiou SH, Lo WL. Inhibition of tumorigenicity and enhancement of radiochemosensitivity in head and neck squamous cell cancer-derived ALDH1-positive cells by knockdown of Bmi-1. Oral oncology. 2010 Mar 1;46(3):158-65.

[49] Destro Rodrigues MF, Sedassari BT, Esteves CM, de Andrade NP, Altemani A, de Sousa SC, Nunes FD. Embryonic stem cells markers Oct4 and Nanog correlate with perineural invasion in human salivary gland mucoepidermoid carcinoma. Journal of Oral Pathology & Medicine. 2017 Feb;46(2):112-20.

[50] Oklejas AE, Nör JE. Overcoming head and neck cancer stem cells. In: Improving the Therapeutic Ratio in Head and Neck Cancer 2020 Jan 1 (pp. 135-158). Academic Press.

[51] Buchwald G, van der Stoop P, Weichenrieder O, Perrakis A, van Lohuizen M, Sixma TK. Structure and E3-ligase activity of the Ring–Ring complex of Polycomb proteins Bmi1 and Ring1b. The EMBO journal. 2006 Jun 7;25(11):2465-74.

[52] Li Z, Cao R, Wang M, Myers MP, Zhang Y, Xu RM. Structure of a Bmi-1-Ring1B polycomb group ubiquitin ligase complex. Journal of Biological Chemistry. 2006 Jul 21;281(29):20643-9.

[53] Cao R, Tsukada YI, Zhang Y. Role of Bmi-1 and Ring1A in H2A ubiquitylation and Hox gene silencing. Molecular cell. 2005 Dec 22;20(6):845-54.

[54] Gray F, Cho HJ, Shukla S, He S, Harris A, Boytsov B, Jaremko Ł, Jaremko M, Demeler B, Lawlor ER, Grembecka J. BMI1 regulates PRC1 architecture and activity through homo-and hetero-oligomerization. Nature communications. 2016 Nov 9;7(1):1-2.

[55] Yadav AK, Sahasrabuddhe AA, Dimri M, Bommi PV, Sainger R, Dimri GP. Deletion analysis of BMI1 oncoprotein identifies its negative regulatory domain. Molecular cancer. 2010 Dec;9(1):1-3.

[56] Jacobs JJ, Kieboom K, Marino S, DePinho RA, Van Lohuizen M. The oncogene and Polycomb-group gene bmi-1 regulates cell proliferation and senescence through the ink4a locus. Nature. 1999 Jan;397(6715):164-8.

[57] Pomerantz J, Schreiber-Agus N, Liégeois NJ, Silverman A, Alland L, Chin L, Potes J, Chen K, Orlow I, Lee HW, Cordon-Cardo C. The Ink4a tumor suppressor gene

product, p19Arf, interacts with MDM2 and neutralizes MDM2's inhibition of p53. Cell. 1998 Mar 20;92(6):713-23.

[58] Lowe SW, Sherr CJ. Tumor suppression by Ink4a–Arf: progress and puzzles. Current opinion in genetics & development. 2003 Feb 1;13(1):77-83.

[59] Liu S, Dontu G, Mantle ID, Patel S, Ahn NS, Jackson KW, Suri P, Wicha MS. Hedgehog signaling and Bmi-1 regulate self-renewal of normal and malignant human mammary stem cells. Cancer research. 2006 Jun 15;66(12):6063-71.

[60] Seo E, Basu-Roy U, Zavadil J, Basilico C, Mansukhani A. Distinct functions of Sox2 control self-renewal and differentiation in the osteoblast lineage. Molecular and cellular biology. 2011 Nov 15;31(22):4593-608.

[61] Kim J, Hwangbo J, Wong PK. p38 MAPK-Mediated Bmi-1 down-regulation and defective proliferation in ATM-deficient neural stem cells can be restored by Akt activation. PLoS One. 2011 Jan 28;6(1):e16615.

[62] Voncken JW, Niessen H, Neufeld B, Rennefahrt U, Dahlmans V, Kubben N, Holzer B, Ludwig S, Rapp UR. MAPKAP kinase 3pK phosphorylates and regulates chromatin association of the polycomb group protein Bmi1. Journal of Biological Chemistry. 2005 Feb 18;280(7):5178-87.

[63] Zhang Y, Xiong Y, Yarbrough WG. ARF promotes MDM2 degradation and stabilizes p53: ARF-INK4a locus deletion impairs both the Rb and p53 tumor suppression pathways. Cell. 1998 Mar 20;92(6):725-34.

[64] Voncken JW, Schweizer D, Aagaard L, Sattler L, Jantsch MF, van Lohuizen M. Chromatin-association of the Polycomb group protein BMI1 is cell cycle-regulated

and correlates with its phosphorylation status. Journal of cell science. 1999 Dec 15;112(24):4627-39.

[65] Li SK, Smith DK, Leung WY, Cheung AM, Lam EW, Dimri GP, Yao KM. FoxM1c counteracts oxidative stress-induced senescence and stimulates Bmi-1 expression. Journal of Biological Chemistry. 2008 Jun 13;283(24):16545-53.

[66] Guo WJ, Datta S, Band V, Dimri GP. Mel-18, a polycomb group protein, regulates cell proliferation and senescence via transcriptional repression of Bmi-1 and c-Myc oncoproteins. Molecular biology of the cell. 2007 Feb;18(2):536-46.

[67] Liu J, Cao L, Chen J, Song S, Lee IH, Quijano C, Liu H, Keyvanfar K, Chen H, Cao LY, Ahn BH. Bmi1 regulates mitochondrial function and the DNA damage response pathway. Nature. 2009 May;459(7245):387-92.

[68] Takahashi A, Ohtani N, Yamakoshi K, Iida SI, Tahara H, Nakayama K, Nakayama KI, Ide T, Saya H, Hara E. Mitogenic signalling and the p16INK4a–Rb pathway cooperate to enforce irreversible cellular senescence. Nature cell biology. 2006 Nov;8(11):1291-7.

[69] Ismail IH, Andrin C, McDonald D, Hendzel MJ. BMI1-mediated histone ubiquitylation promotes DNA double-strand break repair. Journal of Cell Biology. 2010 Oct 4;191(1):45-60.

[70] Rodriguez-Ramirez C, Zhang Z, Warner KA, Herzog AE, Mantesso A, Zhang Z, Yoon E, Wang S, Wicha MS, Nör JE. p53 inhibits Bmi-1-driven self-renewal and defines salivary gland cancer stemness. Clinical Cancer Research. 2022 Sep 1.

[71] Silva J, García JM, Peña C, García V, Domínguez G, Suárez D, Camacho FI, Espinosa R, Provencio M, España P, Bonilla F. Implication of polycomb members

Bmi-1, Mel-18, and Hpc-2 in the regulation of p16INK4a, p14ARF, h-TERT, and c-Myc expression in primary breast carcinomas. Clinical cancer research. 2006 Dec 1;12(23):6929-36.

[72] Kang MK, Kim RH, Kim SJ, Yip FK, Shin KH, Dimri GP, Christensen R, Han T, Park NH. Elevated Bmi-1 expression is associated with dysplastic cell transformation during oral carcinogenesis and is required for cancer cell replication and survival. British Journal of Cancer. 2007 Jan;96(1):126-33.

[73] Wei X, He J, Wang J, Yang X, Ma B. Bmi-1 is essential for the oncogenic potential in CD133+ human laryngeal cancer cells. Tumor Biology. 2015 Nov;36(11):8931-42.

[74] Kim JH, Yoon SY, Kim CN, Joo JH, Moon SK, Choe IS, Choe YK, Kim JW. The Bmi-1 oncoprotein is overexpressed in human colorectal cancer and correlates with the reduced p16INK4a/p14ARF proteins. Cancer letters. 2004 Jan 1;203(2):217-24.

[75] Wang JL, Wu JH, Hong C, Wang YN, Zhou Y, Long ZW, Zhou Y, Qin HS. Involvement of Bmi-1 gene in the development of gastrointestinal stromal tumor by regulating p16Ink4A/p14ARF gene expressions: An in vivo and in vitro study. Pathology-Research and Practice. 2017 Dec 1;213(12):1542-51.

[76] Vonlanthen S, Heighway J, Altermatt HJ, Gugger M, Kappeler A, Borner MM, Van Lohuizen M, Betticher DC. The bmi-1 oncoprotein is differentially expressed in non-small cell lung cancer and correlates with INK4A-ARF locus expression. British journal of cancer. 2001 May;84(10):1372-6.

[77] Xu CR, Lee S, Ho C, Bommi P, Huang SA, Cheung ST, Dimri GP, Chen X. Bmi1 Functions as an Oncogene Independent of Ink4A/Arf Repression in Hepatic

CarcinogenesisBmi1 in Liver Cancer Development. Molecular Cancer Research. 2009 Dec 1;7(12):1937-45.

[78] Svoboda LK, Harris A, Bailey NJ, Schwentner R, Tomazou E, von Levetzow C, Magnuson B, Ljungman M, Kovar H, Lawlor ER. Overexpression of HOX genes is prevalent in Ewing sarcoma and is associated with altered epigenetic regulation of developmental transcription programs. Epigenetics. 2014 Dec 2;9(12):1613-25.

[79] Andreeff M, Ruvolo V, Gadgil S, Zeng C, Coombes K, Chen W, Kornblau S, Barón AE, Drabkin HA. HOX expression patterns identify a common signature for favorable AML. Leukemia. 2008 Nov;22(11):2041-7.

[80] Bhattacharya R, Kwon J, Ali B, Wang E, Patra S, Shridhar V, Mukherjee P. Role of hedgehog signaling in ovarian cancer. Clinical Cancer Research. 2008 Dec 1;14(23):7659-66.

[81] Andrade NP, Warner KA, Zhang Z, Pearson AT, Mantesso A, Guimaraēs DM, Altemani A, Mariano FV, Nunes FD, Nör JE. Survival of salivary gland cancer stem cells requires mTOR signaling. Cell death & disease. 2021 Jan 21;12(1):1-6.

[82] Wang MC, Li CL, Cui J, Jiao M, Wu T, Jing LI, Nan KJ. BMI 1, a promising therapeutic target for human cancer. Oncology letters. 2015 Aug 1;10(2):583-8.

[83] Zaczek A, Jóźwiak P, Ciesielski P, Forma E, Wójcik-Krowiranda K, Cwonda Ł, Bieńkiewicz A, Bryś M, Krześlak A. Relationship between polycomb-group protein BMI-1 and phosphatases regulating AKT phosphorylation level in endometrial cancer. Journal of cellular and molecular medicine. 2020 Jan;24(2):1300-10.

[84] You D, Wang D, Liu P, Chu Y, Zhang X, Ding X, Li X, Mao T, Jing X, Tian Z, Pan Y. MicroRNA-498 inhibits the proliferation, migration and invasion of gastric cancer

through targeting BMI-1 and suppressing AKT pathway. Human Cell. 2020 Apr;33(2):366-76.

[85] Wu Y, Tian S, Chen Y, Ji M, Qu Y, Hou P. miR-218 inhibits gastric tumorigenesis through regulating Bmi-1/Akt signaling pathway. Pathology-Research and Practice. 2019 Feb 1;215(2):243-50.

[86] Guo WJ, Zeng MS, Yadav A, Song LB, Guo BH, Band V, Dimri GP. Mel-18 acts as a tumor suppressor by repressing Bmi-1 expression and down-regulating Akt activity in breast cancer cells. Cancer research. 2007 Jun 1;67(11):5083-9.

[87] Jacobs JJ, Scheijen B, Voncken JW, Kieboom K, Berns A, van Lohuizen M. Bmi-1 collaborates with c-Myc in tumorigenesis by inhibiting c-Myc-induced apoptosis via INK4a/ARF. Genes & development. 1999 Oct 15;13(20):2678-90.

[88] Warner KA, Nör F, Acasigua GA, Martins MD, Zhang Z, McLean SA, Spector ME, Chepeha DB, Helman J, Wick MJ, Moskaluk CA. Targeting MDM2 for Treatment of Adenoid Cystic CarcinomaMDM2 Inhibition in Adenoid Cystic Carcinoma. Clinical Cancer Research. 2016 Jul 15;22(14):3550-9.

[89] Krishnamurthy S, Warner KA, Dong Z, Imai A, Nör C, Ward BB, Helman JI, Taichman RS, Bellile EL, McCauley LK, Polverini PJ. Endothelial interleukin-6 defines the tumorigenic potential of primary human cancer stem cells. Stem cells. 2014 Nov;32(11):2845-57.

[90] Song LB, Li J, Liao WT, Feng Y, Yu CP, Hu LJ, Kong QL, Xu LH, Zhang X, Liu WL, Li MZ. The polycomb group protein Bmi-1 represses the tumor suppressor PTEN and induces epithelial-mesenchymal transition in human nasopharyngeal epithelial cells. The Journal of clinical investigation. 2009 Dec 1;119(12):3626-36.

[91] Yu CC, Lo WL, Chen YW, Huang PI, Hsu HS, Tseng LM, Hung SC, Kao SY, Chang CJ, Chiou SH. Bmi-1 regulates snail expression and promotes metastasis ability in head and neck squamous cancer-derived ALDH1 positive cells. Journal of oncology. 2011 Oct;2011.

[92] Yang MH, Hsu DS, Wang HW, Wang HJ, Lan HY, Yang WH, Huang CH, Kao SY, Tzeng CH, Tai SK, Chang SY. Bmi1 is essential in Twist1-induced epithelial–mesenchymal transition. Nature cell biology. 2010 Oct;12(10):982-92.

[93] Zhang Z, Dong Z, Lauxen IS, Nör JE. Endothelial Cell-Secreted EGF Induces Epithelial to Mesenchymal Transition and Endows Head and Neck Cancer Cells with Stem-like PhenotypeEndothelial EGF and Cancer Stem Cells. Cancer research. 2014 May 15;74(10):2869-81.

[94] Qiao B, Chen Z, Hu F, Tao Q, Lam AK. BMI-1 activation is crucial in hTERT-induced epithelial–mesenchymal transition of oral epithelial cells. Experimental and molecular pathology. 2013 Aug 1;95(1):57-61.

[95] Herzog AE, Warner KA, Zhang Z, Bellile E, Bhagat MA, Castilho RM, Wolf GT, Polverini PJ, Pearson AT, Nör JE. The IL-6R and Bmi-1 axis controls self-renewal and chemoresistance of head and neck cancer stem cells. Cell death & disease. 2021 Oct 23;12(11):1-2.

[96] Kuo SZ, Blair KJ, Rahimy E, Kiang A, Abhold E, Fan JB, Wang-Rodriguez J, Altuna X, Ongkeko WM. Salinomycin induces cell death and differentiation in head and neck squamous cell carcinoma stem cells despite activation of epithelial-mesenchymal transition and Akt. BMC cancer. 2012 Dec;12(1):1-4.

[97] Magaway C, Kim E, Jacinto E. Targeting mTOR and metabolism in cancer: lessons and innovations. Cells. 2019 Dec 6;8(12):1584.

[98] Nakano T, Warner KA, Oklejas AE, Zhang Z, Rodriguez-Ramirez C, Shuman AG, Nör JE. mTOR inhibition ablates cisplatin-resistant salivary gland cancer stem cells. Journal of dental research. 2021 Apr;100(4):377-86.

[99] Andrews A, Warner K, Rodriguez-Ramirez C, Pearson AT, Nör F, Zhang Z, Kerk S, Kulkarni A, Helman JI, Brenner JC, Wicha MS. Ablation of Cancer Stem Cells by Therapeutic Inhibition of the MDM2–p53 Interaction in Mucoepidermoid CarcinomaMDM2 Inhibition and Cancer Stem Cells. Clinical Cancer Research. 2019 Mar 1;25(5):1588-600.

[100] Nör F, Warner KA, Zhang Z, Acasigua GA, Pearson AT, Kerk SA, Helman JI, Sant'Ana Filho M, Wang S, Nör JE. Therapeutic Inhibition of the MDM2–p53 Interaction Prevents Recurrence of Adenoid Cystic CarcinomasMDM2 Inhibition in Adenoid Cystic Carcinoma. Clinical cancer research. 2017 Feb 15;23(4):1036-48.

[101] Kuo SZ, Honda CO, Li WT, Honda TK, Kim E, Altuna X, Abhold E, Wang-Rodriguez J, Ongkeko WM. Metformin results in diametrically opposed effects by targeting non-stem cancer cells but protecting cancer stem cells in head and neck squamous cell carcinoma. International journal of molecular sciences. 2019 Jan 7;20(1):193.

[102] Itoh T, Terazawa R, Kojima K, Nakane K, Deguchi T, Ando M, Tsukamasa Y, Ito M, Nozawa Y. Cisplatin induces production of reactive oxygen species via NADPH oxidase activation in human prostate cancer cells. Free radical research. 2011 Sep 1;45(9):1033-9.

[103] Marullo R, Werner E, Degtyareva N, Moore B, Altavilla G, Ramalingam SS, Doetsch PW. Cisplatin induces a mitochondrial-ROS response that contributes to cytotoxicity depending on mitochondrial redox status and bioenergetic functions. PloS one. 2013 Nov 19;8(11):e81162.

[104] Alajez NM, Shi W, Hui AB, Yue S, Ng R, Lo KW, Bastianutto C, O'sullivan B, Gullane P, Liu FF. Targeted depletion of BMI1 sensitizes tumor cells to P53-mediated apoptosis in response to radiation therapy. Cell Death & Differentiation. 2009 Nov;16(11):1469-79.

[105] Wang G, Liu L, Sharma S, Liu H, Yang W, Sun X, Dong Q. Bmi-1 confers adaptive radioresistance to KYSE-150R esophageal carcinoma cells. Biochemical and Biophysical Research Communications. 2012 Aug 24;425(2):309-14.

[106] Liu ZG, Liu L, Xu LH, Yi W, Tao YL, Tu ZW, Li MZ, Zeng MS, Xia YF. Bmi-1 induces radioresistance in MCF-7 mammary carcinoma cells. Oncology reports. 2012 Apr 1;27(4):1116-22.

[107] Ye L, Wang C, Yu G, Jiang Y, Sun D, Zhang Z, Yu X, Li X, Wei W, Liu P, Cheng J. Bmi 1 induces radioresistance by suppressing senescence in human U87 glioma cells. Oncology letters. 2014 Dec 1;8(6):2601-6.

[108] Sun J, Ye L, Wang C, Li N, Wang D, Li X. MicroRNA-128 increases glioma cell radio-sensitivity by suppressing senescent evasion through oncogene Bmi-1. International Journal of Clinical and Experimental Pathology. 2018;11(3):1423.

[109] Sharaf K, Lechner A, Haider SP, Wiebringhaus R, Walz C, Kranz G, Canis M, Haubner F, Gires O, Baumeister P. Discrimination of Cancer Stem Cell Markers

ALDH1A1, BCL11B, BMI-1, and CD44 in Different Tissues of HNSCC Patients. Current Oncology. 2021 Jul 19;28(4):2763-74.

[110] Mohamed H, Hagström J, Jouhi L, Atula T, Almangush A, Mäkitie A, Haglund C. The expression and prognostic value of stem cell markers Bmi-1, HESC5: 3, and HES77 in human papillomavirus–positive and–negative oropharyngeal squamous cell carcinoma. Tumor Biology. 2019 Mar;41(3):1010428319840473.

[111] Wu TF, Li YC, Ma SR, Bing-Liu, Zhang WF, Sun ZJ. Expression and associations of TRAF1, BMI-1, ALDH1, and Lin28B in oral squamous cell carcinoma. Tumor Biology. 2017 Apr;39(4):1010428317695930.

[112] Jakob M, Sharaf K, Schirmer M, Leu M, Küffer S, Bertlich M, Ihler F, Haubner F, Canis M, Kitz J. Role of cancer stem cell markers ALDH1, BCL11B, BMI-1, and CD44 in the prognosis of advanced HNSCC. Strahlentherapie und Onkologie. 2021 Mar;197(3):231-45.

[113] Häyry V, Mäkinen LK, Atula T, Sariola H, Mäkitie A, Leivo I, Keski-Säntti H, Lundin J, Haglund C, Hagström J. Bmi-1 expression predicts prognosis in squamous cell carcinoma of the tongue. British journal of cancer. 2010 Mar;102(5):892-7.

[114] Fan Z, Li M, Chen X, Wang J, Liang X, Wang H, Wang Z, Cheng B, Xia J. Prognostic value of cancer stem cell markers in head and neck squamous cell carcinoma: a meta-analysis. Scientific reports. 2017 Feb 21;7(1):1-8.

[115] Zhang X, Tian T, Sun W, Liu C, Fang X. Bmi-1 overexpression as an efficient prognostic marker in patients with nonsmall cell lung cancer. Medicine. 2017 Jun;96(26).

[116] Yuan B, Zhao H, Xue X, Zhou J, Wang X, Han Y, Zhang L, Guo X, Zhi Q. Prognostic value and clinicopathological differences of Bmi1 in gastric cancer: a meta-analysis. Anti-Cancer Agents in Medicinal Chemistry (Formerly Current Medicinal Chemistry-Anti-Cancer Agents). 2016 Apr 1;16(4):407-13.

[117] Yu J, Chen L, Bao Z, Liu Y, Liu G, Li F, Li L. BMI 1 promotes invasion and metastasis in endometrial adenocarcinoma and is a poor prognostic factor. Oncology Reports. 2020 May 1;43(5):1630-40.

[118] Kreso A, Van Galen P, Pedley NM, Lima-Fernandes E, Frelin C, Davis T, Cao L, Baiazitov R, Du W, Sydorenko N, Moon YC. Self-renewal as a therapeutic target in human colorectal cancer. Nature medicine. 2014 Jan;20(1):29-36.

[119] Jia L, Zhang W, Wang CY. BMI1 inhibition eliminates residual cancer stem cells after PD1 blockade and activates antitumor immunity to prevent metastasis and relapse. Cell Stem Cell. 2020 Aug 6;27(2):238-53.

[120] Di Pietro A, Polmear J, Cooper L, Damelang T, Hussain T, Hailes L, O'Donnell K, Udupa V, Mi T, Preston S, Shtewe A. Targeting BMI-1 in B cells restores effective humoral immune responses and controls chronic viral infection. Nature Immunology. 2022 Jan;23(1):86-98.

[121] Duan Q, Li H, Gao C, Zhao H, Wu S, Wu H, Wang C, Shen Q, Yin T. High glucose promotes pancreatic cancer cells to escape from immune surveillance via AMPK-Bmi1-GATA2-MICA/B pathway. Journal of Experimental & Clinical Cancer Research. 2019 Dec;38(1):1-3.

[122] Zhang D, Huang J, Wang F, Ding H, Cui Y, Yang Y, Xu J, Luo H, Gao Y, Pan L, Wu Y. BMI1 regulates multiple myeloma-associated macrophage's pro-myeloma functions. Cell death & disease. 2021 May 15;12(5):1-6.

[123] Infante JR, Bedard PL, Shapiro G, Bauer TM, Prawira A, Laskin O, Weetall M, Baird J, Branstrom A, O'Mara E, Spiegel RJ. Phase 1 results of PTC596, a novel small molecule targeting cancer stem cells (CSCs) by reducing levels of BMI1 protein.

[124] Seipel K, Kopp B, Bacher U, Pabst T. BMI1-Inhibitor PTC596 in combination with MCL1 inhibitor S63845 or MEK inhibitor trametinib in the treatment of acute leukemia. Cancers. 2021 Feb 2;13(3):581.

[125] Ismail IH, McDonald D, Strickfaden H, Xu Z, Hendzel MJ. A small molecule inhibitor of polycomb repressive complex 1 inhibits ubiquitin signaling at DNA double-strand breaks. Journal of Biological Chemistry. 2013 Sep 13;288(37):26944-54.

[126] Dey A, Xiong X, Crim A, Dwivedi SK, Mustafi SB, Mukherjee P, Cao L, Sydorenko N, Baiazitov R, Moon YC, Dumble M. Evaluating the mechanism and therapeutic potential of PTC-028, a novel inhibitor of BMI-1 function in ovarian cancer. Molecular cancer therapeutics. 2018 Jan;17(1):39-49.

CHAPTER 4:
Bmi-1 Mediates Resistance of Head and Neck Cancer Stem Cells to Cytotoxic Chemotherapy

4.1 Abstract

Cancer stem cells (CSC) drive therapeutic resistance and recurrence in head and neck squamous cell carcinoma (HNSCC). Bmi-1 is highly expressed in CSCs, and treatment with common antiproliferative chemotherapies such as Cisplatin and Carboplatin augments its expression and the fraction of CSCs. These classes of cytotoxic chemotherapy function by inducing DNA damage, and Bmi-1 is known to play a crucial role in the DNA repair response. Here, we hypothesize that Bmi-1 inhibition will suppress the chemotherapy-mediated increase in the CSC fraction and their self-renewal, thereby overcoming CSC resistance to Cisplatin therapy. We observed that both shRNA-mediated genetic knockdown of Bmi-1 as well as pharmacologic inhibition using the small molecule inhibitor PTC596 abrogates the increase of CSC fraction, sphere formation, and DNA damage response by cytotoxic chemotherapy. HNSCC cells were treated with Cisplatin or Carboplatin *in vitro* and subjected to stemness analyses to evaluate the impact of Bmi-1 signaling on chemoresistance. We observed that Bmi-1 knockdown and inhibition resulted in decreased expression of several stemness markers and signaling effectors, particularly in the IL-6R/STAT3 pathway, even in combination with both chemotherapies. Treatment with PTC596 also suppressed Cisplatin-mediated increase of the CSC fraction in a scaffold xenograft model *in vivo*. These results demonstrate that

Bmi-1 mediates Cisplatin resistance in CSCs and that this may occur through induction of DNA damage. This work unveils crucial molecular mechanisms underlying CSC maintenance and therapeutic resistance, which have the potential to inform novel CSC-targeted therapies for patients with head and neck cancer.

4.2 Introduction

Head and Neck Squamous Cell Carcinoma (HNSCC) is one of the most prevalent solid tumors worldwide yet exhibits unacceptably poor overall patient survival rates (Siegel *et al.,* 2021). Notably, 20-40% of the increasing mortality rate is ascribed to treatment resistance and consequent tumor recurrences or metastases (Carvalho *et al.,* 2005). Current treatment modalities for HNSCC include surgical resection, radiation, and chemotherapy, all of which commonly correlate with increased patient morbidity, disease relapse, and are oftentimes debilitating (Cramer *et al.,* 2019). Though platinum-based antiproliferative chemotherapies such as Cisplatin and Carboplatin remain the cornerstone of systemic treatments for HNSCC through control of tumor growth (Sindhu *et al.,* 2019), residual tumor cells have been shown to undertake a more aggressive phenotype that promotes disease progression and development of evasive resistance (Goldman *et al.,* 2015; Seiwert et al., 2007). Importantly, HPV-negative HNSCC patients present with higher recurrence rates and a worse prognosis as compared with HPV-positive cases (Koneva *et al.,* 2018). Despite modern chemotherapeutic regimes reducing the detectable tumor burden, surviving cancer cells pose a significant threat to long-term disease remission and require the development of more effective treatment strategies.

Cancer stem cells (CSCs) comprise a highly tumorigenic subpopulation of cancer cells shown to be responsible for tumor recurrence and metastasis, as well as resistant

to cytotoxic therapies such as Cisplatin, thus leading to therapeutic evasion (Chinn et al., 2015; Prager et al., 2019). In HNSCC, these cells are characterized by high aldehyde dehydrogenase (ALDH) activity and high CD44 expression (Prince *et al.,* 2007; Krishnamurthy et al., 2010). $ALDH^{+}CD44^{+}$ cells express higher levels of Bmi-1, a master regulator of stem cell self-renewal that has been implicated in mediating HNSCC stemness and tumor formation (Chen *et al.,* 2010). $Bmi\text{-}1^{+}$ CSCs have been shown to mediate chemoresistance and metastasis in HNSCC, and Cisplatin-induced apoptosis was limited to $Bmi\text{-}1^{-}$ cells (Chen *et al.,* 2017). Notably, within the HNSCC tumor microenvironment, endothelial cell-secreted IL-6 promotes CSC tumorigenicity and Bmi-1 expression via STAT3 signaling activation and has been correlated with poor survival of patients with HNSCC (Kim *et al.,* 2017; Duffy *et al.,* 2008). In HNSCC, Cisplatin has been shown to augment the IL-6-mediated induction of the CSC fraction and Bmi-1 expression, and Cisplatin-resistant cells intrinsically exhibit increased Bmi-1 expression (Nör *et al.,* 2014). We have previously demonstrated that IL-6/STAT3 signaling regulates Bmi-1 expression, and that this defines the self-renewal and resistance of HNSCC CSCs (Herzog *et al.,* 2021).

Chemotherapies such as Cisplatin and Carboplatin achieve their cytotoxic activity by crosslinking DNA and inducing its damage. Bmi-1 is a key mediator of the DNA damage response (DDR) pathway (Ismail *et al.,* 2010), and as such may be inadvertently activated in cancer cells after treatment with cytotoxic chemotherapies. In fact, it has been shown that DNA damage following genotoxic chemotherapy results in IL-6 release by tumor-associated endothelial cells, thereby maintaining a subpopulation of cancer cells capable of fueling disease relapse (Gilbert *et al.,* 2010). These findings suggest that

therapeutic ablation of CSCs is crucial for improved efficacy of current chemotherapies and presents compelling arguments for incorporation of a mechanism-based therapy to target Bmi-1 in HNSCC.

Based on our previous findings that therapeutic inhibition of the IL-6R and Bmi-1 signaling axis overcomes chemoresistance of CSCs in HNSCC (Herzog *et al.,* 2021), we here utilize PTC596 (Unesbulin, Selleckchem) to elucidate the role of Bmi-1 in mediating chemoresistance of head and neck CSCs. PTC596 is a second-generation Bmi-1 inhibitor that accelerates Bmi-1 degradation and is currently used in NCI-supported clinical trials (e.g. NCT03605550, NCT03761059, NCT03206645) for advanced solid tumors (Shapiro *et al.,* 2021). Considering our previous findings and the recent promise of Bmi-1 inhibitors as therapeutic agents for cancer, we decided to evaluate the role of Bmi-1 in mediating chemoresistance of head and neck CSCs. Here, we demonstrate that genetic knockdown and pharmacologic inhibition of Bmi-1 inhibits CSC function and suppresses CSC self-renewal induced by cytotoxic chemotherapy, both *in vitro* and *in vivo*. Collectively, these preclinical findings demonstrate clear rationale for therapeutic inhibition of Bmi-1 as a viable strategy to overcome CSC-mediated chemoresistance and to improve the survival and health standard of head and neck cancer patients.

4.3 Results

4.3.1 Bmi-1 knockdown decreases expression of the IL-6/STAT3 signaling axis and regulates cancer cell self-renewal.

To determine the effect of Bmi-1 expression in HNSCC cells, we knocked down Bmi-1 protein levels in UM-SCC-1, UM-SCC-22A, and UM-SCC-22B cells using lentiviral short hairpin RNA (shRNA) constructs. Successful Bmi-1 silencing was obtained with

sequences shBmi-1 (3) in UM-SCC-1 and UM-SCC-22B, and shBmi-1 (2) in UM-SCC-22A, which served as the selected Bmi-1 knockdown sequences for subsequent experiments (**Fig. 4-1A**). We have previously shown that the IL-6/STAT3 signaling axis is upregulated in CSCs and IL-6 augments Cisplatin-induced Bmi-1 expression (Nor et al., 2014; Herzog et al., 2021). Bmi-1 knockdown decreased expression of IL-6Rα and levels of phosphorylated STAT3, whereas the shRNA sequences that resulted in increased Bmi-1 expression correlated with increased expression of these proteins (**Fig. 4-1A**). To determine whether Bmi-1 knockdown affects expression of these signaling effectors in CSCs after treatment with Cisplatin, we employed the orosphere assay to functionally enrich the population for CSCs (Krishnamurthy et al., 2013). As previously shown, Cisplatin increased expression of the IL-6/STAT3 signaling axis and Bmi-1 in orosphere lysates (Herzog et al., 2021), but Bmi-1 knockdown prevented this induction of protein expression (**Fig. 4-1B**). Bmi-1 knockdown resulted in decreased number and size of orospheres formed, even in presence of Cisplatin treatment (**Fig. 4-1C and D,** Supplemental Fig. 4-6A). Of note, the shRNA sequences that resulted in increased Bmi-1 expression promoted higher orosphere formation, which was augmented by Cisplatin. These findings support Bmi-1 as a master regulator of CSC stemness, potentially through regulation of the IL-6/STAT3 signaling axis.

4.3.2 Bmi-1 knockdown suppresses increase in CSC fraction by treatment with cytotoxic chemotherapy and mediates the DNA damage response.

To assess the impact of genotoxic chemotherapies on Bmi-1 expression and the DNA damage response, three different HNSCC cell lines were treated with Cisplatin or Carboplatin. To evaluate the effect on the DNA damage response, we measured

phosphorylated H2AX expression, which plays a key role in the DNA damage repair (DDR) pathway as a marker required for assembly of DNA repair proteins at sites of chromatin damage from double-stranded DNA breaks (Podhorecka *et al.,* 2010). As expected, we observed that Cisplatin and Carboplatin induced Bmi-1 expression and phosphorylation of histone H2AX in a dose-dependent manner in untransfected UM-SCC-1, UM-SCC-22A, and UM-SCC-22B cells (**Fig. 4-2A and B**) and selected the treatment concentration of 1 μM for both chemotherapies for subsequent experiments.

To determine the role of Bmi-1 in regulating IL-6/STAT3 signaling and the DNA damage response in CSCs versus bulk tumor cells, we harvested protein lysates from Bmi-1 knockdown and control cells treated with Cisplatin or Carboplatin, grown under both normal and ultra-low attachment conditions (**Fig. 4-2C and D**). In cells grown under normal attachment conditions, Bmi-1 knockdown prevented the increase of Bmi-1 expression, IL-6/STAT3 signaling, and levels of pH2AX induced by Cisplatin and Carboplatin (**Fig. 4-2C**). Notably, Bmi-1 knockdown was more effective in suppressing this chemotherapy-induced protein expression in orospheres as compared to cells grown under normal attachment conditions (**Fig. 4-2D**). This was particularly apparent in UM-SCC-1 and UM-SCC-22A cell lines, which represent cells isolated from two different primary patient tumors. Orospheres are formed by CSCs and are known to express higher levels of IL-6R and Bmi-1 than cells under normal attachment conditions (Krishnamurthy et al., 2013; Xu et al., 2019; Chen et al., 2016), supporting these findings that Bmi-1 is a key regulator of signaling mechanisms within the CSC population. To assess the significance of Bmi-1 mediating CSC self-renewal, the orosphere assay was employed. Cisplatin and Carboplatin increased orosphere formation in all three cell lines, and Bmi-1

knockdown prevented this increase (**Fig. 4-2E and F**). Cisplatin and Carboplatin did not markedly increase the size of orospheres, whereas Bmi-1 knockdown significantly decreased their size even in presence of either chemotherapy (Supplemental Fig. 4-7A).

Lastly, we directly assessed the effect of Bmi-1 knockdown on the CSC fraction via flow cytometry analysis (**Fig. 4-2G**, Supplemental Fig. 4-7B and C), which showed a decrease in $ALDH^{high}CD44^{high}$ cells (**Fig. 4-2H**). Remarkably, Cisplatin and Carboplatin increased the fraction of CSCs in all three cell lines, and Bmi-1 knockdown successfully prevented this increase. These data support the significance of Bmi-1 as a pivotal regulator of IL-6/STAT3 signaling, DNA damage response, and self-renewal of head and neck CSCs, especially in response to genotoxic chemotherapy.

4.3.3 Bmi-1 inhibition with PTC596 prevents the Cisplatin-induced self-renewal and fraction of CSCs.

To verify our observations of Bmi-1 regulation of CSC chemoresistance with a pharmacologic approach, we utilized the small molecule Bmi-1 inhibitor PTC596. Due to observations that PTC596 induces cancer cell apoptosis in a caspase-3-dependent manner (Wu *et al.,* 2021), we measured protein expression of cleaved-caspase-3 to evaluate apoptosis of HNSCC cells upon treatment with PTC596. We observed that PTC596 decreased Bmi-1 expression and increased cleaved caspase-3 expression in a dose-dependent manner in UM-SCC-1, UM-SCC-22A, and UM-SCC-22B cells (**Fig. 4-3A**) and selected the treatment concentration of 200 nM for subsequent experiments in all three cell lines.

To corroborate our findings of Bmi-1-mediated protein expression changes presented in **Figure 4-2C and D**, we next sought to determine whether PTC596 prevents

the Cisplatin-induced Bmi-1 expression, IL-6/STAT3 activation, and DNA damage response in HNSCC cells grown in both normal attachment conditions as well as orospheres. As previously shown, orospheres express higher levels of Bmi-1 and IL-6/STAT3 signaling effectors at baseline, which is increased upon treatment with Cisplatin (**Fig. 4-3B**). We observed that PTC596 potently suppresses this increase even in combination with Cisplatin in both orospheres and cells grown in normal attachment conditions. PTC596 suppressed the DNA damage response as measured by phosphorylated H2AX in both orospheres and cells grown in normal attachment conditions. Interestingly, orospheres formed by UM-SCC-22B cells exhibited overall higher levels of DNA damage response as compared to their normal attachment culture, which was not the case for either UM-SCC-1 or UM-SCC-22A cells. Of note, PTC596 was shown to preferentially induce activation of caspase-3 in sphere lysates, even in presence of Cisplatin (**Fig. 4-3B**).

To evaluate the efficacy of PTC596 in modulating CSC self-renewal, the orosphere assay was employed (**Fig. 4-3C**). As previously shown, Cisplatin increased the number (**Fig. 4-3D**) and size (**Fig. 4-3C**, Supplemental Fig. 4-8A) of orospheres in all three HNSCC cell lines. However, PTC596 reduced the number and size of orospheres in all cell lines, both as a single agent therapy and in combination with Cisplatin (**Fig. 4-3C and D**, Supplemental Fig. 4-8A). The combination of Cisplatin and PTC596 demonstrated similar efficacy in reducing orosphere formation to PTC596 alone but was more effective in decreasing sphere number formed by UM-SCC-1 cells.

Consistent with the Cisplatin-induced increase in orosphere formation, Cisplatin treatment also increased the CSC fraction in all three cell lines as measured by the

percentage of $ALDH^{high}CD44^{high}$ cells via flow cytometry analysis (**Fig. 4-3E and F**, Supplemental Fig. 4-8B and C). Comparable to our results employing genetic Bmi-1 knockdown, inhibition of Bmi-1 by PTC596 decreased the CSC fraction as compared to baseline and suppressed the Cisplatin-induced CSC fraction in a combinatorial therapy approach (**Fig. 4-3F**). These findings further support Bmi-1 as a pivotal player in overcoming Cisplatin-induction of the CSC population, potentially by inhibiting the DNA damage response and promoting apoptosis in CSCs. Overall, these findings suggest that Bmi-1 signaling is a central regulator of CSC chemoresistance in HNSCC, and that a treatment strategy combining both Cisplatin and PTC596 prevents acquisition of the stem-like phenotype within HNSCC cells observed upon single-agent Cisplatin treatment.

4.3.4 PTC596 suppresses Cisplatin-induced CSC fraction in subcutaneous xenograft model of HNSCC in vivo.

As deduced by the cancer stem cell hypothesis, therapeutic elimination of CSCs is essential to prevent disease relapse in the form of tumor recurrence or metastasis (Reya et al., 2001). To evaluate the therapeutic potential of PTC596 in preventing the Cisplatin-induced increase in CSC fraction in a preclinical scenario, we utilized a HNSCC subcutaneous scaffold xenograft model for a short-term *in vivo* study. As we have previously shown, short term *in vivo* treatment with Cisplatin and a CSC-targeted agent are both sufficient and preferred to assess the therapeutic effect on the CSC fraction as opposed to long-term tumor growth (Herzog et al., 2021; Sahara et al., 2023). Once tumors grew to an average volume of 180 mm^3 (Supplemental Fig. 4C), mice were randomly allocated to treatment groups (n = 10) including treatment with either vehicle, Cisplatin, PTC596, or the combination of Cisplatin and PTC596. Treatments were

administered on days 0, 3, and 6, and mice were euthanized on day 7 (**Fig. 4-4A**). As mentioned, the primary purpose of this short-term experiment was to determine the therapeutic effect on tumor CSC fraction, as opposed to tumor growth. As such, we did not expect to observe a difference in tumor growth over the course of this experiment (**Fig. 4-4B-D,** Supplemental Fig. 4-9D and E). Notably, mice did not experience any weight loss as compared to their pretreatment weight throughout the course of this treatment (Supplemental Fig. 4-9B).

To directly evaluate the effect of this treatment on the tumor CSC fraction *in vivo*, we performed flow cytometry analysis of ALDH activity and CD44 expression of tumor cells (**Fig. 4-4F**). Congruous with our previous findings (Herzog et al., 2021; Nör et al., 2014), treatment with Cisplatin increased the CSC fraction in subcutaneous xenograft tumors formed by UM-SCC-22A cells (**Fig. 4-4G**). Importantly, treatment with PTC596 alone decreased the CSC fraction in tumors as well as prevented the Cisplatin-mediated increase of the CSC fraction. Western blot analyses of tumor tissue lysates confirmed increased Bmi-1 and STAT3 signaling after treatment with Cisplatin and demonstrated that PTC596 inhibited Bmi-1 expression and STAT3 activation *in vivo*, even when combined with Cisplatin treatment (**Fig. 4-4E**, Supplemental Fig. 4-9A). As shown *in vitro,* PTC596 suppressed the DNA damage response and activated caspase-3 within tumors even in combination with Cisplatin.

These results corroborate our *in vitro* findings, where PTC596 suppressed increase of the CSC fraction induced by Cisplatin, as well as activation of the IL-6/STAT3 signaling axis. These data emphasize that although cytotoxic therapies such as Cisplatin are regarded as the gold standard for treatment in HNSCC, a CSC-targeting agent such

as PTC596 is necessary to prevent the increase of the tumor CSC fraction. Similarly, due to the fraction of CSCs only encompassing a small proportion of total tumor cells, any CSC-targeted therapy must be combined with a chemotherapy that is effective in targeting the bulk tumor cells.

4.3.5 Bmi-1 defines the self-renewal capacity of HNSCC cells.

The sphere formation assay has been universally accepted as a functional method to enrich for stem cell populations in physiological and pathological cell cultures without the need for specific cell markers. However, the conventional sphere assay utilizing ultra-low attachment dishes or well plates presents limitations in experimental setup and analysis of resultant spheres, e.g. lack of high-throughput, standardized single-sphere treatment and imaging. Here, we utilized an automated liquid handler robot and imaging system to enable analysis of orospheres formed by Bmi-1 knockdown and control cells treated with Cisplatin or Carboplatin on a single-sphere basis. In an initial concentration assay, we determined the ideal cell seeding number of 4,500 cells per well for all three cell lines (Supplemental Fig. 4-10A and B). Regardless of the initial number of cells seeded, Bmi-1 knockdown strongly inhibited orosphere formation in all cell lines. Orospheres that were able to form from Bmi-1 knockdown cells were significantly smaller than orospheres formed by control cells (**Fig. 4-5A-C**, Supplemental Fig. 4-10A and B), as measured by transmitted light images or fluorescence images of GFP signal expressed from the shRNA plasmid construct of transfected Bmi-1 knockdown and control cells.

To evaluate the consequence of Bmi-1 knockdown on CSC stemness and self-renewal in context of treatment with cytotoxic chemotherapy, we treated orospheres either on day 1 or day 3 after cell seeding. Treatment on day 1 attempts to prevent

maturation of orospheres, thus targeting cancer cell stemness, whereas treatment on day 3 attempts to eradicate matured orospheres, thus targeting cancer cell self-renewal. Interestingly, Cisplatin and Carboplatin did not affect orosphere size for either treatment strategy, but Bmi-1 knockdown significantly decreased orosphere size (**Fig. 4-5A-C**). This decrease was more evident upon treatment on day 3 (**Fig. 4-5C**), particularly in UM-SCC-22B cells which did not exhibit a difference in size upon treatment on day 1 (**Fig. 4-5B**). This supports our previous data that Bmi-1 is a crucial regulator of CSC self-renewal, as well as a mediator of CSC stemness. To assess the effect of cytotoxic chemotherapy on eliminating cells within orospheres formed by Bmi-1 knockdown and control cells, we stained them with propidium iodide at termination of these experiments. Bmi-1 knockdown decreased the percentage of PI^+ cells upon treatment on day 1 only in the UM-SCC-22A cell line and to a more significant extent upon treatment on day 3, as well as in the UM-SCC-1 cell line for treatment on day 3 (**Fig. 4-5D and E**). Bmi-1 knockdown and treatment with either chemotherapy agent did not affect PI^+ cells in the UM-SCC-22B cell line in either treatment strategy. These results suggest that Bmi-1 signaling contributes to chemotherapeutic resistance, as observed by the significant effect on cell death as measured by the PI^+ cell percentage within orospheres.

4.4 Discussion

Preventing HNSCC disease relapse in the form of tumor recurrence or metastasis remains as great of a challenge as attempting to treat the resultant disease. CSCs have been identified as the subpopulation of tumor cells responsible for more aggressive tumor phenotypes and disease relapse, particularly as refractory cells to conventional treatments that persist to drive tumor recurrence or metastasis. We previously evinced

the clinical importance of Bmi-1 in HNSCC patient outcomes by demonstrating that high Bmi-1 expression in patient tumor samples significantly correlated with worse recurrence-free survival time, which supports the CSC-driven nature of disease relapse (Herzog et al., 2021). In this study, we showed that both genetic and pharmacologic inhibition of Bmi-1 can resolutely overcome the resistance of CSCs to cytotoxic chemotherapy. We have shown here that Bmi-1 knockdown suppressed IL-6/STAT3 signaling in CSC-enriched cultures as well as bulk tumor cells and prevents the CSC fraction increase induced by both Cisplatin and Carboplatin. Further, we showed that treatment with the Bmi-1 inhibitor PTC596 suppressed the Cisplatin-mediated increase in the CSC fraction and self-renewal both *in vitro* and *in vivo.* Lastly, we established a link between both Bmi-1 inhibition and knockdown causing an abrogated DNA damage response and apoptosis in presence of genotoxic chemotherapies, suggesting a potential mechanism by which Bmi-1 may elicit its effect on CSCs. The preclinical studies described herein provide rationale for the incorporation of a CSC-targeted therapy based on Bmi-1 inhibition in HNSCC where no such therapy currently exists.

These results support and extend upon our recently published findings that IL-6/STAT3 signaling regulates Bmi-1 expression and controls chemoresistance of head and neck CSCs (Herzog et al., 2021). In the former study, we demonstrated that therapeutic inhibition of the IL-6 receptor as a CSC-targeted therapy prevented their increase in response to concurrent treatment with Cisplatin. IL-6 secreted by endothelial cells within the perivascular tumor niche supports CSC survival, self-renewal, and tumorigenic potential (Krishnamurthy *et al.,* 2014; Kim *et al.,* 2017). We've also previously shown that Cisplatin activates the IL-6 pathway (McDermott *et al.,* 2018), which reinforces the

Cisplatin-mediated increase in Bmi-1 expression and the CSC fraction (Nör *et al.,* 2014). Within this molecular context, Gilbert *et al.* provide a riveting explanation for the observed increase in CSCs following DNA damage by chemotherapy. The authors show that pro-survival IL-6 secretion is released from endothelial cells within the tumor microenvironment in a p38-dependent manner in response to genotoxic chemotherapeutic stress, thereby creating a chemo-resistant niche (Gilbert et al., 2010). These findings deepen the compelling connection between IL-6/STAT3 signaling and Bmi-1 activity in cancer cells and provide a possible explanation for the mechanism by which genotoxic chemotherapy activates this signaling network.

The mechanistic link between Bmi-1 inhibition and the DNA damage response remains unclear and warrants studies for further investigation, yet Bmi-1 has been widely implicated in promoting efficient DNA damage response in cancer cells, with loss of Bmi-1 having been shown to impair the repair of double-stranded DNA breaks by homologous recombination and subsequent accumulation of cells in G_2-M (Ginjala *et al.,* 2011). Unrepaired DNA damage induces genome instability and promotes tumorigenesis, making it essential for cells to harbor mechanisms responsible for recognizing these events and regulating cell cycle checkpoints to repair the damage. Phosphorylation of H2AX is involved in activation of checkpoint proteins that result in cell cycle arrest, and Bmi-1 is involved in facilitating the phosphorylation of H2AX by ATM along with recruiting other repair proteins to sites of double-stranded DNA damage (Podhorecka *et al.,* 2010; Ginjala *et al.,* 2011). This, along with findings that PTC596 and Bmi-1 knockdown induces caspase-dependent apoptosis via downregulation of Mcl-1, could explain our observed decrease in pH2AX and increase in cleaved caspase-3 expression after Bmi-1

knockdown or inhibition. However, further mechanistic studies to dissect this signaling cascade are needed.

Bmi-1 is a master regulator of stem cell self-renewal, and as such functional assessment of its activity is commonly performed via sphere forming assays (Jacobs *et al.,* 1999). Since different methods of performing sphere forming assays harbor unique limitations, we utilized complimentary assay methods to dissect different aspects of the functional role of Bmi-1 in context of CSC self-renewal (Pastrana *et al.,* 2011). In our conventional orosphere assays, we observed robust inhibition of sphere formation with Bmi-1 inhibition and knockdown, even in combination with cytotoxic chemotherapies. The automated orosphere assay enabled a high-throughput analysis of the effect of therapy on sphere size and cell death on a single-sphere basis, whereas its utility in analyzing sphere forming ability is biased by nature of the steep meniscus formed in a 96-well plate promoting a higher degree of aggregation of cancer cells. In the automated orosphere assay, Bmi-1 knockdown significantly decreased the size of resultant spheres and interestingly was shown to decrease the percentage of PI^+ cells within orospheres treated with Cisplatin or Carboplatin. This may be explained by the fact that under the more conducible sphere formation conditions of the automated orosphere assay, Bmi-1 knockdown cells were still able to form spheres, albeit significantly smaller. Those cells still able to form spheres may represent a more aggressive, chemoresistant phenotype. Though the heterogeneity of tumors spheres has not been characterized in depth, it has been shown that not all HNSCC spheres are created equal and harbor differing self-renewal, tumorigenic, and clonogenic potential (Almeida *et al.,* 2016). As such, using

these complimentary methods of analyzing the functional role of Bmi-1 is necessary and provides avenues for future studies.

The clinical development and approval process for new cancer therapeutics requires rigorous assessment of its safety, tolerability, and preliminary efficacy. PTC596 is a tubulin-binding agent at the colchicine site and the resulting decrease in Bmi-1 protein levels and function are secondary to potent induction of G_2-M mitotic arrest. Importantly, this drug demonstrates high oral bioavailability, readily crosses the blood brain barrier, and is not a substrate for drug efflux via P-glycoprotein, making it an attractive candidate for anticancer therapeutics (Jernigan *et al.,* 2021). Reassuringly, no clinical trials to date have described significant adverse effects, such as neuropathy typically produced by microtubule-targeting agents, while the anticancer effect of PTC596 in a phase 1 clinical trial to target CSCs is proving to be promising (Infante et al., 2017). In this study, we provided evidence for PTC596 reducing the CSC fraction in tumors from a HNSCC subcutaneous xenograft model even in combination with Cisplatin treatment, whereas the therapeutic effect of Bmi-1 inhibition in decreasing tumor growth of HNSCC in a longer-term *in vivo* study has been shown elsewhere (Chen et al., 2017). Here, we introduce a therapeutic strategy specifically to suppress the adverse effects of cytotoxic chemotherapy treatment that result in an increase in CSC.

In addition to their resistance to a plethora of conventional chemotherapy agents, CSCs also exhibit resistance to immunotherapy and have become a relevant immune-oncology target (Ning *et al.,* 2012; Lu *et al.,* 2015; Kaur *et al.,* 2017). Anti-PD-1 immunotherapy has been approved as first-line treatment for HNSCC and is commonly combined with Cisplatin. However, this has been shown to increase CSCs and lead to

evasive resistance, ultimately resulting in poor response rates and relapsing disease (Jia *et al.,* 2020). Jia *et al.* recently showed that Bmi-1 inhibition with the first-generation small-molecule inhibitor PTC209 prevented the Cisplatin-mediated induction of Bmi-1$^+$ CSCs and enabled anti-PD-1 therapy to prevent relapse of HNSCC. Moreover, they demonstrated that Bmi-1 inhibition activated the tumor cell-intrinsic immune response by recruitment of CD8$^+$ T cells, which supports the use of a CSC-targeted therapy via Bmi-1 inhibition in combination with HNSCC immunotherapy.

Collectively, these exciting results provide preclinical evidence for a novel mechanism-based treatment strategy that is based on targeted elimination of CSCs with a small molecule Bmi-1 inhibitor in combination with a genotoxic chemotherapy such as Cisplatin to debulk the tumor for improved outcomes of patients with head and neck squamous cell carcinoma.

4.5 Materials and Methods

4.5.1 Cell culture

Human HNSCC cell lines UM-SCC-1, UM-SCC-22A, and UM-SCC-22B (from T. Carey, University of Michigan, Ann Arbor) were cultured in Dulbecco's Modified Eagle Medium (Invitrogen, Carlsbad, CA, USA) with 10% fetal bovine serum (Atlanta Biologicals, Flowery Branch, GA, USA), 1% L-Glutamine (Invitrogen, Carlsbad, CA, USA), 1% Antibiotic-Antimycotic solution (Sigma, Burlington, MA, USA), and .05% Plasmocin (InvivoGen, San Diego, CA, USA). The origin, confirmation of identity, and authentication by STR profiling of these cell lines are described elsewhere (44) and tested negative for mycoplasma (Mycoplasma Detection Kit, Invitrogen).

4.5.2 Bmi-1 gene silencing

HEK293T cells were used to produce lentiviral particles by co-transfecting packaging vectors pMD2.G and psPAX2 with either shRNA-control or shRNA-Bmi-1 constructs on a pGIPZ backbone (University of Michigan Vector Core) using the calcium phosphate method. The supernatant was collected, and UM-SCC cells were infected overnight with the supernatant in the presence of 4 μg/ml polybrene (Sigma, Burlington, MA, USA). Successfully infected cells were selected with 1 μg/ml puromycin (InvivoGen, San Diego, CA, USA).

4.5.3 Conventional orosphere assay

HNSCC cells were cultured in ultra-low attachment (ULA) culture ware (Corning, Corning, NY, USA) using serum-free Dulbecco's Modified Eagle Medium (Invitrogen, Carlsbad, CA, USA) supplemented with 1% GlutaMAX (Invitrogen, Carlsbad, CA, USA), 1% Antibiotic-Antimycotic solution (Sigma, Burlington, MA, USA), 1% N-2 Supplement (Invitrogen, Carlsbad, CA, USA), 10 ng/mL epidermal growth factor (R&D Systems, Minneapolis, MN, USA), and 10 μg/mL Insulin (Sigma, Burlington, MA, USA). On Day 0, 12,000 cells/well were seeded in 6-well ULA plates for sphere counting experiments or 500,000 cells were seeded in 100 mm ULA dishes for harvesting protein lysates (Corning, Corning, NY, USA). 24 hours later on Day 1, cells were treated with 0-1 μM Cisplatin, 0-1μM Carboplatin, and/or 0-200 nM PTC-596 (Selleckchem, Houston, TX, USA). Orospheres were cultured by gradually adding feeding media every 2 days while maintaining final treatment concentration. Orospheres were defined as non-adherent spheres containing ≥ 25 cells, as observed at high power magnification, and counted or harvested on Day 6. Representative pictures were taken via light microscope at 40X and

100X magnification. All experiments are representative of at minimum two independent experiments performed in triplicate experimental conditions.

4.5.4 Automated orosphere assay

HNSCC cells were cultured in the same media and conditions as in the conventional orosphere assay, described above. Cells were seeded on Day 0 by the automated liquid handler OT-2 (Opentrons, New York, NY, USA) in ultra-low attachment round-bottom 96-well plates (Sarstedt, Nümbrecht, Germany). After seeding, sphere formation was allowed for at least 24 hours before treatment with Cisplatin (1 μM) or Carboplatin (1 μM) on Day 1 or Day 3 using the automated liquid handler. Images and size measurements for cell seeding concentration assays were obtained daily from day 1 until day 4 using EVOS FL Auto Imaging System (ThermoFisher Scientific). To stain for dead cells, propidium iodide was added at a concentration of 1:50. Fluorescence images were obtained using the ImageXpress Micro 4 (Molecular Devices, San Jose, CA, USA) on Day 2 or Day 4 after 24 hours of treatment. Sphere size and cell death was quantified using the ImageXpress software.

4.5.5 Western blot

Cells were plated, serum-starved overnight, and treated with 0-1 μM Cisplatin, 0-1 μM Carboplatin, and/or 0-200 nM PTC-596. HNSCC cells, orospheres, and tumor tissues were lysed in NP-40 lysis buffer, loaded, and separated on 9-15% SDS-PAGE gels, and then transferred to nitrocellulose membranes. Membranes were blocked with 5% nonfat milk in TBST, then incubated with the following primary antibodies overnight at 4°C: rabbit anti-human Bmi-1, mouse anti-human phosphorylated STAT3, rabbit anti-

human STAT3, rabbit anti-human gp130, rabbit anti-human phosphorylated H2AX, rabbit anti-human H2A, rabbit anti-human cleaved Caspase-3 (Cell Signaling Technology, Danvers, MA, USA), mouse anti-human IL-6Ra (Santa Cruz Biotechnology, Dallas, TX, USA), glyceraldehyde-3-phosphate-dehydrogenase (GAPDH) (MilliporeSigma, Burlington, MA, USA). Membranes were exposed to affinity-purified anti-mouse or anti-rabbit secondary antibodies conjugated with HRP (1:1000) (Jackson Laboratories, Bar Harbor, ME, USA). Immunoreactive proteins were then visualized by Super-Signal West Pico Chemiluminescent Substrate (Thermo Scientific, Rockford, IL, USA).

4.5.6 Flow cytometry

Tumors were resected from mice, dissociated by collagenase and hyaluronidase (Stem Cell Technologies), incubated in ACK red blood cell lysis buffer (Invitrogen), and filtered through a sterile 40-μm cell strainer. ALDH activity was measured via Aldefluor Kit (Stem Cell Technologies) or AldeRed ALDH Detection Assay (EMD Millipore). Briefly, $1x10^6$ cells were incubated with activated ALDH substrate or the equivalent volume of ALDH inhibitor diethyl aminobenzaldehyde (DEAB). Cells were rinsed with PBS and stained for CD44 with either CD44-V450 (BD Horizon) or CD44-APC (R&D Systems) for 15 minutes at 4°C. Human cells were identified by anti-HLA-ABC (PE, BD Pharmingen). Viable cells were stained with DAPI (Molecular Probes). All flow cytometry analysis was conducted by the Bigfoot Spectral Cell Sorter (Invitrogen). Results were analyzed with FlowJo software (LLC) in triplicate per condition.

4.5.7 HNSCC subcutaneous scaffold xenograft model

HNSCC subcutaneous xenograft tumors were generated as previously described (46) without the inclusion of HDMEC cells. Briefly, 1 x 10^5 tumor cells (UM-SCC-22A) were seeded with a cell growth media and Matrigel (Corning, Corning, NY, USA) mixture in poly-(L)-lactic acid biodegradable scaffolds and subsequently implanted into the dorsal subcutaneous space of immunodeficient mice (CB-17 SCID, Charles River, Wilmington, MA, USA). Tumor volume (mm^3) was calculated by L x $W^2/2$ (L, length; W, width). Once tumors grew to an average volume of 180 mm^3, mice were randomly allocated to treatment groups (n = 4-5, due to unexpected death of one mouse in the vehicle group): 5 mg/kg Cisplatin; 5 mg/kg PTC596; 5 mg/kg PTC596 + 5 mg/kg Cisplatin; or vehicle treatment. Cisplatin was administered on day 0 and 6 intraperitoneally, whereas PTC596 was administered on days 0, 3, and 6 via oral gavage. Vehicle mice were administered saline intraperitoneally and solvents for PTC596 via oral gavage (water, tween-80, and PEG300). Mice were euthanized, and tumors retrieved 24 hours after the end of treatment on day 7. All procedures and treatments were conducted under protocols reviewed and approved by UCUCA.

4.5.8 Statistical analyses

All statistical analysis was performed using GraphPad Prism. Sample sizes for both *in vitro* and *in vivo* studies were determined by power calculations from data previously published. All experiments were performed with at least three biological replicates. One-way ANOVA followed by appropriate post hoc tests (Tukey test) was used to analyze comparisons between two or more groups. Data were summarized as mean ± S.D. Statistical significance was defined at $p<0.05$ throughout the manuscript.

4.6 Acknowledgements

We thank Dr. Thomas Carey for generously providing us with the UM-SCC-1, UM-SCC-22A, and UM-SCC-22B cell lines. We thank the University of Michigan Flow Cytometry core for their aid with experimental design, protocol troubleshooting, and data handling. All schematic diagrams were created with BioRender.com. This work was funded by NIH/NIDCR F30-DE029097 (AEH), R01-DE21139 (JEN), and R01-DE23220 (JEN).

4.7 Figures

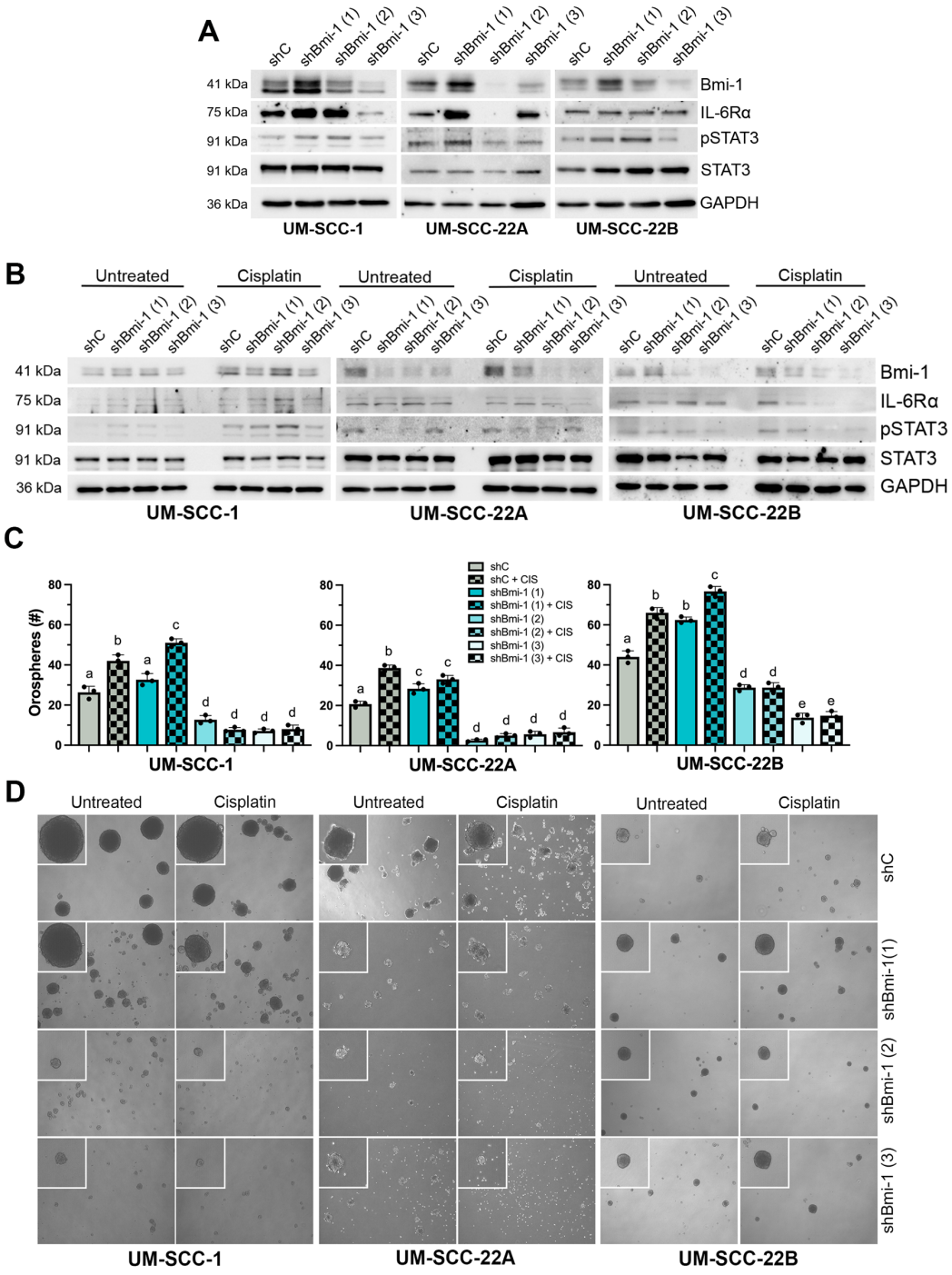

Figure 4-1: Bmi-1 knockdown decreases activation of the IL-6/STAT3 signaling axis and regulates cancer cell self-renewal.

(A) Western blots showing baseline protein levels in Bmi-1 knockdown and control cells grown in normal attachment conditions. **(B)** Western blots showing baseline protein levels in lysates

isolated from primary orospheres formed by Bmi-1 knockdown and control cells treated with Cisplatin (0-1 μM). **(C)** Quantification depicting number of primary orospheres per well. Three wells were counted per treatment group. Bar graphs display mean ± S.D. (n=3) and significance denoted by letters at p≤0.05. **(D)** Representative images (40x) of primary orospheres on day 6 formed by Bmi-1 knockdown and control cells. Cells were treated with Cisplatin (0-1 μM) the day after plating in ULA sphere conditions. Inserts at 100x magnification. Pictures acquired of five fields per well in three wells per treatment group.

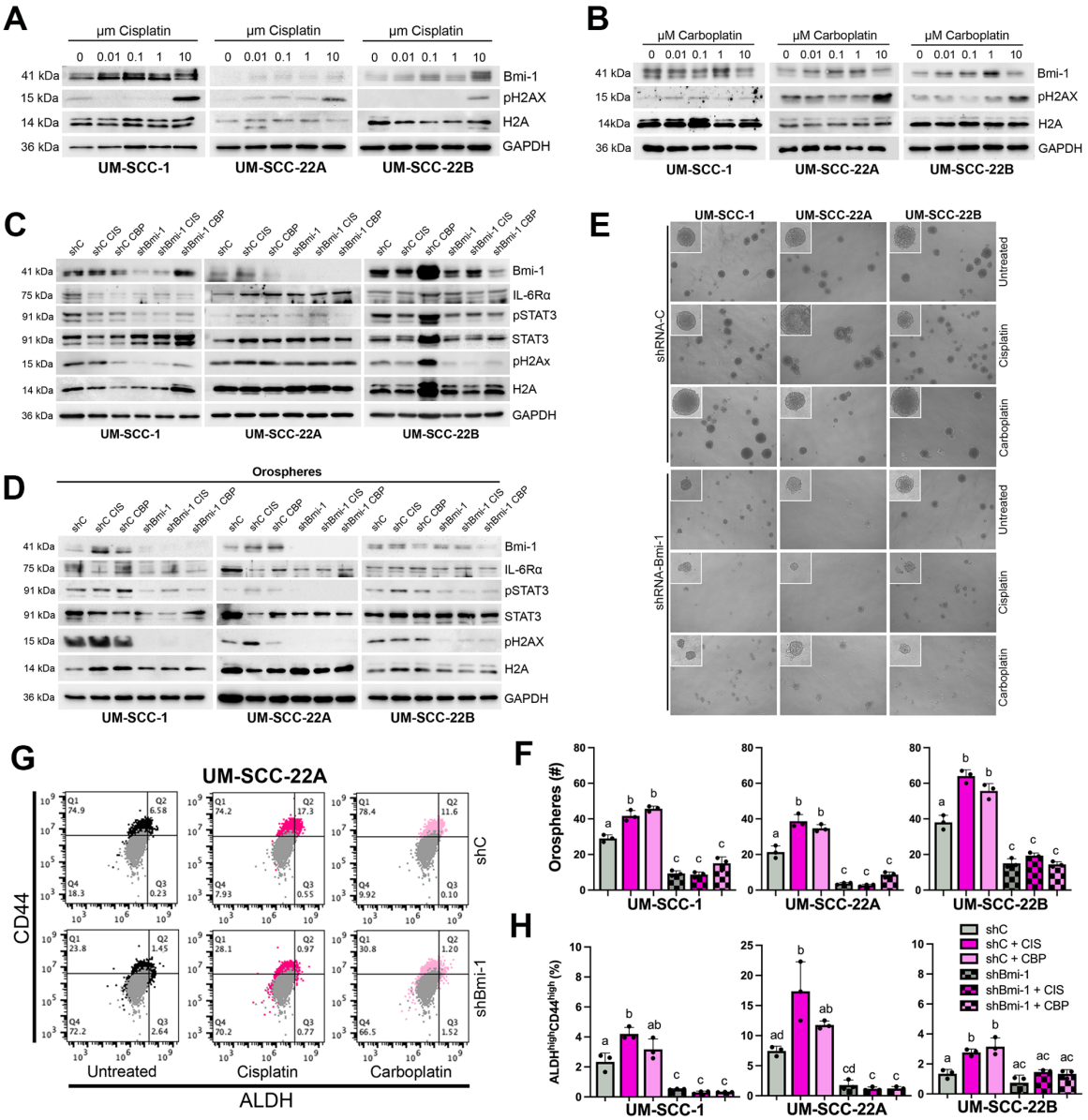

Figure 4-2: Bmi-1 knockdown suppresses increase in CSC fraction by treatment with cytotoxic chemotherapy and mediates the DNA damage response.

(A) Dose response western blot analysis of UM-SCC-1, UM-SCC-22A, and UM-SCC-22B cells treated with Cisplatin (0-10 μM). **(B)** Dose response western blot analysis of UM-SCC-1, UM-SCC-22A, and UM-SCC-22B cells treated with Carboplatin (0-10 μM). **(C)** Western blot analysis of Bmi-1 knockdown and control cells grown under normal attachment conditions and treated with Cisplatin (0-1 μM) or Carboplatin (0-1 μM). **(D)** Western blot analysis of Bmi-1 knockdown and control cells grown under ultra-low attachment conditions and treated with Cisplatin (0-1 μM) or Carboplatin (0-1 μM). **(E)** Representative images (40x) of primary orospheres on day 6 formed by Bmi-1 knockdown and control cells treated with Cisplatin (0-1 μM) or Carboplatin (0-1 μM). Cells were treated the day after plating in ULA sphere conditions. Inserts at 100x magnification. Pictures acquired of five fields per well in three wells per treatment group. **(F)** Quantification depicting number of primary orospheres per well. Three wells were counted per treatment group. Bar

graphs display mean ± S.D. (n=3) and significance denoted by letters at p≤0.05. **(G)** Flow cytometry graphs depicting DEAB/IgG controls (gray) in UM-SCC-22A cells for Aldefluor and CD44, respectively. One experimental replicate per group is shown to demonstrated gate setting strategy. $ALDH^{high}CD44^{high}$ cells were identified based on these gates. **(H)** Flow cytometry graphs depicting CSC fraction percentage ($ALDH^{high}CD44^{high}$ cells) in HNSCC cell lines. Bar graphs display mean ± S.D. (n=3) and significance denoted by letters at p≤0.05.

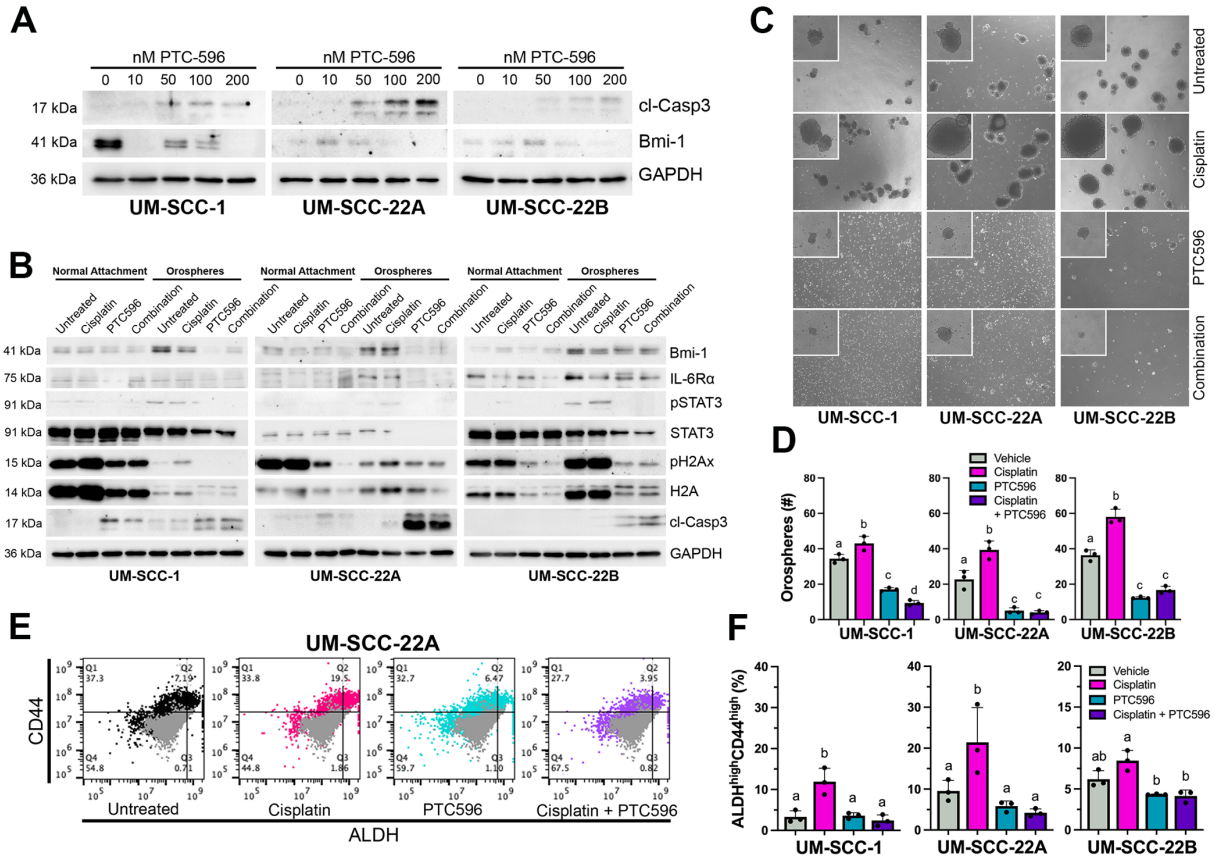

Figure 4-3: Bmi-1 inhibition with PTC596 prevents the Cisplatin-induced self-renewal and fraction of CSCs.

(A) Dose response western blot analysis of UM-SCC-1, UM-SCC-22A, and UM-SCC-22B cells treated with PTC596 (0-200 nM). **(B)** Western blot analysis of HNSCC cells grown under normal attachment or ultra-low attachment conditions and treated with Cisplatin (0-1 μM) and/or PTC596 (0-200 nM). **(C)** Representative images (40x) of primary orospheres on day 6 formed by HNSCC cells treated with Cisplatin (0-1 μM) and/or PTC596 (0-200 nM). Cells were treated the day after plating in ULA sphere conditions. Inserts at 100x magnification. Pictures acquired of five fields per well in three wells per treatment group. **(D)** Quantification depicting number of primary orospheres per well. Three wells were counted per treatment group. Bar graphs display mean ± S.D. (n=3) and significance denoted by letters at p≤0.05. **(E)** Flow cytometry graphs depicting DEAB/IgG controls (gray) in UM-SCC-22A cells for Aldefluor and CD44, respectively. One experimental replicate per group is shown to demonstrated gate setting strategy. $ALDH^{high}CD44^{high}$ cells were identified based on these gates. **(F)** Flow cytometry graphs depicting CSC fraction percentage ($ALDH^{high}CD44^{high}$ cells) in HNSCC cell lines. Bar graphs display mean ± S.D. (n=3) and significance denoted by letters at p≤0.05.

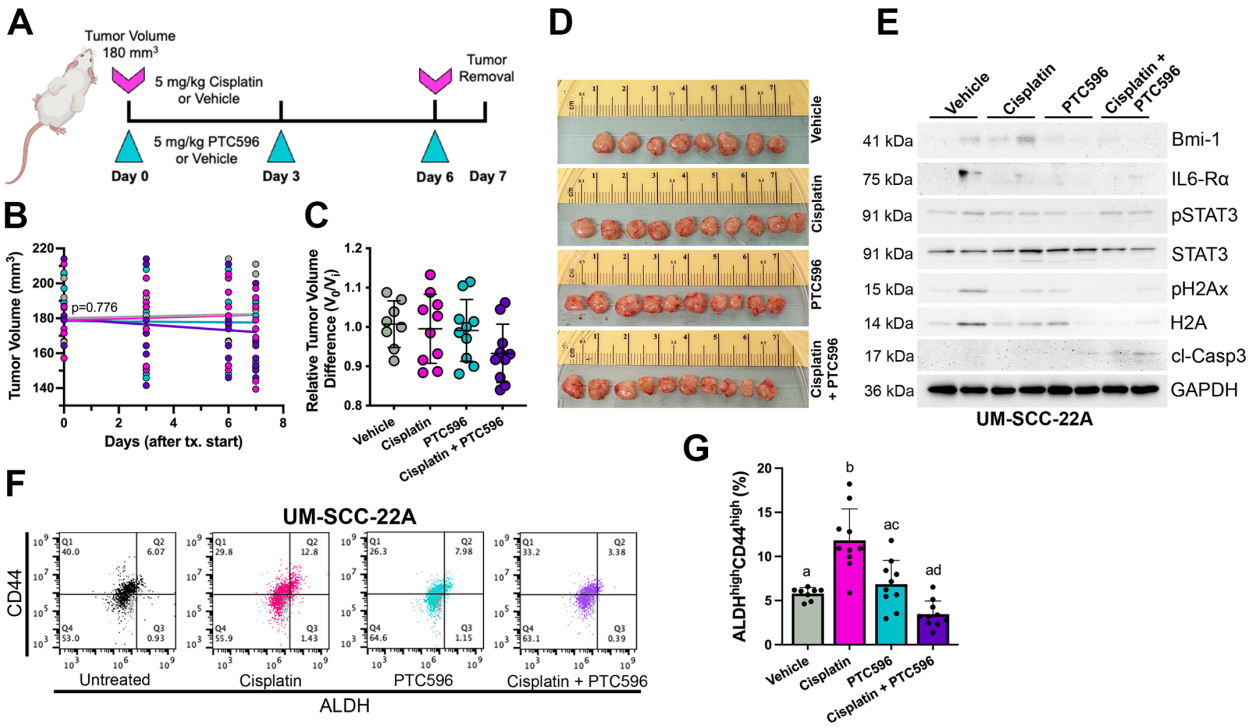

Figure 4-4: PTC596 suppresses Cisplatin-induced CSC fraction in subcutaneous xenograft model of HNSCC *in vivo.*

A) Treatment schematic. Mice harboring UM-SCC-22A subcutaneous xenograft tumors began treatment for 7 days (3 doses total), receiving either vehicle treatment, Cisplatin (5 mg/kg, I.P.) and/or PTC596 (5 mg/kg, oral gavage). Mice were euthanized 24 hours after last dose. **(B)** Simple linear regression model of mean tumor volumes over the duration of the treatment course. **(C)** Graphs depicting tumor volume at the end of experiment (V_0) normalized against tumor volume at treatment start (V_i). **(D)** Macroscopic images of subcutaneous xenograft tumors generated with UM-SCC-22A and treated with Cisplatin (5 mg/kg, I.P.) and/or PTC596 (5 mg/kg, oral gavage). **(E)** Western blot of representative tumor tissue lysates from each treatment group. **(F)** Flow cytometry graphs depicting DEAB/IgG controls (gray) for Aldefluor and CD44, respectively. One experimental replicate per group is shown to demonstrated gate setting strategy. $ALDH^{high}CD44^{high}$ cells were identified based on these gates. **(G)** Flow cytometry graphs depicting CSC fraction percentage ($ALDH^{high}CD44^{high}$ cells) in subcutaneous xenograft tumors.

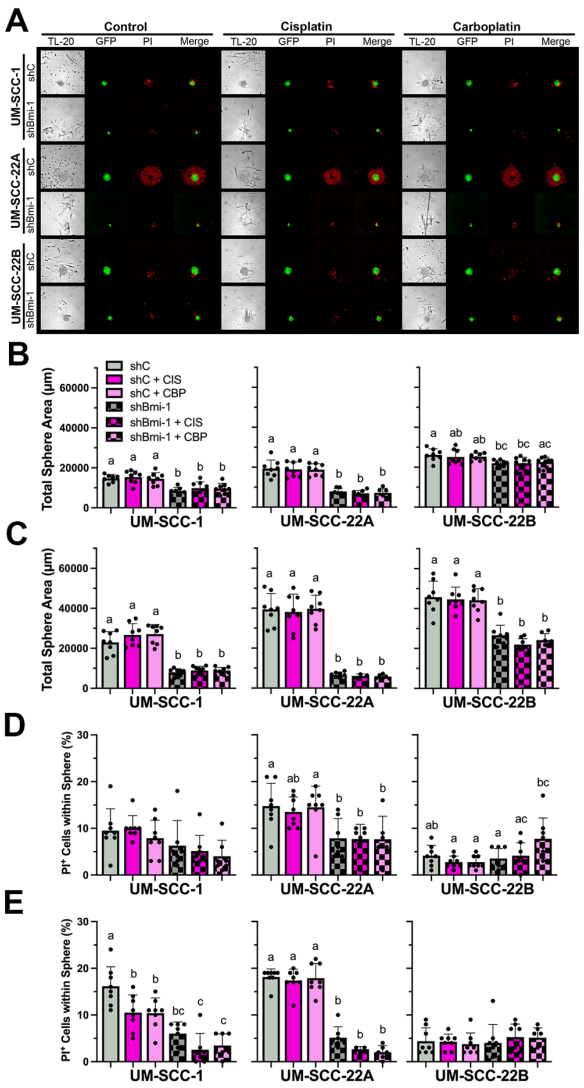

Figure 4-5: Bmi-1 defines the self-renewal capacity of HNSCC cells.

(A) Representative images of orospheres generated from Bmi-1 knockdown and control cells treated with Cisplatin (0-1 µM) or Carboplatin (0-1 µM). Transmitted light and fluorescence images (GFP from shRNA constructs and PI-TexasRed) were acquired for each orosphere. **(B,C)** Bar graphs depicting the area of orospheres generated from Bmi-1 knockdown and control cells treated with Cisplatin (0-1 µM) or Carboplatin (0-1 µM) as measured from images acquired on day 2 **(B)** and day 4 **(C)** of experiment. **(D,E)** Bar graphs depicting the percentage of PI^+ cells within orospheres generated from Bmi-1 knockdown and control cells treated with Cisplatin (0-1 µM) or Carboplatin (0-1 µM) as measured from images acquired on day 2 **(D)** and day 4 **(E)** of experiment. Eight wells were analyzed per treatment group. Bar graphs display mean ± S.D. (n=8) and statistical significance is denoted by different letters at $p \leq 0.05$.

4.8 Supplemental Figures

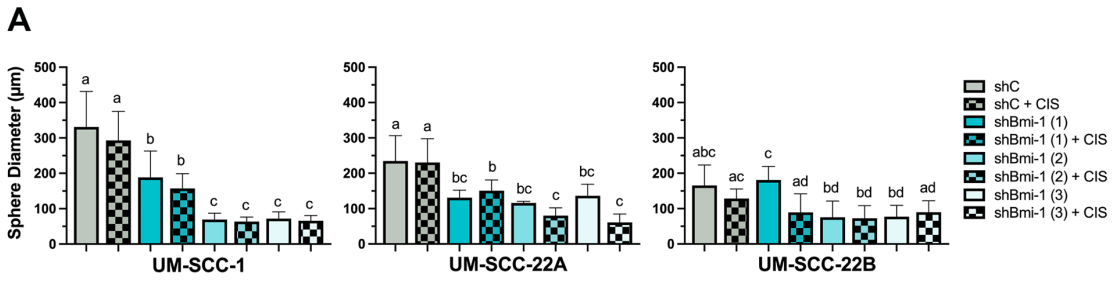

Figure 4-6: Orosphere size measurements for analysis of Bmi-1 knockdown cells.

(A) Bar graphs depicting the size of orospheres generated from Bmi-1 knockdown cells treated with Cisplatin (0-1 µM). Different lowercase letters depict statistical significance at $p \leq 0.05$.

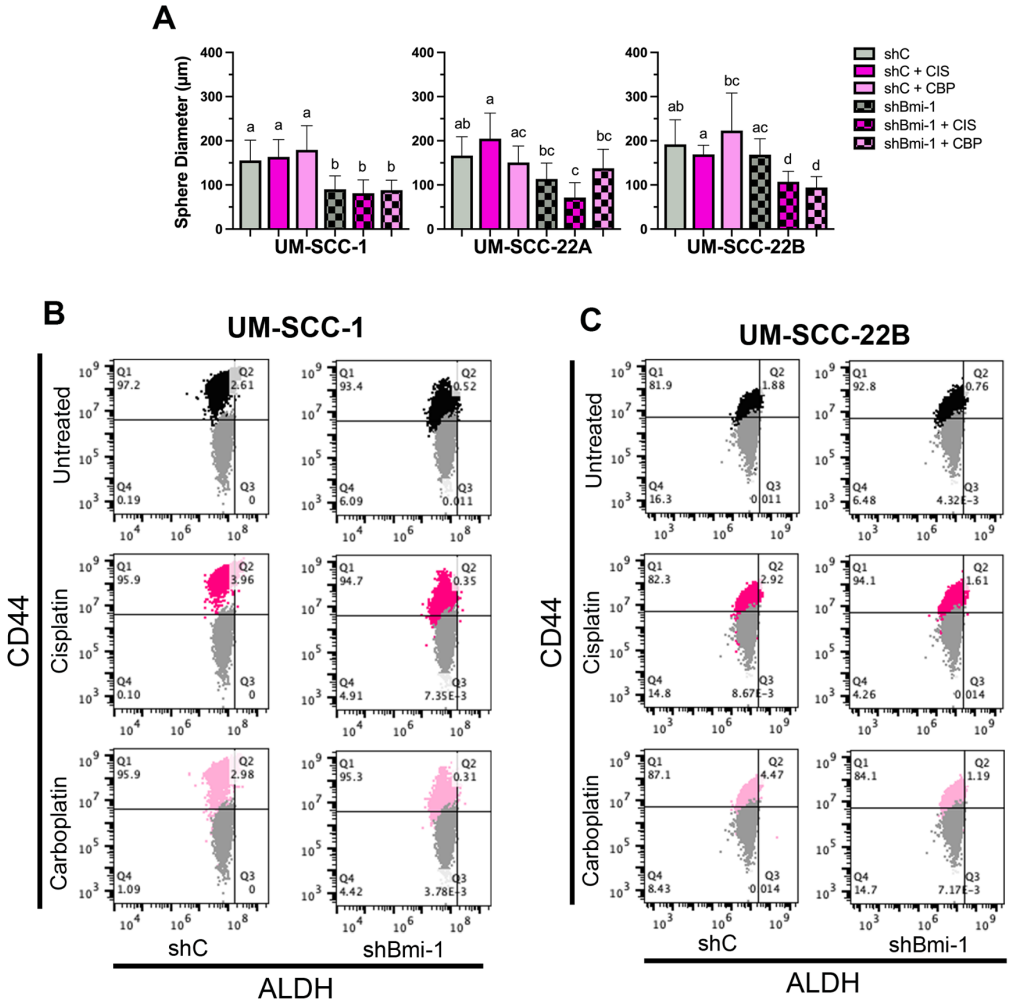

Figure 4-7: Orosphere size measurements and flow cytometry gating strategy for analysis of Bmi-1 knockdown cells treated with Cisplatin or Carboplatin.

(A) Bar graphs depicting the size of orospheres generated from Bmi-1 knockdown cells treated with Cisplatin (0-1 µM) or Carboplatin (0-1 µM). Different lowercase letters depict statistical significance at p≤0.05. **(B)** Flow cytometry graphs depicting DEAB/IgG controls (gray) for Aldefluor and CD44 in UM-SCC-1 cells, respectively. **(C)** Flow cytometry graphs depicting DEAB/IgG controls (gray) for Aldefluor and CD44 in UM-SCC-22B cells, respectively. One experimental replicate per group is shown to demonstrated gate setting strategy. $ALDH^{high}CD44^{high}$ cells were identified based on these gates.

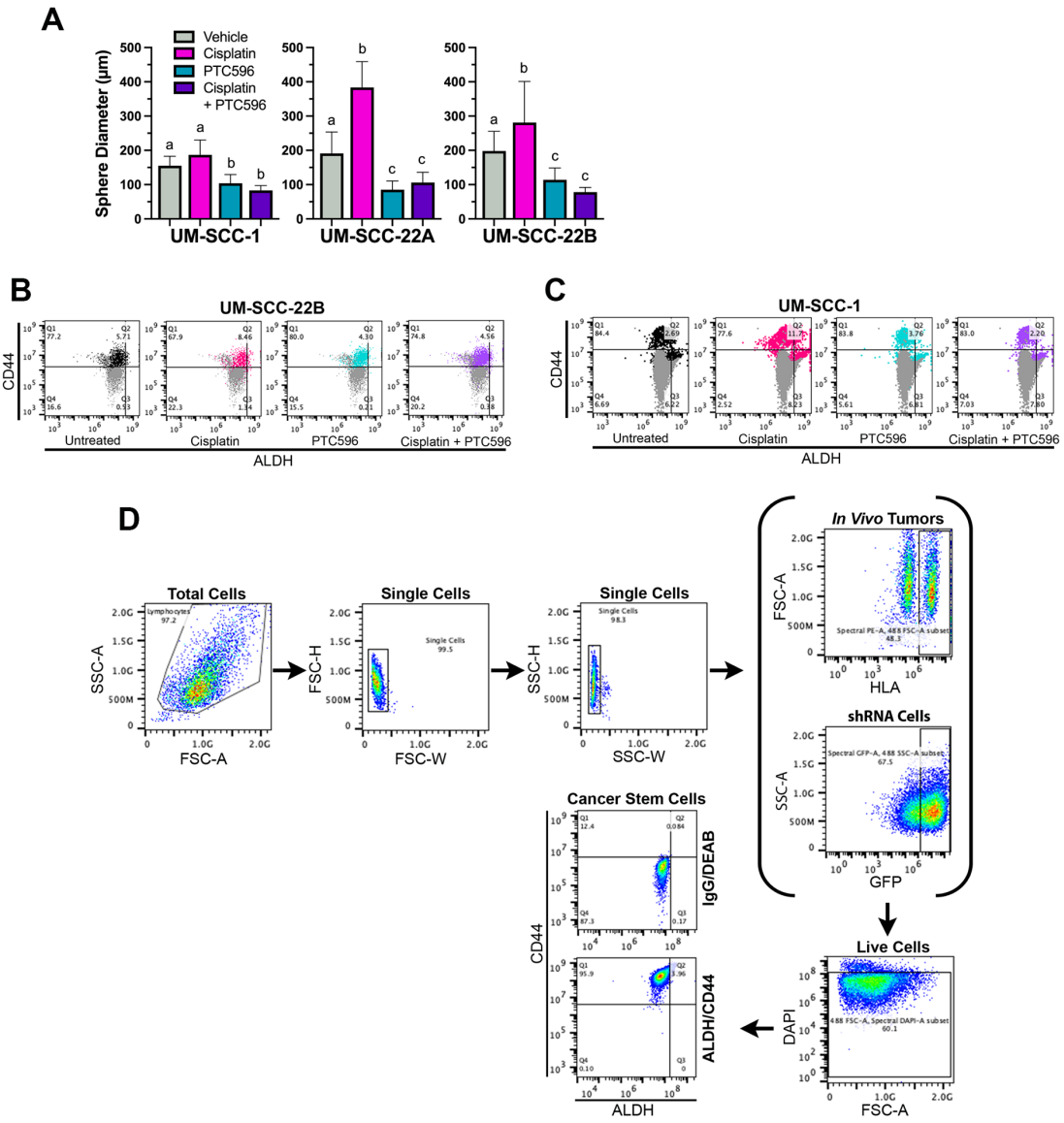

Figure 4-8: Orosphere size measurements and flow cytometry gating strategy for analysis of HNSCC cells treated with Cisplatin and/or PTC596.

(A) Bar graphs depicting the size of orospheres generated from Bmi-1 knockdown cells treated with Cisplatin (0-1 µM) and/or PTC596 (0-200 nM). Different lowercase letters depict statistical significance at p≤0.05. **(B)** Flow cytometry graphs depicting DEAB/IgG controls (gray) for Aldefluor and CD44 in UM-SCC-22B cells, respectively. **(C)** Flow cytometry graphs depicting DEAB/IgG controls (gray) for Aldefluor and CD44 in UM-SCC-1 cells, respectively. One experimental replicate per group is shown to demonstrated gate setting strategy. $ALDH^{high}CD44^{high}$ cells were identified based on these gates. **(D)** General gating strategy schematic for all flow cytometry experiments.

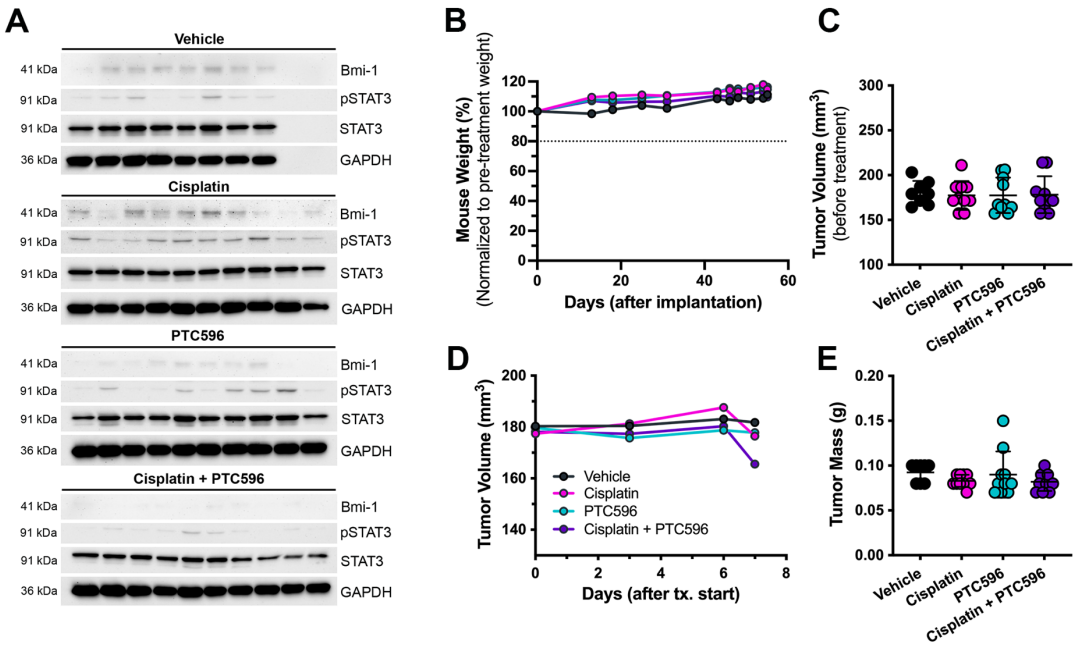

Figure 4-9: Therapeutic effect of PTC596 and/or Cisplatin in *in vivo* HNSCC subcutaneous xenograft model.

(**A**) Western blots depicting the impact of Cisplatin and/or PTC596 on the expression of STAT3 and Bmi-1 in subcutaneous xenograft tumors generated with UM-SCC-22A cells. Lysates were prepared from whole tumors upon dissociation (n=8-10). **(B)** Graph depicting mouse weight during the experimental period. Data points were normalized to pretreatment weight. Line indicated animal protocol cutoff weight loss of 20% for this experiment. **(C)** Graphs depicting tumor volumes at treatment start for each experimental condition. **(D)** Line graph depicting mean tumor volume over time in the subcutaneous xenograft model after treatment with Cisplatin and/or PTC 596. **(E)** Graphs depicting tumor mass after tumor resection at treatment end for each experimental condition.

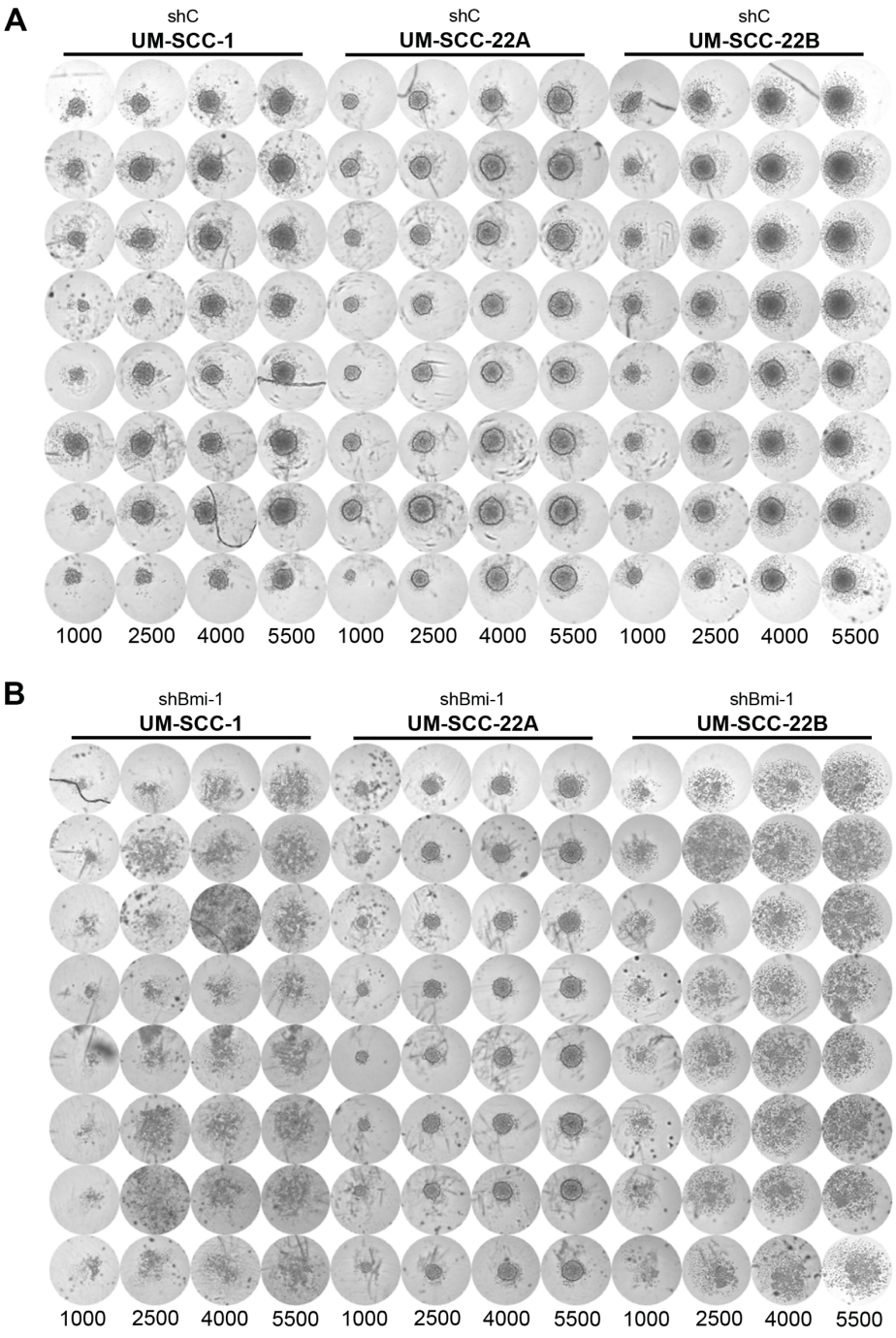

Figure 4-10: Optimization of cell seeding number for orosphere assay using an automated liquid handler.

(A,B) Transmitted light microscope images of UM-SCC-1, UM-SCC-22A, and UM-SCC-22B Bmi-1 knockdown and control orospheres grown from different cell seeding numbers in ultra-low attachment round-bottom 96-well plates. Images were acquired on day 4 after cell seeding.

4.9 References

Almeida LO, Guimarães DM, Squarize CH, Castilho RM. Profiling the behavior of distinct populations of head and neck cancer stem cells. Cancers. 2016 Jan 4;8(1):7.

Carvalho, A.L., Nishimoto, I.N., Califano, J.A. & Kowalski, L.P. Trends in incidence and prognosis for head and neck cancer in the United States: a site-specific analysis of the SEER database. Int. J. Cancer 114(5), 806-816 (2005).

Chen YC, Chang CJ, Hsu HS, Chen YW, Tai LK, Tseng LM, Chiou GY, Chang SC, Kao SY, Chiou SH, Lo WL. Inhibition of tumorigenicity and enhancement of radiochemosensitivity in head and neck squamous cell cancer-derived ALDH1-positive cells by knockdown of Bmi-1. Oral oncology. 2010 Mar 1;46(3):158-65.

Chen, D. et al. Targeting BMI1+ cancer stem cells overcomes chemoresistance and inhibits metastases in squamous cell carcinoma. Cell Stem Cell 20(5), 621-634, e6 (2017).

Chen, Y.C. et al. High-throughput single-cell derived sphere formation for cancer stem-like cell identification and analysis. *Scientific reports* **6**(1), 1-2 (2016).

Chinn, S.B. et al. Cancer stem cells: mediators of tumorigenesis and metastasis in head and neck squamous cell carcinoma. *Head Neck* **37**(3), 317-326 (2015).

Cramer JD, Burtness B, Le QT, Ferris RL. The changing therapeutic landscape of head and neck cancer. Nature reviews Clinical oncology. 2019 Nov;16(11):669-83.

Gilbert, L.A. & Hemann, M.T. DNA damage-mediated induction of a chemoresistant niche. Cell 143(3), 355-366 (2010).

Ginjala V, Nacerddine K, Kulkarni A, Oza J, Hill SJ, Yao M, Citterio E, van Lohuizen M, Ganesan S. BMI1 is recruited to DNA breaks and contributes to DNA damage-

induced H2A ubiquitination and repair. Molecular and cellular biology. 2011 May 1;31(10):1972-82.

Goldman, A. et al. Temporally sequenced anticancer drugs overcome adaptive resistance by targeting a vulnerable chemotherapy-induced phenotypic transition. Nat. Commun. 6, 6139 (2015).

Herzog AE, Warner KA, Zhang Z, Bellile E, Bhagat MA, Castilho RM, Wolf GT, Polverini PJ, Pearson AT, Nör JE. The IL-6R and Bmi-1 axis controls self-renewal and chemoresistance of head and neck cancer stem cells. Cell death & disease. 2021 Oct 23;12(11):988.

Infante JR, Bedard PL, Shapiro G, Bauer TM, Prawira A, Laskin O, Weetall M, Baird J, Branstrom A, O'Mara E, Spiegel RJ. Phase 1 results of PTC596, a novel small molecule targeting cancer stem cells (CSCs) by reducing levels of BMI1 protein.

Ismail IH, Andrin C, McDonald D, Hendzel MJ. BMI1-mediated histone ubiquitylation promotes DNA double-strand break repair. Journal of Cell Biology. 2010 Oct 4;191(1):45-60.

Jacobs, J.J., Kieboom, K., Marino, S., DePinho, R.A. & van Lohuizen, M. The oncogene and Polycomb-group gene bmi-1 regulates cell proliferation and senescence through the ink4a locus. *Nature* **397**(6715), 164-168 (1999).

Jernigan F, Branstrom A, Baird JD, Cao L, Dali M, Furia B, Kim MJ, O'Keefe K, Kong R, Laskin OL, Colacino JM. Preclinical and early clinical development of PTC596, a novel small-molecule tubulin-binding agent. Molecular Cancer Therapeutics. 2021 Oct 1;20(10):1846-57.

Jia L, Zhang W, Wang CY. BMI1 inhibition eliminates residual cancer stem cells after PD1 blockade and activates antitumor immunity to prevent metastasis and relapse. Cell Stem Cell. 2020 Aug 6;27(2):238-53.

Kaur, K. et al. Novel Strategy to Expand Super-Charged NK Cells with Significant Potential to Lyse and Differentiate Cancer Stem Cells: Differences in NK Expansion and Function between Healthy and Cancer Patients. *Front. Immun*. **8**, 297 (2017)

Kim, H.S. et al. Endothelial-derived interleukin-6 induces cancer stem cell motility by generating a chemotactic gradient towards blood vessels. *Oncotarget* **8**(59), 100339-100352 (2017).

Koneva, L.A. et al. HPV Integration in HNSCC Correlates with Survival Outcomes, Immune Response Signatures, and Candidate Drivers. *Mol. Cancer Res.* **16**(1), 90-102 (2018).

Krishnamurthy, S. et al. Endothelial cell-initiated signaling promotes the survival and self-renewal of cancer stem cells. Cancer Res. 70(23), 9969-9978 (2010).

Krishnamurthy, S. & Nör, J.E. Orosphere assay: a method for propagation of head and neck cancer stem cells. *Head Neck* **35**(7), 1015-1021 (2013).

Krishnamurthy, S. et al. Endothelial interleukin-6 defines the tumorigenic potential of primary human cancer stem cells. *Stem Cells* **32**(11), 2845-2857 (2014).

Lu, L. et al. Cancer stem cell vaccine inhibits metastases of primary tumors and induces humoral immune responses against cancer stem cells. *Oncoimmunology* **4**(3), e990767, (2015).

McDermott, S.C., Rodriguez-Ramirez, C., McDermott, S.P., Wicha, M.S. & Nör, J.E. FGFR signaling regulates resistance of head and neck cancer stem cells to Cisplatin. *Oncotarget* **9**(38), 25148-25165 (2018).

Ning, N. et al. Cancer stem cell vaccination confers significant antitumor immunity. *Cancer Res.* **72**(7), 1853-1864 (2012).

Nör, C. et al. Cisplatin induces Bmi-1 and enhances the stem cell fraction in head and neck cancer. Neoplasia 16(2),137-146 (2014).

Pastrana E, Silva-Vargas V, Doetsch F. Eyes wide open: a critical review of sphere-formation as an assay for stem cells. Cell stem cell. 2011 May 6;8(5):486-98.

Podhorecka M, Skladanowski A, Bozko P. H2AX phosphorylation: its role in DNA damage response and cancer therapy. Journal of nucleic acids. 2010 Oct;2010.

Prager BC, Xie Q, Bao S, Rich JN. Cancer stem cells: the architects of the tumor ecosystem. Cell stem cell. 2019 Jan 3;24(1):41-53.

Prince, M.E. et al. Identification of a subpopulation of cells with cancer stem cell properties in head and neck squamous cell carcinoma. Proc. Natl. Acad. Sci. USA 104(3), 973-978 (2007).

Reya, T., Morrison, S.J., Clarke, M.F. & Weissman, I.L. Stem cells, cancer, and cancer stem cells. *Nature* **414**(6859),105-111 (2001).

Sahara S, Warner KA, Herzog AE, Zhang Z, Nör JE. Therapeutic inhibition of Bmi-1 ablates chemoresistant cancer stem cells in adenoid cystic carcinoma. Oral Oncology. 2023 Jul 1;142:106437.

Seiwert, T.Y., Salama, J.K. & Vokes, E.E. The chemoradiation paradigm in head and neck cancer. *Nat. Clin. Pract. Oncol.* **4**(3), 156-171 (2007).

Shapiro GI, O'Mara E, Laskin OL, Gao L, Baird JD, Spiegel RJ, Kaushik D, Weetall M, Colacino J, O'Keefe K, Branstrom A. Pharmacokinetics and Safety of PTC596, a Novel Tubulin-Binding Agent, in Subjects With Advanced Solid Tumors. Clinical Pharmacology in Drug Development. 2021 Aug;10(8):940-9.

Siegel RL, Miller KD, Fuchs HE, Jemal A. Cancer statistics, 2021. Ca Cancer J Clin. 2021 Jan 12;71(1):7-33.

Sindhu SK, Bauman JE. Current concepts in chemotherapy for head and neck cancer. Oral and Maxillofacial Surgery Clinics. 2019 Feb 1;31(1):145-54.

Wu K, Woo SM, Seo SU, Kwon TK. Inhibition of BMI-1 Induces Apoptosis through Downregulation of DUB3-Mediated Mcl-1 Stabilization. International Journal of Molecular Sciences. 2021 Sep 18;22(18):10107.

Xu, R., Chen, L. & Yang, W.T. Aberrantly elevated Bmi1 promotes cervical cancer tumorigenicity and tumor sphere formation via enhanced transcriptional regulation of Sox2 genes. *Oncology reports* **42**(2), 688-696 (2019).

CHAPTER 5:
Conclusion

5.1 Summary

Despite being the most common head and neck cancer, head and neck squamous cell carcinoma (HNSCC) continues to present a challenge in treatment with unacceptably high recurrence rates (Carvalho *et al.,* 2005). This challenge is suspected to arise from the evidence that while conventional chemotherapy is effective in debulking the tumor, it does not eradicate the uniquely resistant cancer stem cells (CSCs) that have been shown to drive tumor initiation, therapeutic evasion, and disease progression. Using a CSC-targeted approach as a monotherapy, however, would eliminate the small fraction of CSCs while leaving behind the bulk tumor cells that still harbor growth potential and plasticity to recapitulate the CSC nice. Therefore, we embarked on elucidating potentially impactful processes that define the acquisition and maintenance of the CSC phenotype, which may be targeted in combination with conventional chemotherapy to achieve optimal therapeutic outcomes in HNSCC.

In Chapter 1, we delved into the heterogeneity of the cancer cell population, as well as other cells within the tumor microenvironment and their influence on cancer cell survival and stemness. In this chapter, we explored the biology and clinical relevance of the CSC population, which can be therapeutically targeted. We reviewed signaling circuits that compose impactful roles in the maintenance of CSCs, which when targeted might sensitize them to commonly used cytotoxic chemotherapy.

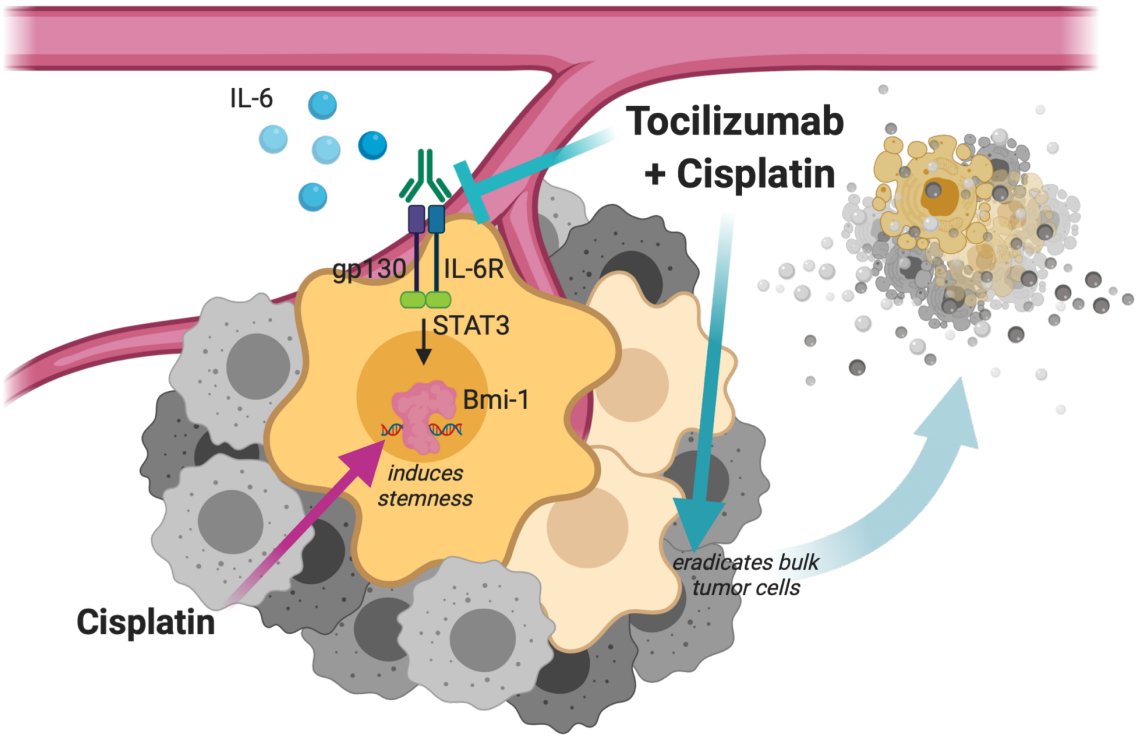

Figure 5-1: The IL-6R and Bmi-1 axis controls self-renewal and chemoresistance of head and neck cancer stem cells.

The role of endothelial cell-secreted IL-6 within the perivascular niche in promoting maintenance of the CSC pool and their invasive properties has been extensively described by our lab (Kim *et al.,* 2017; Krishnamurthy *et al.,* 2014). In Chapter 2, we expand on previous observations that IL-6 augments Cisplatin-induced increase in cancer cell stemness, implicating the IL-6/STAT3 signaling axis as a key mediator of chemoresistance in HNSCC tumors via downstream Bmi-1 activation that results in a more aggressive phenotype. In this chapter, we showcased a promising therapeutic strategy to suppress the adverse molecular effects of Cisplatin treatment that provoke an increase in CSC (**Fig. 5-1**). We demonstrated both genetic and pharmacologic inhibition of IL-6R signaling could suppress Cisplatin-mediated induction of the CSC fraction, Bmi-1 expression, and self-renewal of HNSCC cells. We also showed that increased Bmi-1

expression in patient tumor specimens correlated with a poorer recurrence-free survival, underlining the importance of Bmi-1 in the context of disease relapse. Lastly, we presented that therapeutic IL-6R inhibition with Tocilizumab can resolutely prevent the CSC increase by Cisplatin and suppress the growth of Cisplatin-resistant tumors. Of note, our results using Tocilizumab are applicable in an immune-incompetent setting. Considering the increasing prominence of immune checkpoint targeting cancer immunotherapy, the interface of CSC and immune cells remains to be investigated.

Bmi-1 has emerged as a prominent player in CSC biology and, in Chapter 2, was

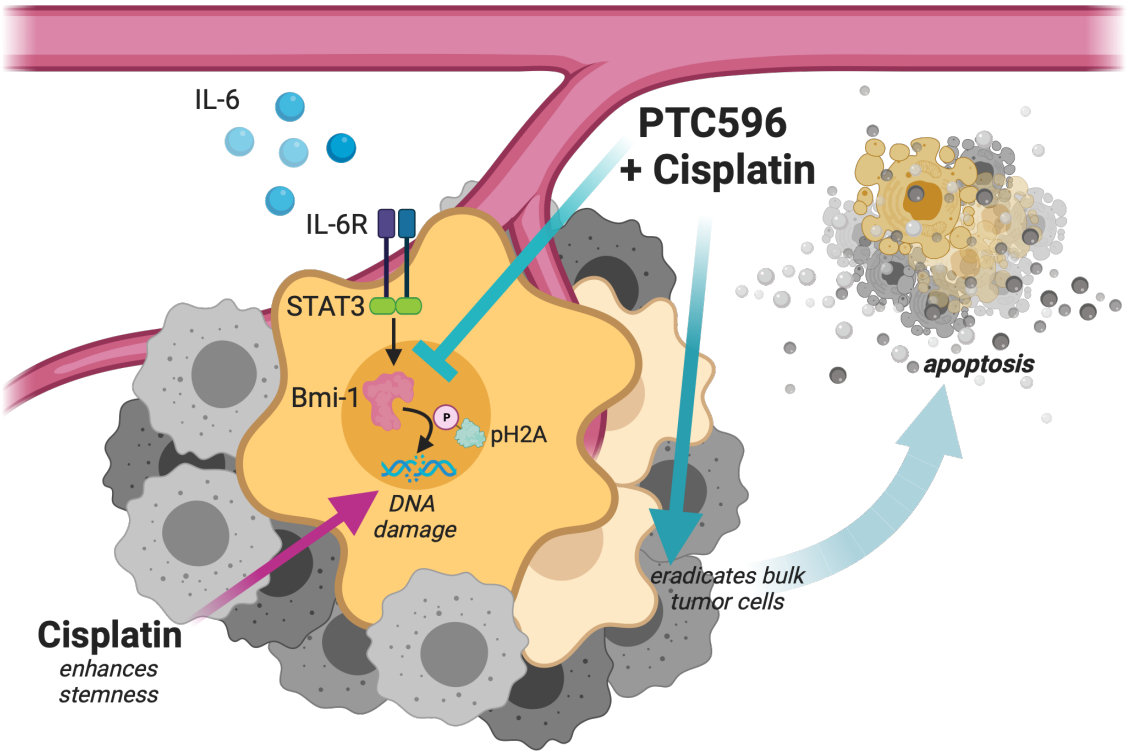

Figure 5-2: Bmi-1 mediates resistance of head and neck cancer stem cells to cytotoxic chemotherapy.

found to control self-renewal and chemoresistance as part of the IL-6/STAT3 signaling axis. In Chapter 3, we sought to dig deeper into the role of Bmi-1 as a master regulator of stem cell self-renewal and discussed the parallels in the role of Bmi-1 in stem cell biology of health and disease. We explored how the functional role of Bmi-1 in CSC-

mediated disease progression may be leveraged to advance clinical treatment strategies as an attractive target for mechanism-based, developmental therapeutics.

Lastly, in Chapter 4, we used both genetic and pharmacologic approaches to inhibit Bmi-1, which overcame resistance of CSCs to cytotoxic chemotherapy. We showed that Bmi-1 knockdown suppressed IL-6/STAT3 signaling in CSC-enriched cultures as well as bulk tumor cells and prevents the CSC fraction increase by both Cisplatin and Carboplatin. Further, we showed that treatment with the Bmi-1 inhibitor PTC596 suppressed the Cisplatin-mediated increase in the CSC fraction and self-renewal both *in vitro* and *in vivo.* Additionally, we established a link between both Bmi-1 inhibition and knockdown causing an abrogated DNA damage response and apoptosis in presence of genotoxic chemotherapies, suggesting a potential mechanism by which Bmi-1 may elicit its effect on CSCs (**Fig. 5-2**).

The preclinical studies described in this dissertation provide rationale for the incorporation of a CSC-targeted therapy based on inhibition of the IL-6 and Bmi-1 signaling axis in HNSCC where no such therapy currently exists.

5.2 Future Directions

5.2.1 Biological processes underlying Bmi-1-mediated CSC fraction changes

It is yet unclear whether the observed changes in CSC fraction occurs due to a numerator or a denominator effect, i.e. whether changes in the CSCs or the bulk tumor cells are driving the proportionate change within the overall tumor population. Additionally, the question by which mechanism these changes occur remain unanswered – namely, is the CSC proportion changing due to preferential apoptosis, induced cellular senescence, or shift towards differentiation? To attempt to address aspects of these questions, we

performed immunocytochemistry staining for ALDH and Bmi-1 of HNSCC cells grown in chamber slides in Chapter 2 of this dissertation, where we found that Cisplatin and IL-6 inhibition did not induce overall shifts in fluorescence within the entire cell population, but rather within a subset of cells to a greater extent. We also reviewed in Chapter 3, that downstream Bmi-1 signaling mediates a plethora of cellular processes as a master regulator of stemness and key player in cell cycle regulation. In Chapter 4, we found that Bmi-1 inhibition with PTC596 induced apoptosis as measured by cleaved caspase-3 expression. Undoubtedly, Bmi-1 is a protein with a vast repertoire of cellular functions and further investigation into biological processes underlying its regulatory role within the CSC pool is warranted.

It has been shown that Cisplatin-induced apoptosis was limited to Bmi-1$^-$ cells, supporting the rationale that the increase in the resulting CSC fraction may be due to a relative decrease in non-CSC tumor bulk cells being eliminated by cytotoxic chemotherapy (Chen *et al.,* 2017). To address this point within the context of the manuscript in preparation for submission encompassed in Chapter 4, we plan to analyze more closely the PTC596-mediated apoptosis within CSC versus tumor bulk cells via immunofluorescence staining of *in vitro* cultured cancer cells and tumor tissues from our *in vivo* study. Bmi-1 is a direct regulator of the cell cycle, as reviewed in Chapter 3, particularly via tight regulation of cell senescence as described earlier in this thesis. Interestingly, others have shown that genotoxic chemotherapy promotes IL-6 release acutely following DNA damage, and that this was coincident with a gradual induction of cancer cell senescence (Gilbert *et al.,* 2010). This observation may establish a link between IL-6 acting as a trigger to Bmi-1-induced senescence in context of genotoxic

chemotherapy treatment. At the intersection of the DNA damage response and cell cycle regulation lies p53, which is commonly mutated in HNSCC. Our lab has previously shown in MEC that p53 inhibits Bmi-1 driven CSC self-renewal by driving cells towards differentiation (Rodriguez *et al.,* 2022). Understanding the details of the cell cycle-related fate of CSCs remains an area of further investigation. Aside from inducing potential cell senescence, Bmi-1 is a master regulator of self-renewal. In the milieu of CSCs, this is directly related to the balance of symmetric (self-renewing) versus asymmetric (differentiating) cell divisions. Such future studies may require the development of reporter systems, as current identification of CSCs relies on enzymatic ALDH assays, and utilization of cell cycle reporter systems such as the FUCCI system (Fischer *et al.,* 2023).

5.2.2 Untangling the Bmi-1-mediated DNA damage response

The mechanism of action of many genotoxic chemotherapies, such as Cisplatin, involves causing DNA crosslinks that elicit the DNA damage response (DDR) in which Bmi-1 is a key mediator (Ismail *et al.,* 2010). As such, the increase in Bmi-1 expression and subsequent CSC fraction may be regarded as a molecular side effect of genotoxic chemotherapies. Loss of Bmi-1 impairs the repair of double-stranded DNA breaks by homologous recombination and subsequent cell cycle arrest in G_2-M (Ginjala *et al.,* 2011), however the mechanistic link between Bmi-1 and the DNA damage response in HNSCC has not yet been investigated.

Interestingly, studies have begun to investigate the potential of treatment optimization by combining poly-adenosine diphosphate-ribose polymerase inhibitors (PARPi) with chemotherapy or immunotherapy in HNSCC (Moutafi *et al.,* 2021). Others have shown that patients with HNSCC show defective DDR pathway activity and higher

levels of oxidative stress, which appeared to correlate with a response to Cisplatin therapy (Psyrri *et al.,* 2021). Additionally, the combination of the PARP inhibitor Olaparib with platinum-based chemotherapy has shown promise, as cancer cells use PARP to repair platinum-induced DNA damage to escape apoptosis (Ledermann *et al.,* 2019). As previously mentioned, Bmi-1 is a key component in recruiting DDR machinery and was shown to co-purify with PARP-1 (Facchino *et al.,* 2010). Remarkably, this study showed that Bmi-1 confers radioresistance to CSCs through recruitment of DNA damage response machinery in glioblastoma. As another avenue for future investigation, combination of a PARP inhibitor with Cisplatin in HNSCC may provide insight into the mechanism of Bmi-1-mediated cancer cell stemness.

Conversely, future studies to dissect the underlying cause of the observed increase in Bmi-1 expression following Cisplatin and Carboplatin treatment may include investigating relevant chemotherapeutics for HNSCC that function through different mechanisms of action from platinum-based agents (e.g. Paclitaxel). Such studies would enable determining whether the increase of Bmi-1 expression and CSC fraction is specific to platinum-based chemotherapeutics and may shed further light on mechanisms underlying chemoresistance of CSCs.

5.2.3 Bmi-1 as a putative prognostic marker

In this dissertation, we have discussed extensively that tumor cells derive many of their malignant features from the acquisition of stem-like characteristics. We reviewed in Chapter 3 that CSCs are a highly tumorigenic subpopulation of tumor cells that share characteristics of self-renewal and multipotency with physiological stem cells and drive neoplastic processes including tumor initiation, metastasis, recurrence, and therapeutic

evasion. Another area of future directions lies within the investigation of premalignant dysplastic oral lesions and their progression to carcinoma. Early premalignant lesions are heterogeneous, the tumor-initiating cell type is largely unknown, and currently there is no way to predict whether a dysplastic lesion will progress to cancer or not. Scientific evidence suggests that oral epithelial stem cells are targeted by carcinogens and may function as cancer stem cells in driving carcinogenesis (Trosko *et al.,* 2008).

There are multiple potential mechanisms by which CSCs could initiate a cancer within the oral epithelium, and advancements in the knowledge of the biology underlying acquisition of the CSC phenotype may provide scientific rationale for novel preventative and treatment strategies. For example, in breast cancer the role of CSCs in tumor initiation and disease progression is well-defined, but their contribution to the progression of premalignant lesions is still unclear. It has recently been shown that within heterogeneous precancerous lesions, both mammary stem cells and more differentiated cells rapidly progress to cancer through induction of the *Wnt1* oncogene (Bu et al. 2019), which maintains stemness in both normal and cancerous cells (Lindvall et al. 2007). However, the resulting tumors are vastly different in protein expression and histopathology. *Wnt* stimulation induced cancer cell stemness in precancerous lesions, even in those derived from more differentiated cells (Bu et al. 2019), suggesting that cancer cell stemness may play a role in multiple steps of carcinogenesis. Similarly, in human papillomavirus-driven cervical precancers, $CD66^{high}$ cells exhibited both stem-like and differentiated characteristics, which were thought to concurrently be permissive of neoplastic development and viral life cycle events, respectively (Pattabiraman et al. 2014). Irrespective of a particular mechanism, Smith *et al.* showed in pan-cancer findings

that a molecular signature of DNA methylation marks variants of adult stem cells that was enriched in aggressive epithelial cancers (Smith *et al.,* 2018). The identification of CSC has more recently also been augmented vial spatial transcriptomics methods that have potentiated in silico modeling approaches to inform pan-cancer insights into pathobiology and putative therapeutics (Arora *et al.,* 2023). With the rise in artificial intelligence, these trends will likely continue broadening the interface of different areas of cancer research.

As mentioned throughout this thesis, endothelial cell-mediated IL-6 signaling is indispensable in facilitating the acquisition of the CSC phenotype in HNSCC. Others from our laboratory group have reviewed elsewhere (Polverini et al., 2023) that IL-6 signaling may also play a crucial role in promoting the malignant transformation of dysplastic lesions (**Fig. 5-3**). Considering our findings of IL-6/STAT3 signaling controlling Bmi-1 expression and subsequently the CSC phenotype, Bmi-1 presents an attractive candidate in the development of prognostic factors for HNSCC. In Chapter 2, we showed that increased Bmi-1 expression in patient samples within a tissue microarray significantly correlated with decreased recurrence-free survival time, which supports other published findings of Bmi-1 and CD44 as indicators for poorer prognosis of overall and disease-free survival in HNSCC, implicating Bmi-1 as a potential prognostic factor (Jakob *et al.,* 2021). In a model of HNSCC, Bmi-1^{+} lingual epithelial stem cells were shown to function as cancer stem cells (Tanaka et al., 2016). Here, a multicolor lineage tracing mouse model underwent chemical induction of oral cancer by 4-NQO, which demonstrated polyclonal tumor formation from single cells over the course of 1-3 months. More specifically, in a gene-specific multicolor lineage tracing method, the authors demonstrated that Bmi-1^{+}

cells give rise to single-colored clusters in developing tumors and may potentially serve as CSCs.

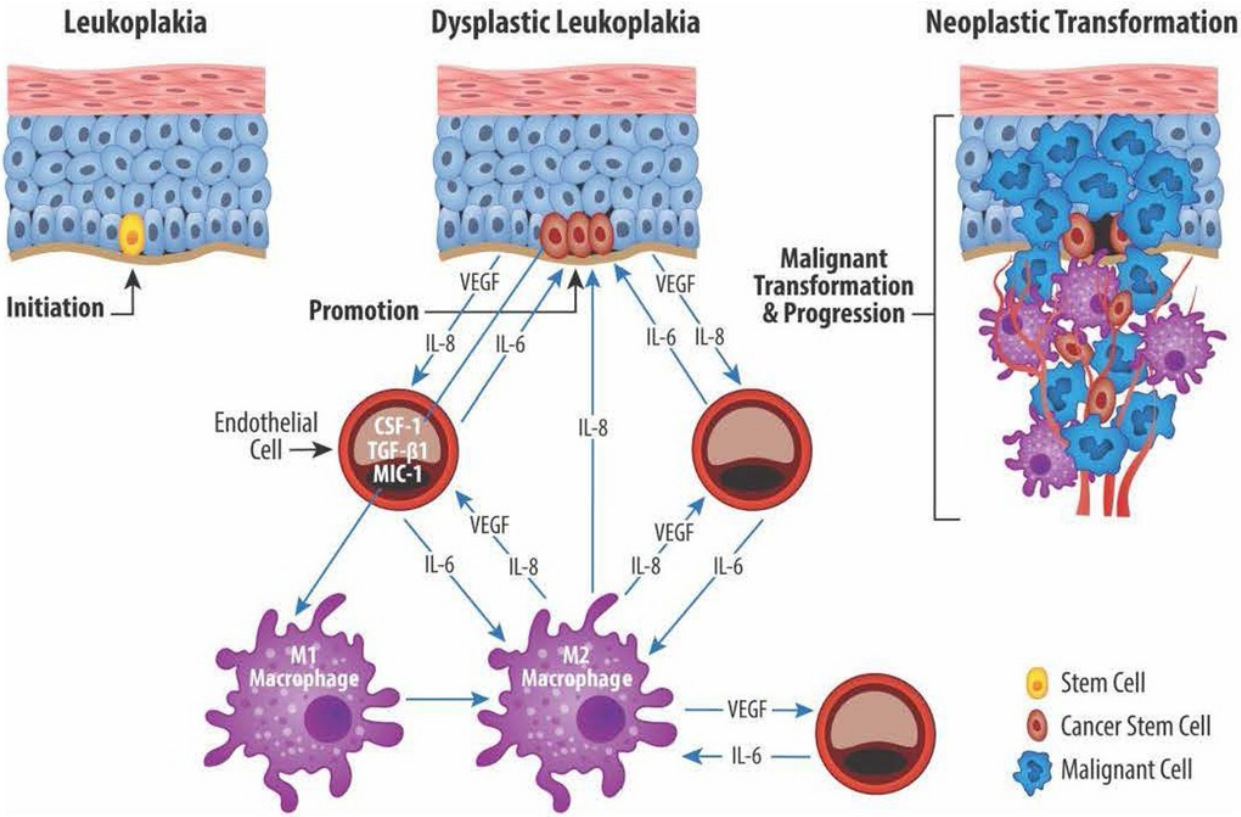

Figure 5-3: Reciprocal exchange of cytokine mediators between cancer stem cells (CSC), endothelial cells (EC), and macrophages (M1 and M2).

CSC located in the basal layer of dysplastic epithelium produce, among others, the angiogenic mediators VEGF and IL-8. EC in turn produce IL-6 which plays an important role in maintaining the CSC stemness. EC also play a role in transitioning proinflammatory M1 macrophages to protumor M2 macrophages via production of IL-6. This figure was adapted from Polverini *et al.,* 2023.

Evidently, a subset of physiological stem cells plays a crucial role in the progression of precancerous dysplasia which later contributes to the observed cancer cell stemness. This thesis work elucidated key signaling mechanisms that promote the CSC phenotype, which may be significant in mediating the transformation of epithelial stem cells to ultimately initiate tumor growth and warrant future investigation. With limited

success in curbing the incidence of HNSCC, especially given the increase in percentage of younger patients developing human papillomavirus (HPV) related HNSCC (Ang *et al.,* 2010), it is apparent that early identification of premalignant lesions at risk for malignant transformation has the potential to change the landscape of HNSCC diagnosis and treatment.

5.3 Concluding Remarks

A consequential challenge preventing long-term survival and quality of life of patients with head and neck cancer is the failure of current treatment modalities to eliminate cancer stem cells within a tumor, ultimately originating from a lack of understanding of molecular mechanisms underlying the acquisition and maintenance of the cancer stem cell phenotype. The work completed in this thesis project elucidated mechanisms underlying IL-6/STAT3-mediated chemoresistance of cancer stem cells. These studies also provided potential mechanism-based, therapeutic strategies based on IL-6 and Bmi-1 inhibition to target cancer stem cells, capable of suppressing the Cisplatin-mediated increase in fraction of cancer stem cells *in vitro* and *in vivo.* Collectively, expanding our understanding of cancer stem cell-mediated chemoresistance will enhance our ability to design novel therapeutics to minimize disease-relapse and improve the outcomes for patients with head and neck cancer.

5.4 References

Ang KK, Harris J, Wheeler R, Weber R, Rosenthal DI, Nguyen-Tân PF, Westra WH, Chung CH, Jordan RC, Lu C, Kim H. Human papillomavirus and survival of patients

with oropharyngeal cancer. New England Journal of Medicine. 2010 Jul 1;363(1):24-35.

Arora R, Cao C, Kumar M, Sinha S, Chanda A, McNeil R, Samuel D, Arora RK, Matthews TW, Chandarana S, Hart R. Spatial transcriptomics reveals distinct and conserved tumor core and edge architectures that predict survival and targeted therapy response. Nature Communications. 2023 Aug 18;14(1):5029.

Bu W, Liu Z, Jiang W, Nagi C, Huang S, Edwards DP, Jo E, Mo Q, Creighton CJ, Hilsenbeck SG, Leavitt AD, Lewis MT, Wong STC, Li Y. Mammary Precancerous Stem and Non-Stem Cells Evolve into Cancers of Distinct Subtypes. Cancer Res. 2019 Jan 1;79(1):61-71.

Carvalho, A.L., Nishimoto, I.N., Califano, J.A. & Kowalski, L.P. Trends in incidence and prognosis for head and neck cancer in the United States: a site-specific analysis of the SEER database. Int. J. Cancer 114(5), 806-816 (2005).

Chen, D. et al. Targeting BMI1+ cancer stem cells overcomes chemoresistance and inhibits metastases in squamous cell carcinoma. Cell Stem Cell 20(5), 621-634, e6 (2017).

Facchino S, Abdouh M, Chatoo W, Bernier G. BMI1 confers radioresistance to normal and cancerous neural stem cells through recruitment of the DNA damage response machinery. Journal of Neuroscience. 2010 Jul 28;30(30):10096-111.

Gilbert, L.A. & Hemann, M.T. DNA damage-mediated induction of a chemoresistant niche. Cell 143(3), 355-366 (2010).

Ginjala V, Nacerddine K, Kulkarni A, Oza J, Hill SJ, Yao M, Citterio E, van Lohuizen M, Ganesan S. BMI1 is recruited to DNA breaks and contributes to DNA damage-induced

H2A ubiquitination and repair. Molecular and cellular biology. 2011 May 1;31(10):1972-82.

Jakob M, Sharaf K, Schirmer M, Leu M, Küffer S, Bertlich M, Ihler F, Haubner F, Canis M, Kitz J. Role of cancer stem cell markers ALDH1, BCL11B, BMI-1, and CD44 in the prognosis of advanced HNSCC. Strahlentherapie und Onkologie. 2021 Mar;197(3):231-45.

Kim, H.S. et al. Endothelial-derived interleukin-6 induces cancer stem cell motility by generating a chemotactic gradient towards blood vessels. Oncotarget 8(59), 100339-100352 (2017).

Krishnamurthy, S. et al. Endothelial interleukin-6 defines the tumorigenic potential of primary human cancer stem cells. Stem Cells 32(11), 2845-2857 (2014).

Moutafi M, Economopoulou P, Rimm D, Psyrri A. PARP inhibitors in head and neck cancer: Molecular mechanisms, preclinical and clinical data. Oral Oncology. 2021 Jun 1;117:105292.

Lindvall C, Bu W, Williams BO, Li Y. Wnt signaling, stem cells, and the cellular origin of breast cancer. Stem Cell Rev 2007;3:157–68.

Pattabiraman C, Hong S, Gunasekharan VK, Pranatharthi A, Bajaj J, Srivastava S, Krishnamurthy H, Ammothumkandy A, Giri VG, Laimins LA, Krishna S. CD66+ cells in cervical precancers are partially differentiated progenitors with neoplastic traits. Cancer Res. 2014 Nov 15;74(22):6682-92.

Polverini PJ, Nör F, Nör JE. Crosstalk between cancer stem cells and the tumor microenvironment drives progression of premalignant oral epithelium. Frontiers in Oral Health. 2023 Jan 10;3:1095842.

Psyrri A, Gkotzamanidou M, Papaxoinis G, Krikoni L, Economopoulou P, Kotsantis I, Anastasiou M, Souliotis VL. The DNA damage response network in the treatment of head and neck squamous cell carcinoma. ESMO open. 2021 Apr 1;6(2):100075.

Rodriguez-Ramirez C, Zhang Z, Warner KA, Herzog AE, Mantesso A, Zhang Z, Yoon E, Wang S, Wicha MS, Nör JE. p53 inhibits Bmi-1-driven self-renewal and defines salivary gland cancer stemness. Clinical Cancer Research. 2022 Nov 1;28(21):4757-70.

Smith BA, Balanis NG, Nanjundiah A, Sheu KM, Tsai BL, Zhang Q, Park JW, Thompson M, Huang J, Witte ON, Graeber TG. A human adult stem cell signature marks aggressive variants across epithelial cancers. Cell reports. 2018 Sep 18;24(12):3353-66.

Tanaka T, Atsumi N, Nakamura N, Yanai H, Komai Y, Omachi T, Tanaka K, Ishigaki K, Saiga K, Ohsugi H, Tokuyama Y, Imahashi Y, Hisha H, Yoshida N, Kumano K, Okazaki K, Ueno H1. Bmi1-positive cells in the lingual epithelium could serve as cancer stem cells in tongue cancer. Sci Rep. 2016 Dec 22;6:39386.

Trosko JE. Human adult stem cells as the target cells for the initiation of carcinogenesis and for the generation of “cancer stem cells”. Int J Stem Cells. 2008 Nov 31;1(1):8-26.